UNIVERSITY OF SOUTHAMPTON

FACULTY OF MEDCINE, HEALTH AND LIFE SCIENCES

SCHOOL OF MEDICINE

Division of Infection Inflammation & Repair (IIR)

Allergy & Inflammation Research (AIR)

The expression and function of the asthma susceptibility gene, A Disintegrin and Metalloprotease (ADAM) 33, in airways of normal and asthmatic subjects and in developing lungs

By

Hans Michael Haitchi MD, MMed

Thesis for the degree of Doctor of Philosophy

February 2008

To

ἰχθύς (ichthys)

&

Gerhild

UNIVERSITY OF SOUTHAMPTON

ABSTRACT

FACULTY OF MEDCINE, HEALTH AND LIFE SCIENCES
SCHOOL OF MEDICINE

Doctor of Philosophy

THE EXPRESSION AND FUNCTION OF THE ASTHMA SUSCEPTIBILITY GENE, A DISINTEGRIN AND METALLOPROTEASE (ADAM) 33, IN AIRWAYS OF NORMAL AND ASTHMATIC SUBJECTS AND IN DEVELOPING LUNGS

by Hans Michael Haitchi

Asthma affects 1 in 12 adults and 1 in 10 children in the UK. It is a complex disease involving genetic and environmental factors. *ADAM33* is an asthma susceptibility gene whose polymorphic variation has been linked to asthma and bronchial hyperresponsiveness, as well as decline in lung function in asthma and COPD and reduced lung function in young children. ADAM33 mRNA is almost exclusively expressed in mesenchymal cells, such as fibroblasts, myofibroblasts and smooth muscle cells. These cells play an important role in modelling of the airways during lung development and in remodelling of the airway in established disease. As the function of ADAM33 and its role in asthma is not known, this thesis tested the hypotheses that:

ADAM33 is differentially expressed in normal and asthmatic lungs; and

ADAM33 is involved in embryonic/fetal lung development where the influence of an allergic maternal environment affects ADAM33 to contribute to the development of asthma.

To test the hypothesis that ADAM33 is differentially expressed in asthma, bronchial biopsies and brushings from adult subjects were examined. Using RT-qPCR all previously described splice variants were detected in the biopsies. No disease specific difference for any of the mRNA splice variants could be detected. Using immunohistochemistry, it was shown, for the first time that ADAM33 is found mainly in the bronchial smooth muscle, consistent with its genetic association with BHR. Computer-aided image analysis of ADAM33 expression did not reveal a disease-specific difference, consistent with the mRNA data. No expression of ADAM33 could be demonstrated in bronchial brushings containing more than 95% epithelial cells.

To test the hypothesis that ADAM33 is involved in embryonic lung development human embryonic lung (HEL) and mouse tissues were examined. Using RT-qPCR, the same splice variants were detected in HEL as in adult bronchial tissue, however Western blot analysis revealed an extra ADAM33 protein band in HELs compared to adult lungs suggesting a different role of ADAM33 in developing lung. Expression of ADAM33 increased in HELs from 7 to 9 weeks post conception and a similar increase occurred when HELs were cultured in a newly developed HEL explant culture system suggesting that this is a useful model for studying human lung development. ADAM33 could be successfully knocked down using siRNA in the mesenchymal progenitor cells grown in culture from HELs paving the way for knock-down in whole HEL tissue. When ADAM33 mRNA expression was studied during murine lung development it was detectable from as early as embryonic day 11 and two significant increments in expression could be seen. The first occurred during the pseudoglandular stage when spontaneous peristaltic contractions occur and the second one after birth when the lungs inflate at the beginning of air breathing, suggesting that mechanical forces might induce ADAM33.

To test the hypothesis that ADAM33 and asthma are influenced by maternal allergy, a mouse model using bronchial hyperresponsiveness susceptible mice (A/J mice) was used. Maternal allergy was induced using ovalbumin and the offspring were studied for ADAM33 expression and lung function. Maternal allergy had a suppressive effect on ADAM33 mRNA directly after birth which was similar to the findings in HEL cultured for 18 days in the presence of IL-13. Maternal allergy also induced increased BHR to methacholine in 4 weeks old offspring. Although no direct causal relationship with ADAM33 was established, these findings suggest a potential gene-environment interaction.

In conclusion this thesis provides novel data regarding the expression and localisation of ADAM33 in embryonic and adult lung. It also suggests a potential role for ADAM33 in lung development and highlights the effect that maternal allergy has on airway reactivity of offspring that carry the ADAM33 susceptibility gene, consistent with a role for ADAM33 in the early-life origins of asthma.

Table of content

List of figures

List of tables

List of movies

(CD attached in hard copy)

Declaration of authorship

I, HANS MICHAEL HAITCHI,
declare that the thesis entitled

THE EXPRESSION AND FUNCTION OF THE ASTHMA SUSCEPTIBILITY GENE, A DISINTEGRIN AND METALLOPROTEASE (ADAM) 33, IN AIRWAYS OF NORMAL AND ASTHMATIC SUBJECTS AND IN DEVELOPING LUNGS

and the works presented in it are my own. I confirm that:

- this work was done wholly or mainly while in candidature for a research degree at this University;
- where any part of this thesis has previously been submitted for a degree or any other qualification at this University or any other institution, this has been clearly stated;
- where I have consulted and published work of others, this is always clearly attributed;
- where I have quoted from the work of others, the source is always given. With the exception of such quotations, this thesis is entirely my own work;
- I have acknowledged all main sources of help;
- where the thesis is based on work done by myself jointly with others, I have made clear exactly what was done by others and what I have contributed myself;
- part of this work has been published as: See Appendix!

Signed: ……

Date: …….

Acknowledgements

First of all I would like to thank my supervisors Professors Donna Davies and Stephen Holgate who have supported and encouraged me throughout my postgraduate studies. Particular thanks to Stephen who is a fountain of knowledge and a real encourager and special thanks to Donna for her generous giving of time (many very late afternoons), her expertise as well as deep insight and understanding of pathophysiological mechanisms.
Many thanks go to all my colleagues and friends from the IRR Division and in particular the Roger Brooke Lab, who have been really great to work with and of whom I have become very fond over the years: Dr Rob Powell, who trained me in RT-qPCR and who has become a dear friend; Dr James Wicks, for teaching me how to extract RNA and culture cells; Dr Lynn Andrews, for her assistance with Western blotting; Dr Fabio Bucchieri for his assistance with tissue culture; Drs Chrissy Boxall, Lynnsey Hamilton, Sarah Puddicombe, Yun Pang for helping a clinician to become a 'lab rat'; Sue Martin for teaching me good laboratory practice. Apologies to anyone not mentioned by name.
Further thanks should be attributed to:
Drs Tim Shaw, Peter Wark, Ian Yang, Timothy Howell, Suresh Babu, David Sammut, Peter Howarth for performing bronchoscopies and providing bronchial samples; the research nurses Lou Little and her team from Allergy and Inflammation Research (AIR) and the staff and nurses from Wellcome Trust Clinical Research Facility for their assistance with bronchoscopies; Dr Anton Page, Roger Alston from the Biomedical Imaging Unit for assistance with image capture and analysis; Dr Susan Wilson, Jon Ward, Helen Rigden, and Janet Underwood from the Histochemistry Research Unit for their assistance with processing and cutting GMA resin-embedded tissue.
Mrs Jas Barley, Kerry Taylor and Michael Broome from the Biomedical Research Facility for animal husbandry; Professors Neil Hanley and David Wilson from the Human Genetics Division for providing human embryonic/fetal lungs and expertise in embryonic developmental biology.
Special thanks go to Professor David Bassett and Xiufeng Gao from Wayne State University, Detroit, MI, USA. Using their Ford Motor Company Exposure facility enabled the study of a maternal allergy mouse model. I am grateful to them for doing the allergen exposure and challenging experiments, testing the lung function, harvesting the lungs and shipping all the samples for analysis to Southampton. It has been a pleasure to collaborate with them.

Research is like art and would never be possible without the 'benefactors' who financially supported my work. Many thanks to the Asthma, Allergy and Inflammation Research Charity (AAIR, UK), HOPE Wessex Medical Research (UK), the British Lung Foundation (BLF, UK) and Medical Research Council (MRC, UK), and in particular to Roger Brooke for his generous personal research fellowship through his Roger Brooke Charitable Trust (UK).

I would also like to thank my parents Johann and Maria Haitchi who have created a loving and caring environment in the home where I grew up. I thank them for supporting my inquisitive mind and for enabling me to attend university. I am grateful for the love and support of my sister Sonja and brother Gerhard and their families (U,S,M,T & S) during all my graduate and postgraduate studies. Thanks also to my ABC family, and I am particular grateful to our adopted English parents Dr Bill & Shirley Lees for their support, prayers and encouragement during my work and completion of this thesis.

Finally, I would like to thank my dear wife Gerhild for her love and support and for bearing with me all the long evenings and weekends I spent in the lab doing exciting experiments. Without her love, patience and constant support I would have not been able to complete this work.

"The scientist does not study nature because it is beautiful; he studies it because he delights in it, and he delights in it because it is beautiful. If nature were not beautiful, it would not be worth knowing, and if nature were not worth knowing, life would not be worth living. Of course I do not speak of the beauty that strikes the senses, the beauty of qualities and appearances; not that I undervalue such beauty, far from it, but it has nothing to do with science; I mean that profounder beauty which comes from the harmonious order of the parts, and which pure intelligence can grasp."
French mathematician and philosopher of science: Henri Poincaré
"As you do not know the path of the wind, or how the body is formed in a mother's womb, so you cannot understand the work of God, the Maker of all things." Ecclesiastes 11 Verse 5
Science has become an exciting part of my life, trying to understand 'the harmonious order of parts' by following the thoughts of 'God, the Maker of all things'.

Definitions & abbreviations

18S rRNA	18S ribosomal RNA
28S rRNA	28S ribosomal RNA
3'UTR	3'untranslated region
ADAM	A Disintegrin And Metalloprotease
ADAM33cat	Catalytically active ADAM33
Ago-2	Aronaute-2 protein
AIR	Allergy & Inflammation Research
AM	Adult mouse
ANOVA	Analysis of variance
Anti-IgE	Omalizumab
APP	Amyloid precursor protein
APS	Ammonium persulphate
ASM	Airway smooth muscle
ASOs	Antisense oligonucleotides
B2A	Beta-2 agonist
BALF	Bronchoalveolar lavage fluid
BALT	Bronchus-associated lymphoid tissue
BBR	Bronchial brushing
BBX	Bronchial biopsy
BDP	Beclomethasone dipropionate
BHR	Bronchial hyperresponsiveness
BM	Basement membrane
BMP	Bone morphogenic protein
Bp	Base pair
BRF	Biomedical Research Facility
BT	Bronchial thermoplasty
BTS	British Thoracic Society
C/EBPa	CCAT/enhancer binding protein a
cDNA	Complementary DNA
CHO cells	Chinese Hamster Ovary cell
COPD	Chronic obstructive pulmonary disease
Ct	Threshold cycle
CTGF	Connective tissue derived growth factor
CTLA	Cytotoxic T-lymphocyte associated antigen
CXCL10	Chemokine (C-X-C motif) ligand 10
CYT	Cytoplasmic
DAB	Diaminobenzidine chromogen
DC	Dendritic cell
Dh1,2,3,4	DharmaFECT transfection reagents 1,2,3,4
DharmaFECT	Transfection reagent
Dicer	Ribonuclease III enzyme
Dis	Disintegrin
DMEM	Dulbecco's Modified Eagle Medium
DNase	DNA cleaving endonuclease
dNTP	Deoxyribonucleotide triphosphate
DPP-4	Dipeptidyl peptidase-4 (CD26)
dsRNA	Double stranded RNA
E346A	Mutation of the zinc binding domain
ECM	Extracellular matrix
ECS	Enhanced chemiluminescence
ED12	Embryonic day 12

EDTA	Ethylenediaminetetracetic acid
EGF	Epidermal growth factor
EGFR	Epidermal growth factor receptor
EMTU	Epithelial mesenchymal trophic unit
ENFUMOSA	Europ. Network for Understanding Mechanisms Of Severe Asthma
ETS-2, -3	Ets family transcription factor
FEV1	Forced expiratory volume in the first second
FGF-10	Fibroblast growth factor-10
FGF-2	Fibroblast growth factor 2
Foxa1	Forkhead box a1
Foxj1	Forkhead box j1
FRET	Fluorescence resonant energy transfer
g	Relative centrifugal force in gravities
GFP	Green fluorescent protein
GINA	Global Initiative for Asthma
Gli	Transcription factor
GMA	Glycol methacrylate
GM-CSF	Granulocyte monocyte colony stimulating factor
GPRA	G-protein coupled receptor
GSTP1	Glutathione S-transferase
GTPase	Guanosine triphosphatase
H292	Human Negroid lung, mucoepidermoid carcinoma cell line
HBSS	Hank's balanced salt solution
HEK 293	Human embryonic kidney cells
HEL	Human embryonic lung
HEPES	4-(2-Hydroxyethyl)piperazine-1-ethanesulfonic acid
HKG	House keeping gene
HLA	Human lymphocyte antigen
HLA-G	Human lymphocyte antigen-G
HPABF	Human primary adult bronchial fibroblast
HPELF	Human primary embryonic lung fibroblast
HPLC	High performance liquid chromatography
Hybond-P PVDF	Hydrophobic polyvinylidene difluoride membrane
ICAM-1	Intercellular adhesion molecule 1 (CD54)
ICC	Immunocytochemistry
ICOSL	Inducible T-cell co-stimulator ligand
ICS	Inhaled corticosteroids
IgE	Immunoglobulin E
IGF	Insulin growth factor
IgG	Immunoglobulin G
IHC	Immunohistochemistry
IL	Interleukin
IL-13	Interleukin13
INF-β	Interferon beta
INF-γ	Interferon gamma
INF-δ	Interferon delta
IRR	Infection Inflammation & Repair
ISAAC	International Study of Asthma and Allergies in Childhood
ISH	In situ hybridisation
k_{cat}/K_m	Specificity constants
kD	Kilo-Dalton
KL-1	Kit-ligand-1
LABA	Long acting beta agonist
LTC4	Leukotriene C4
M3R	Muscarinic acetylcholine receptor subtype 3

MALDI-TOF	Matrix-assisted-laser-desorption/ionisation time-of-flight
MCH II	Major histocompatibility complex class II
MCP-1,-2,-3	Monocyte chemoattractant protein
MDC	Monocyte-derived chemokine
miRNA	Micro RNA
MMP	Matrix metalloprotease
MP	Metalloprotease
mRNA	Messenger ribonucleic acid
MUC5AC	Mucin 5ac
MUC8	Mucin 8
N	Nucleus
NAC MAAS	NAC Manchester Asthma & Allergy Study
NAC	National Asthma Campaign
NB	Newborn
NHS	National Health Service
NOS	Neuronal nitric oxide synthetase
OS	Offspring
OVA	Ovalbumin
Ox40	Tumour necrosis factor receptor superfamily, member 4
Ox40L	Tumour necrosis factor (ligand) superfamily, member 4
p.c.	Post conception
PBS	Phosphate buffered saline
PCR	Polymerase chain reaction
PD1	Post partum day 1
PDDH-1	Protocaherin-1 gene
PDGF	Platelet derived growth factor
Penh	Enhanced pause in expiration
PEP	Pressure on expiration
PFA	Paraformaldehyde
PGD2	Prostaglandin D2
PGD2	Prostaglandin D2
PIP	Pressure on inspiration
piRNA	Piwi interacting RNA
PMA	Phorbol 12-Myristate 13-Acetate
PNA	Peptide nucleic acid
pp	Post partum
PRO	Pro-domain
PTGDR	Prostaglandin D2 receptor
RANTES	Regulated upon activation, normal T cell expressed and secreted
RISC	RNA-induce silencing complex
RNAi	RNA interference
RNase	Ribonuclease
RT	Reverse transcriptase assay
RT-qPCR	Reverse Transcription quantitative Polymerase Chain Reaction
SB	Sample buffer
SCF	Stem cell factor
SDS	Sodium dodecyl sulphate
SDS-PAGE	Sodium dodecyl sulphate polyacrylamide gel electrophoresis
SFM	Serum-free medium
Shh	Sonic hedge hog
shRNA	Small hairpin RNA
SIGN	Scottish Intercollegiate Guidelines Network
siRNA	Small interfering ribonucleic acid
SNP	Single nucleotide polymorphism
SOCS	Suppressor of cytokine signalling

SPINK5	Serine protease inhibitor Kazal type 5
SRF	Serum response factor
SS	Signal sequence
STAT	Signal transducer and activator of transcription
TACE	Tumour necrosis factor converting enzyme (ADAM17)
TARC	Thymus and activation regulated chemokine
TCR	T-cell receptor
TGF-α	Transforming growth factor-alpha
TGF-β	Transforming growth factor beta
Th0	T-helper type 0 lymphocyte (naïve T-cell)
Th1	T-helper type I lymphocyte
Th2	T-helper type II lymphocyte
TIMP	Tissue-inhibitors of metalloprotease
TIP	Tension induced/inhibited protein
TLR	Toll like receptor
T_m	Melting temperature
TM	Transmembrane
TNF-α	Tumour necrosis factor alpha
TRANCE	Tumour necrosis factor-related activation induced cytokine
Treg	T regulatory cells
Tris-HCl	Tris (hydroxymethyl) aminomethane hydrochloride
TSLP	Thymic stromal lymphopoietin (IL-7)
UK	United Kingdom
US	United States
VCAM-1	Vascular cell adhesion molecule 1
VEGF	Vascular endothelial growth factor
VEGFR	Vascular Endothelial Growth Factor Receptor
wpp	Weeks post partum
XG	X-tremeGENE transfection reagent
X-Gal	5-bromo-4-chloro-3-indolyl-β-D-galactopyranoside
X-tremeGENE	Transfection reagent
Zn^{++}	Zinc
αSMA	Alpha-smooth muscle actin
ΔΔCT	Delta delta CT

Chapter 1 Introduction

1.1 What is asthma?

In 1859, Henry Hyde Salter was the first to describe asthma: he described it as "a disease of reversible airway obstruction" (Salter HH 1859) which is still true today almost 150 years later.

Asthma is a chronic inflammatory disorder of the airways involving mast cells, eosinophils, and T-lymphocytes that is associated with airway remodelling and bronchial hyperresponsiveness. In susceptible individuals, this inflammation and structural airway wall changes cause recurrent episodes of wheezing, breathlessness, chest tightness, and cough, particularly at night and/or the early morning. These symptoms are usually associated with widespread but variable airflow limitations that are at least reversible either spontaneously or with treatment (Tattersfield *et al.* 2002; Elias *et al.* 2003; Lemanske and Busse 2003; Global Initiative for Asthma 2007). Although these pathological changes are mostly true for adult asthma they do not necessarily apply to the pre-school wheeze syndrome in childhood. Wheezing infants do not have inflammation and remodelling of the airways (Saglani *et al.* 2005) in contrast to pre-school children with confirmed wheezing (Saglani *et al.* 2007). This suggests that structural changes of the airways in form of impaired lung growth might happen early even before birth independent of inflammation (Bush 2008).

1.2 Asthma, a global and UK burden

Asthma is a serious global health problem with an estimated 300 million affected individuals worldwide. The prevalence of asthma has been increasing in adults and particular in children over the past ten to thirty years (Lenfant and Khaltaev 1995) (Masoli *et al.* 2004b; Masoli *et al.* 2004a; Eder *et al.* 2006).

The UK has been identified as amongst those countries with the highest prevalence for asthma worldwide (Global Initiative for Asthma 2007) and Europe-wide which was shown in the International Study of Asthma and Allergies in Childhood (ISAAC) (Beasley 1998; Kaur *et al.* 1998; ISSAC Steering Committee 1998) and the European Respiratory Health Survey (Sunyer *et al.* 1999; Pearce *et al.* 2000). The National Asthma Campaign Asthma Audit 2001 revealed that 7.8% of adults and 12.5-15.5% of children are afflicted by current symptomatic asthma in England. (National Asthma Campaign 2001). In the UK with a population of 60 million there are 5.2 million people (1.1 million children and 4.11 million adults) currently receiving treatment for asthma (Asthma UK 2004b) which is about 1 in 12 adults. Asthma is more widespread in children and is the most common long-term childhood medical condition affecting 1 in 10 children. Morbidity has a big impact on the quality of life

of asthmatic patients (Asthma UK 2004a). Although mortality had reached its peak 20 to 30 years ago, about 1400 people in the UK still die from asthma each year (Asthma UK 2004b). Asthma is not just a burden for the individual sufferer but also a major financial burden for the health care system and society. In 2001 the annual costs to the National Health Service (NHS) was estimated to be £889 million in the UK (Asthma UK 2004b). At least 12.7 million lost working days are not included leading to an extra cost for lost productivity of £1.2 billion (Asthma UK 2004b). The trend in asthma prevalence with its attendant persistent morbidity and disease burden, as well as the estimated costs for asthma, are likely to rise worldwide despite the availability of anti-inflammatory and bronchodilator drugs and guidelines for their use (Global Initiative for Asthma 2007; British Thoracic Society (BTS) and Scottish Intercollegiate Guidelines Network (SIGN) 2007; Expert Panel Report 3 2007). Although asthma has a strong genetic predisposition (Zhang *et al.* 2008), the increase in prevalence (Global Initiative for Asthma 2007) of the disease that has been observed over the last 30 years has occurred too rapidly to be due to new genetic changes. Instead, it is likely that factors related to the environment or to lifestyle are involved in the worldwide differences in asthma prevalence and its rise, and that these factors have exposed and interacted with pre-existing genetic susceptibilities (Holgate 1999; Sengler *et al.* 2002). Therefore, it is most important and urgent to understand the origins and mechanisms underlying the development of asthma and its progression in order to make advance in terms of prevention, diagnosis and treatment.

1.3 Pathology & Pathophysiology

1.3.1 History

Asthma is a complex and multifactorial syndrome whose underlying cause is unclear. More than a century ago Sir William Osler suggested that asthma is due to spasm of bronchial muscles, the attack is due to swelling of the bronchial mucous membrane and in many cases it is a special form of inflammation of the smaller bronchioles (Osler 1892). In the meantime our knowledge of asthma pathogenesis has increased substantially but reversible airway obstruction, bronchial hyperresponsiveness (BHR), airway inflammation and remodelling are still the key pathophysiological characteristics of asthma (Global Initiative for Asthma 2007).

Due to the progress made in new techniques to investigate asthma the understanding of the disease has vastly increased. Much of the early asthma studies relied upon the use of measurements of airflow restriction and inflammatory cells in the peripheral blood. Histopathological examination of lungs of patients that had died of asthma allowed studying the changes that took place in the airways directly after an acute attack significant enough to cause death. Nevertheless, these early techniques revealed several features that are specific to asthma. Mucus plugging of the airways, containing mucus and serum proteins mixed with cellular debris was one of the major features parallel to epithelial sloughing, basement membrane thickening, oedema and leukocyte infiltration (mainly eosinophils) of the submucosal structures, hyperplasia of mucous glands and hypertrophy or hyperplasia of bronchial smooth muscle (Dunnill *et al.* 1969; Dunnill 1971).

It was only until the use of fiberoptic bronchoscopy was deemed to be safe in asthma research in the late 1980s (Rankin *et al.* 1984; National Institute of Health 1985; Laursen *et al.* 1988; Beasley *et al.* 1989) that the progression of the pathology of asthma could be studied in vivo. Fiberoptic bronchoscopy is now an established and commonly used tool in the field of respiratory disease research. It allows the collection of bronchial biopsies, epithelial cells from brushings and bronchoalveolar lavage fluid (BALF) containing luminal secretions.

Immunohistochemical analysis of biopsies from asthmatic compared with normal subjects gave rise to detailed description of the asthmatic airway histology, showing submucosal infiltration with inflammatory cells (**inflammation**) such as, mast cells, eosinophils and T-lymphocytes and also structural airway wall changes (**remodelling**) such as damaged epithelium, thickened basement membrane, glandular hypertrophy and increased vessel formation and smooth muscle mass (Figures 1.2B & 1.3).

1.3.2 Immunological features (Inflammation)

The immunological differences associated with asthmatic airways compared to normal airways have been studied extensively. Normal airways contain typically very few immunological features, such as resident macrophages and a few leukocytes that are part of the first response mechanisms to foreign antigens. However, in contrast, asthmatic airways have an infiltration of a great number of leukocytes such as activated neutrophils, basophils, eosinophils, mast cells, macrophages and T cells (Jeffery *et al.* 1989; Foresi *et al.* 1990; Howarth *et al.* 1991; Sampson 2000; The ENFUMOSA Study Group 2003). These cells together with structural cells release inflammatory mediators (Pease and Williams 2006; Nakajima and Takatsu 2007) that contribute to the inflammation and symptoms even in the absence of infection.

The majority of asthma in adults and even more in children occurs in association with atopy, the predisposition to generate IgE to common environmental allergens through a Th2 cell-dependent mechanism.

Allergic immune response

Allergic disease is an aberrant immune response to harmless environmental antigens (allergens) resulting in induction of T helper (Th) 2 cells and specific IgE responses. Dendritic cells within the bronchial epithelium play an important role in allergic asthma (Van Rijt and Lambrecht 2005; Steinman and Banchereau 2007). One of their functions is to capture inhaled allergens, process them and present a modified peptide via the major histocompatibility complex class II (MCH II) to naive $CD4^+$ T-cells. These develop via a Th0 to either Th2 cells that produce interleukin (IL)-4, IL-5, IL-9, IL-13 cytokines or Th1 cells that produce interferon (INF)-γ, IL-2, TNF-α. This cytokine production is crucial in inducing and maintaining a tolerant or inflammatory context following allergen recognition. It was hypothesised that a non-allergic phenotype results due to immunologic ignorance (failure to recognise the allergen) or due to the expression of a 'protective' Th1 cytokine profile. However, recently it has been suggested that an active regulatory mechanism is important in maintaining tolerance to allergens in healthy individuals. Natural and/or adaptive T regulatory (Treg) cells (Tr1 and Th3) that produce IL-10 and/or TGF-β are responsible for this regulatory mechanisms and an impaired expansion of Treg cells leads to the development of allergy and asthma with a predominant Th2 cell response. (Larche 2007; Umetsu and DeKruyff 2006; Rouse 2007).

In asthma, recruitment and activation of mast cells, basophils and eosinophils into the airways following exposure to allergen or respiratory viruses is orchestrated by Th2 lymphocytes that exhibit evidence of increased activation and cytokine production. IL-4 and

IL-13, act as IgE heavy chain isotype switch factors on B-cells leading to the production of IgE. IL-4, IL-5 and IL-9 enhance the survival of eosinophils and their progenitors. IL-9 acts as a growth factor for mast cells and IL-13 has been associated with goblet cell hyperplasia, mucus hypersecretion and BHR. Thymus and activation-regulated chemokine (TARC) and monocyte-derived chemokine (MDC) from Th2 cells recruit more Th2 cells to the sites of allergic inflammation (Larche 2007; Umetsu and DeKruyff 2006). Only recently it has been shown that thymic stromal lymphopoietin (TSLP; IL-7) is highly expressed in asthmatic epithelial cells and might play a central role in the allergic immune response. Allergen or virus induced epithelial (as well as fibroblast or mast cell) damage leads to the release of TSLP. TSLP activates dendritic cells which release large quantities of Th2 cell chemokines TARC and MDC, eosinophil chemokine eotaxin and IL-8, a chemokine for neutrophils. It also co-stimulates mast cells to produce IL-5, IL-13, GM-CSF and IL-6. This initiates the innate phase of the allergic immune response. TSLP also up-regulates the co-stimulatory molecule, Ox40L on mature dendritic cells that migrate to the draining lymph node and initiates the adaptive phase of allergic immune response via Th2 polarisation (Holgate 2007; Larche 2007; Seshasayee *et al.* 2007; Wang and Liu 2007) (Figure 1.1).

Studies of allergic reactions have focused on the ability of allergen to cross-link IgE receptors on mast cells or basophils and the subsequent release of mediators such as histamine. This reaction develops in minutes, persists for several hours, and is associated with mast cell degranulation resulting in the release of mediators including histamine, prostaglandin D2 (PGD2), leukotrienes C4 (LTC4), and tryptase. This causes bronchoconstriction and airway narrowing by mechanisms that include smooth muscle constriction and oedema (Larche 2007). Following allergen exposure and an acute response, the late phase reaction begins after 3–12 hours, lasts for many hours and is associated with an infiltration of activated $CD4^+$ Th2 cells and eosinophils. The release of Th2 cytokines, in particular IL-5 lead to recruitment of bone morrow derived eosinophils and their progenitors. The release of eotaxin by structural cells at the site of allergen exposure and an increase in vascular permeability, and the expression of a range of adhesion molecules by the endothelium (including E-selectin, VCAM-1, and ICAM-1) in the lung are likely to be involved in the recruitment of inflammatory cells, such as eosinophils into the airways. Eosinophils are the key effector cells in the late-phase allergic response in the airways, causing epithelial damage through release of toxic granule proteins, bronchoconstriction through leukotrienes and BHR (Haitchi *et al.* 2005a) (Larche 2007) (Figure 1.1)

Airway inflammation

While there is overwhelming evidence to indicate that airway inflammation underlies the pathophysiology of asthma, its relationship to disease severity is less clear. The recruitment

of eosinophils and T cells from the microvasculature is an important contributor to the inflammatory airway response in severe and chronic disease. However, increased mast cell, eosinophil, and T-cell survival through cytokine-mediated inhibition of apoptosis is likely to be just as important as granulocyte recruitment in maintaining eosinophilic inflammation of the airway mucosa. The presence of eosinophils in the sputum, a persistent blood eosinophilia, and increased circulating levels of eosinophil granule proteins along with other surrogate markers such as increased circulating soluble receptors broadly relate to disease severity (Busse and Rosenwasser 2003; Busse and Lemanske 2001). Furthermore, severe asthma shows less atopy and a predominantly neutrophilic inflammation, suggesting that it might even be a different form of asthma, that poorly responses to anti-inflammatory treatment (The ENFUMOSA Study Group 2003; Holgate and Polosa 2006).

However, there are large intraindividual and interindividual variations that have yet to be explained. Similarly, although the numbers of activated eosinophils and T cells in bronchial mucosal biopsies have been linked to clinical disease severity and BHR, there is sufficient variation to question a single cause and effect relationship. Inflammation plays an important role in airway dysfunction of asthma. However, tissue specific events (Davies *et al.* 2003) and the airway compartments might be important in disease expression (Brightling *et al.* 2002). Locally-expressed tissue susceptibility genes might create a microenvironment that sustains the chronic immune and inflammatory responses in the airways.

This hypothesis is supported by the discovery of asthma susceptibility genes that are not expressed in inflammatory cells but in the epithelia cells, such as ESE-3, SPINK5, GPRA that are expressed in epithelial cells (Silverman *et al.* 2002; Kabesch *et al.* 2004; Laitinen *et al.* 2004; Vendelin *et al.* 2005) or the mesenchymal compartment of the airways such as ADAM33 (Van Eerdewegh *et al.* 2002). It is important to remember that human asthma is a complex disease involving multiple gene-gene and gene-environment interactions.

Recently three possible models of the interaction of changes of the airway wall structure and airway inflammation have been discussed (Saglani and Bush 2007). The conventional model where chronic and recurrent inflammation leads to structural airway wall changes resulting in secondary remodelling is a common perception (Elias *et al.* 2003) but its correctness has to be questioned. The alternative model postulates that an underlying ‘asthma factor’ (‘X-factor’) drives both processes of airway inflammation and remodelling in parallel. The view of the EMTU model was described as a primary event of injury and repair in an abnormal epithelial and/or mesenchymal airway tissue causes secondary inflammation. (Saglani and Bush 2007; Bush 2008). However, an alternative view of the EMTU model is that interactions between environmental factors and susceptibility genes (Sengler *et al.* 2002) might cause a change in the airway micro environment in the EMTU. Environment and genetic predisposition can be seen as the ‘asthma factors’. Atopy/inflammation genes and

structural cell asthma susceptibility genes interact with the environment and drive stress-injury and repair in the EMTU in parallel to airway inflammation. Predominance of either structural cell or atopy/inflammation asthma susceptibility genes might determine the origin of disease in early life before airway inflammation and symptoms occur resulting in either intrinsic asthma (without atopy) or allergic asthma (Davies *et al.* 2003).

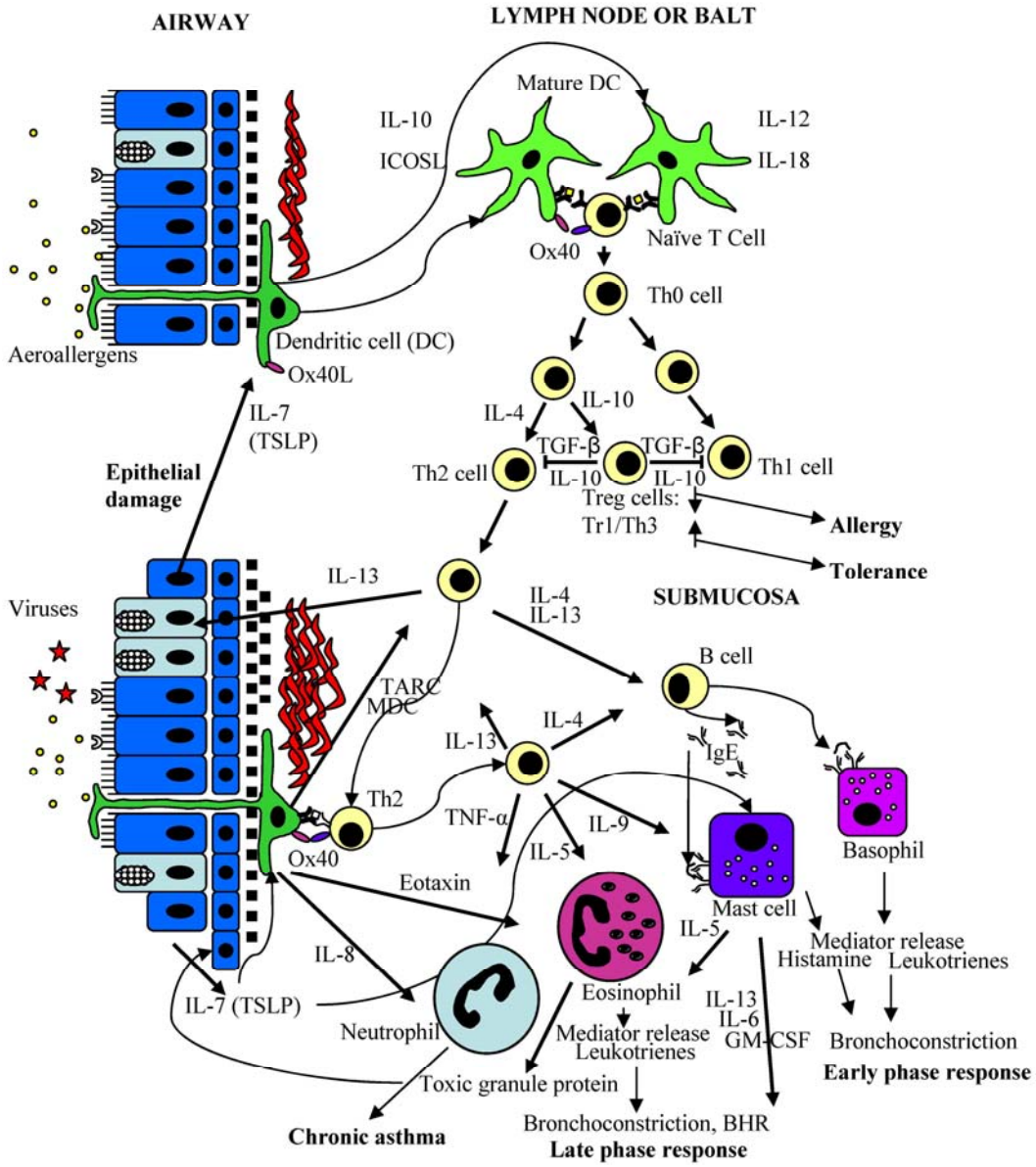

Figure 1.1 Network of cellular interactions in allergic airway inflammation.

(adapted from Haitchi et al, Mucosal Immunology, Chapter 82: Asthma: Clinical Aspects and Mucosal Immunology, Elsevier Academic Press 2005)

1.3.3 Structural features

In addition to the airway inflammation seen in asthma structural changes or remodelling of the architecture of the airways take place. Modelling and remodelling in the EMTU occurs during normal lung development and growth (Minoo and King 1994) or in response to injury, which is inappropriate when it occurs chronically resulting in abnormal tissue structure or function in asthma (Bai and Knight 2005)

Typical pathological findings in bronchial walls from asthmatic patients are epithelial damage, goblet cell hyperplasia, increased wall thickness and in particular a thickened reticular basement membrane, enlargement of the bronchial smooth muscle mass, submucosal gland hypertrophy, and angiogenesis (Jeffery 2004) (Tang *et al.* 2006; Fixman *et al.* 2007) (Figure 1.2 & 1.3).

Epithelium dysfunction

The bronchial epithelium has a considerable barrier function for the majority of inhaled allergens and toxins that are deposited on the surface of the airways. However, its immunomodulatory function by expression of cytokines, growth factors, adhesion molecules and mediators seems to be of equal importance in the remodelling and inflammatory mucosal processes in asthma. The bronchial epithelium seems to be in a key position to translate gene-environmental interactions to the underlying mesenchymal cells. In asthma it is either disrupted or damaged resulting in shedding of the columnar cells into the airway lumen. Inflammation is a natural response to tissue injury and therefore an abnormal injury and repair response might lead to airway inflammation and remodelling in asthma (Davies 2001) (Holgate 2007). Several mechanisms have been implicated resulting in a damaged epithelium with impaired barrier function due to disrupted tight junctions or defective antioxidant pathways (Holgate 2007).

An abnormal epithelium in asthma is also the source for a wide range of cytokines, chemokines and growth factors that cause changes in the basement membrane, the mucus producing goblet cells and submucosal glands resulting in inflammation and remodelling (Holgate 2007). The thickened basement membrane seen in adult and children with asthma (Bourdin *et al.* 2007; Payne *et al.* 2003) might be due to the increased number of activated sub-epithelial myofibrolasts that produce new matrix and collagens I, III, IV (Roche *et al.* 1989). Goblet cell hyperplasia induced by IL-9 (Vermeer *et al.* 2003) and IL-13 (Atherton *et al.* 2003) is more predominant than submucosal gland hypertrophy in asthma (Rose and Voynow 2006). Only recently it has been shown that a defect in INF-β and -λ production in asthmatic epithelial cells results in impaired Rhinovirus clearance and increased cytotoxic

cell death that might be responsible for increased susceptibility of asthmatic airways to common cold virus infections (Wark *et al.* 2005; Contoli *et al.* 2006)

Fibroblast/Myofibroblast

The locally resident attenuated fibroblast sheath below the airway basement membrane (Evans *et al.* 1999) and/or circulating fibrocytes (Schmidt *et al.* 2003) are the most common source for myofibroblasts or airway smooth muscle cells. Myofibroblast differentiation requires at least three local events such as accumulation of biologically active TGF-β, presence of extracellular matrix (ECM) protein such as fibronectin and an extracellular mechanical stress (Hinz *et al.* 2007). The proliferation and activation of subepithelial fibroblasts to become myofibroblasts is a consequence of epithelial damage (Evans *et al.* 1999; Holgate 2007). Both IL-4 and IL-13 activate bronchial epithelial cells and induce the release of TGF-β2, a profibrotic cytokine, that transforms bronchial fibroblast into myofibroblasts (Richter *et al.* 2001). Myofibroblasts produce cytokines, such as GM-CSF, SCF, and IL-8, which may be important in maintaining the inflammatory response. These cells are also believed to be responsible for the deposition of a number of extracellular matrix proteins such as collagen types I, III and V and fibronectin below the basement membrane (Roche *et al.* 1989; Holgate 2000).

Airway smooth muscle

Contraction of airway smooth muscle (ASM) is of critical importance in producing BHR and typically reversible airway obstruction, both during the early phase and, to a lesser extent, during the late phase response. Bronchial smooth muscle is under autonomic nervous control providing an opportunity for intervention by bronchodilator drugs such as β-agonists and anti-cholinergics. Airway smooth muscle mechanical function and proliferation is influenced by contractile mediators (histamine, leukotrienes, adenosine, endothelin), cytokines (IL-1β, TNF-α) and growth factors (PDGF, FGF-2, EGF, IGF) resulting in an increased ASM mass in chronic persistent asthma (Hirst *et al.* 2000) leading to persistent structural changes. Both, hyperplasia (increase in number of airway smooth muscle cells) and/or hypertrophy (increase in size of airway smooth muscle cells) have been recognised in asthma (Shore 2004; Lazaar and Panettieri, Jr. 2005).

TNF-α and IL-8 upregulate the expression of substance P and muscarinic M3 receptors on airway smooth muscle, possibly contributing to the pathogenesis of BHR. Several other mediators, including autacoid mediators (histamine, PGD_2, leukotriene (LT) C_4, proteases (tryptase, chymase) and cytokines (IL-4, IL-5, IL13) from mast cells, can induce airway smooth muscle responsiveness and airway wall remodelling. Mast cells can also be found within the ASM bundles in patients with asthma but not in patients with eosinophilic

bronchitis or normal subjects (Brightling *et al.* 2002) with a significant correlation between ASM mast cell number and BHR within the asthmatic group (Bradding 2007). However, it has been recently recognized that ASM may also serve synthetic and immunomodulatory functions in the form of active secretion of pro-inflammatory cytokines, chemokines and mediators as well as growth factors (IL-1, IL-5, IL-6, IL-8, IL-11, GM-CSF, MCP-1,-2,-3, eotaxin, RANTES, VEGF, PGDF, IGF, stem cell factor) and expression of cell adhesion molecules (ICAM-1, VCAM-1, CD44, integrins) and pattern recognition receptors (TLR-2, -3, -4) (Amrani and Panettieri 2003; Tliba *et al.* 2008), which lead to interactions with inflammatory cells like T-cells, eosinophils, neutrophils, monocytes and mast cells that accumulate around the ASM (Brightling *et al.* 2002). Therefore, ASM is not just increased in mass but has an modulatory function in asthma by promoting inflammation, subepithelial fibrosis and bronchial neovascularisation resulting in airway remodelling (Lazaar and Panettieri, Jr. 2005).

Recently, there seems to be increasing evidence that there is a difference in ASM phenotype between asthmatic and normal subjects. ASM cells from asthmatic patients secreted more TGF-β, induced connective tissue-derived growth factor (CTGF) (Burgess *et al.* 2003), produced more CXCL10, a chemokine for mast cells (Brightling *et al.* 2005), and proliferated faster (Johnson *et al.* 2001). The anti-proliferative effect of glucocorticosteroids is impaired in asthmatic compared to normal ASM cells due to lack of transcription factor CCAAT/enhancer binding protein a (C/EBPa) (Roth *et al.* 2004). These findings suggest an intrinsic abnormality in ASM cells in asthma. However, it still needs to be determined if these in vitro cultured cells were myofibroblasts or smooth muscle cells and what implications this has on the smooth muscle of asthmatic patients (Borger *et al.* 2006; Wenzel and Balzar 2006). Nevertheless, the interaction of dysfunctional epithelial, mesenchymal and inflammatory cells might add to the perpetuation and intensity of airway wall inflammation and remodelling (Davies *et al.* 2003) through chemotactic, autocrine or paracrine effects (McKay and Sharma 2002).

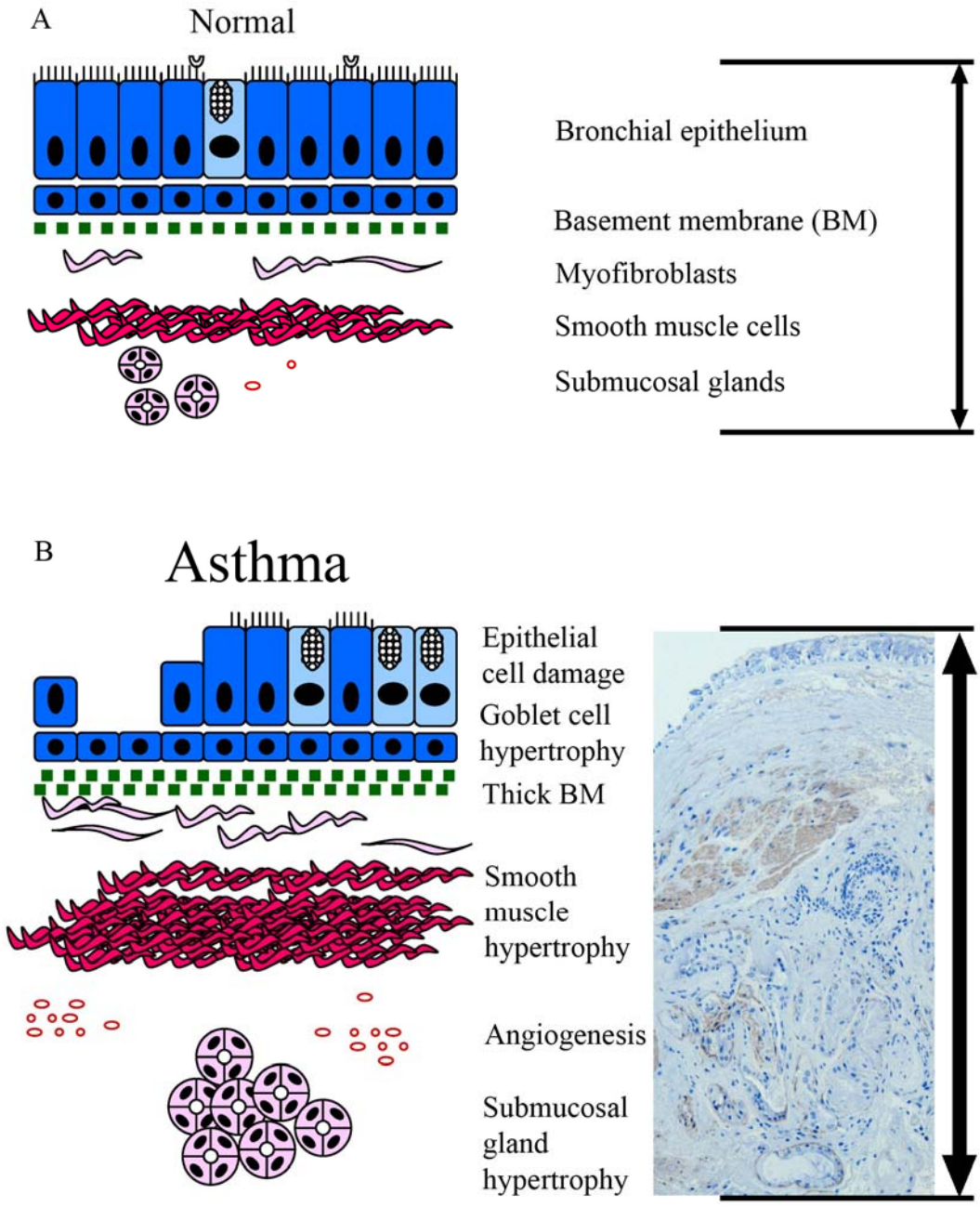

Figure 1.2 Diagram of bronchial wall in normal and asthmatic airways.

A Diagram of normal airway wall. B Pathological changes in asthmatic airway wall resulting in increase wall thickness; immunohistochemistry for αSMA of a mild asthmatic bronchial biopsy (unpublished data).

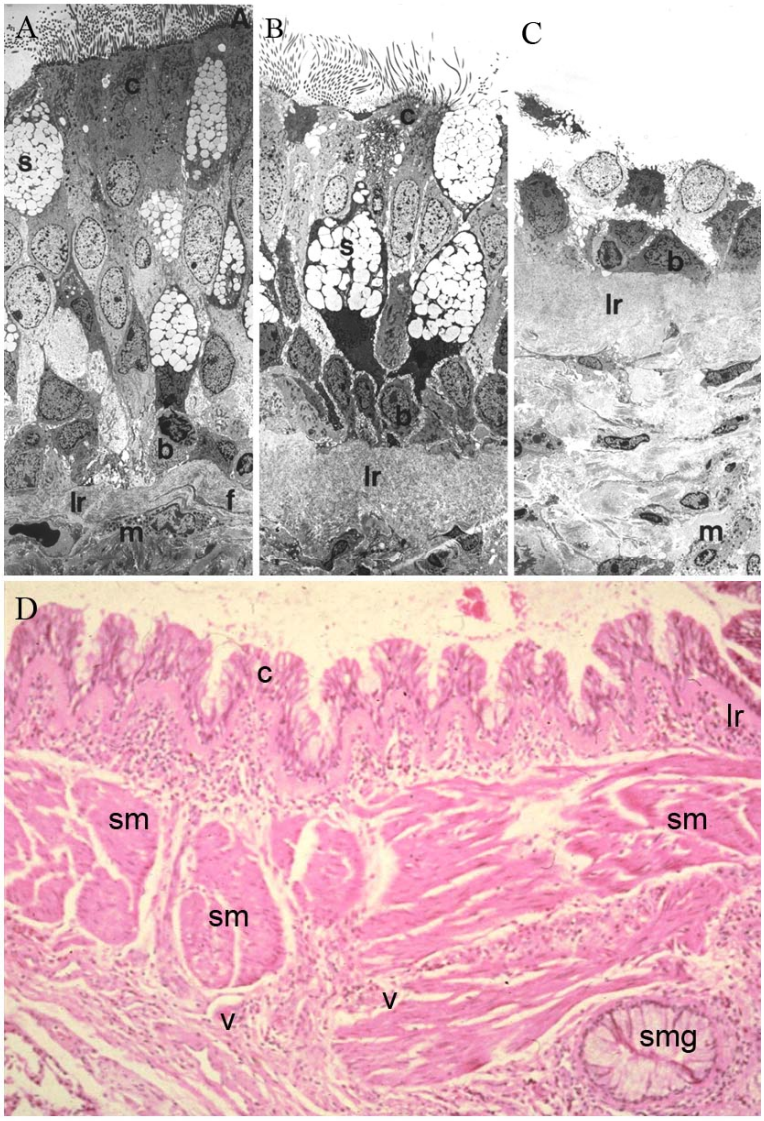

Figure 1.3 Electron and light microscopy of bronchial biopsy.

A: Electron microscopy of normal bronchial epithelium. B&C: Asthmatic epithelium with basal cells (b), columnar epithelial cells (c), (myo)fibroblasts (f), lamina reticularis (lr), mast cell (m) and secretory goblet cells (s). Magnification x1600. D Haematoxylin-eosin stain of bronchial biopsy of severe asthmatic patient showing the enlarged smooth muscle (sm) with columnar epithelial cell (c) damage and increase of goblet cells and a submucosal gland (smg) and vessels (v). (adapted from Holgate et al, 2000)

1.3.4 Bronchial hyperresponsiveness

Bronchial hyperresponsiveness (BHR), the exaggerated narrowing of the airways after inhalation of various stimuli, is a fundamental feature of asthma (Cockcroft and Davis 2006). Explanations for BHR include mucosal swelling (James *et al.* 1989) excessive airway smooth muscle (ASM) shortening (Wiggs *et al.* 1990; Gil and Lauzon 2007), an increase in ASM mass causing greater force generation (Seow *et al.* 1998) and an excessive velocity of contraction linked to altered cross-bridge cycling (Fredberg 1998; Gil and Lauzon 2007) and biophysical muscle cell adaption (An and Fredberg 2007; An *et al.* 2007). Morphometric studies have shown a graded increase in smooth muscle mass in proportion to disease severity suggesting that ASM hyperplasia and hypertrophy are important abnormalities that contribute to BHR (Lambert *et al.* 1993; An *et al.* 2007). The ASM is an important tissue (Amrani and Panettieri 2003) being part of the epithelial-mesenchymal trophic unit (EMTU) (Holgate *et al.* 2000) and a rich source of pro-inflammatory cytokines, chemokines and growth factors (McKay and Sharma 2002). As described above these are involved in bi-directional cross-talk with T-lymphocytes (Hakonarson *et al.* 2001) (Black and Johnson 2002) and mast cells (Page *et al.* 2001) (Brightling *et al.* 2002) that supports the central role of ASM not only in airway inflammation and remodelling (Black *et al.* 2001) but also BHR (An *et al.* 2007). The central role of ASM in BHR is supported by the fact that anti-inflammatory therapy can control the inflammation, however, BHR can persists in asthmatics, even in the absence of airway inflammation.

Therefore, asthma seems to be more than an inflammatory disease and the existence of tissue-specific processes in the EMTU might occur either first or in parallel rather than sequentially to the inflammatory events (Holgate 2002; Davies *et al.* 2003).

Evidence is available that bronchial hyperresponsiveness is genetically determined in the mouse and that human and several genes might be involved in its clinical expression (De Sanctis *et al.* 2001) (Postma *et al.* 2000; Holgate *et al.* 2007). It is likely that factors related to the environment or to lifestyle have exposed, and interacted with, pre-existing genetic susceptibilities (Sengler *et al.* 2002) (Holgate 1999) (Holgate *et al.* 2007).

1.4 Treatment

Relatively cheap and safe therapies are effective in controlling most asthmatic patients and there are good guidelines for the treatment of asthma (Global Initiative for Asthma 2007; British Thoracic Society (BTS) and Scottish Intercollegiate Guidelines Network (SIGN) 2007; Expert Panel Report 3 2007). Nevertheless, there is still a need to reduce their side effects and find new therapeutic approaches especially on the severe side of asthma (Holgate and Polosa 2006).

Currently available asthma treatment can be classified into controller and reliever medications. Rapid acting β_2-agonists are the medication of choice for relieving acute bronchoconstriction or as pre-treatment of exercise induced asthma, in both adults and children of all ages. Inhaled glucocorticosteroids (ICS) are the most effective medications currently available that are used on a long-term basis to keep asthma under clinical control through their anti-inflammatory action. These may be used in combination with long-acting β_2-agonists when control of asthma is not achieved on medium dose of ICSs. Leukotriene modifiers may be used as alternative treatment in mild persistent asthma and aspirin-sensitive asthma. Theophylline might be used as an add-on therapy to ICSs. Sodium chromoglycate and nedocromils have a limited role in the long-term treatment of adult asthma; however, they are frequently used in paediatric asthma. Only recently, anti-IgE (omalizumab) has become available as a new add-on asthma therapy in patients with severe allergic asthma. Oral or systemic glucocorticosteroids may be required for asthma exacerbations or severely uncontrolled asthma. In selected patients and under appropriate supervision, methotrexate, cyclosporin and gold have been used mainly as corticosteroid sparing medications and have been shown to be effective in some patients. Allergen and modified allergen-specific immunotherapy (Larche *et al.* 2006) is the only therapy so far available that has disease modifying properties and seems to be safe and effective in allergic asthma.

ICSs are also the most effective controller therapy in children of all ages; however, their systemic side effects have to be taken in consideration. Other controller medications for children include leukotriene modifiers, long-acting inhaled and oral β_2-agonists, theophylline, and chromones (Global Initiative for Asthma 2007). Very few new treatments have been added to the currently predominantly anti-inflammatory medications. Anti-TNF-α seems to be a promising new potential treatment for severe asthma (Howarth *et al.* 2005) (Berry *et al.* 2006). Presently there are good controller and reliever medications available and several new treatment strategies are currently in development but there is still a lack of treatment that would have an effect on the cause and progression of asthma. Bronchial thermoplasty (BT) is a new bronchoscopic procedure to reduce mass of airway smooth

muscle using radiofrequency ablation. Although BT was safe and resulted in an improvement in asthma control in moderate and severe asthmatic subjects one year after treatment only one study showed also significant improvement of FEV1 (Pavord *et al.* 2007). However, the treatment had no effect on bronchial hyperresponsiveness (Cox *et al.* 2007). Genetics that are associated with the origin of the disease and in particular 'pharmacogenetics' and 'pharmacogenomics' might be of help to find new disease modifying therapies (Haitchi and Holgate 2004).

1.5 Genetics of Asthma

Asthma is a complex disorder which has an inheritable component as it seems to run in families. The risk of a child developing asthma is 3 times increased in families with one asthmatic parent and 6 times in families with 2 asthmatic parents (Litonjua *et al.* 1998). Of interest is that several studies have demonstrated that maternal asthma is a greater risk factor than paternal asthma suggesting that genetic factors and *in utero* or postnatal exposures might be attributing factors (Hohlberg *et al.* 1998; Aberg 1993).
The involvement of multiple genes and in particular the gene-gene and gene-environment interactions add to the complexity of the disease. Although asthma is multigenetic, evidence seems to suggest that a few genes with moderate effect rather than many genes with small effects might be responsible for the development of asthma (Holloway *et al.* 2003).
To date, over 100 genes have been reported to show association with asthma or related phenotypes (Zhang *et al.* 2008) highlighting the complexity of the disease. Many of these susceptibility genes and their gene products are involved in the immune response and atopy that are intrinsically associated with asthma. However, some of the genes are mainly expressed in the structural cells of the airways and appear to modulate normal airway function. Many of the association studies have been replicated in different populations; however, differences are often found between different association studies. These could be explained by differences in ethnic groups, environmental influences and differences in definition of asthma phenotypes studied.

Two main efforts have been used to study the genetic variations that are associated with asthma or its partial phenotypes: candidate gene and positional cloning approach. The candidate gene approach looks at genetic variations in molecules that are known to play a role in the pathophysiology. The positional cloning approach uses linkage and association studies to identify chromosomal regions of interest and then pinpoint genes that might be responsible for the signal (Holloway *et al.* 2003).

Candidate genes

A great number of candidate gene association studies have revealed the involvement of different pathways. The ‘pro-allergic’ immunological pathways include human lymphocyte antigen (HLA), T-cell receptor (TCR), cytotoxic T-lymphocyte-associated antigen (CTLA)-4, Th2 cytokines and their receptors. Molecules that are potentially involved in protective ‘anti-allergic’ pathways are CD14, toll-like receptor (TLR)-4 and -9. Other candidate genes might have association with airway function and disease severity such as β2-adrenoreceptor, transforming growth factor (TGF)-β, leukotriene (LT) C4 synthetase, glutathione-S-

transferase (GST P1), tumour necrosis factor (TNF)-α, TNF-β and neuronal nitric oxide synthetase (NOS). Genes that have effects on both inflammatory and structural cells include IL-4, IL-9, IL-13 and their receptors, signal transducer and activator of transcription (STAT)-6, suppressor of cytokine signalling (SOCS)-1, SOCS box and TLRs (Holgate *et al.* 2007).

Disease linkage analysis and positional cloning genes

Several genome wide screens have been published that showed linkage with asthma or its phenotypes in regions of 23 chromosomes and several putative novel susceptibility genes have been identified by positional cloning. Regions on chromosome 11p3encoding epithelium specific transcription factors ETS-2 and ETS-3 showed strong association with BHR and asthma (Zamel *et al.* 1996; Tugores *et al.* 2001). On chromosome 5q31-34 was another region of interest for asthma. This region encodes IL-4 gene cluster, β2-adrenoreceptor and the corticosteroid receptor but also contains a gene encoding a serine protease inhibitor Kazal type 5 (SPINK 5). Polymorphisms in this gene are strongly associated with defective epithelial function and asthma and eczema (Walley *et al.* 2001; Kabesch *et al.* 2004). Protocadherin-1 gene (PDDH-1) in chromosome 5q31 is associated with BHR and is expressed in bronchial epithelium (Whittaker 2003). Strong linkage was also shown on chromosome 2q14 which resulted in the identification of dipeptidyl peptidase (DPP)-4 (CD26) that is also expressed in epithelial cells (Allen *et al.* 2003). G-protein-coupled receptor (GPRA) on chromosome 7p has two isoforms (A, B) which showed differential protein distribution in bronchial biopsies. A-isoform was located in epithelial cells of healthy subjects and B-isoform in smooth muscle of asthmatic patients (Laitinen *et al.* 2004). Mucin 8 (MUC8) on chromosome 12q23-ter is yet another gene expressed in the bronchial epithelium (Keith *et al.* 2004). The prostaglandin (PG) D2 receptor (PTGDR) on chromosome 14q22.1 is expressed on smooth muscle, blood vessel and mast cells and human lymphocyte antigen (HLA)-G on chromosome 6p21 is expressed by bronchial epithelial cells (Oguma *et al.* 2004). Another candidate gene for asthma and BHR is a disintegrin and metalloprotease (ADAM)-33 on chromosome 20p13 which is strongly expressed in airway mesenchymal cells, such as fibroblasts, myo-fibroblasts and smooth muscle (Van Eerdewegh *et al.* 2002; Holgate *et al.* 2007).

The number of asthma susceptibility genes discovered by genetic studies is still increasing; however, the functional consequences of these genes and their polymorphisms on asthma need to be further studied.

ADAM33 was the first asthma susceptibility gene discovered by positional cloning by a team from the Infection, Inflammation and Repair (IRR) Division of the University of Southampton in collaboration with 2 US groups in 2002 (Van Eerdewegh *et al.* 2002). This

novel gene is strongly associated with asthma and BHR and is not expressed in inflammatory cells or epithelial cells but in mesenchymal cells suggesting an important role in airway remodelling. The lack of knowledge about expression and function of ADAM33 made it an exciting new target to study in asthma and early origin of asthma during lung development. Therefore, the focus has been placed on ADAM33 for the purpose of this thesis.

1.6 ADAM33

1.6.1 Genetics of ADAM33

The *ADAM33* gene was mapped to human chromosome 20p13 and the mouse ortholog of ADAM33 was mapped to the mouse chromosome 2 (73.9cM) (Yoshinaka *et al.* 2002; Gunn *et al.* 2002) close to the trait locus for bronchial hyperresponsiveness (bhr1) to a region on mouse chromosome 2 (74cM) (De Sanctis *et al.* 1995). They share a 70% similarity in their amino acid sequence. Human ADAM33 is most closely related to human ADAM12, ADAM15, ADAM19 and *Xenopus* ADAM13. ADAM33 is a tissue specific candidate gene whose polymorphic variation contributes to the population attributable risk for asthma (Van Eerdewegh *et al.* 2002). Its discovery has been acknowledged as a major breakthrough in providing a molecular mechanism(s) for BHR, a fundamental feature of asthma (Drazen and Weiss 2002; Shapiro and Owen 2002; Ahmadi and Goldstein 2002; Tattersfield *et al.* 2002; Lemanske and Busse 2003).

Multiple genomic regions are linked to asthma, and a genome-wide scan on 460 Caucasian families identified polymorphic variation in *ADAM33,* located at the short arm of chromosome 20, as a genetic determinant for the development of asthma and BHR (Van Eerdewegh *et al.* 2002). 460 Caucasian affected sib-pair (children having the same biological parents) families from the UK and US were scanned. They were phenotyped by physician's diagnosis of asthma on active asthma medication and further analysed for BHR, elevated serum total IgE or positive specific IgE. The asthma plus BHR reduced the sample size to 218 nuclear families, but contributed most strongly to the linkage signal on chromosome 20p13. Association studies using a case control study design, in which 135 nucleotide polymorphisms (SNPs) were analysed in 23 genes, revealed that the *ADAM33* region showed the most significant association signal in the linkage region. Multiple SNPs were analysed of which six were significant in the combined UK/US population (Q-1, S1, ST+4, ST+7, V-1), seven in the UK (F+1, Q-1, S1, S2, ST+4, V-1) and six in the US population (I1, L-1, M+1, T1, T2, T+1) (Table 1.1). When haplotype pairs were constructed and their frequencies compared between cases and control an even higher significance than individual SNPs could be found (Table 1.1). To date about 100 polymorphisms have been identified in *ADAM33*. Significant SNPs are located in non-coding regions (introns and 3' untranslated region (3'UTR)) which may affect alternative splicing, splicing efficiency or the turnover of mRNA. In the UK population significant SNPs and two haplotypes were located in the 3'region of the gene. This included an amino acid substitution in the transmembrane domain and an amino acid change in the cytoplasmic tail plus a SNP in the 3'UTR (Figure 1.4). In the US population SNPs were found in the catalytic domain and 2 amino acid changes in the

cytoplasmic domain which could have an influence on signalling (Van Eerdewegh *et al.* 2002).

The association of ADAM33 with asthma has been replicated in several other populations, such as African American, US Caucasian, US Hispanic, Dutch, German, Korean, Japanese, Australian and South Han Chinese (Howard *et al.* 2003; Werner *et al.* 2004; Lee *et al.* 2004; Sakgami *et al.* 2003; Noguchi *et al.* 2006; Kedda *et al.* 2006; Hirota *et al.* 2006; Sakagami *et al.* 2007; Qiu *et al.* 2007a). However, a few studies in a Puerto Rican and Mexican, Chinese, British, Icelandic, US European and Hispanic population failed to replicate the association (Lind *et al.* 2003; Wang *et al.* 2006; Blakey *et al.* 2005; Hersh *et al.* 2007) and two studies in a US Caucasian and German population found only weak associations (Raby *et al.* 2004) (Schedel *et al.* 2006), which is a common occurrence in diseases with complex genetic trails (Ioannidis *et al.* 2001; Raby and Weiss 2004). This may be due to insufficient statistical power, genotypic and phenotypic heterogeneity across study groups, as well as environmental interactions (Ioannidis *et al.* 2001; Ioannidis *et al.* 2003). However, a large meta-analysis of replication studies included 8 populations and several populations which, when analysed on its own, failed to show significance but when analysed together resulted in strong association. Data from these eight separate populations showed SNPs F+1 and ST+7 were significantly associated with asthma and these variants would potentially account for about 50 000 excess asthma cases in UK population (Blakey *et al.* 2005; Holgate and Holloway 2005). (Table 1.2)

Of further support for the importance of ADAM33 in the development and progression of asthma are the findings that when eight SNPs in *ADAM33* were analysed in a Dutch cohort of 200 asthma patients followed over 20 years that the S-2 polymorphism was significantly associated with a more rapid decline in FEV1 (Jongepier *et al.* 2004). Furthermore, when a Dutch general population cohort was followed for 25 years with regular lung function measurements an association with SNPs S1, S2 and Q-1 with decline in lung function was demonstrated. A subgroup of this cohort that was diagnosed with chronic obstructive pulmonary disease (COPD) showed association of SNPs F+1, S1 and S2 with lung function decline (van Diemen *et al.* 2005a). A recent study linked several SNPs (ST+5, T1, T2, S2) to the pathophysiology of COPD, confirming its additional role as a susceptibility gene for COPD (Gosman et al. 2007). Another important work studying children from the National Asthma Campaign Manchester Asthma and Allergy Study (NACMAAS) cohort has also shown that SNPs in ADAM33 predict a low lung function in children aged 3 (F+1 SNP) and 5 years (F+1, S1, ST+5, V4 SNPs) (Simpson *et al.* 2005b) suggesting that the influences of ADAM33 commence early in life. (Table 1.2)

To date no functional variation is known, however, a recent study, mining public data, showed a peak of recombinatory rate at ADAM33 exons S to V (Wjst 2007). With S2 being

the most frequently associated variant, in exon 19 that codes for the ADAM33 transmembrane domain, suggests a potential role in protein-protein interaction in the cell membrane. Furthermore, it has also only recently been shown that a disease-associated genetic variant, BC+1 might have a promoter repressive effect, suggesting that in the BC intron exists a regulatory element that might be involved in the pre-mRNA processing and modulation ADAM33 gene expression (Del Mastro *et al.* 2007).

Although this might be the first SNP with a function ascribed to it, all associated SNPs need to be further elucidated in biological functional studies to shed more light on the function of ADAM33 and to dissect its genetic associations with asthma (Blakey *et al.* 2005; Van Eerdewegh *et al.* 2002) and chronic obstructive pulmonary disease (Gosman *et al.* 2007; van Diemen *et al.* 2005b).

Single SNPs significant at p<0.05				
Allele frequency				
SNP Name	Allele	Control	Case	P-value
Combined UK and US				
Q - 1	C	85.0%	91.2%	0.02
S1	G	89.5%	94.6%	0.02
ST + 4	A	51.5%	60.1%	0.03
ST + 7	G	78.1%	85.8%	0.02
V - 1	C	85.2%	92.4%	0.006
V4	C	76.7%	83.6%	0.03
UK				
F + 1	G	64.1%	74.2%	0.03
Q - 1	C	86.1%	92.3%	0.04
S1	G	89.4%	95.2%	0.03
S2	G	72.9%	84.0%	0.004
ST + 4	A	48.0%	59.2%	0.02
V - 1	C	86.4%	93.8%	0.01
V4	C	75.4%	83.7%	0.03
US				
I1	G	87.2%	70.4%	0.01
L - 1	A	8.0%	22.2%	0.01
M + 1	G	92.0%	77.8%	0.01
T1	C	7.8%	24.1%	0.003
T2	T	7.4%	20.4%	0.02
T + 1	C	92.0%	80.0%	0.03
SNP haplotypes (2-at-atime) significant at P<0.001				
	Combined		*UK*	
SNP-pair	P-value	SNP-pair	P-value	
ST + 4/V - 3	0.00004	S2/ST + 4	0.0003	
ST + 4/V - 2	0.00004	S + 1/ST + 4	0.0004	
V1/V4	0.0004	ST + 4/ST + 5	0.0005	
V2/V4	0.0004	ST + 4/V - 3	0.000003	
V4/V5	0.0003	ST + 4/V - 2	0.000005	

Table 1.1 Single nucleotide polymorphisms (SNPs) and haplotypes.

Single nucleotide polymorphisms (SNPs) and haplotypes in case-control study of *ADAM33* (adapted from Van Eerdewegh et al, Nature 2002 (Van Eerdewegh *et al.* 2002))

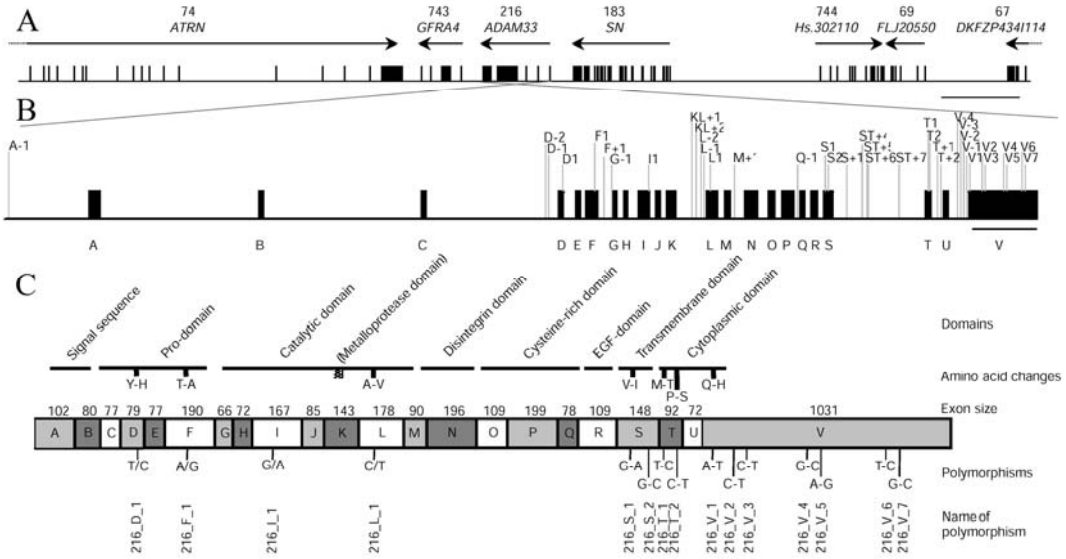

Figure 1.4 ADAM33 Gene, Exons and Domain structure.

ADAM33 chromosomal region on chromosome 20p13. A. Genomic structure of genes flanking *ADAM33*. B. The exon (A-V) intron structure of *ADAM33* and SNPs in *ADAM33* indicated above the gene. C. Domain organisation of the *ADAM33* gene and location of coding and 3'UTR SNPs and sizes of exons given in base pairs. (taken and adapted from Van Eerdewegh et al, Nature 2002 (Van Eerdewegh *et al.* 2002))

Population	Disease	SNPs	References
UK case-control	Asthma	F+1, Q–1, S1, S2, ST+4, V–1, V4	(Van Eerdewegh *et al.* 2002)
US case-control	Asthma	I1, L-1, M+1, T1, T2, T+1	(Van Eerdewegh *et al.* 2002)
Dutch case-control	Asthma	ST+7, V4	(Howard *et al.* 2003)
African American case-control	Asthma	S2	(Howard *et al.* 2003)
US Caucasian case-control	Asthma	ST+7, T1, T2	(Howard *et al.* 2003)
US Hispanic case-control	Asthma	S2, T2	(Howard *et al.* 2003)
Mexican-Puerto Rican case-control	Asthma	No association	(Lind *et al.* 2003)
German case-control	Asthma	ST+7	(Werner *et al.* 2004)
German asthma family study	Asthma	F+1, ST+4, ST+5	(Werner *et al.* 2004)
Dutch cohort	Asthma FEV1 decline	S2	(Jongepier *et al.* 2004)
Korean case-control	Asthma	T1	(Lee *et al.* 2004)
US Caucasian family study	Asthma childhood	Haplotype only	(Raby *et al.* 2004)
African American family study	Asthma childhood	No association	(Raby *et al.* 2004)
Hispanic	Asthma childhood	T1, T+1	(Raby *et al.* 2004)
Japanese case-control	Allergic rhinitis	F+1, L-1, S2, T1, T2, T+1	(Cheng *et al.* 2004)
Icelandic case-control	Asthma	No association	(Blakey *et al.* 2005)
UK family study	Asthma	No association	(Blakey *et al.* 2005)
US/UK, Mexican, Puerto Rican, Dutch, US, German, UK, Iceland meta-analysis	Asthma	F+1, ST+7	(Blakey *et al.* 2005)
UK children cohort age 3 years	Reduced lung function	F+1	(Simpson *et al.* 2005a)

UK children cohort age 5 years	Reduced lung function	F+1, S1, ST+5, V4	(Simpson *et al.* 2005a)
Dutch cohort whole population	Lung function decline	S1, S2, Q-1	(van Diemen *et al.* 2005b)
Dutch cohort COPD	Lung function decline	F+1, S1, S2	(van Diemen *et al.* 2005b)
Japanese family study	Asthma affected offspring	S+1, ST+4, T2	(Noguchi *et al.* 2006)
Australian Caucasian case-control	Asthma	Haplotype only (combination V-1, ST+7)	(Kedda *et al.* 2006)
German case-control	Asthma childhood	Haplotype only	(Schedel *et al.* 2006)
German cohort	Asthma childhood	No association	(Schedel *et al.* 2006)
Japanese case-control	Asthma	T1, T2, S2, V-3	(Hirota *et al.* 2006)
Chinese case-control	Asthma	No association (only 3 SNPs genotyped)	(Wang *et al.* 2006)
Japanese case-control	Asthma aspirin intolerant	ST+7, V-1, V5	(Sakagami *et al.* 2007)
South China Han case-control	Asthma	T1	(Qiu *et al.* 2007a) (Qiu *et al.* 2007b)
Dutch case study	COPD, BHR, Inflammation	ST+5, T1,T2, S2	(Gosman *et al.* 2007)
US-European family study	Asthma childhood	No association	(Hersh *et al.* 2007)
Hispanic	Asthma childhood	No association	(Hersh *et al.* 2007)
French family study	Psoriasis	ST+4, ST+5, V Haplotype	(Lesueur 2007)

Table 1.2 ADAM33 genetic association studies since 2002.

1.6.2 Expression of ADAM33

Localization of ADAM33

As described above human and mouse *ADAM33* genes on chromosome 20p13 and 2 respectively were identified and their product described as a novel ADAM protein with potential metalloprotease activity by Yoshinaka (Yoshinaka *et al.* 2002) and Gunn (Gunn *et al.* 2002) in 2002. Human *ADAM33* consists of 22 exons (Figure 1.4 & 1.5) and the protein shows a 70% homology with mouse ADAM33 and 44% with *Xenopus* ADAM13, 40 and 39% with human ADAM19 and 12 respectively (Yoshinaka *et al.* 2002). Using a human cDNA panel, ADAM33 could be detected in large variety of organs, except the liver, with high expression in placenta, lung, spleen and veins (Yoshinaka *et al.* 2002). Unlike other members of the ADAM family, ADAM33 showed almost exclusive expression in smooth muscle containing organs, such as urethra, bladder, vasculature, intestine, trachea, bronchus and no expression in kidney, liver, pancreas, bone marrow or spleen and cells derived from epithelial origin analysed by real-time quantitative PCR or Northern blotting (Umland *et al.* 2003). In situ hybridisation (ISH) showed selective expression in mesenchymal cells, such as reactive fibroblasts and smooth muscle in duodenal ulcer granulation tissue as well as bronchial subepithelial fibroblasts and smooth muscle but none in epithelial cells (Umland *et al.* 2003). Mouse ADAM33 is also widely expressed, most highly in adult brain, heart, kidney, lung and testis (Gunn *et al.* 2002).

In human lung, ADAM33 mRNA is expressed in fibroblasts, smooth muscle cells but not epithelial cells (Van Eerdewegh *et al.* 2002). As will be discussed in this thesis immunohistochemistry showed that ADAM33 protein is expressed in the smooth muscle cells and (myo)fibroblasts in bronchial biopsies from adult asthmatic and normal subjects (Haitchi *et al.* 2005b) which was subsequently confirmed by other studies(Lee *et al.* 2006; Ito *et al.* 2007; Foley *et al.* 2007) suggesting that ADAM33 might play a role in the control of contractility and tonus and/ or differentiation of the smooth muscle. Detection of increased expression of ADAM33 mRNA and protein in asthmatic smooth muscle and bronchial epithelial cells (Ito *et al.* 2007; Foley *et al.* 2007) has been reported, however, there are some controversies about these findings which will be elaborated on in chapter 3 of this thesis.

The expression of ADAM33 in bronchial mesenchymal cells strongly suggests that alterations in its activity underlie abnormalities in the function of airway fibroblasts and smooth muscle cells in the EMTU (Davies *et al.* 2003) leading to airway remodelling, and important component of asthma pathophysiology, that is linked to BHR in asthma. Consistent with genetic studies (Van Eerdewegh *et al.* 2002; Blakey *et al.* 2005), recent studies suggest that ADAM33 could play an important role in the pathogenesis of asthma,

since levels of a soluble form of ADAM33 containing the metalloprotease domain are higher in bronchial alveolar lavage (gain of function) from asthmatic compared with normal subjects (Lee *et al.* 2006). Using an antibody against the metalloprotease (catalytic) domain for Western blotting showed a strong 55 kDa band in bronchial alveolar lavage fluid (BALF) from asthmatic subjects compared with a weak band in control subjects. This was confirmed by integrated optical density analysis of dot blots comparing BALF from mild and moderate severe asthmatic subjects using the same antibody. ADAM33 levels in BALF were found to be related to disease severity and showed an inverse correlation with Forced Expiratory Volume in the first second (FEV1) % predicted). ADAM33 protein expression detected with an anti-catalytic antibody was also detected by immunohistochemical analysis of bronchial mucosal tissue from bronchoscopies and showed an increase expression in the smooth muscle layers and basement membrane with some positive staining of the epithelium only in subjects with asthma (Lee *et al.* 2006). Despite the controversy on the expression pattern of ADAM33 in bronchial biopsies, the increase of a soluble form of ADAM33 in BALF of asthmatic subjects and its correlation with disease severity could represent a novel target in the treatment of asthma.

1.6.3 Function of ADAM33

ADAM 33 is one of the most recently described members of the A Disintegrin and Metalloprotease (ADAM) gene family of Zn++-dependent metalloproteases (MPs) (Yoshinaka *et al.* 2002; Gunn *et al.* 2002) that includes the well known TNF-α converting enzyme (ADAM 17, TACE). There are currently 40 members of the ADAM family of proteins described (White and Wolfsberg 2004).
(http://www.people.virginia.edu/~jw7g/Table_of_the_ADAMs.html)
Since its discovery in 2002, ADAM33 has been extensively characterized at molecular and structural levels (Zou *et al.* 2004; Zou *et al.* 2005; Bridges *et al.* 2005; Umland *et al.* 2003; Meng *et al.* 2007; Orth *et al.* 2004), but its biological functions have remained elusive. This might be due to the complex domain structure where multiple functions are possible, and the fact that ADAM33 exists as multiple alternatively spliced variants.

Domains and motifs

ADAM proteins are membrane anchored multifunctional molecules as reflected by their complex domain structure (Figure 1.5). ADAM33 comprises a full-length molecule of 813 amino acids including 8 domains: Signal sequence Pro-, Metalloprotease (MP)- , Disintegrin- , Cysteine-rich- , EGF-like- , Transmembrane-Domain and Cytoplasmic Tail (Yoshinaka *et al.* 2002), to which specific functions have been attributed.
Based on information from other ADAM proteins, ADAM33 might have sheddase activity and catalyse the release of different growth factors or receptors from the cell surface (Black and White 1998; Blobel 2000).
Alternatively, adhesion (Nath *et al.* 1999), migration (Nath *et al.* 2000), and membrane fusion (Evans 2001) are other important functions of ADAM proteins that might be relevant for growth and proliferation of ADAM33 expressing fibroblast and smooth muscle cells (Davies *et al.* 2003).
A number of ADAM proteins, including those most closely related to ADAM33 exist as alternatively spliced transcripts. These have been shown to produce protein products with distinct functions, either by the deletion of functional domains, or by altering the cellular localisation through the production of secreted and intracellular isoforms (Gilpin *et al.* 1998; Kurisaki *et al.* 2002; Cerretti *et al.* 1999; Hotoda *et al.* 2002; Roberts *et al.* 1999; Sagane *et al.* 1999; Yavari *et al.* 1998). Several alternatively spliced variants of ADAM33, including the α- and β-isoform (lack of exon Q) and a putative secreted variant, have been detected in bronchial fibroblasts with the majority lacking exons encoding the MP domain (Powell *et al.* 2004). The very low abundance of the MP domain suggests that the catalytic function of ADAM33 in smooth muscle and other mesenchymal cells need to be tightly controlled.

Human ADAM33 has been expressed as a recombinant protein in CHO cells where some protein was detected on the cell surface, with the majority of protein detected intracellularily; mutation of the zinc binding domain (E346A) had no significant effect on protein processing (Garlisi *et al.* 2003). Studies of the alpha and beta isoforms of murine ADAM33 expressed in HEK293 cells have also been undertaken (Umland *et al.* 2004). Expression of the alpha isoform of ADAM33 resulted in detection of two major protein isoforms of ~120 and 100 kD, each detectable with antibodies specific to peptides in the catalytic or cytoplasmic domains. However, only the larger protein was detected by an antibody to the pro-domain, indicating that it was the non-processed pro-form of ADAM33. This conclusion was supported by pulse chase experiments which showed the time-dependent disappearance of the ~120-kD protein and appearance of the ~100-kD form. The beta isoform of the ADAM33 protein consisted of only one form of ~110 kD, whose intensity and mobility was unaffected by cell trypsinization or biotinylation. Thus, it was concluded that this form was exclusively located intracellularly.

ADAM33 MP domain

The activity of the Zinc-dependent MP-domain is inhibited by the Pro-domain. The MP-domain becomes enzymatically active when the Pro-domain is cleaved by a furin endopeptidase at a furin recognition site at the N-terminal end of the MP-domain (Zou *et al.* 2004) (Figure1.5). The MP (catalytic) domain of ADAM proteins is implicated in shedding of cytokines, growth factors or receptors (sheddase activity), (Kheradmand and Werb 2002; Seals and Courtneidge 2003) (Figure 1.5). The catalytic domain of ADAM33 has been most extensively studied. It has been expressed as a recombinant protein in *Drosophila* S2 cells and purified from conditioned media where the majority of the protein remaining composes the MP domain in non-covalent association with the pro-domain (Prosise *et al.* 2004). The crystal structure of the catalytic domain of ADAM33 with its polypeptide fold and active site are similar to other metalloproteases with a unique substrate-binding site that will allow the design of specific inhibitors (PDB ID: Ir54 resolution 1.85 Å; Ir55, resolution 1.58 Å) (Orth *et al.* 2004). The activity of recombinant ADAM33 was evaluated using a high performance liquid chromatography (HPLC)-based cleavage assay which revealed four potential substrates out of 39 tested peptides known to be cleaved by other ADAMs. These four peptides were beta-amyloid precursor protein (APP), Kit-ligand-1 (KL-1), tumour necrosis factor-related activation-induced cytokine (TRANCE) and insulin B chain. Substrate peptide was incubated with or without recombinant catalytically active ADAM33 (ADMA33cat) for 2 hours. The samples were then run through an HPLC column. The eluate was monitored at 210nm and percentage of peptide cleavage was calculated. The cleavage sites of the peptide were identified by either electrospray or matrix-assisted laser-desorption/ionisation time-of-

flight (MALDI-TOF) mass spectrometry. The same cleavage assay was performed in the presence or absence of different classes of protease inhibitors for 2 hours using ADAM33cat and KL-1 peptide substrate. Although four peptides were cleaved by ADAM33, specificity constants (k_{cat}/K_m values) for each of the synthetic substrates suggested that these were not efficient substrates for ADAM33. Furthermore, co-expression of ADAM33 with KL-1 revealed only weak constitutive shedding of KL-1 in a transfected cell system, which was not regulated by protein kinase C activation via PMA stimulation (Zou *et al.* 2004). More efficient substrates for ADAM33 have yet to be identified, although ADAM33 has recently been implicated as a sheddase of a mutant form of CD23, the low-affinity IgE receptor (Meng *et al.* 2007), arising from a nonsynonymous (R62W) single nucleotide polymorphism (SNP). This mutation has been associated with enhanced T-cell responses to antigen in allergic subjects which may be linked to its influence on the stability of membrane CD23 molecules (Meng *et al.* 2007).

Several hydroxamate compounds, such as IK682 (γ-Lactam Hydroxamic Acid, Bristol-Myers Squibb (Duan *et al.* 2002)) and the Immunex compound 1 (*N*-{R-[2-(hydroxyamino-carbonyl)methyl]-4 methylpentanoyl}-L-3-(*tert*butyl)glycyl-L-alanine 2-Aminoethylamide), both known to inhibit ADAM17 or Marimastat ((2R,3S)-N-[(2S)-3,3-dimethyl-1-methylamino-1-oxobutan-2-yl]-N',3-dihydroxy-2-(2-methylpropyl) butanediamide, British Biotech), a MMP inhibitor were tested as ADAM33 inhibitors (Zou *et al.* 2004). IL682 was the most potent inhibitor of ADAM33 (Ki value of 23±7 nM) followed by Marimastat (Ki value of 160± 40nM) and then Immunex compound (Ki value of 2800 ±150nM (Zou *et al.* 2004)).

Endogenous human inhibitors of MMPs and ADAMs, tissue inhibitors of metalloprotease (TIMP) -1, -2, -3, -4, were also tested. TIMP-3 and TIMP4 showed strongest inhibition of ADAM33 (Ki values: 60±20 nM; 220±20 nM) whereas TIMP-1 had no inhibitory effect at 2 μM and TIMP-2 only a weak effect (Ki value of 760±160 nM). In contrast ADAM17 was strongly inhibited by TIMP-2, -3, and -4 and only weakly by TIMP-1 (Zou *et al.* 2004).

The development of the synthetically improved substrate β-amyloid precursor protein (APP) by a single amino acid change resulted in a 20-fold more efficient substrate. This allowed the development of a sensitive fluorescence resonance energy transfer (FRET) assay using a fluorogenic derivative of APP, which was used to obtain accurate Ki values for TIMP and small molecule compounds. In this assay the hydroxamate-based compounds IL682 and marimastat showed good inhibitory effects ((Ki values: 15±3 nM and 120±30 nM). No effect of the natural MMP inhibitor TIMP-1 was observed and the Ki values for TIMP-2 to 4 were: 660±150 nM, 7±1 nM, 40±10 nM (Zou *et al.* 2005).

Other MMP specific inhibitors (from Calbiochem, now Merck Chemicals Ltd) and one broad spectrum hydroxamic acid inhibitor (GM6001) (N-[(2R)-2-(Hydroxamidocarbonylmethyl)-

4-methylpentanoyl]-L-tryptophan methylamide; Ilomastat, Galardin, Quick-Med Technologies, Inc.) have been tested as potential inhibitors of ADAM33. In FRET peptide cleavage assays, a MMP-8 inhibitor I ((3R)-(+)-[2-(4-methoxybenzenesulfonyl)-1,2,3,4-tetrahydroisoquinoline-3-hydroxamate) was the most potent (IC_{50} = 371nM) and showed similar effect to that reported for Marimastat (Ki values: 120±30 nM). A MMP-3 inhibitor (N-Isobutyl-N-(4-methoxyphenylsulfonyl)-glycylhydroxamic Acid) showed an IC_{50} of 3355nM whereas the MMP-2/-9 inhibitor I ((2R)-2-[(4-Biphenylylsulfonyl)amino]-3-phenylpropionic Acid) and GM6001 achieved only about 40% inhibition at 5μM (Pang *et al.* 2006; Pang 2007).

These findings suggest that the catalytic activity of ADAM33 can be inhibited by several hydroxamate inhibitors and small molecule compounds that might be used in the treatment of asthma and potentially other ADAM33 related diseases (Li *et al.* 2005). (Figure 1.6)

Other ADAM33 domains

The Disintegrin-domain is potentially involved in cell adhesion and migration (Seals and Courtneidge 2003) and it has also recently been shown that the ADAM33 Disintegrin-domain is potentially involved in cell adhesion and migration and can interact with the leukocyte integrin alpha9beta1 (Bridges *et al.* 2005) and it inhibits cell migration mediated by alpha4beta1 and alpha5beta1 integrins (Huang *et al.* 2005). As the integrin alpha9beta1 is also expressed on mesenchymal cells, including fibroblasts and smooth muscle like cells (Wiester and Giachelli 2003), these data together suggest a role for ADAM33 in cell-cell adhesion (Figure 1.5).

As suggested from other ADAM proteins, the Cysteine-rich- and EGF-like domains might be involved in cell fusion (Seals and Courtneidge 2003). The Transmembrane-domain anchors the ADAM33 protein in the cell membrane allowing it to interact with potential substrates in the membrane or in the extracellular matrix. The Cytoplasmic domain might play an active role in intracellular signal transduction that regulates trafficking and activation of the ADAM protein (Kheradmand and Werb 2002) (Blobel 2000; Van Eerdewegh *et al.* 2002; Duffy *et al.* 2003) (Figure 1.5).

All these activities need to be further elucidated in biological functional studies to shed more light on the function of ADAM33 and to dissect its genetic associations with asthma (Blakey *et al.* 2005; Van Eerdewegh *et al.* 2002) and chronic obstructive pulmonary disease (Gosman *et al.* 2007; van Diemen *et al.* 2005b).

Mouse model

A recent ADAM33 knock out mouse model did not add much to elucidate the function of ADAM33 as it showed normal development and fertility (Chen *et al.* 2006) which might be

explained by compensation of ADAM33 function by other ADAMs or metalloproteases. The same mice used in an animal model of allergic asthma showed normal allergen-induced airway hyperreactivity, immunoglobulin E production, mucus metaplasia and airway inflammation (Chen *et al.* 2006) suggesting that a loss of ADAM33 function might not be the pathophysiological mechanism in the development of asthma.

Potential targets

The enzymatic activity of the MP domain of ADAM33 seems to be an important target due to the fact that soluble ADAM33, containing the catalytic domain, is increased in BALF from asthmatic subjects. Its inhibition by small molecules, cyclic hydroxamates or siRNA may be of benefit in disease. However, interfering with the Disintegrin- or EGF-domain could also present a potential target (Figure 1.6).

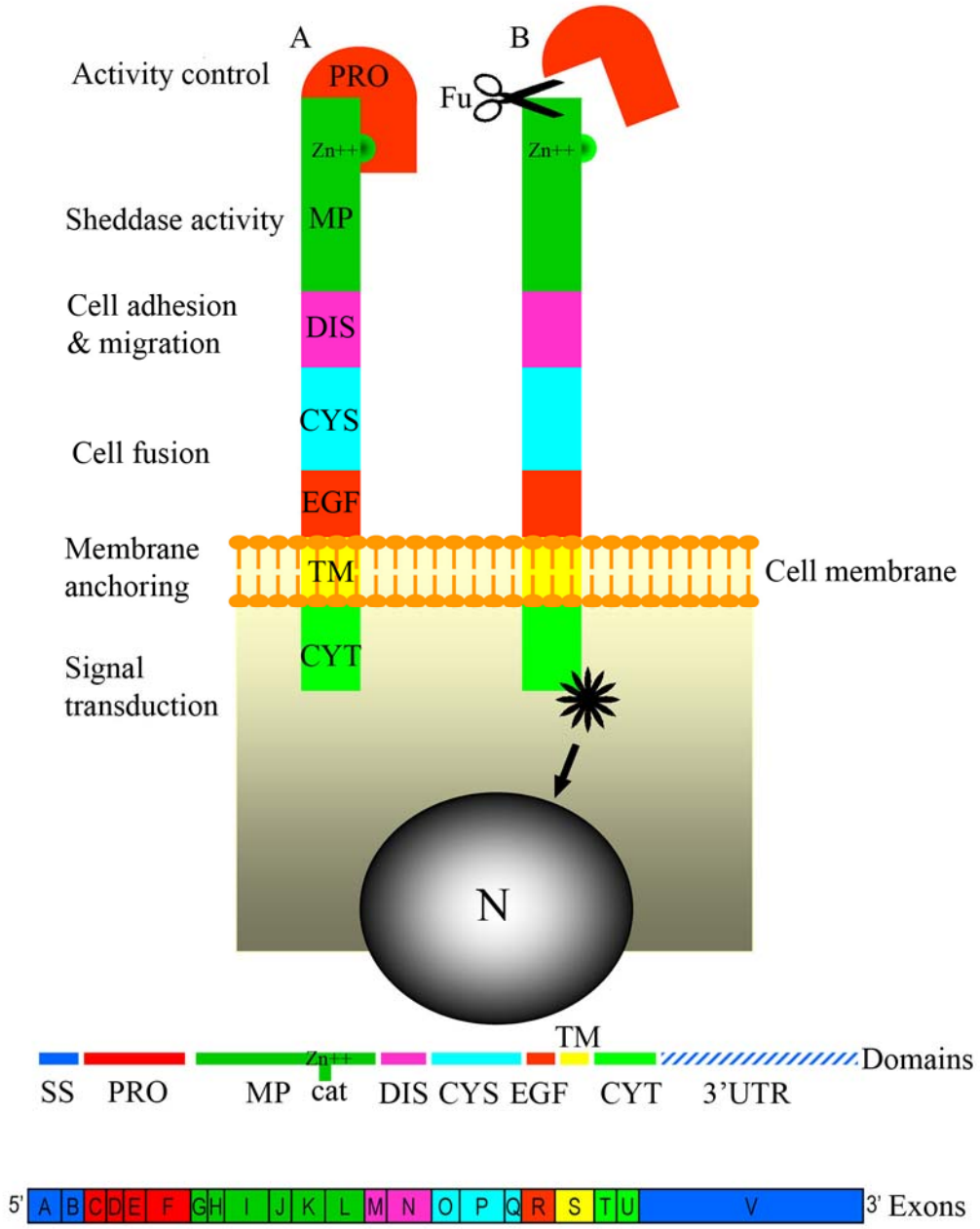

Figure 1.5 Diagrams of ADAM33 Exons, Domains and Functions.

A Cell membrane anchored ADAM33 with its different domains and functions. B Activation of ADAM33 metalloprotease domain (MP) containing the zinc (Zn++) dependent catalytically active site (cat) by cleavage of the pro-domain (PRO) by a furin endopeptidase (Fu). Cytoplasmic domain is probably involved in intra cellular signalling (*). Signal sequence (SS), disintegrin domain (DIS), cysteine rich domain (CYS), epithelial growth factor like domain (EGF), transmembrane domain (TM), Cytoplasmic domain (CYT), nucleus (N).

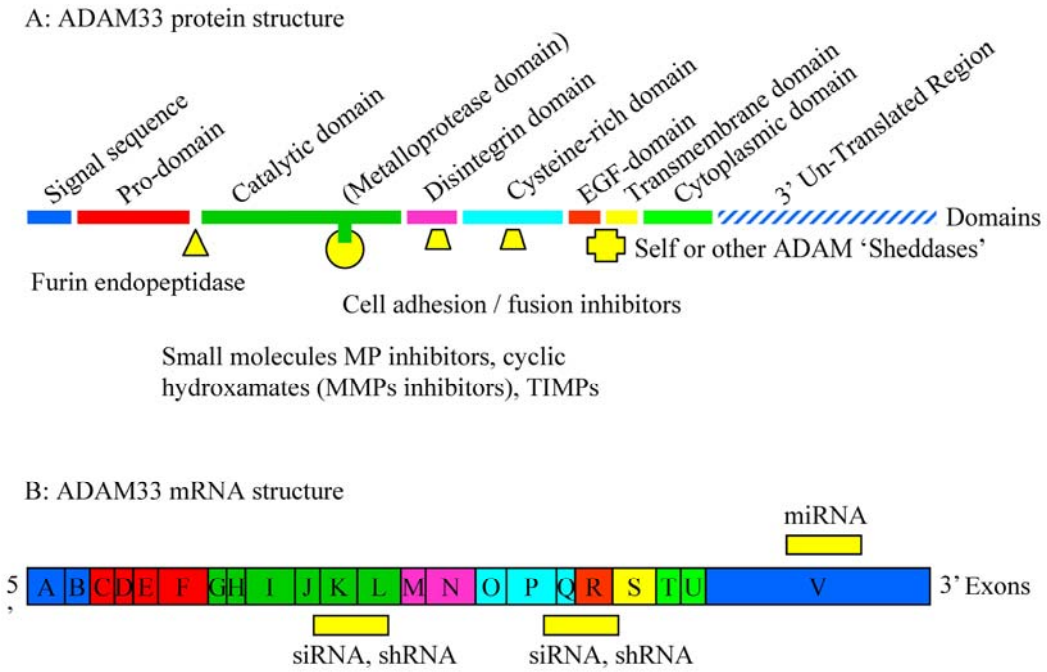

Figure 1.6 Treatment targets in ADAM33 mRNA and protein structure.

Potential therapeutic targets at the ADAM33 protein level (A) or the mRNA level (B) (adapted from (Haitchi *et al.* 2008).

1.7 Early origin of asthma

In the Western world asthma is the most common chronic childhood disease, which has been described as 'repeated attacks of airway obstruction and intermittent symptoms of increased airway responsiveness to triggering factors, such as exercise, allergen exposure and viral infections' (Illi *et al.* 2006). However, its diagnosis is difficult particular in pre-school children and it can only be clinically diagnosed with certainty by the age of 5years (Bacharier *et al.* 2008). Recurrent episodes of bronchial symptoms such as coughing and/or wheezing are common in infants and pre-school children but these symptoms are often associated with viral lower respiratory tract infections and are frequently transient and about 60% will be symptom-free at school age (Bacharier *et al.* 2008).

Most childhood asthma begins before the age of 3 years with their first episode of wheeze due to viral infections. The natural history of asthma progression from childhood to adulthood has been studied in several longitudinal cohort studies. The population-based cohort in Tucson, where children have been followed up from birth, have been divided into 4 phenotypes: never wheezers (NW), transient early wheezers (TEW; before age 3 but not at age 6), persistent wheezers (PW; before age 3 and at age 6), and late on-set wheezers (LOW) at the age of six. A recent follow-up study of this cohort through adolescence showed that the pattern of wheezing and lung function seemed to be established by the age of six with no significant changes at the age of sixteen. There was no difference in prevalence of wheeze at ages 8, 11, 13 and 16 between NW and TEW compared to a significant increase in PW and LOW (Morgan *et al.* 2005). It was suggested that the first 6 year of life play an important role of asthma expression and lung function achievement later in life which might be influenced by environmental and genetic factors (Morgan *et al.* 2005).

Between 40 and 75% of children with asthma will have complete resolution by adulthood and the relapse rate after a period of remission ranges between 12 and 35% (Koh and Irving 2007). Episodic asthma has generally a good outcome whereas children with persistent and severe persistent asthma continue to have asthma symptoms in adulthood (89%). Duration of asthma, BHR, smoking and atopy were all associated with increased symptoms in adulthood (Koh and Irving 2007; Piippo-Savolainen and Korppi 2008). This raised the question if anti-inflammatory therapy would have an effect on the outcome of childhood asthma. A longitudinal study comparing inhaled glucocorticoids (ICS) with nedocromil and placebo (for 6 years) in children 5-12 years old with mild to moderate asthma did not have an effect on changes in lung function but improved BHR and control of asthma (The Childhood Asthma Management Program Research Group 2000). Recently, a study using intermittent ICS did not have an effect on the progression from episodic wheezing to persistent wheezing in infants followed for 3 years (Bisgaard *et al.* 2006) and another study showed that 2years

of ICS therapy in pre-school children at high risk for asthma had an effect on symptom and exacerbation reduction but did not have a subsequent disease-modifying effect after ICS were stopped (Guilbert *et al.* 2006). All these studies seem to suggest that anti-inflammatory treatment does not change the course of asthma in childhood (Gold and Fuhlbrigge 2006) and a proportion of asthma in particular severe asthma has its origin in childhood.

Computer tomography and bronchial biopsy studies have shown that eosinophilic-neutrophilic airway inflammation, matrix deposition and epithelial injury exist in children with asthma (Cokugras *et al.* 2001; Payne *et al.* 2003; Payne *et al.* 2004; Pohunek *et al.* 2005; de Blic *et al.* 2005; Fedorov *et al.* 2005; Barbato *et al.* 2006) (Saglani *et al.* 2007) and in children who subsequently develop clinically diagnosed asthma at a later stage (Pohunek *et al.* 2000) (Pohunek *et al.* 2005), indicating that pathological changes occur early in life, although inflammation and remodelling seems not to be present in wheezing infants (Saglani *et al.* 2005). Taken all these findings together would transfer the origin of asthma into the intrauterine or early postnatal developmental phases where susceptibility genes might be activated by environmental influences (Saglani and Bush 2007).

In-utero exposure to maternal cigarette smoke and a family history of asthma are associated with reduced lung function in newborn infants suggesting adverse effects of these factors on lung development in utero (Stick *et al.* 1996). Significantly, exposure to maternal tobacco smoke is one of the strongest environmental risk factors for developing asthma (Dezateux *et al.* 1999; Dezateux *et al.* 2001; London *et al.* 2001) through its effects on lung morphogenesis linked to altered mesenchymal function (Sekhon *et al.* 1999; Sekhon *et al.* 2002). For example, it has been shown in monkeys that maternal nicotine exposure resulted in abnormal fetal lung development (Sekhon *et al.* 1999) and upregulation of collagen gene expression (Sekhon *et al.* 2002). Prenatally and postnatally maternal smoking results in increased inner airway wall thickness in children who die from sudden infant death syndrome (Elliot *et al.* 1998). These findings might partially explain abnormal lung mechanics in infants of smoking mothers.

The early life origins of atopy might be caused by transplacental allergen exposure that produces neonatal T cell memory (Holt 1996; Szepfalusi *et al.* 2000) and after maternal smoking, atopic predisposition is another strong risk factor for developing bronchial hyperresponsivenes and asthma (Young *et al.* 1991). Another potential important mechanism in the pathogenesis of lung disease and in particular asthma is the interplay between maternal smoking and the fetal immune system. Cord blood from children whose mothers smoked during pregnancy had lower concentrations of IL-4 and INF-γ which was associated with an increased risk of wheeze at age six (Macaubas *et al.* 2003). Maternal smoking also attenuated cord blood mononuclear cell responses to toll-like receptor ligands suggesting that

the innate immune response is inhibited (Noakes *et al.* 2006). Of interest is a study that showed that cord blood INF-γ responses are inversely related to the frequency of viral respiratory infections in the first year of their life (Copenhaver *et al.* 2004). Another study demonstrated that cord blood mononuclear cell proliferation significantly increased in response to the allergen house dust mite in neonates with a history of maternal smoking (Devereux *et al.* 2002). It has also been shown that maternal smoking during pregnancy modifies the fetal immune system with a significantly higher neonatal Th2 response (in form of IL-13 protein) in response to allergens such as ovalbumin or house dust mite (Noakes *et al.* 2003).

Previous work in Southampton has demonstrated that interleukin-4 (IL-4) and IL-13 stimulate release of the EGFR ligand TGF-α (a homologue of EGF) (Lordan *et al.* 2002) and the profibrotic cytokine TGF-β (Richter *et al.* 2001) from adult bronchial epithelial cells. As these growth factors regulate branching morphogenesis, a Th2 environment might influence airway development. IL-13 overexpression in transgenic mice also leads to subepithelial fibrosis (Zhu *et al.* 1999; Elias *et al.* 2003). Of interest is the combined effect of maternal smoking (in utero exposure to smoking) and IL-13 polymorphisms on the development of persistent wheezing and persistent childhood asthma showing a possible genetic-environmental interaction (Sadeghnejad *et al.* 2008). In support of the environmental influences is the recent report that children with the TGB-β1 polymorphism have an increased risk to develop asthma (Salam *et al.* 2007). Furthermore, exhaled nitric oxide (eNO) which is a marker for airway inflammation in asthma was increased in infants exposed to postnatal maternal smoking in the presence of maternal atopic disease (Frey *et al.* 2004). This underlines the additional complex interaction between maternal and environmental factors in airway disease development.

Of importance is the recent report that ADAM33 polymorphisms are associated with impaired lung functions in 3 and 5 year old children (Simpson *et al.* 2005a) suggesting an important role of ADAM33 early in life either in utero or post partum.

Thus, events taking place during the gestational period might play a significant role in determining whether or not a genetic susceptibility becomes translated into a disease process. Although much is known about how the EMTU influences lung growth and maturation, how this becomes disordered by environmental exposures or Th2 cytokines to predispose to asthma remains unknown. Interactions between environmental stimuli and susceptibility genes and their proteins might be critically involved in these pathological responses that might be initiated even in the early stages of lung development in utero.

1.8 Embryonic & Lung development

1.8.1 Human embryonic development

Human pregnancy (38-40 weeks) can be divided into 3 periods: the pre-embryonic, the embryonic and foetal periods. The pre-embryonic phase covers the period from fertilization (=conception) up to about 14 days post conception (p.c.), at which time the process of gastrulation (formation of 3 germinal layers: ectoderm, endoderm, mesoderm) begins with the appearance of the intra-embryonic mesoderm and the primitive streak as first indication of the embryonic axis. This phase starts after human conception (fertilization) occurs by penetration of the haploid male pronuclei (sperm with one of each autosome plus either an X or Y chromosome) into the haploid oocyte (ovum with one of each autosome plus an X chromosome) in the ampullary region of the Fallopian tube to form the zygote (single diploid cell). During this time the zygote divides by mitosis into the morula stage (4-16 cells) and blastocoele stage (60-120 cells) that becomes the blastocyst. The blastocyst attaches around day 4 p.c. and implants at day 7 p.c. with primitive streak formation at around day 13 p.c. during which time the first size increase from 0.1 to 0.2 mm occurs (Table 1.3) (Strachan *et al.* 1997).

In the early stage of embryonic development the blastocyst develops into the Inner cell Mass and Trophoectoderm (Trophoblast). The Inner cell Mass becomes the Epiblast and Hypoblast and the Hypoblast later the Extra-embryonic endoderm. Out of the Epiblast the Ectoderm, Endoderm, and Mesoderm develop from which all embryonic tissue is generated (Figure 1.7). The Ectoderm also contributes to the Amniotic ectoderm and the Mesoderm to the Extraembryonic mesoderm. The endoderm gives rise to germ cells and epithelial tissue in the digestive tube, lungs, liver, and urinary tract. Out of the mesoderm the skeleton, striated muscle, connective tissue, parts of the scull and jaw, blood cells, vessels, bone marrow, reproductive and excretory organs are formed. The ectoderm changes into the epidermis, including the skin, hair and eyes and the nervous tissue (Figure 1.8).

The second phase of embryonic development, the embryonic period covers the processes of embryogenesis and the majority of organogenesis and lasts until week 8 p.c. (appearance of centres of ossification in the humerus) to week 10 p.c. (major events of organogenesis completed, although brain and the rest of central nervous system and the respiratory system continue to differentiate for some time after birth). The third phase, the fetal period between week 11 p.c. and full term, represents the period of consolidation and growth (Strachan *et al.* 1997).

Carnegie Stage	Age (days)	Size (mm)	Major features
1	1	0.1	Fertilization
2	1.5	0.1	2-16 cells
3	4	0.1	Blastocyst
4	5	0.1	Attaching blastocyst
5	7	0.1	Implantation
6	13	0.2	Chorionic villi formation; primitive streak
7	16	0.4	Notochord formation
8	18	1.25	Gastrulation; neural fold formation
9	20	2	Somite formation
10	22	2.75	Start of neural tube fusion
11	24	3.5	Optic vesicle formation; anterior neuropore closes
12	26	4	Upper limb buds appear
13	28	5	Lower limb buds, lens disc and optic vesicle appear
14	32	6	Optic cup appears
15	33	8	Formation of nasal pit, hand plate and cerebral hemispheres
16	37	9.5	Auricular hillocks and foot plate appear
17	41	12.5	Finger rays distinct; nasofrontal groove appears
18	44	15	Ossification begins; eyelid folds
19	47.5	17	Trunk elongation and straightening
20	50.5	20	Upper limbs longer and bent at elbow
21	52	23	Fingers longer; hands approach each other
22	54	25.5	Eyelids and external ears more distinct
23	56.5	29	External genitalia well developed

Table 1.3 Carnegie staging of human embryos.

(adapted from Strachan et al. 1997)

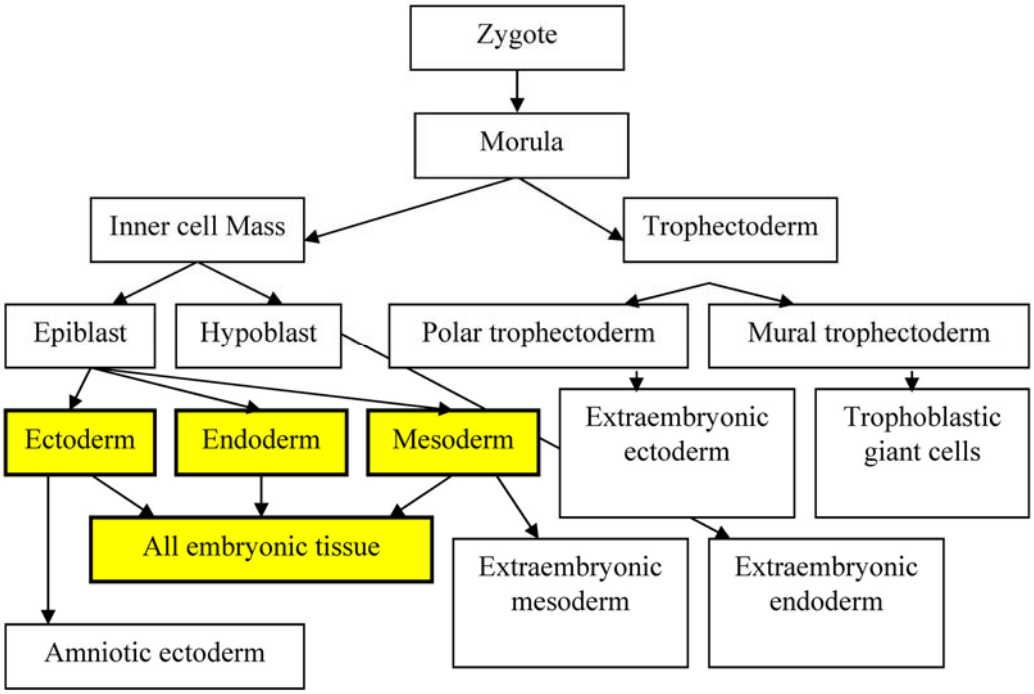

Figure 1.7 Cell lineage during development.

(adapted from MuriTech webpage: www.muritech.com
http://www.muritech.com/embryoj/lineage.htm)

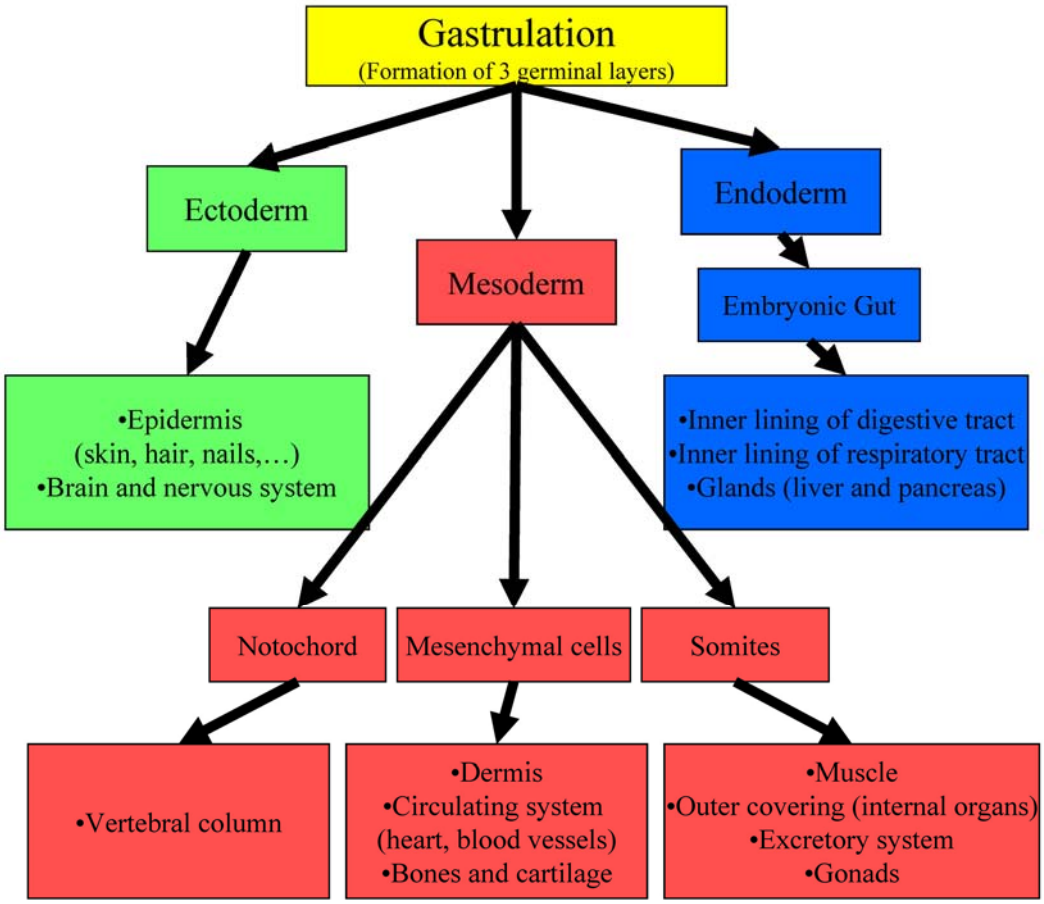

Figure 1.8 Gastrulation with Ectoderm, Mesoderm and Endoderm.

Gastrulation with formation of 3 germinal cell layers with their derivative cell lineages.

1.8.2 Embryonic lung development

The mammalian lung starts as an evagination, the laryngo-tracheal groove, from the floor of the primitive pharynx (foregut endoderm; embryonic gut) and grows into two lung buds into the surrounding splanchnic mesenchyme. Larynx and trachea grow out from the proximal portion and right and left main stem bronchial buds from the distal portion of the ventro-lateral side of the laryngo-tracheal groove at about embryonic day (ED) 9.5 in mouse and 3 to 4 weeks of gestation in human. As the lung buds grow, they elongate and branch repeatedly forming the primary bronchi and stem bronchi and the foregut gets separated into oesophagus and trachea. The lung buds continue to grow into the coelomic cavity and are covered by mesoderm that gives rise to the visceral and parietal pleura. Endodermally derived epithelium lining the lung buds differentiates into respiratory epithelium that lines the airways and specialised epithelium that lines the alveoli. Innervation is derived from the Ectoderm and the Mesoderm contributes the blood vessels, smooth muscle, cartilage and other connective tissue (Figure 1.8).

Histologically lung development can be divided into five different stages in mouse / human: lung premordium (ED 8-9 / 3-4 weeks), pseudoglandular (ED 10-16 / 5-17 weeks), canalicular (ED16-18 / 16-26 weeks), saccular (ED 18-20 up to 5 days after birth / 24-38 weeks), alveolar (birth to 4 weeks postnatal / 36 weeks to 1-2 years after birth (Warburton *et al.* 2000; Chinoy 2003).

In the mouse four lobes form in the right lung and a single lobe in the left lung whereas in humans the right lung is trilobed (upper, middle, lower) and the left lung bilobed (upper, lower). Several generations of dichotomous branching of the secondary bronchi occur to form 16-25 generations of primitive airways ending in bronchioles which are followed by secularisation and alveolarisation. (Table 1.4) (Chinoy 2003; Gaultier *et al.* 2000; Rosenthal and Bush 2002). The lobation of the lungs and bronchial branching for the first 16 to 23 generations in humans is stereotypic. The later lower airways branching phase is non-stereotypic following a proximal-distal fractal pattern that repeats itself at least 50 million times (Warburton *et al.* 2005; Cardoso 2000; Chinoy 2003; Aliotta *et al.* 2005; Warburton *et al.* 2000; Warburton *et al.* 2003). The stereotypic branch pattern of the lung seems to be well-conserved as a genetically hard-wired programme that is directed by transcriptional factors interacting with peptide growth factors signalling pathways, hypoxia and physical forces (Warburton *et al.* 2003; Warburton *et al.* 2000; Warburton *et al.* 2005; Perl and Whitsett 1999; Cardoso 2000). Many complex mechanisms are involved in the organogenesis of the lung, such as interactions between cells originating from two germ layers, endoderm and mesoderm. Interactions between epithelium and mesenchyme and/or

endothelium as well as genes regulating architecture, growth pattern and differentiation are crucial in lung branching morphogenesis.

Epithelial cells derived from the endoderm and mesenchymal cells from the mesoderm form the Epithelial Mesenchymal Trophic Unit (EMTU) which is an important unit in normal branching morphogenesis and lung development as well as later in remodelling in asthma (Holgate *et al.* 2000) (Davies *et al.* 2003). Normal lung development is subject to a fine balance between these different cell types and their multiple positive and negative signalling factors (Warburton *et al.* 2000; Cardoso 2001; Warburton *et al.* 2001; Perl and Whitsett 1999; Chinoy 2003; Cardoso and Lu 2006) and transcription factors (Whitsett 1998).

These complex mechanisms transform a fluid filled lung into an air breathing organ that will be able to sustain a newborn life. Respiratory gas exchange, a main function in the mature mammalian lungs, has been developed by diffusion through very thin cells. The human lung achieves a final gas diffusion surface of 70 m^2 in area by 0.1 μm in thickness in early adulthood and is capable to support systemic oxygen consumption in the range of 250 ml/min at rest and 5500 ml/min during maximal exercise. A parallel capillary network develops which is in close proximity to the alveoli and accommodates pulmonary blood flow rising from 4 l/min to 40 l/min during max exercise (Warburton *et al.* 2000).

(Databases on lung: http://www.ana.ed.ac.uk/anatomy/database/lungbase/lunghome.html)

Stages of lung development			
Stage	**Time period (mouse)**	**Time period (human) / Airway epithelium**	**Morphometric correlates**
Embryonic		1-7(1-6) weeks 4 weeks: primitive epithelial cells	Lung buds appear as out pouching of forgut. Mesenchyme driven branching of airways. First appearance of primitive pulmonary arteries and veins. Ventral outpouching of foregut – laryngeal cleft Two bronchi – right and left main stem Asymmetric dichotomous branching to form bronchi 6-7 weeks vascular connection with atria
Pseudoglandular	9.5-16.2 embryonic days (ED)	5-17(6-16) weeks 8weeks: neurosecretory cells appear 10-12 weeks: presecretory and preciliated 14 weeks: ciliated cells, neuroepithelial bodies	Virtually the complete branching structure of the future bronchial tree is laid down. Cellular differentiation (cartilage, neuronal tissue, ciliated cells, smooth muscle) commences from proximal to distal. The pre-acinar vascular patern is fully mature at the end of this period. Continued airway branching to terminal bronchioles Mucus glands and cartilage Smooth muscle and epithelial cell differentiation Closure of pleural peritoneal cavities
Canalicular	16.6-17.4 EDs	16-26 weeks 20-22 weeks: pre-clara cells 24 weeks: Type I and Type II 24-26 weeks: clara cells	Early acini become visible under the light microscope. Capillaries from a meshwork within the mesnchyme. Type-1 and -2 cell differentiation. Respiratory bronchioles, acinar tubules Capillary bed comes in close apposition with tubules Epithelial differentiation more complex (Surfactant protein begins to be expressed) General thinning of both mesenchyme and epithelium Survival possible
Saccular	17.4 EDs to 5 days after birth	24 weeks to term (26-36)	Blind saccules start to divide, and alveolarization commences. The capillary network beomes closer together, and the walls between the sacs contain a double capillary network. Secondary crests subdivide saccules First true alveoli at about 36 weeks Maturation of epithelium – Type II cells Flattening of Type I cells
Alveolar	Day 5-day 30 after birth	36 weeks - 3 years	Formation of alveoli, mostly in first 6 months, virtually complete by 2 yrs. Formation of new double capillary layers, followed by remodelling to form the mature single layer. Septation of alveoli and iuncreasing size Growth of capillary network matching alveoli formation 85% of alveoli form postnatally Most alveoli formed before year 3
Postnatal		+3years	Alveolar formation: 85% Fusion of double capillary network complete at 18 – 24 months Increased mucus cells Collateral ventilation Pores of Kohn between alveoli Canals of Lambert (terminal bronchioles and alveoli)

Table 1.4 Stages of lung development.

adapted from(Rosenthal and Bush 2002; Have-Opbroek 1991; Perl and Whitsett 1999)

1.8.3 Mechanisms of lung development

Complex cell-cell interactions of endodermal derived epithelium and mesenchyme derived from the splanchnic mesoderm, the EMTU, are characteristic in lung morphogenesis and repair (Minoo and King 1994; Shannon and Hyatt 2004; Demayo *et al.* 2002) (Cardoso and Lu 2006). The mesenchyme gives rise to several soluble factors that are responsible for branching morphogenesis distal to the trachea. This was shown by grafting distal pulmonary mesenchyme of ED 13-14 rat lungs onto a stretch of tracheal epithelium from which the mesenchyme had been removed. This resulted in normal branching pattern and induction of type II cell differentiation (Shannon 1994). When tracheal mesenchyme was grafted onto peripheral epithelial cell buds, no branching was observed but cyst formation with epithelium containing ciliated and mucous secretory cells (Shannon *et al.* 1998). Fibroblast growth factor (FGF)-10 from the mesenchyme and FGF-Receptor (FGFR) on the epithelial cells play an important role during lung development (Celli *et al.* 1998; Sekine *et al.* 1999) that might be controlled by TGF-β which inhibits FGF-10 expression in mesenchymal cells (Cardoso and Lu 2006). Deficiency and disruption of the retinoic acid pathway results in total lung agenesis (Mendelsohn *et al.* 1994) and it has only recently been shown that retinoic acid induces FGF-10 expression in the mesoderm next to the laryngo-tracheal groove which can be blocked by blockade of the retinoic acid receptor pathway (Desai *et al.* 2004). This suggests that retinoic acid signalling from the laryngo-tracheal groove might induce the early FGF-10 dependent bud formation and later bronchial morphogenesis. It has also been shown that separate embryonic cell lineages form the trachea and the peripheral lung which was demonstrated by permanently marking endodermally derived peripheral lung epithelial cells using a tetracycline driven SpC-Cre recombination system (Perl *et al.* 2002). Recently it has been shown in Foxj1-GFP transgenic mouse lungs that labelled ciliated epithelial cells appear in a proximal to distal pattern during embryogenesis (Rawlins *et al.* 2007). The larynx, trachea, determination of left-right laterality and septation of the trachea from the oesophagus are genetically distinguishable from the distal airways (Warburton *et al.* 2005).

ASM develops, in contrast to the epithelial cells, in a distal to proximal pattern alongside the bronchial tree originating from local mesenchymal cells that are located around the tips of the growing epithelial buds. Mechanical tension and epithelial paracrine factors seem to regulate bronchial myogenesis which begins in the onset of the pseudoglandular stage (embryonic day 11 in the mouse and about 5 weeks post conception in human). ASM precedes vascular muscle development by several days.

Laminin-1 and -2 are components of the EMTU basement membrane and that are newly synthesised around the developing airways. Embryonic mesenchymal precursor cells bind to

these proteins and elongate which induces smooth muscle myogenesis (Badri *et al.* 2008). Stretch is another mechanisms that induces ASM myogenesis of undifferentiated lung mesenchymal cells and an increase of hydrostatic pressure in mouse embryonic lung explants increased α-smooth muscle positive cells around the bronchial tree (Yang *et al.* 2000). It was recently suggested that lack of ASM cell development in amyogenic mice is due to the lack of skeletal muscle and therefore lack of fetal breathing (Inanlou *et al.* 2006) which would also result in absent or abnormal spontaneous peristaltic airway contractions moving amniotic fluid in the lungs through the bronchial tree an important mechanism for branching morphogenesis (Schittny *et al.* 2000).

The molecular mechanisms that lead to embryonic ASM differentiation are largely unknown, however, serum response factor (SRF) and its dominant-negative isoform SRFΔ5 play an important role in ASM myogenesis. SRF is a transcription factor that regulates smooth muscle gene expression. Both isoforms are expressed in mesenchymal progenitor cells and when the cells are exposed to mechanical stress SRF increases whereas SRFΔ5 is suppressed, which might induce myogenesis (Yang *et al.* 2000). RhoA is a small guanosine triphosphatase (GTPase) signalling protein which is highly expressed in undifferentiated embryonic mesenchymal progenitor cells and prevents those becoming ASM cells. LN-1 and LN-2 inhibit its expression and activity and it is suppressed during spread- and stretch induced myogenesis (Beqaj *et al.* 2002).

A new factor has recently been discovered, tension-induced/inhibited proteins (TIP). TIPs contain functions of nuclear receptor co-regulators and chromatin remodelling enzymes. TIP-1 is induced by tension and promotes myogenesis by interaction with the SRF promoter and acetylating histones 3 and 4 on this promoter resulting in activation of SRF transcription (Jakkaraju *et al.* 2005)

Several epithelial-derived morphogens and their effectors have been shown to modulate ASM myogenesis in several transgenic mouse models. This are molecules such as sonic hedgehog (Shh), Gli transcription factors, Forkhead box (Fox_a1 and Foxa2), fibroblast growth factor (FGF), bone morphogenic protein (BMP)-4, noggin, Wnt signalling. Changes of these factors in experimental mouse models resulted in either increased or decreased ASM development (Badri *et al.* 2008)

1.8.4 The role of ADAMs in lung development

In embryonic development 'ectodomain shedding' of membrane proteins from the cell surface plays an important role and is facilitated by proteolytic proteins ('sheddases'), such as ADAM proteins (Kheradmand and Werb 2002). TNF-α-converting enzyme (TACE/ADAM17) is part of the ADAM protein family. It is a sheddase that processes TNF-α, TNF-related activation-induced cytokines (TRANCE), TNF receptors, transforming growth factor-α (TGF-α), L-selectins, fractalkine, amyloid protein precursor (APP), and cellular prion protein (Garton *et al.* 2001; Tsou *et al.* 2001; Vincent *et al.* 2001; Peschon *et al.* 1998; Buxbaum *et al.* 1998; Lum *et al.* 1999; Moss *et al.* 1997; Black *et al.* 1997). ADAM17 is the first of the ADAM proteins describe to play a role in embryonic lung development. ADAM17-deficient mice show pulmonary hypoplasia and develop respiratory stress at birth (Zhao *et al.* 2001a). When cultured in serum free medium, ADAM17-/- embryonic lungs branch poorly compared with wild type lungs, but can be rescued by addition of exogenous TGF-α. Inhibition of branching morphogenesis in vitro can also be achieved using specific antisense oligonucleotides (ASOs) that prevent ADAM17 expression; this can also be reversed with TGF-α (Zhao *et al.* 2001b) providing evidence that ADAM-mediated protein shedding is important for lung development by regulation of growth factor availability.

The role of ADAM33 in lung embryonic lung development is not known and very little is known about the embryonic expression of ADAM33. Using semi quantitative PCR for a mouse cDNA panel expression was studied in whole mouse embryos at day 8.5, day 9.5, day 12,5 and day 19 with the highest expression at embryonic day 19 (Gunn *et al.* 2002). In human ADAM33 expression was shown in embryonic lung fibroblasts, MRC-5 fibroblasts (Garlisi *et al.* 2003) (Umland *et al.* 2003) and in all human fetal tissue including the fetal lung except the brain with highest expression in the fetal uterus (using a cDNA library of human fetal tissue) (Umland *et al.* 2003).

Analysis of the off-spring from heterozygous breeding pairs (ADAM33 -/-, ADAM33-/+) did not reveal gross morphological differences from the wild type mice and histological examination could not show apparent differences in the major organs (Chen *et al.* 2006). The function of ADAM33 might be compensated by other ADAM or matrix metalloproteinases. However, it is not known if there were any differences in morphology and histology during the embryonic and fetal stages of organ development.

Therefore, more light needs to be shed on ADAM33 and its role in lung growth and development.

1.9 Summary and hypothesis

Asthma is a disease that runs in families and has a complex genetic background. Several asthma susceptibility genes have been discovered of which one of them is ADAM33. Polymorphisms have been linked to asthma and in particular bronchial hyperresponsiveness, decline in lung function in asthma and COPD and in young children. ADAM33 is almost exclusively expressed in mesenchymal cells, such as fibroblasts, myofibroblasts and smooth muscle cells. These cells play an important role in the epithelial mesenchymal trophic unit in modelling of the airways during lung development. They are also linked to airway remodelling and hyperresponsiveness in asthma and might play an important role in the origins of the disease

Therefore, it is hypothesised that ADAM33 is differentially expressed in normal and asthmatic lungs and that ADAM33 is involved in embryonic/fetal lung development and is influenced by an allergic maternal environment.

1.10 Aims

The overall aims of this project are to study ADAM33 in:

Human adult lung

- by examining the expression of ADAM33 at the mRNA and protein level in bronchial biopsies from normal and asthmatic subjects.

Human embryonic/fetal lung

- by examining the expression of ADAM33 at the mRNA and protein level in human embryonic lungs.
- by developing a human embryonic/fetal lung explant model and studying the influence of a maternal allergic (IL-13) environment on ADAM33 expression.
- by investigating the effect of ADAM33 knock down, in contrast to knock out on human embryonic lung and primary fibroblasts.

Mouse lung

- by examining the expression of ADAM33 during all stages of mouse embryonic, fetal and postnatal lung development.
- by investigating the in vivo influence of a maternal allergic environment on ADAM33 expression in the lung and on lung function in offspring from allergic mouse mothers.

Chapter 2 Materials & Methods

2.1 Section: Clinical

2.1.1 Human adult subjects

Following ethical approval from the Southampton and South West Hampshire Joint Local Research Ethics Committee, bronchial biopsies and brushings were obtained from healthy and asthmatic subjects. Subjects were characterized according to symptoms, lung function, medication and skin prick test to common-allergens. Asthma severity was assessed according to the Global Initiative for Asthma (GINA) guidelines(Global Initiative for Asthma 2004; Global Initiative for Asthma 2006; Global Initiative for Asthma 2007). Recruitment of most subjects was done by the team of research nurses from Allergy and Inflammation Research (AIR).

Subjects healthy versus mild to moderate asthmatic

Initially bronchial biopsies were obtained for study from 21 normal subjects and 19 subjects with mild to moderate asthma. All asthmatic subjects were using β2-agonists (B2A) as required, and 14 were using additional inhaled corticosteroids (ICS) (beclomethasone dipropionate (BDP) equivalent median dose = 670 (range: 200-2000) ug/day) (Table 2.1). 13 biopsies from the normal and 14 from asthmatic subjects, 2 on B2A only and 12 plus ICS, were used for RNA extraction and RT-qPCR analysis. 15 biopsies from normal and 12 biopsies from asthmatic subjects (5 on B2A and 7 plus ICS) were used for immunohistochemistry and analysis. On average 2.5 biopsies (range: 1-4) were obtained from each subject for immunohistochemistry.

Subjects healthy versus severe asthmatic

Subsequently further bronchial biopsies/brushings were obtained from 8/6 normal and 15/9 severe asthmatic subjects. All asthmatic subjects were using B2A as required, ICS (BDP equivalent median dose = 2000 (range: 500-4000) μg/day) and long acting beta-agonists (LABA) (Table 2.2 & 2.3). 15 biopsies (mean 1.9) and 14 brushings (mean 2.3), from the normal and 23 biopsies (mean 1.5) and 16 brushings (mean 1.8) from the asthmatic subjects were used for RNA extraction and RT-qPCR analysis.

2.1.2 Bronchoscopy

Fibreoptic bronchoscopy was performed according to the BTS guidelines (British Thoracic Society Bronchoscopy Guidelines Committee 2001) and the local departmental standard

operation procedure in the Wellcome Trust Clinical Research Facility. Bronchoscopies were performed by clinician colleagues Tim Shaw, Peter Wark, Ian Yang, Timothy Howell, Suresh Babu, Peter Howarth and David Sammut.

Bronchial biopsies

Biopsies were taken with a disposable alligator forceps (Bard, Ref 100503, size: 1.8mm) (KeyMed (Medical & Industrial Equipment) Ltd., OLYMPUS Group Company, Southend-on-Sea, UK) after local anaesthetics from carinae of the right upper lobe (6 – 8 biopsies) and further processed for GMA embedding and immunohistochemistry, fibroblast cell culture, whole mount microscopy, and RNA extraction. On average 2.5 biopsies (range: 1-4) were taken from each subject in both groups (asthmatic and controls) for immunohistochemistry.

Bronchial brushings

Bronchial brushings were performed with disposable cytology brushes (Olympus, Ref BC-202D-2010, size: 2mm) (KeyMed (Medical & Industrial Equipment) Ltd., OLYMPUS Group Company, Southend-on-Sea, UK) after local anaesthetics from the bronchial epithelial layers of the segmental bronchi of the right lower lobe (4 – 8 brushings) and collected in sterile phosphate buffered saline (PBS). They were further processed for primary epithelial cell cultures and RNA extraction.

Bronchial alveolar lavage

Bronchial alveolar lavage was performed by installing about 100 - 120ml pre-warmed (37°C) normal saline into the segments of the right lower lobe and then aspirating the fluid by suction (about 80 – 100ml) into a bronchial lavage fluid trap.

TABLE. BRONCHIAL BIOPSIES SUBJECT CHARACTERISTICS		
	Control Subjects	Subjects with Mild to Moderate Asthma
Number of subjects	21	19
Number of BBX/mean per subject	53/2.5	48/2.5
Sex, F/M	13/8	7/12
Age: Mean (range) years	36 (21-54)	34 (21-65)
FEV1, % predicted ± 10%	107 ± 10%	90 ± 10%*
ICS (BDP equivalent, µg/day)	0	670(200-2000)
LABA, yes/no	0	0/19
Definition of abbreviations: F = females; M = males; FEV1 = forced expiratory volume in 1 second; ICS = inhaled corticosteroids; BDP = beclomethasone diproprionate; LABA = long acting beta-agonists; BBX = bronchial biopsies, * significant difference ($p<0.05$)		

Table 2.1 Subject characteristics. I.

Bronchial biopsies subject characteristics from normal control and mild to moderate asthmatic subjects.

TABLE. BRONCHIAL BIOPSIES SUBJECT CHARACTERISTICS		
	Control Subjects	Subjects with Severe Asthma
Number of subjects	8	15
Number of BBX/mean per subject	15/1.9	23/1.5
Sex, F/M	3/5	11/4
Age: Mean (range) years	41 (19-64)	44 (17-71)
FEV1, % predicted (range)	105 (90-134)	70 (30-125)*
Atopy, yes/no	5/3	9/6
ICS (BDP equivalent, μg/day)	0	2000(500-4000)
LABA, yes/no	0	15/0
Definition of abbreviations: F = females; M = males; FEV1 = forced expiratory volume in 1 second; ICS = inhaled corticosteroids; BDP = beclomethasone diproprionate; LABA = long acting beta-agonists; BBX = bronchial biopsies, * significant difference ($p<0.05$)		

Table 2.2 Subject characteristics. II.

Bronchial biopsies subject characteristics from normal control and severe asthmatic subjects.

TABLE. BRONCHIAL BRUSHINGS SUBJECT CHARACTERISTICS		
	Control Subjects	Subjects with Severe Asthma
Number of subjects	6	9
Number of BBR/mean per subject	14/2.3	16/1.8
Sex, F/M	1/5	6/3
Age: Mean (range) years	42 (19-64)	47 (17-63)
FEV_1, % predicted (range)	106 (90-134)	64 (30-119)*
Atopy, yes/no	3/3	5/4
ICS (BDP equivalent, μg/day)	0	2000(50-4000)
LABA, yes/no	0	9/0
Definition of abbreviations: F = females; M = males; FEV_1 = forced expiratory volume in 1 second; ICS = inhaled corticosteroids; BDP = beclomethasone diproprionate; LABA = long acting beta-agonists; BBR = bronchial brushings, * significant difference ($p<0.05$)		

Table 2.3 Subject characteristics. III.

Bronchial brushings subject characteristics from normal control and severe asthmatic subjects.

2.1.3 Human embryonic subjects

The collection and use of human embryonic material was carried out under the guidelines of the Polkinghorne Committee following ethical approval from the Southampton and South West Hampshire Joint Local Research Ethics Committee and Newcastle Health Authority and informed consent from the donor. Human embryonic tissue was collected, staged, and processed by Professors David Wilson and Neil Hanley as described previously (Hanley *et al.* 2000). Fetal foot length measurement was used as most accurate method for dating gestational age (age calculated from the first day of the last menstrual period) (Hern 1984; Drey *et al.* 2005). The gestational age was between 9 and 13 weeks and developmental age (=gestational age minus 14 days) between 7 and 11 weeks (www.fpnotebook.com/OB3.htm). Expertise in embryogenesis and human embryonic/fetal lung tissue was provided by Professors David Wilson and Neil Hanley, Division of Human Genetics, Southampton University.

2.2 Section: Culture

All media and supplements were purchased from Invitrogen Ltd, UK unless otherwise specified. Cells were grown in a humidified Haraeus incubator at 37°C, 5% CO_2. Fibroblasts were grown in DMEM (Dulbecco's Modified Eagle Medium) supplemented with 10% v/v heat inactivated fetal bovine serum, 50 IU/ml penicillin, 50 µg/ml streptomycin, 2mM L-glutamine, 100x non-essential amino-acids and 100mM sodium pyruvate, unless otherwise stated.

2.2.1 Human adult cell culture

Human primary adult bronchial fibroblasts (HPABF)

Prior to use, all media and trypsin were pre-warmed to room temperature. Primary human bronchial fibroblasts were grown from biopsies obtained by fiberoptic bronchoscopy. Biopsies were placed into one well of a 6-well plate with 3ml of supplemented DMEM. The biopsy was cut into small tissue pieces and anchored into grooves upon the surface of the well freshly scored with a sterile scalpel blade. The tissue was cultured for approximately one week during which time fibroblast migrated from the tissue and proliferated on the base of the well.

The fibroblasts cultures were then grown in the same supplemented DMEM (changed every other day) until confluent and then passaged. Fibroblasts for cultures were used for assays up to passage 9.

To passage confluent cultures, the cell monolayer was washed twice for one minute with Hank's Balanced Salt Solution (HBSS) without Ca^{2+} and Mg^{2+}. 3-5 ml of 1xTrypsin ethylenediaminetetracetic acid (EDTA) solution diluted in HBSS without Ca^{2+} and Mg^{2+} was then washed over the cells and removed. The cultures were then incubated at 37°C for 1-3 minutes. The flask was then sharply tapped and the detached cells collected in supplemented DMEM.

2.2.2 Human embryonic cell culture

Human primary embryonic/fetal lung fibroblasts (HPELF)

Primary human embryonic/fetal lung fibroblasts were grown from embryonic fetal lungs obtained from terminated pregnancies. Embryonic/fetal lungs were placed into 100mm petri dishes with 3ml of supplemented DMEM. The lungs were cut into small tissue about 1mm pieces and anchored into grooves upon the surface of the dish freshly scored with a sterile

scalpel blade. The pieces of tissue was cultured in 10ml of medium for approximately one to two weeks during which time embryonic/fetal fibroblasts migrated from the tissue and proliferated on the base of the well.

The embryonic/fetal fibroblasts were then further cultured and passaged in the same way as the human adult fibroblasts.

2.2.3 Human embryonic/fetal explant culture

HELs developmental age between 7 and 11 weeks (Figure 2.1), were dissected and cut into 1 to 2mm pieces in a laminar flow hood to be used for explant cultures.
Based on a method for culturing embryonic mouse lung explants (as early as embryonic day 11 and 12) using an air medium interface in a transwell inserts (Tollet *et al.* 2002), a new human embryonic lung (HEL) explant culture model was developed. To mimic the intrauterine environment HEL tissue pieces were placed onto the membrane of the insert and additionally embedded in Matrigel™ Matrix that gets semi-solid at 37°C (air-matrigel-medium interface) with medium only at the bottom in the well (Figure2.2). This new system allowed culturing and studying of HELs for several weeks in contrast to earlier described HEL explant culture methods that used only an air-medium interface (Snyder *et al.* 1981; Gonzales *et al.* 1986; Cossar *et al.* 1990).
The pieces of lung tissue were placed onto a polyester membrane of clear transwells that were inserted into 24 Well Clusters/Case (Corning Incorporated, Costar® Transwell® 3470-Clear, NY, USA) and 340µl of serum free medium were pipetted into the wells. Pipette tips kept at -20°C were used to pipette ice-cold 50 to 60 µl of Growth Factor Reduced (GFR) Matrigel™ Matrix (BD Biosciences, Oxford, UK) onto the explants (Figure 2.2). The explants were incubated at 37°C and 5% CO_2 in a Heraeus HERAcell 150 incubator (Kendro Laboratory Products plc, Bishop's Stortford, UK) for 6 – 18 days (Figure 2.3 A-D). Medium in the wells was collected and replaced every third day. Time lapse microscopy was performed for 8 days to demonstrate branching morphogenesis (Figure 2.4) (See movie 1 in attached CD) and lungs could be grown and cultured in this model up to 6 weeks.

In vitro exposures

Using this newly developed explant culture system, HELs were cultured in the presence of the Th2 cytokine recombinant human IL-13 at 1ng/ml (Catalogue # 213-IL, R&D Systems, Inc., Abingdon, UK). The tissue was harvested into Trizol® for RNA extraction at 6, 12 and 18 days. Phase contrast images were taken at day 0, 6, 12 and 18 using a LEICA DM IRB inverted microscope. (Leica Microsystems GmbH, Wetzlar, Germany) (Figure 2.3). Some

tissue was harvested into Acetone for GMA embedding, 4% paraformaldehyde for whole mount confocal fluorescent immunochemistry.

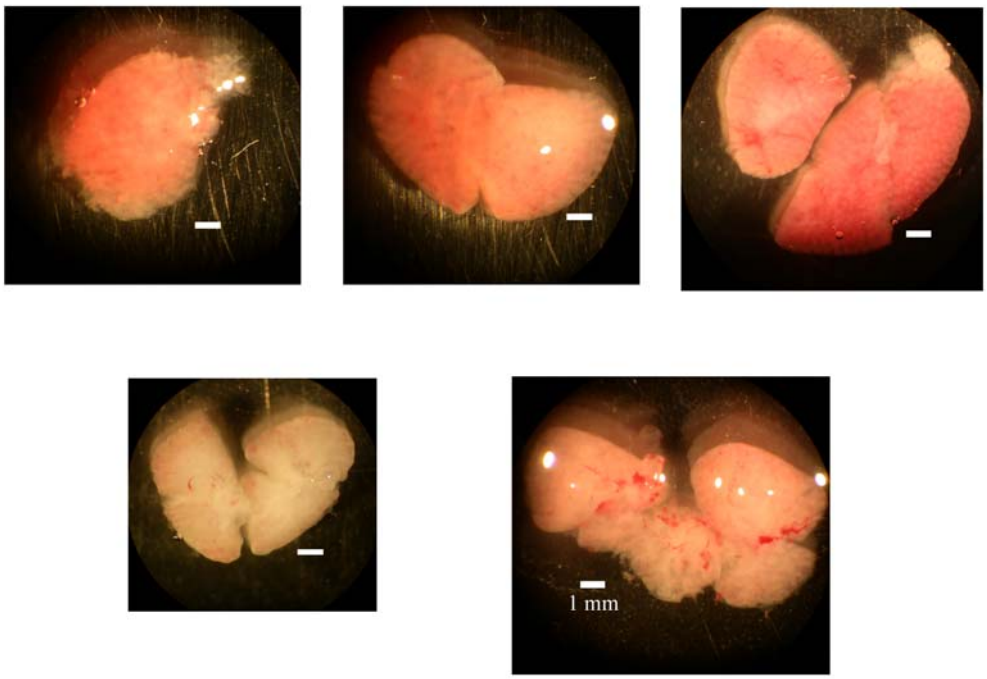

Figure 2.1 Whole and single lobes of HELs.

Freshly collected HELs before dissection showing whole singular lobes developmental age 7-9 weeks from 5 subjects.

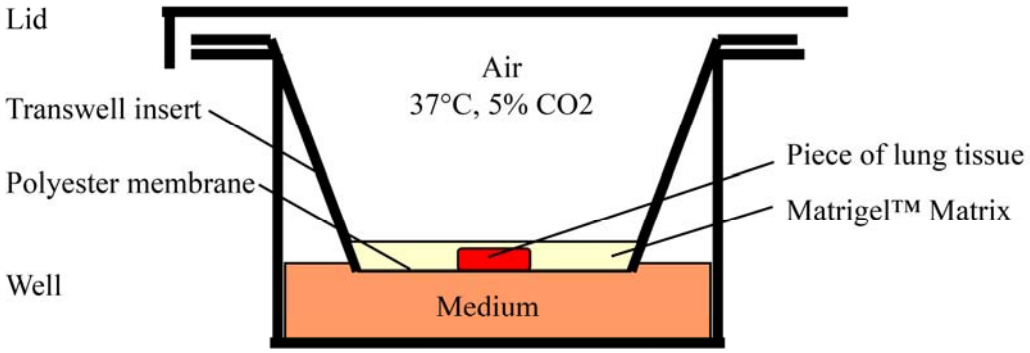

Figure 2.2 Human embryonic/fetal lung explant culture model.

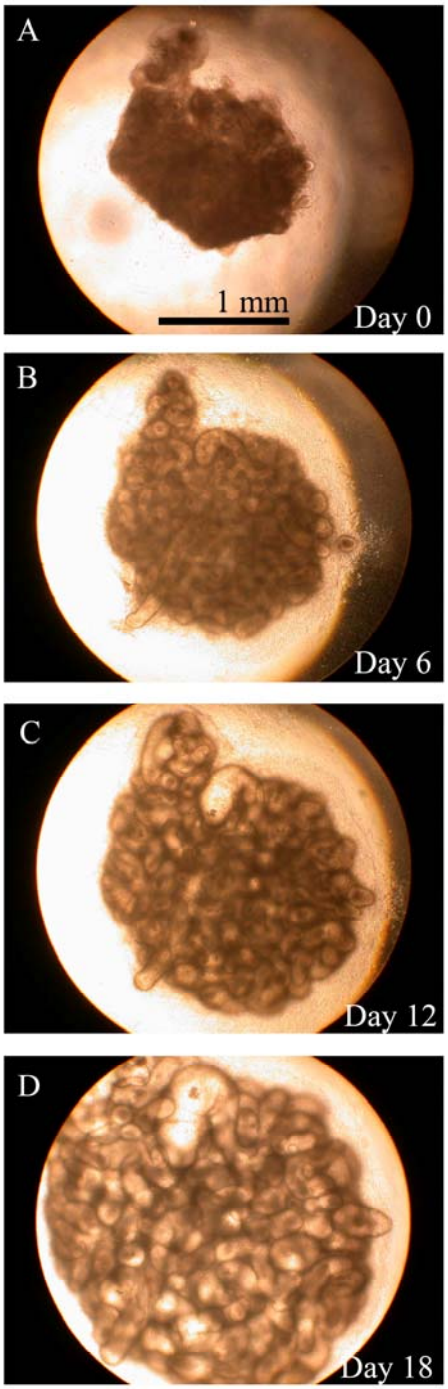

Figure 2.3 Phase contrast microscopy of HEL explant cultures.

Phase contrast images of HELs that were dissected into 1 to 2 mm big tissue pieces (A) and grown in serum-free medium (UltraCulture) for 6 days (B), 12 days (C) and 18 days (D).

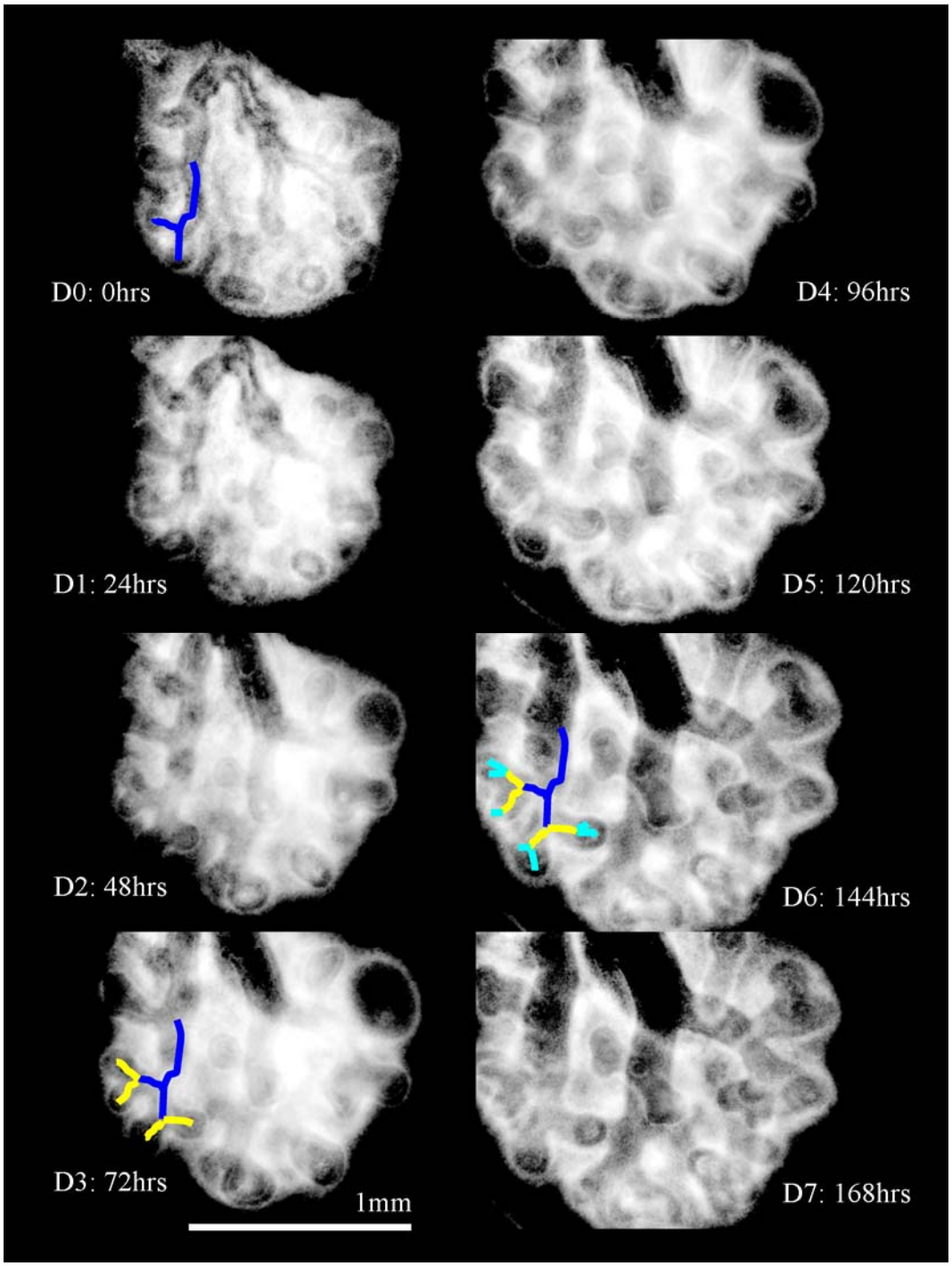

Figure 2.4 Time lapse microscopy of HEL explant culture.

Time lapse of HEL grown for 8 days showing branching morphogenesis (blue, yellow, green) in inverted single images at 24 hours (hrs) intervals for 7 days (D) (See movie 1 in attached CD)

2.2.4 Knock down experiments

Theory

In 1998 Andrew Fire and Craig Mello discovered post-transcriptional sequence-specific gene silencing using small interfering RNA (siRNA) in nematodes (Fire *et al.* 1998) for which they received the Nobel price for Medicine as early as in 2006 (Bernards 2006). This underlines their groundbreaking discovery. However, the discovery that RNA interference (RNAi) is also active in mammals (Elbashir *et al.* 2001; McCaffrey *et al.* 2002) opened the use of this exciting novel technology for basic and clinical research in 2001/2002.
RNAi is a cellular mechanism that occurs naturally and induces post-transcriptional gene silencing via siRNA and micro RNA (miRNA) (Bentwich *et al.* 2005) or epigenetic activation via Piwi-interacting RNA (piRNA) (Aravin *et al.* 2007; Yin and Lin 2007). siRNA lead to mRNA degradation whereas miRNA suppress the translation of target genes by binding at the 3'UTR of the gene of interest.
Only the mechanism of siRNA gene 'knockdown' will be discussed in this chapter as it will be used in this work.

siRNAs are short duplexes of RNA (21-23 nucleotides) that are derived from long double-stranded RNA (dsRNA) which is cleaved by Dicer, a multidomain ribonuclease (RNase) III enzyme. In lower organisms RNAi is thought to protect against viruses that generate long dsRNA as replication intermediate (primitive immune system). In mammalian cells long dsRNA activates an interferon response pathway as part of an antiviral defence mechanism which induces a global shutdown of protein synthesis (Bernards 2006). Short dsRNA (siRNA) fragments associate with a multiprotein complex known as the RNA-induced silencing complex (RISC). Exogenous synthetic siRNA can be administered without activating the interferon response when used in low concentrations. It is also associated with RISC which exposes the antisense strand of siRNA and allows it to recognise the complementary sequence of target mRNA. Upon binding of mRNA to RISC, the targeted mRNA is cleaved by the slicer enzyme Argonaute-2 protein (Ago-2), a critical component of RISC, and is further degraded by cellular nucleases (RNases) and RISC is recycled. This mechanisms suppresses mRNA and hence protein expression (Figure 2.5) (Gilmore *et al.* 2004; Grimm and Kay 2007).

Two mechanisms will be discussed to deliver specifically designed and synthetically produced siRNA into tissue and cells for RNAi. One of the mechanisms is the use of a DNA based vector encoding short hairpin RNA (shRNA), using Baculovirus A to transfect the

cells. The other mechanism is the use of lipid based transfection reagents (cationic liposomes) (Figure 2.5) (Gilmore *et al.* 2004).

The modified Baculovirus *Autographa californica* multiple nuclear polyhedris virus (ACMNPV; Baculovirus A) vector was initially chosen for transfection experiments as it is an insect virus and does not carry the problems of animal derived viruses that include the potential for a pre-existing immune response to the virus or the danger to form replication competent viruses. This method was used in whole tissue in the expectation to achieve high transfection efficiency.

Additionally lipid based transfection reagents were used as a siRNA delivery method. Transfection conditions were optimised for each model, in whole tissue and cells

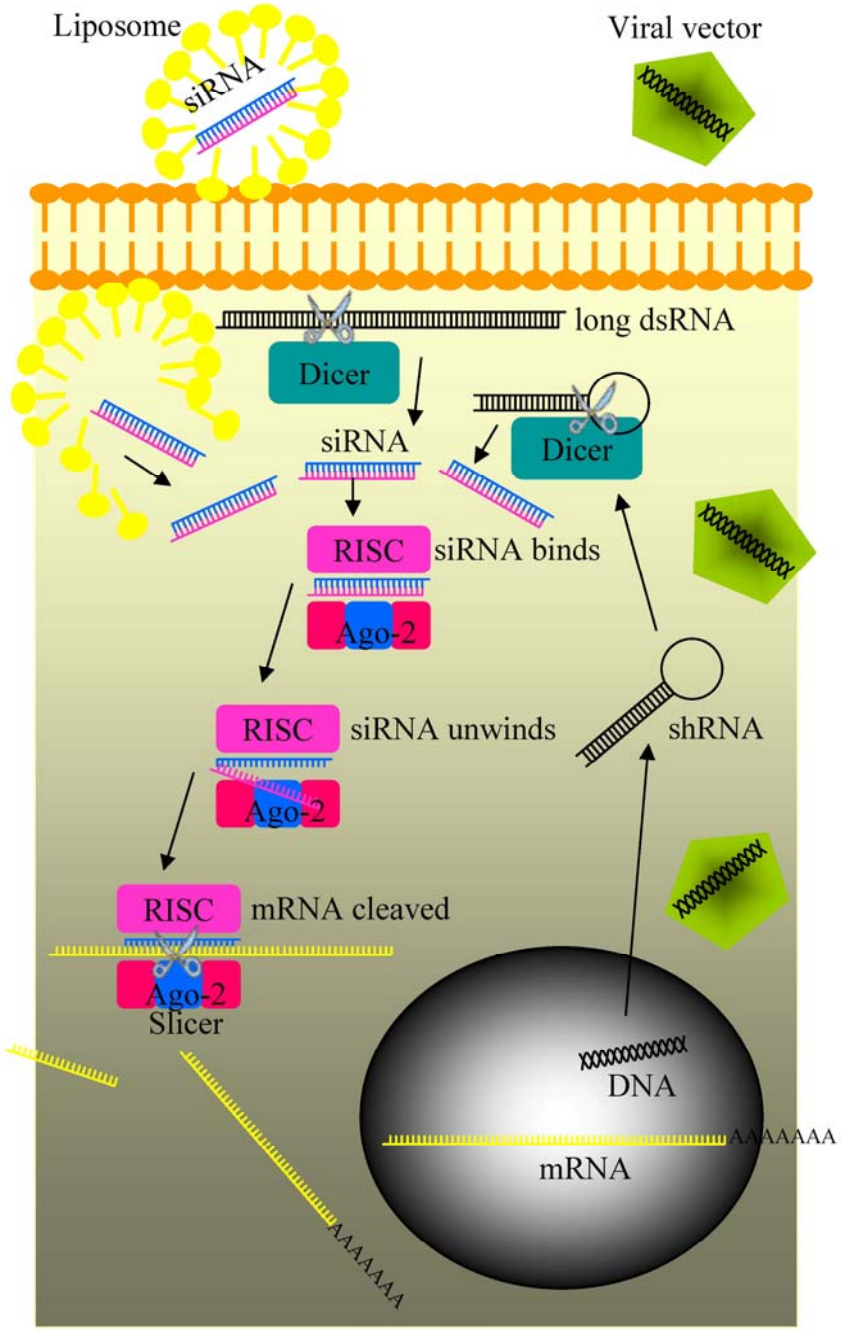

Figure 2.5 RNA interference with siRNA.

A ribonuclease III (Dicer) cleaves endogenously double-stranded RNA (dsRNA) to form siRNA. Two transfection methods used for delivery of siRNA into target cells: DNA based viral vector encoding short hairpin RNA (shRNA) & lipid based transfection reagents (cationic liposomes). shRNA is also cleaved by Dicer. siRNA is bound to the RNA-inducing silencing complex (RISC) which unwinds the siRNA and exposes the anti-sense strand to allow it to bind to the complementary sequence of the target mRNA. The mRNA is cleaved by the Slicer Argonaute-2 protein (Ago-2) of RISC and degraded, which results in posttranscriptional silencing of target gene expression (modified from (Grimm and Kay 2007)).

HELs + Baculovirus

Human embryonic/fetal lungs were dissected and cut into 1 to 2 mm tissue pieces in a laminar flow tissue culture cabinet and 3 pieces were placed into 100µl serum free medium (UltraCULTURE™ supplemented with 50 IU/ml penicillin, 50 µg/ml streptomycin, 2mM L-glutamine) in single wells of a 96-well plate.

The modified Baculovirus *Autographa californica* multiple nuclear polyhedris virus (ACMNPV; Baculovirus A) vector, carrying the bacterial (Escherichia coli K12) gene *lacZ* that encodes the reporter protein β-D-galactosidase (gift from Christopher McCormick), at a stock concentration of $1.7x10^9$ plaque forming units per ml (pfu/ml) was used to infect HEL tissue pieces. In bacteria, β-D-galactosidase cleaves the disaccharide lactose into glucose and galactose and therefore it is able to cleave X-gal (5-bromo-4-chloro-3-indolyl-β-D-galactopyranoside) into galactose and a colourless indoxyl monomer that forms a homodimers resulting in a halogenated indigo which is very stable and insoluble blue product which can be visualised.

HEL tissue pieces were incubated at different virus concentrations ($5x10^6$, $8x10^6$, $1x10^7$, $2x10^7$, $3x10^7$, $4x10^7$ and $5x10^7$ pfu/ml) at 37°C in 5% CO_2 for 24 hours. HEL tissue pieces were also grown without being transfected with the Baculovirus A vector to control for background activity of endogenous β-D-galactosidase or its isozymes. After 24 hours HEL tissue pieces were stained in situ for β-galactosidase activity according to a modified protocol from the β-Galactosidase Enzyme Assay System (Cat. # E2000; Promega, Southampton, UK). HEL tissue pieces were twice washed in 1xPBS which was completely removed after final wash. Tissue was fixed in 150µl/well 4% paraformaldehyde/PBS solution (PFA), pH 7.4, for 30 minutes at room temperature. 4%PFA was removed and tissue was washed 4 times with 1xPBS which was completely removed after final wash. 100µl of 0.2% X-Gal solution/well as a substrate for β-Galactosidase was added and incubated for 1 to 16 hours after which the X-Gal solution was removed and replaced with 1xPBS. HELs were then assessed for β-Galactosidase activity (blue staining) with a inverted microscope LEICA DM IRB (Leica Microsystems GmbH, Wetzlar, Germany) and phase contrast and light microscopy images were taken with a digital camera (NIKON Coolpix 995 from Nikon UK Limited Kingston upon Thames, UK) (See chapter 4 Figures 4.13, 4.14, 4.15).

siRNA & transfection reagents

siRNA was purchased from DHARMACON part of Thermo Fisher Scientific, US. 5nmol of siGLO-RISC free control siRNA, siGLO-Cyclophillin control siRNA (both labelled with DY-547 (Filter: Cy™3, Rhodamine, or PE, Absorbance: 557, Emission: Max: 570nm.), GAPDH control siRNA, SMARTpool® control siRNA, SMARTpool® ADAM33 siRNA,

and single siGENOME ADAM33 duplexes (Table 2.6 and see chapter 4, tables 4.1 & 4.2) were resuspended in 250µl of 1x siRNA buffer (20nM KCL, 6 mM HEPES-pH 7.5, 0.2 mM $MgCl_2$; provided by Dharmacon) and divided into aliquots of 25µl stock siRNA at 20 µM concentration and stored at -20°C.

Transfection reagents DharmaFECT™ 1, 2, 3 and 4 were purchased from DHARMACON and X-tremeGENE siRNA Transfection Reagent from Roche Applied Science, UK.

HELs + siRNA

Human embryonic/fetal lungs were cut into 1 to 2 mm tissue pieces in a laminar flow tissue culture cabinet and placed into 100µl serum free medium without antibiotics (UltraCULTURE™ supplemented only with L-Glutamine) in 96 wells.

For initial optimisation experiments siGLO-RISC free control siRNA (labelled with DY-547 at 100nM was used to transfect HEL whole tissue pieces with DharmaFECT™ 1, 2, 3 and 4 (Dh1 to 4) (Table 2.4) at different concentrations for Dh1, Dh2 and Dh4 at: 0.2, 0.4 and 0.8µl/100 µl total medium and for Dh3at: 0.4, 0.8 and 1.6µl/100µl total medium all in triplicate according to the Basic DharmaFECT™ Transfection Protocol (Table 2.5).

Before use of siRNA, 20 µM stock siRNA was first diluted to 2 µM with 1x siRNA buffer. 2µM siRNA (Tube 1) and appropriate DharmaFECT™ transfection reagent (Tube 2) was prepared in serum-free and antibiotic-free medium (SFM: UltraCULTURE™) in separate tubes (Table 2.5). Two master mixes (Tube 1 and 2) were prepared (total 350µl for distribution of 100µl/well in triplicate in a 96 well-format). In tube 1, 17.5µl of 2µM siRNA was added to 17.5µl of serum free medium to a total of 35µl. In tube 2, the appropriate volume of desired DharmaFECT transfection reagent was added to SFM (for example 0.4µl of Dh1 plus 34.6µl SFM to total volume of 35µl).

The content of each tube was gently mixed by pipetting up and down and incubated for 5 minutes at room temperature. Then the contents of tube 1 and 2 were combined (total volume 70µl), mixed by carefully up and down pipetting and incubated for 20 minutes at room temperature. After this sufficient UltraCULTURE™ was added to the mix to reach the desired transfection volume (280µl for a total of 350µl). The culture medium from the wells of the 96-well plate was removed and 100 µl of the appropriate transfection mix was added to each well containing a tissue piece of dissected HELs. The plate was incubated at 37°C in 5% CO_2 for 24 to 48 hrs. Phase contrast images and immunofluorescent images were taken after 24 and 48 hours using a LEICA DM IRB inverted microscope (Leica Microsystems GmbH, Wetzlar, Germany). After 48 hours pieces of tissue were fixed in 4% paraformaldehyde for confocal microscopy using a LEICA TCS SP2 confocal microscope (Leica, Mannheim, Germany).

Primary fibroblasts + siRNA using DharmaFECT™ transfection reagent

Primary human adult bronchial fibroblasts and primary human embryonic/fetal lung fibroblasts were grown in 96-well plates and 24-well plates in the presence of supplemented DMEM until about 60-70% confluence. DMEM was then replaced with Serum-free Medium UltraCULTURE™ supplemented only with L-Glutamine without antibiotics (Lonza Biologics plc, Slough, UK) overnight. For initial optimisation experiments Dh1 and Dh4 transfection reagents (both had showed the least toxicity in HEL tissue transfection experiments) were used at 0.2µl/100 µl total transfection medium with siGLO-RISCfree control siRNA in triplicate for 48 hours, using the same protocol as for HEL tissue transfections (See section above). Phase contrast and fluorescence imaging of the cells was performed after 24 and 48 hours using a LEICA DM IRB inverted microscope (Leica Microsystems GmbH, Wetzlar, Germany). Transfection was also performed using 3 control siRNAs, siGLO RISC-free, siGLO Cyclophilin B, and siCONTROL GAPDH siRNA using the protocol described above. After 24 and 48 hours cells were harvested in TRIzol for RNA extraction and RT-qPCR.

DharmaFECT™ transfection reagents			
DharmaFECT™	**Properties**	**Use (µl/100µl medium/96 well)**	**Range**
Dh1	highest efficiency	0.4	0,05 – 0.4
Dh2	least toxicity	0.4	0.1 – 0.4
Dh3	efficient certain cells	0.8	to 1.6
Dh4	mouse & rat	0.4	0.4 – 0.8

Table 2.4 DharmaFECT™ transfection reagents.

Four different DharmaFECT™ transfection reagents, their main properties and recommended concentration of use in one well from a 96-well plate.

DharmaFECT transfection protocol						
Plate Format		**Tube 1 Volumes per well**		**Tube 2 Volumes per well**		**Plating Volume (µl/well)**
wells/plate	**cm^2/well**	**2µM siRNA (µl)**	**SFM (µl)**	**Dh1-4 (µl)**	**SFM (µl)**	**Transfection Medium**
96	0.3	5	5	0.05 – 0.5	9.95-9.5	100
24	2	25	25	0.5 – 2.0	49.5-48.0	500
12	4	50	50	1.0 – 3.0	99.0-97.0	1000
6	10	100	100	2.0 – 6.0	198.0-194.0	2000

Table 2.5 DharmaFECT™ transfection reagent protocols.

Recommended volumes for transfecting 100nM siRNA in various plating formats. DharmaFECT™ volumes per well represent guidelines that needed to be optimised (adapted from Dharmacon Basic DharmaFECT™ Transfection Protocol).

DHARMACON siRNA				
	Catalogue Nr	**Gene description**	**Target accession Nr**	**Use**
siGLO RISC-Free siRNA*	D-001600-01-05	-	Non-targeting + RISC-Free modification	Control
siGLO Cyclophilin B siRNA*	D-001610-01-05	Cyclophilin	NM_000942(Human) NM_011149(Mouse) NM_022536(Rat)	Control
siCONTROL GAPDH siRNA	D-001140-01-05	GAPDH	NM_002046(Human)	Control
siCONTROL NonTargeting siRNA Pool	D-001206-13-05	-	Non-targeting 4 mismatches	Control
siGENOME SMARTpool siRNA	M-004525-00	ADAM33	NM_025220(Human) NM_153202(Human)	Target
siGENOME SMARTpool siRNA	M-004525-01	ADAM33	NM_025220(Human) NM_153202(Human)	Target
siGENOME Duplex 1	D-004525-01	ADAM33		Target
siGENOME Duplex 5	D-004525-05	ADAM33		Target
siGENOME Duplex 6	D-004525-06	ADAM33		Target
siGENOME Duplex 7	D-004525-07	ADAM33		Target
* labelled with DY-547 (Filter: Cy^{TM}3, Rhodamine, or PE, Absorbance: 557, Emission: Max: 570nm.				

Table 2.6 Details of control and target siRNAs from DHARMACON.

Primary fibroblasts + siRNA using X-tremeGENE transfection reagent

Primary human embryonic/fetal lung fibroblasts were grown in 24-well plates in the presence of supplemented DMEM until about 60-70% confluence. DMEM was then replaced with Serum-free Medium Opti-MEM®-1 Reduced Serum Medium without supplements (GIBCO, Invitrogen Ltd, Paisley, UK) overnight.

X-tremeGENE siRNA Transfection Reagent (XG) was a newly available reagent for transfection of siRNA into animal cells (Roche Applied Science, Mannheim, Germany). It was tested as it has the advantages of low cyto-toxicity which does not require the change of media after addition of transfection complex, and it functions also well in the presence or absence of serum, eliminating the need to change media.

Initial experiments were performed to optimise the concentration of XG transfection reagent and siRNA using siGLO-RISCfree non-functional non-targeting control siRNA and siGLO Cyclophilin B silencing control siRNA to evaluate transfection efficiency, toxicity and knock down effect according to the adapted X-tremeGENE transfection protocol.

20 µM stock siRNA was first diluted to 2µM with 1x siRNA buffer. 2µM siRNA (Tube A) and appropriate X-tremeGENE transfection reagent (Tube B) was prepared at different concentrations in both, serum- and antibiotic-free medium (SFM: Opti-MEM-1) in separate tubes (Tables 2.7 & 2.8). The two master mixes (Tube A and B) were prepared for a final transfection mixture volume of 100µl per well in a 24 well-format. In tube A different volumes of desired X-tremeGENE transfection reagent were added to different volumes of SFM (for example 5µl of XG plus 45µl SFM for a total volume of 50µl). In tube B different small volumes of 2µM siRNA were added to 50µl of serum free medium. The content of each tube was gently mixed by pipetting up and down and incubated for maximum 5 minutes at room temperature. Then the contents of tube A and B were combined (total volume about 100µl), mixed by carefully up and down pipetting and incubated for 15 to 20 minutes at room temperature. All mixtures were prepared in triplicate and 100 µl of the appropriate transfection mix was added drop-wise to each well containing cells growing in 400µl Opti-MEM-1 (total transfection medium volume: 500µl). The plate was cautiously swirled to ensure even distribution over the entire plate surface before it was incubated at 37°C in 5% CO_2 for 24 to 48 hrs. Phase contrast images and immunofluorescent images were taken after 24 and 48 hours using a LEICA DM IRB inverted microscope (Leica Microsystems GmbH, Wetzlar, Germany). After 48 hours cells were harvested in TRIzol for RNA extraction and RT-qPCR. All these different optimisation concentrations of XG transfection reagent and siRNA were tested in triplicate.

X-tremeGENE transfection optimisation protocol 1				
		Tube 5	**Tube 2.5**	**Tube 1**
Tube A	Opti-MEM-1 (µl)	45	47.5	49
	XG (µl)	5	2.5	1
Tube B	Opti-MEM-1 (µl)	50	50	50
	2µM siRNA (µl)	7.5	3.75	1.5
24-well plate				
Total transf. medium/well	Opti-MEM-1 (µl)	500	500	500
siRNA/well	nM	30	15	7.5

Table 2.7 X-tremeGENE transfection optimisation protocol 1.

Transfection optimisation protocol using different concentrations of X-tremeGENE transfection reagent (XG) and siGLO siRNA in one well of a 24-well plate (adapted from X-tremeGENE siRNA Transfection Reagent Protocol).

X-tremeGENE transfection optimisation protocol 2					
		Tube 2	**Tube 1**	**Tube 0.5**	**Tube 0.33**
Tube A	Opti-MEM-1 (µl)	48	49	49.5	49.67
	XG (µl)	2	1	0.5	0.33
Tube B	Opti-MEM-1 (µl)	50	50	50	50
	2µM siRNA (µl)	15	7.5	3.75	2.5
24-well plate					
Total transfec. Medium/well	Opti-MEM-1 (µl)	500	500	500	500
siRNA/well	nM	60	30	15	10

Table 2.8 X-tremeGENE transfection optimisation protocol 2

Transfection optimisation protocol using different concentrations of X-tremeGENE transfection reagent (XG) and siGLO siRNA in a well of 24-well plates (adapted from X-tremeGENE siRNA Transfection Reagent Protocol).

2.3 Section: Gene expression

2.3.1 RNA extraction

Harvesting of mouse tissue

Specific pathogens free 6 weeks old out bred MF-1 mice (obtained from Harlan UK Limited, Bicester, UK) were kept and time mated by detection of a vaginal plug in the Biomedical Research Facility (BRF). This day was taken as embryonic day (ED) 0. Pregnant mice between ED 10-20, newborn and juvenile mice were killed using a Schedule 1 method (cervical dislocation). Breeding, time mating and killing of animals were performed by Mrs Jas Barley and her team, Kerry Taylor and Michael in the BRF. Gravid uteri were removed under sterile conditions and embryos killed according to schedule 1 method (neural tube dissection, cervical dislocation). Maternal adult, embryonic and postpartum lungs, hearts and brains were dissected in a laminar flow hood. Embryos were dissected under a dissecting microscope (LEICA WILD M3Z, Wetzlar, Germany) (Figure 2.6). The dissected lungs, hearts, and brains were then placed in RNA*later*® (Catalogue# AM7020; Ambion®, Applied Biosystems, Warrington, UK) or directly homogenised in TRIzol® (Invitrogen, Paisley, UK) and stored for later RNA extraction. Usually 10-18 embryos could be obtained from one pregnant mouse.

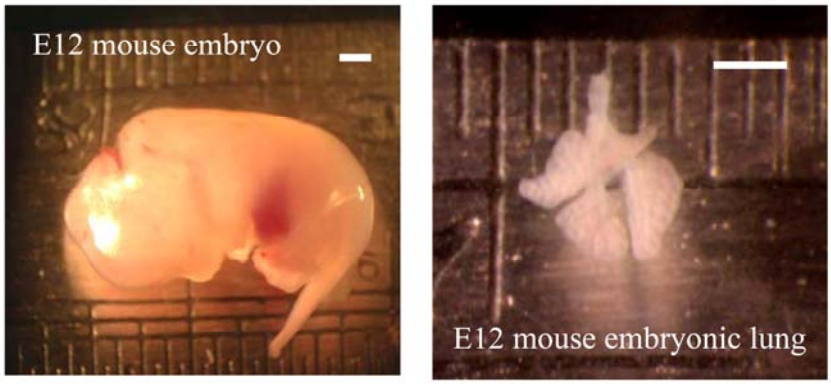

Figure 2.6 ED12 mouse embryo and lungs.

Whole embryonic day 12 mouse embryo and dissected lung, containing one left lobe and four right lobes. White bar is 1mm.

Homogenisation of tissue and cells

Immediately after harvesting, fresh tissues from bronchial biopsies or mouse organs were homogenised (ribolysed) in Lysing Matrix D impact-resistant 2.0 ml tubes containing 1.4 mm ceramic spheres (Qbiogene, UK) and 1ml of TRIzol® ((Invitrogen, Paisley, UK) using a Hybaid RiboLyser™ Cell Disrupter (Thermo Life Sciences, Hybaid UK) at speed settings 6.0 and for 40 seconds. Tubes were cooled on ice for 2 minutes and ribolysed for a second time with the same settings to completely homogenise the pieces of bronchial tissue and then cooled down on ice for 2 minutes and incubated at room temperature for 5 minutes.

Human embryonic/fetal lungs were dissected under a dissecting microscope in a laminar flow cell culture cabinet. One to three small pieces of HEL lung tissue were placed into 250µl of Trizol in 0.5ml RNase- and DNAse-free Eppendorf microtubes (Sigma-Aldrich, Gillingham, Dorset, UK or STAR LAB Milton Keynes, UK) containing 3 to 5 ceramic spheres from the Lysing Matrix D tubes. Tissue was ribolysed in the Hybaid RiboLyser at speed settings 6.0 for 10 seconds then cooled on ice for 2 minutes and incubated at room temperature for 5 minutes.

Cells grown in wells of 24-well or 96-well plates were solubilised in 250 - 500µl or 100µl (depending on surface area) of TRIzol by pipetting up and down and then incubated at room temperature for 5 minutes. The homogenate was then collected in 500 or 1500µl Eppendorf microtubes for storage or RNA extraction.

After homogenisation, tissue or cells samples were either processed immediately for RNA extraction or stored at -80°C.

RNA extraction (adapted from TRIzol® Reagent protocol)

All RNA extractions and RNA processing were performed in a specifically designated RNA processing area in the Roger Brooke Laboratory. The RNA work bench was cleaned with RNaseZap (R-2020, Sigma-Aldrich Company Ltd., Gillingham, UK) and DNA-Remover (Minerva Biolabs GmbH, Berlin, Germany) to prevent RNA degradation and DNA contamination of the samples before the start of each experiment. To prevent contaminations from pipettes ART® Aerosol Resistant barrier tips (Molecular BioProducts, Inc., San Diego, CA, USA) were used for all experiments.

200µl of chloroform, minimum 99% (C2432-500ml, Sigma, UK) per ml of TRIzol (Chomczynski and Piotr 1994) (or proportional volumes) were added to tubes containing the freshly homogenised tissues or cells or the defrosted samples. Samples were shaken vigorously by hand for 15 seconds and incubated at room temperature for 2 to 3 minutes. They were then spun at 12,000g (relative centrifugal force in gravities) for 15 minutes at 4°C in a Heraeus® Biofuge® fresco or primo R (Thermo Fisher Scientific, Inc, UK). After centrifugation the mixture separated into a lower red, organic phenol-chloroform phase

containing the protein, an interphase containing the DNA, and a colourless upper aqueous phase, which exclusively contains the RNA. The volume of the aqueous phase is about 60% of the volume of TRIzol Reagent used for homogenisation. The aqueous phase was carefully (to avoid carry over of genomic DNA from the interphase) transferred into fresh Eppendorf microtubes. The organic phase and interphase were stored at minus 20°C for protein and DNA extraction at a later stage. For small quantities of tissue (1 to 10mg) or cells (10^2 to 10^4) samples, prior to the precipitation with isopropyl alcohol, 5 to 10ug RNase-free glycogen (Cat. No 10814, Sigma-Aldrich, UK) was added to the aqueous phase as a carrier for the RNA. To precipitate RNA 500µl of isopropyl alcohol (2-Propanol, for molecular biology, minimum 99%, I9516-500ml, Sigma, UK) per 1ml of TRIzol Reagent used for the initial homogenisation was added to the aqueous phase. The samples were either left to incubate at 15 to 30°C for 10 minutes or overnight at minus 20°C to increase the precipitation of RNA. If kept in the freezer overnight, samples were first vortexed for 10 seconds and then centrifuged at 12,000g for 30 minutes at 4°C. The RNA precipitate, often invisible before centrifugation, formed a gel-like pellet on the side and bottom of the tube. The supernatant was removed by pouring it off under visual control to prevent loss of the pellet. The RNA was washed in 75% ethanol (made from ultrapure water (Milli-Q Biocel System, Millipore Ltd, Watford, UK) and Ethanol absolute 3221, Riedel-de Haën (Sigma-Aldrich, Seelze, Germany)), by adding at least 1ml of 75% ethanol per 1ml of TRIzol Reagent used for initial homogenisation. The samples were mixed and centrifuged at 7,500g for 5 minutes at 2 to 8°C. The supernatant was poured off under visual control to prevent loss of the pellet and the samples were shortly pulse spun to collect all ethanol left on the walls of the tubes, after which the ethanol was carefully removed with a pipette using a 200µl pipette tip. The pellet was air dried for 5 to 10 minutes (not completely to prevent decrease of its solubility) before it was dissolved in the DNase treatment mixture.

DNase treatment (adapted from DNA-free™ Kit)

To remove trace contamination by genomic DNA samples were treated with DNase using DNA-free™ (Cat# AM1906, Ambion, UK) for DNase treatment and removal. The dry RNA pellet was dissolved in 20 (or 30µl) of total DNase digestion reagents. This was made up by 17µl (or 26µl) nuclease-free water, 2µl (or 3µl) 10x DNase I buffer (100mM Tris-HCl pH 7.5, 25mM $MgCl_2$, 5mM $CaCl_2$) and 1µl of recombinant DNase I (2Units/µl). The samples were incubated in a water bath (Grant W28, Grant Instruments Cambridge, UK) at 37°C for 60 minutes after which the DNase was inactivated by adding 5µl of the DNase Inactivation Reagent to the samples and incubating them for 2 minutes at room temperature and occasionally mixing them. The samples were spun at 12,000g for 2 minutes and the RNA was stored at -80°C or immediately used for quantification and reverse transcription.

Quality check and quantitation of RNA

Three different methods of quality check and quantitation of total mRNA were used. The first involved analysing the quality and quantity of RNA using an 1% Agarose gel run using a Wide Mini-Sub® Cell GT Cell and PowerPac™ (BIO-RAD Laboratories, Hercules, CA, USA). 1 gram of Agarose (Certified Molecular Biology Agarose, Cat# 161-3102, BIO-RAD Laboratories, Hercules, CA, USA) was added to 100ml of 1xTBE (made of 5x stock TBE: 54g of Tris base, 27.5 of boric acid and 20ml of 0.5M EDTA (pH 8.0) in 1 litre of water). The mixture was boiled in a microwave oven (at middle power) until the agarose was dissolved completely and the solution was clear. The solution was allowed to cool down and ethidium bromide was added to a concentration of 0.5µg/ml. A gel-tray was sealed at the ends with a tape and a 20-well comb was positioned about 3cm from one end and about 1-2mm above the surface of the tray. The cooled (to about 50°C) gel solution was poured into the tray to a depth of about 7mm and the gel allowed to solidify about 20 minutes at room temperature. Before running the gel, the tape and the comb were gently removed. The gel was placed into an electrophoresis chamber and covered with electrophoresis buffer (1xTBE) just until wells were submerged. Two µl of RNA sample was added to 8 µl of 1x loading buffer (containing Bromphenol blue) and wells were loaded with 10 µl of these sample mixtures. To quantify the RNA a 0, 0.5, 1, 2, 3, and 4µl of control-RNA (0.2µg/µl) were added to 10, 9.5, 9, 8, 7, and 6µl of 1x loading buffer and also loaded to the wells. The gel was run at 80mA for about 30 minutes and the bands were viewed with UV light and images were taken using a Molecular Imager Gel Doc XR System (BIO-RAD Laboratories, Hercules, CA, USA) (Figure 2.7). Densitometry of the RNA bands was performed and RNA concentration calculated using the RNA Standard Curve from the control-RNA bands (Figure 2.8).

The second method for RNA assessment involved using micro-fluid electrophoresis with a RNA 6000 Nano LabChip® kit in an Agilent Bioanalyser 2100 (Agilent Technologies Limited, Stockport, UK). 1µl of an RNA ladder and 1 µl of 12 RNA samples were loaded into micro-wells of a RNA 6000 Nano LabChip® kit and run on the Bioanalyser 2100. This allowed assessment of the quality of RNA extracted from whole HEL tissue pieces. Data were converted to a gel-like format allowing analysis of 18S and 28S rRNA (Figure 2.9.A-E). By using an RNA ladder as standard, the concentration of the RNA samples could also be quantified.

The third method used to assess the quality and quantity of RNA was a spectrophotometric approach using a Nanodrop ND 1000 (Nanodrop Technologies, Wilmington, DE, USA). 1µl of total undiluted RNA was placed into the machine on a pedestal that formed a sample column by surface tension (1mm path length) when the apparatus was closed. This sample retention system eliminates the need of cuvettes and capillaries. The absorbance at 260 and

280nm using a 10mm light path equivalent was measured and this was used to determine the RNA concentration and purity (pure RNA: A260/A280 ratio: 1.8 to 2.1) (Figure 2.10).

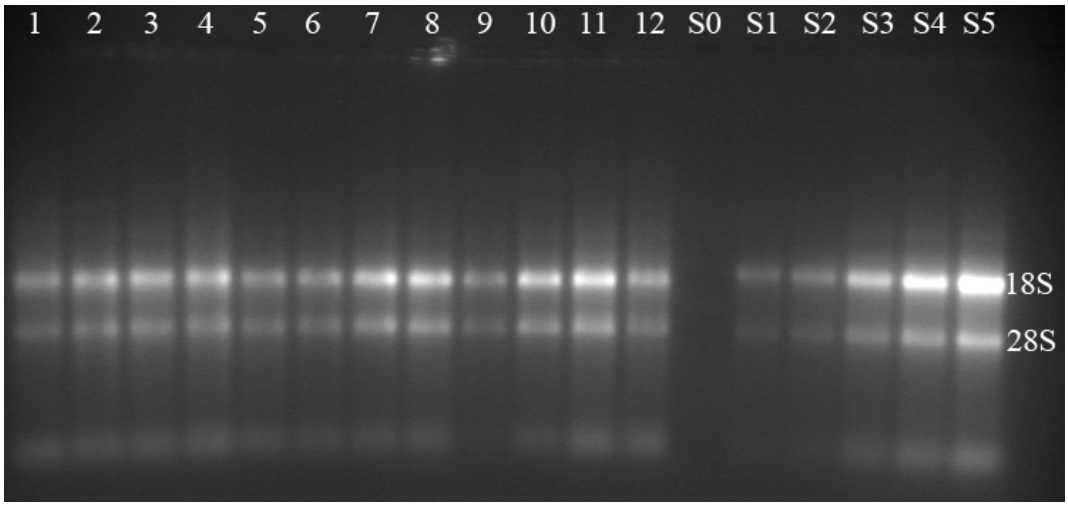

Figure 2.7 Agarose gel of 18S and 28S rRNA.

Agarose gel (1%) analysis of RNA samples 1 to 12 (primary lung fibroblasts) and Standard RNA S0 (0ng), S1 (100ng), S2 (200ng), S3 (400ng), S4 (600ng) and S5 (800ng) showing the ribosomal RNA 18S and 28S bands.

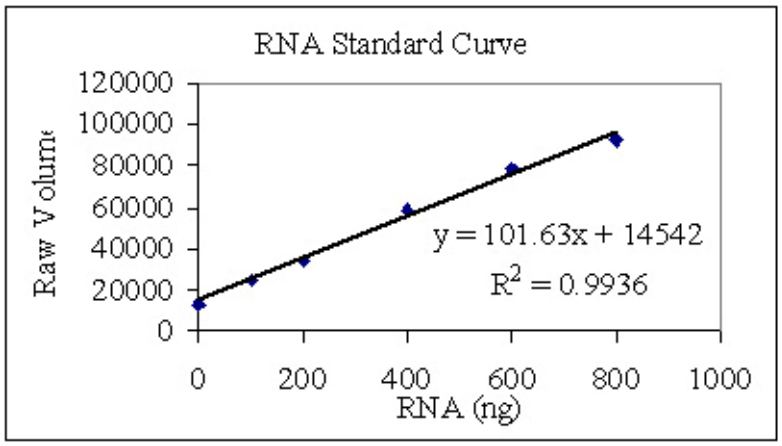

Figure 2.8 18S rRNA standard curve.

Typical RNA Standard Curve from densitometry measurement of 18S rRNA bands on Agarose Gel used to quantify RNA concentration in the RNA samples.

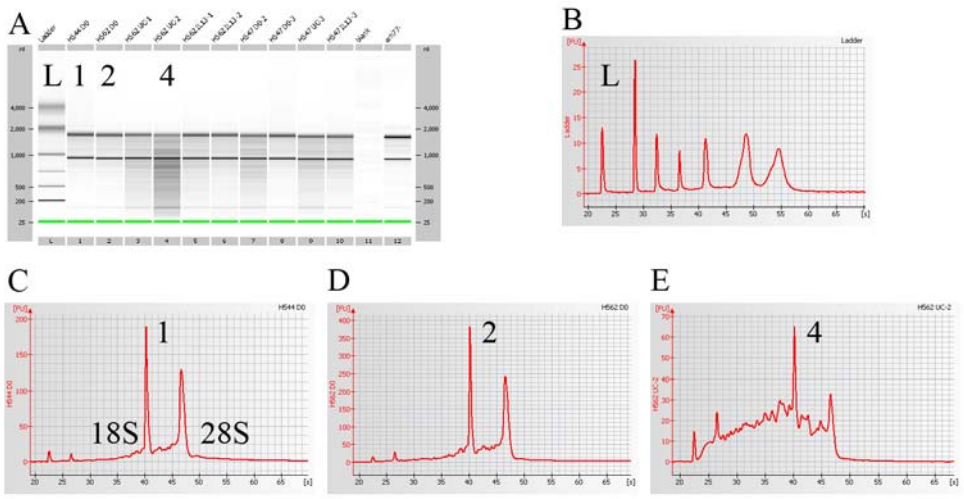

Figure 2.9 RNA assessment with Agilent 2100 bioanalyser.

RNA quality control and quantitation of human embryonic tissue samples using an Agilent 2100 bioanalyser: showing the gel-like image (A) with the RNA ladder (L) and 12 samples and electrophoresis data (B,C,D,E) of the ladder and 3 samples (1,2,4). Samples 1 and 2 show intact total RNA (C and D) and sample 4 showed partially degraded RNA (E). The RNA ladder is used to quantify the RNA concentration.

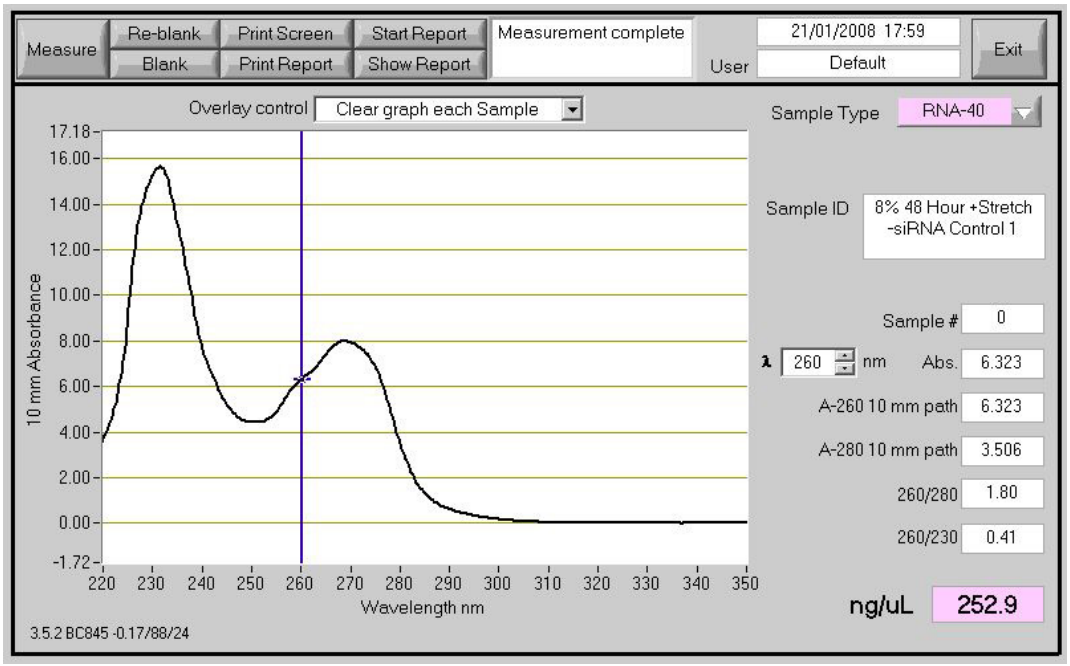

Figure 2.10 RNA assessment with Nanodrop ND 1000 spectrophotometer.

RNA quantitation and quality control of human embryonic fibroblast samples from a single well of a 6 well-plate using a Nanodrop ND 1000 spectrophotometer: showing the Absorbance curve with the concentration of RNA of 252.9 ng/µl and the 260/280 ratio of 1.80 which demonstrated relative pure RNA quality.

2.3.2 Reverse transcriptase (RT) assay

(adapted from Precision™ Reverse Transcription kit protocol; www.primerdesign.co.uk)

RNA was reverse transcribed to create cDNA which is the template used for the quantitative PCR reactions. The RT reaction has two stages 'annealing', when the primer is bound to the template and 'extension' to form new single stranded DNA
1 µg of total mRNA, determined by the methods described above was used for each reverse transcription reaction in sterile DNase-, RNase- and DNA-free thin walled 0.2ml 8 tube strips (T320-2N, Simport, Beloveil, Qc, Canada; THER-A8N, Elkay Laboratory Products Ltd, Basingstoke, UK) using Precision™ Reverse Transcription kits (Precision™ Reverse Transcription kit PrimerDesign Ltd., Southampton, UK). The volume containing 1µg total RNA was made up to 10µl by adding ultrapure water. An annealing mastermix comprising of 1µl of random Hexamer primers, 2µl of Oligo dT primer/dNTP mix and 2µl of ultrapure water per reaction was prepared. 5µl of this master mix was pipetted into each microtube and the 10µl of RNA was added. This mix was heated to 65°C for 5 minutes on a thermocycler (Eppendorf® Mastercycler® gradient, Eppendorf UK Limited, Cambridge, UK) after which it was 'snap cooled' on dry ice in ethanol or ice from minus 80°C freezer. In the meantime a second extension mastermix was prepared containing 4µl of 5x MMLV transcription buffer, 0.8µl of MMLV reverse transcriptase and 0.2µl ultrapure water per reaction. 5µl of this mix was added to the 'snap cooled' microtubes and placed into a water bath (Grant W28, Grant Instruments Cambridge, UK) at 37°C for 10 to 15 minutes and then at 42°C for 60 minutes. The RT-product, cDNA (DNA that is complementary to mRNA), was then either stored at minus 20°C or diluted 1 in 5 or 1 in 10 by adding 80µl or 180µl of ultrapure water to the 20µl of RT-product and used as template for RT-qPCR at 2.5 or 5µl template
.

2.3.3 RT-qPCR

(adapted from Precision™ qPCR Mastermix protocol; www.primerdesign.co.uk)

Theory

Polymerase Chain Reaction or PCR has become an important and widely used tool for amplifying DNA in molecular biology worldwide where a polymerase enzyme synthesises a complementary sequence of bases to any single strand of DNA that has a double stranded starting point. By adding primers (forward and reverse primers) that are complementary to the sequence of interest in the DNA/cDNA sample a target gene can be selected which enables the polymerase to bind and begin copying the gene of interest (Figure 2.11).

Changes of temperature are used to control the activity of the polymerase and the binding of primers to the target gene during the PCR. At the start the temperature is raised to 95°C to denature double stranded DNA into single strands. The reaction is then cooled down to 55°C which allows the primers to anneal to the gene of interest, which allows the polymerase to bind and to begin extending and amplifying the DNA sequence of interest. The temperature is then raised to 72°C, which is the optimal working temperature for the polymerase with maximum enzyme activity. Primers (forward and reverse primers) are directed to both single strands of the DNA which will result in a doubling in DNA copy numbers of the target gene after each cycle. A single cycle (95°C, 50°C and 72°C) can be repeated 40 to 50 times resulting in exponential amplification of the DNA of interest.

Real-Time PCR or Reverse Transcription quantitative PCR (RT-qPCR) is a novel form of standard PCR that allows the monitoring of the process in real-time by using a camera or detector that can detect fluorescently labelled DNA/cDNA product (gene copies) during each PCR cycle (Figure 2.11). As the number of gene copies increases during the reaction so does the fluorescence increase, which allows us to see the efficiency and rate of reactions taken place.

Different techniques and fluorescent dyes are used to monitor DNA amplification in real-time. Sybr green is an intercalating fluorescent dye that emits a fluorescent signal only when it is bound to double stranded DNA, which results in low specificity as the dye will also report 'miss-primed' DNA that might have also been amplified. Alternatively, fluorescent probes, Taqman-type probes, are used that are oligonucleotides (about 20-25 bases) containing at one end a fluorogenic reporter dye, such as FAM (6-carboxyfluorescein) and at the other end a quencher dye such as TAMRA (6-carboxy-N,N,N',N'-tetramethylrhodamine) (Table 2.9). The probe is complementary to a target sequence of the cDNA and binds specifically to a selected region of interest, between the forward and reverse primers. During the cycle, the Taq polymerase will bind and extend the cDNA. The Taq polymerase has 3'exonuclease activity and when in contact with the probe will cleave the FAM from the probe. This causes an increase in fluorescent intensity of the reporter dye due to its detachment from the quencher. Therefore, the faster the fluorescence reaches a set threshold (CT value), the greater is the amount of cDNA encoding the gene of interest in the reaction mix.

When two probes are used in the same TaqMan reaction (multiplexing), the emission wavelengths of the two probes have to be far enough apart to allow their individual detection. FAM (490) and Cy5 (670) fluorophores are sufficiently different to allow simultaneous detection (Table 2.9).

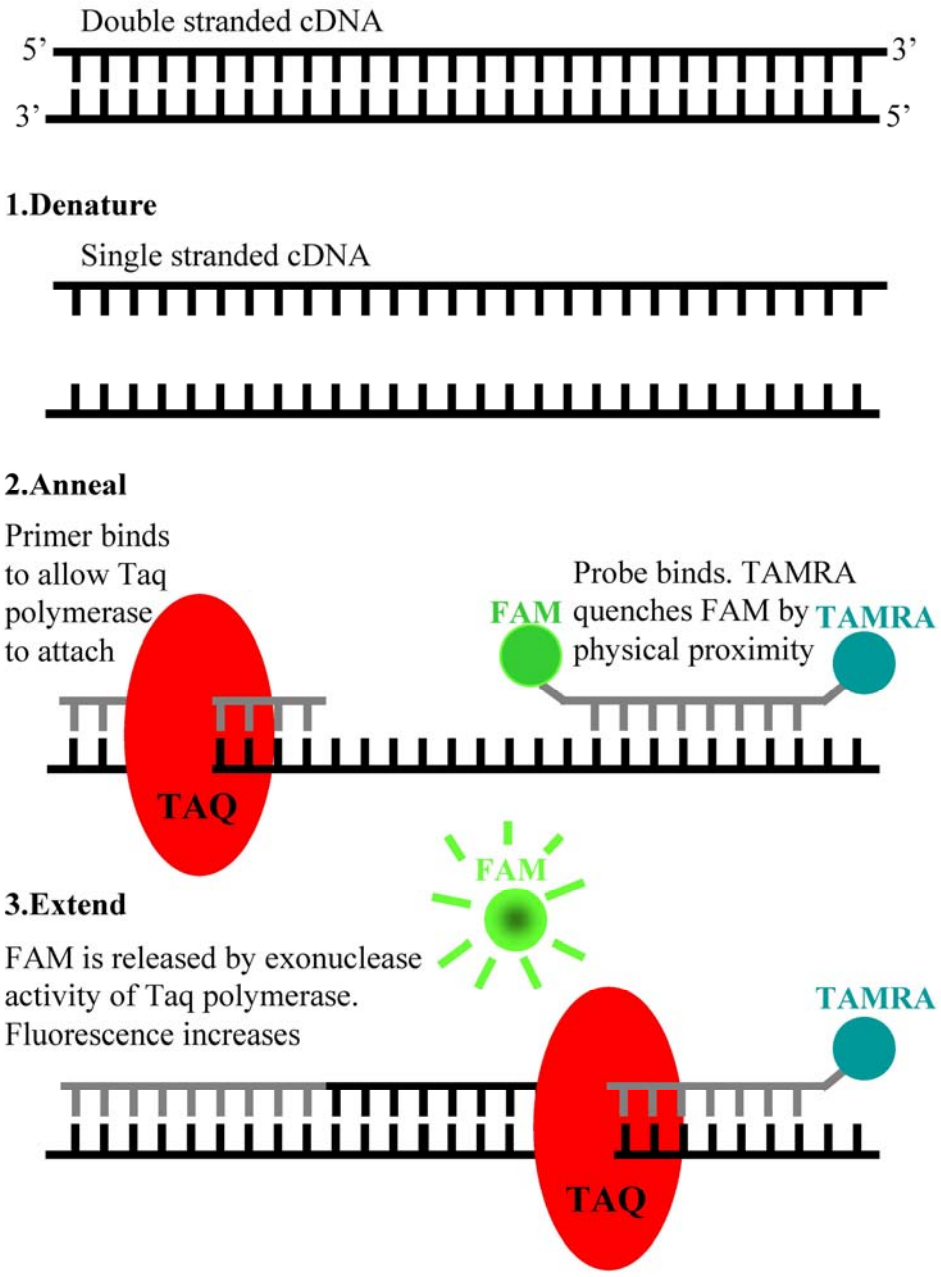

Figure 2.11 Diagram of TaqMan RT-qPCR.

Schematic representation of molecular events involved in TaqMan RT-qPCR.

Probe	Reporter: 5'-end	Emission	Quencher: 3'-end
FAM	FAM carboxyfluorescein	520nm	TAMRA
VIC	Yakima Yellow	549nm	Eclipse® DarkQuencher
Cy5	Cy5 Indocarbocyanin	667nm	ElleQuencher

Table 2.9 RT-qPCR probes labelled with different Reporters and Quenchers.

Primers and probes

Forward and reverse primers were ordered from MWG-BIOTECH (Ebersberg, Germany) and the probes from Oswell (Southampton, UK) and complete RT-qPCR assays were purchased from PrimerDesign Ltd (Southampton, UK). Primers and probes specifically for ADAM33 (Powell *et al.* 2004) and other genes were designed by Dr Robert M. Powell using Beacon Designer 3.0 (PREMIER Biosoft, Palo Alto, CA, USA) (Table 2.10) Where possible the primers were designed to span two exons on the genes of interest to prevent exponential amplification of genomic DNA. Primers and probes should not be able to amplify traces of genomic DNA, which were not eliminated by DNase treatment, but only cDNA reverse transcribed from the mRNA.

6µl of forward primer (100pmol/µl) and 6µl of reverse primer (100pmol/µl) were mixed and 300pmol of probe was added. The primer mix was made up to 100µl with ultrapure water resulting in 6pmol/µl forward and reverse primers and 3pmol/µl probe. Primers and probe mixes purchase from PrimerDesign Ltd had the same concentrations.

Target	Primers and Probe	Dye
hADAM33 3'UTR	F: 5'-GGCCTCTGCAAACAAACATAATT-3' R: 5'-GGGCTCAGGAACCACCTAGG-3' P: 5'-CTTCCTGTTTCTTCCCACCCTGTCTTCTCT-3'	Fam
hADAM33 EGF α & β (exon R)	F: 5'-CAACCATAACTGCCACTGTGCT-3' R: 5'-TGTCCATGCTGCCACCAA-3' P: 5'-CCACCCTTCTGTGACAAGCCAGGCT-3'	Fam
hADAM33 β Form	F: 5'-ACCCAGTGTGGACCTAGAATGGTTTGCAAT3' R: 5'-TGTCCATGCTGCCACCAA-3' P: 5'-CCACCCTTCTGTGACAAGCCAGGCT-3'	Fam
hADAM33 EGF α (exon PQR)	F: 5'-CTGCCACAGCCACGGGGTTTG-3' R: 5'-TGTCCATGCTGCCACCAA-3' P: 5'-CCACCCTTCTGTGACAAGCCAGGCT-3'	Fam
hADAM33-Disintegrin	F: 5'-CAGGCCATGGGTGACTGT-3' R: 5'-GGTGAGCCGTCCAGTAGGTAA-3' P: 5'-CGGGCACCTCCTCCCACTGTCC-3'	Fam
hADAM33 MP-GH	F: 5'-CCTGGAACTGTACATTGTGGCA-3' R: 5'-GTCCACGTAGTTGGCGACTTC-3' P: 5'-CCACACCCTGTTCTTGACTCGGCAT-3'	Fam
hADAM33 MP-FGHI	F: 5'-GATCCTGGGAACAAAGCGGG-3' R: 5'-TCAGGACTCTGGACATTCAGGT-3' P: 5'-CCACACCCTGTTCTTGACTCGGCAT-3'	Fam
hADAM33 soluble	F: 5'-CTGCCACATCCACGGGGCTG-3' R: 5'-TGTCCATGCTGCCACCAA-3' P: 5'-CCACCCTTCTGTGACAAGCCAGGCT-3'	Fam
hαSMA	F: 5'-GACAGCTACGTGGGTGACGAA-3' R: 5'-TTTTCCATGTCGTCCCAGTTG-3' P: 5'-TGACCCTGAAGTACCCGATAGAACATGGCT3'	Fam
hMUC5AC	F: 5'-ATGACAAACGAGATCATCTTCAACA-3' R: 5'-CGGGATGGTCGCGTACAT-3' P: 5'-TCTCGCGCATCGGCGTCAAT-3'	Fam
hTGFβ1	F: 5'-TGGACATCAACGGGTTCACTAC-3' R: 5'-AAGCAGGAAAGGCCGGTT-3' P: 5'-CGAGGTGACCTGGCCACCATTCATT-3'	Fam
hCOLLAGEN	F: 5'-CCCTGGAAAGAATGGAGATGAT-3'	Fam

1A	R: 5'-AAACCACTGAAACCTCTGTGTCC-3' P: 5'-CGGGCAATCCTCGAGCACCCTT-3'	
rRNA 18S	F: 5'-CATTCGAACGTCTGCCCTATC-3' R: 5'-TGATGTGGTAGCCGTTTCTCAG-3' P: 5'-ACTTTCGATGGTAGTCGCCGTGCCT-3'	Fam
hβ-ACTIN	F: 5'-GCAAGCAGGAGTATGACGAGT-3' R: 5'-CAAGAAAGGGTGTAACGCAACTAA-3' P: 5'-CCCCTCCATCGTCCACCGCAAATG-3'	Fam
hGAPDH	F: 5'-GACAGTCAGCCGCATCTTCTT-3' R: 5'-TCCGTTGACTCCGACCTTCA-3' P: 5'-CGTCGCCAGCCGAGCCACATCG-3'	Cy5
hUBC (Ubiquitin C)	F: 5'-GAGGTTGATCTTTGCTGGGAAAC-3' R: 5'-GGTGGACTCTTTCTGGATGTTGTA-3' P: 5'-ACAGGGTGCGTCCATCTTCCAGC-3'	Fam
hCyclophilin B (PPIB)	F: 5'-TCCGAACGCAACATGAAGGTG-3' R: 5'-GGCAGCAGCAGGAAGAAGAC-3' P: -	Sybr
hGAPDH/UBC multiplex house keeping gene kit	F: PrimerDesign R: PrimerDesign P: PerfectProbe™, PrimerDesign	Cy5 Fam
hA2/UBC multiplex house keeping gene kit	F: PrimerDesign R: PrimerDesign P: PerfectProbe™, PrimerDesign	Cy5 Fam
mADAM33 cyto tail	F: 5'-CCTCCATCTCTTGACTTGCTCTC-5' R: 5'-GGTCCTCAGGGTGCTTCCAT-5' P: 5'-TGGAACTCAATCTGTAGACCAGGCTGCTTCA3	Fam
mADAM33 MMP	F: 5'-GCAGGATCTCAGTCGATCA-3' R: 5'-GGCGCCACTGTAGGAAAGC-3' P: 5'-TCAGGACGCAAACGAAACGCTCTGT-3'	Fam
mADAM33 PRO	F: 5'-ATGGACCTCTTGCCAACAGC-3' R: 5'-GCTGCTTCAGAGGGTAGTTCTTAGG-3' P: 5'-TGACTTGCTCTCAGACCCTGCGAACTCT-3'	Fam
mαSMA	F: 5'-TGAAGAGGAAGACAGCACAGC-3' R: 5'-GGAGCATCATCACCAGCGAA-3' P: 5'-CAGAGCCCAGAGCCATTGTCGCAC-3'	Fam

mFOXA1	F: 5'-CCAGACCCGTGCTAAATACTTC-3' R: 5'-TGTGGTTGGTTTGGTGTGTG-3' P: -	Sybr
mGAPDH	F: PrimerDesign R: PrimerDesign P: PerfectProbe™, PrimerDesign	Vic Fam
mATP5B	F: PrimerDesign R: PrimerDesign P: PerfectProbe™, PrimerDesign	Fam
mCYC1	F: PrimerDesign R: PrimerDesign P: PerfectProbe™, PrimerDesign	Fam
mβ-ACTIN	F: PrimerDesign R: PrimerDesign P: PerfectProbe™, PrimerDesign	Fam

Table 2.10 Primer & probe sequences.

Sequences of primers and probes for human and mouse genes. F: Forward primer, R: Reverse primer, P: Probe (All primers and probes were designed by Dr Robert M Powell).

TaqMan Master mix

TaqMan master mix for probe-based or Sybr Green RT-qPCR assays was used. The qPCR MasterMix Plus and qPCR MasterMix Plus for Sybr® Green I w/ fluorescein contain a 2xbuffer with dNTP/dUTP, HotGoldStar, UNG, $MgCl_2$ and stabilisers without or with Sybr® Green and fluorescein (Eurogentec Ltd, Southampton, UK). The Precision™ qPCR Mastermix from PrimerDesign contains 2x reaction buffer, 0.0025U/µl Taq Polymerase, 5nM $MgCl_2$, dNTP Mix (200µM each dNTP) without or with Sybr® Green and fluorescein (PrimerDesign Ltd, Southampton, UK).

TaqMan reaction

Each RT-product containing 20µl cDNA (from 1µg of RNA reverse transcribed) was diluted 1 in 10 in ultrapure water to give a concentration of 5ng/µl. Template cDNA, 5µl containing 25ng was added to 7.5µl qPCR Master mix and 1µl of target primer and probe mix plus 1.5µl ultrapure water into each well in a 96-well iCycler iQ™ thin-wall PCR plate (Cat# 2239441, BIO-RAD, Hercules, CA, USA) to a total volume of 15µl. 1µl of stock primers and probe mix in a total volume of 15µl TaqMan reaction gives a final concentration of 400nM forward and reverse primers of 200nM probe. For house-keeping genes, 5µl of template containing 25ng of cDNA was added to 12.5µl of qPCR master mix and 1µl of primers and probes of multiplexed housekeeping gene detection kits for GAPDH (Cy5)/UBC (Fam) and A2 (Cy5)/UBC (Fam) (PrimerDesign Ltd., Southampton, UK) and 6.5µl ultrapure water into each well in a 96-well PCR plate to a total volume of 25µl. Parallel to the cDNA samples an RT minus control sample (sample that had not been reverse transcribed) and a negative control sample (containing ultrapure water as a template) were used on every plate and experiment. The RT minus control enabled detection of significant genomic DNA contamination was detected. The water negative control sample enabled detection of DNA contamination of the reagents used in the experiments. All samples and controls were analysed in duplicate.

96-well thin-walled PCR plates were sealed with Microseal® 'B' Adhesive Film (Cat# MSB1001, BIO-RAD, Hercules, CA, USA) and spun at 1200g for 2 minutes at 4°C in a large capacity refrigerated benchtop centrifuge, MSE Mistral 3000i (MSE Limited, London, UK). After this it was placed into an iCycler iQ™ Real-Time PCR Detection System (BIO-RAD, Hercules, CA, USA) and run with the appropriated amplification protocol for the different probe base or Sybr green based detection assays.

cDNA amplification

qPCR reactions were performed on an iCycler iQ™ Multi-Color Real-Time PCR Detection System (BIO-RAD, Hercules, CA, USA) under standard cycling conditions. For TaqMan

and Sybr® Green I gene detection RT-qPCR assays the Taq polymerase was heat activated on heating at 95°C for 10 minutes, followed by 50 cycles of denaturation at 95°C for 15 seconds and annealing, extension and data collection at 60°C for 1 minute (Table 2.11). This resulted in a typical amplification curve (Figure 2.12A). Where Sybr Green was used, a meltcurve was run immediately after each gene detection RT-qPCR run to assess specificity and detect miss-priming of the primers. The RT-qPCR products were denaturated at 95°C for 3 minutes, allowing them to re-anneal at 50°C followed by 90 melting cycles by increasing the temperature by 0.5°C every 10 seconds and measuring the fluorescence after each step (Table 2.11). The meltcurve measures the melting temperature (T_m) of double stranded DNA molecules which have Sybr® Green I dye incorporated and are brightest when the two strands of DNA are annealed. Since Sybr Green binds to any double-stranded DNA molecule, it is impossible to distinguish between multiple amplification products in the same reaction. However, the number of amplified products can be identified by melt curve analysis. As the T_m is reached, DNA product will denature and release Sybr Green I resulting in a sharp decline in fluorescence which is plotted as Fluorescence vs. Temperature (Figure 2.12 B). When the negative first derivative of this data versus the temperature change (-dF/dT vs Temperature) is plotted it results in a melting peak and T_m for each amplified product (Figure 2.12 C). The T_m for each peak is dependent on the length of the amplified DNA as well as the G/C content of the sequence. Primer-dimers are typically shorter and melt at a much lower T_m than the product of interest. Secondary or non-specific products can be of varying lengths and thus have a wider range of possible melting curves. Identification of primer-dimers and non-specific products using a meltcurve are important to understand amplification plots using Sybr Green gene detection assays (BIO-RAD 2001).

For PerfectProbe™ gene detection RT-qPCR assays the Taq polymerase was heat activated on heating at 95°C for 10 minutes, followed by 50 cycles of denaturation at 95°C for 15 seconds, data collection at 50°C for 30 seconds and annealing and extension at 72°C for 15 seconds (Table 2.11).

AMPLIFICATION PROTOCOLS			
Taqman® gene detection assay		**Time**	**Temp**
Enzyme activation	Hot Start	10 min	95°C
Cycling x50	Denaturation	15 sec	95°C
	Data collection	60 sec	60°C
Sybr® Green gene detection assay		**Time**	**Temp**
Enzyme activation	Hot Start	10 min	95°C
Cycling x50	Denaturation	15 sec	95°C
	Data collection	60 sec	60°C
Meltcurve	Denaturation	3 min	95°C
Cycling x90	Data collection	10sec	50°C + 0.5°C every 10 sec step
PerfectProbe™ gene detection assay		**Time**	**Temp**
Enzyme activation	Hot Start	10 min	95°C
Cycling x50	Denaturation	15 sec	95°C
	Data collection	60 sec	50°C
	Extension	15 sec	72°C

Table 2.11 RT-qPCR amplification protocols.

Amplification protocols for 3 different gene detection assays used with an iCycler iQ™ Multi-Color Real-Time PCR Detection System (BIO-RAD, Hercules, CA, USA) (adapted from PrimerDesign, Precision™ qPCR Mastermix protocol).

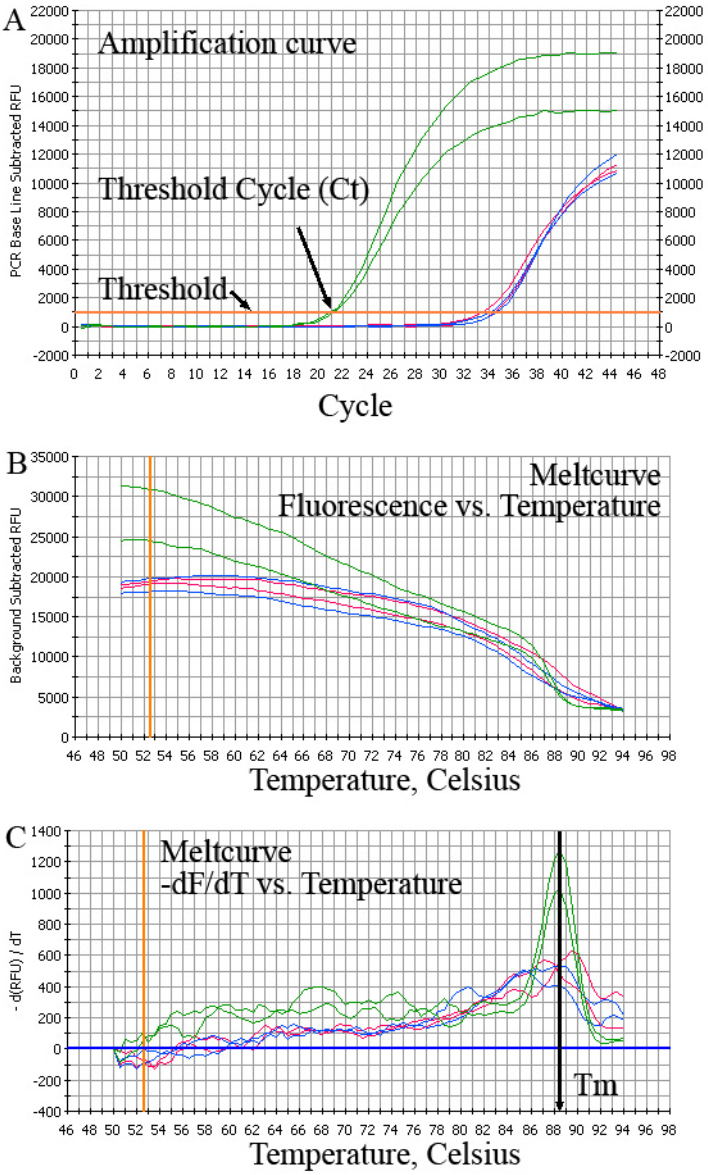

Figure 2.12 Amplification and melt curves of Sybr Green RT-qPCR.

A: Typical amplification curve generated with iCycler iQ™ Software (BIO-RAD, Hercules, CA, USA) for Cyclophilin B Sybr Green gene detection assay (representative for TaqMan and PerfectProbe based assays). It shows the sample amplification curve (green) crossing the Threshold (arrow) set at 1000 at the Threshold Cycle (Ct) at 21 (arrow) and the control sample (Negative water control: blue; RT minus control: red) at Ct of 34. B: Meltcurve with Fluorescence vs. Temperature blot showing the steep loss of fluorescence when the melting temperature (T_m) is reached. C: Meltcurve with negative first derivative of data versus the temperature change (-dF/dT vs. Temperature) blot showing the specific peak at T_m for Cyclophilin (green) compared to the multiple non-specific peaks for the negative water (blue) and RT minus (red) control suggesting primer dimmer or non-specific product formation.

Analysis of RTqPCR data by $\Delta\Delta C_T$ method.

Data processing was done using the iCycler iQ™ Software Version 3.1 (BIO-RAD, Hercules, CA, USA) and quantitation of PCR products from real-time detection was done using the $\Delta\Delta C_T$ method in Microsoft Office Excel 2003 (Microsoft Cooperation, USA). The cycle number is determined by dropping a perpendicular line from the exponential trace of a well in the amplification curve (fluorescence emission versus time) when it crosses the threshold, which is the Ct value. The threshold is automatically set by the iCycler iQ™ Software. The software calculates the standard deviation of the readings between cycles 2 and 10 in the PCR Base Line Subtracted plot (Figure 2.12 A). The mean of all standard deviations is multiplied by the default factor 10 and this level of fluorescence is considered the threshold (BIO-RAD 2001). The Ct values are exported into an Excel file for analysis of the level of gene of interest expression relative to one or the geometric mean of more than one normalising genes (ΔC_T). The ΔC_T value is the result of the gene of interest Ct value (e.g.: ADAM33-3'UTR) minus the normalising gene Ct value (e.g.: 18S-rRNA).
A difference between two Ct values of 1 unit (=1 cycle) represents a two-fold and of 2units (=2 cycles) a four-fold increase in the expression of the target gene. This method is based on the assumption that the normalising genes are always stably expressed in each cell or tissue. To make the data easier to interpret and visualise an arbitrary point from each data set was chosen to which all other gene expression levels were expressed relatively. This manipulation of the ΔC_T calculation is known as the $\Delta\Delta C_T$ calculation. Relative gene expression can then be obtained by exponential transformation of the $\Delta\Delta C_T$ values: (Table 2.12).

$$=2^{-(\Delta CT - (\text{arbitrary1 } \Delta CT))}$$

Relative expression levels of for example all ADAM33 mRNA splice variants in bronchial biopsies were calculated using the $\Delta\Delta C_T$ method and expressed relative to the average of ΔC_T values of all the ADAM33-3'UTR relative to 18S-rRNA from the normal subjects. This resulted in values distributed around 1 for the 3'UTR and the other splice variants were presented relative to the expression of the 3'UTR (Table 2.12) (See chapter 3, Figure 3.1).

$\Delta\Delta C_T$ calculation					
Gene of interest	**Ct**	**Ct HKG**	**ΔC_T**	**$\Delta\Delta C_T$**	**$2^{-(\Delta\Delta CT)}$**
A	X1	Y1	X1-Y1 (ΔC_T1)	ΔC_T1-(average (ΔC_T1 + ΔC_T2))	$2^{(-\Delta\Delta CT1)}$
A	X2	Y2	X2-Y2 (ΔC_T2)	ΔC_T2-(average (ΔC_T1 + ΔC_T2))	$2^{(-\Delta\Delta CT2)}$
B	A1	Y3	A1-Y3 (ΔC_T3)	ΔC_T3-(average (ΔC_T1 + ΔC_T2))	$2^{(-\Delta\Delta CT3)}$
B	A2	Y4	A2-Y4 (ΔC_T4)	ΔC_T4-(average (ΔC_T1 + ΔC_T2))	$2^{(-\Delta\Delta CT4)}$
ADAM 33	**Ct**	**Ct HKG**	**ΔC_T**	**$\Delta\Delta C_T$ (ΔC_T -7.75)**	**$2^{(-\Delta\Delta CT)}$**
3'UTR	26	18.5	7.5	-0.25	1.1892
3'UTR	26.5	18.5	8	0.25	0.8408
MP	28.5	18	11	3.25	0.1051
MP	29	18.5	10.5	2.75	0.1486

Table 2.12 $\Delta\Delta C_T$ calculation method.

$\Delta\Delta C_T$ calculation used for analysis of RT-qPCR. X1 and X2 represent data. of 2 samples tested for gene A expression and A1 and A2 represent data of 2 samples tested for gene B which are analysed relative to the HKG (ΔC_T) and then relative to the average of ΔC_T1 + ΔC_T2 from the A gene data ($\Delta\Delta C_T$). Below is an example for a calculation for ADAM33 3'UTR and MP with real numbers.

2.3.4 geNorm

For accurate gene expression data, it is essential to normalise results from RT-qPCR experiments to a fixed reference that is not affected by experimental conditions. Normalising to a constitutively expressed housekeeping gene is a common method; however, there is no universal reference gene that is constant in all experimental conditions. This is of particular importance in embryonic development that is a complex process during which significant changes in gene expression occur.

To establish the ideal reference genes during mouse embryonic development geNorm™ analysis was performed using geNorm™ Housekeeping Gene Selection Kit for 12 different candidate reference genes (Table 2.13) (PrimerDesign Ltd., Southampton, UK). geNorm™ Analysis Software (Vandesompele *et al.* 2002) is a Microsoft Excel applet that is freely available and can be downloaded from the geNorm webpage (http://medgen.ugent.be/~jvdesomp/genorm/). It was designed to identify optimum HKGs, and hence to generate a measure of stability for each gene.

This measure relies on the principle that, regardless of the conditions, the expression ration of two normalising genes will remain constant in all samples. Hence, any variation in expression ratio between the two is indicative of one or both genes being variably expressed. Base on the stability of each HKG geNorm software also predicts the number of measured HKGs that are required to achieve optimum normalisation (See Chapter 5).

geNorm analysis

1µg of total mRNA from 44 mouse lung samples, two from each developmental time point (embryonic day (ED)11,12,13,14,15,16,17,18,19, postpartum day (PD)1 to 59 and adult mouse (AM)) were reverse transcribed. RTqPCR was performed using 12 different housekeeping gene PerfectProbe gene detection kits. All plates (in total 12 96-well PCR plates) were poured at the same occasion, each plate containing 1 different reference gene. All data points were run in duplicate according to the appropriate amplification protocol as described above. The Ct values were transferred into a Microsoft Excel sheet and transformed into relative quantification data using the ΔC_T method by subtracting the highest Ct value from all other Ct values for each gene measured. The resulting ΔC_T values, with the highest becoming 0 and all the others becoming less than 0, were then exponentially transformed using the equation: $2^{(-\Delta CT)}$. This results in the expression of the data relative to the expression of the least expressed gene. An input file for geNorm analysis was prepared in Microsoft Excel with the first column containing the sample names and the first row containing the 12 different reference gene names. The file was saved in the InputData directory of geNorm. After closing all running Microsoft Excel files, the geNorm applet was

started by clicking on the *geNorm.xls* file and enabling the prompted macro in Excel. The data Input file was loaded and automated analysis was performed. The first geNorm chart was generated showing the average expression stability values of remaining control genes and the most stable expressed genes (Figure 2.13 A). After clicking the automated analysis icon for a second time a second geNorm chart was generated showing the determination of the optimal number of control genes for normalisation (Figure 2.13 B).
geNorm analysis was also performed using the same protocols as above for mouse heart and brain tissues.

Accession Number	Mus musculus Sequence Definition
NM_007393	actin, beta, cytoplasmic (**ACTB**), mRNA.
NM_001001303	glyceraldehyde-3-phosphate dehydrogenase (**GAPDH**), mRNA.
NM_019639	ubiquitin C (**UBC**), mRNA.
NM_009735	beta-2 microglobulin (**B2M**), mRNA.
NM_011740	phospholipase A2 (**YWHAZ**), mRNA.
NM_009438	ribosomal protein L13a (**RPL13A**), mRNA.
NM_007597	calnexin (**CANX**), mRNA.
NM_025567	cytochrome c-1 (**CYC1**), mRNA.
NM_023281	succinate dehydrogenase complex, subunit A (**SDHA**), mRNA.
X00686	18S rRNA gene
NM_013506	eukaryotic translation initiation factor 4A2 (EIF4A2), mRNA.
NM_016774	ATP synthase subunit (**ATP5B**), mRNA.

Table 2.13 12 mouse HKGs detection kit used with geNorm.

Accession numbers and gene names of 12 mouse 'house keeping genes' used for GeNorm analysis in lung development to find the best normalisation genes.

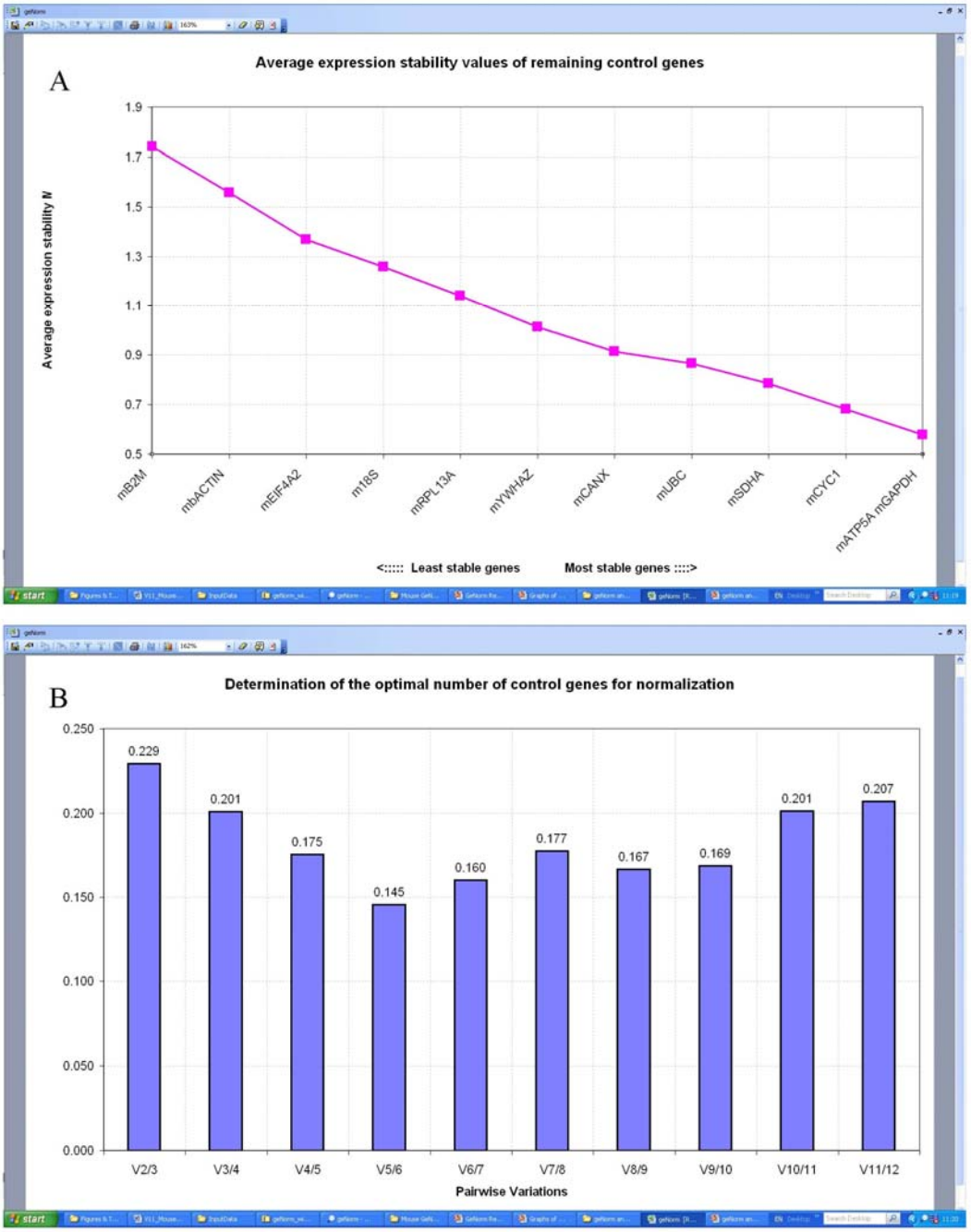

Figure 2.13 geNorm graphs of stability and optimal number for HKGs.

geNorm analysis samples of snapshots of output file graphs. A: Gene stability graphs. B: Optimal gene number graph.

2.3.5 SDS-polyacrylamide gel electrophoresis & Western blotting

In addition to RT-qPCR to study ADAM33 splice variants, SDS-polyacrylamide gel electrophoresis (SDS-PAGE) followed by Western blotting was used for detection of protein isoforms of ADAM33.

All solutions and buffers used for SDS-PAGE and Western blotting are listed in Table 2.15.

Sample preparation

Bronchial biopsies and HEL tissue pieces were freshly homogenised in 1x sample buffer (SB)(made of 5x sample buffer: 0.3125M Tris-HCl pH6.8, 50% glycerol, 25% 2-mercaptoethanol, 10% SDS, 0.01% bromophenol blue). Fresh bronchial biopsies were placed in 200µl 1x SB into Lysing Matrix D impact-resistant 2.0 ml tube containing only about 20% of the original filling with 1.4 mm ceramic spheres and ribolysed in the Hybaid RiboLyser™ Cell Disrupter at speed settings 6.0 for 40 seconds. This was followed by a pulse spin to reduce the foam formed in the tubes and a second ribolysing session.

HEL tissue pieces were placed into 250µl of 1xSB into 0.5ml Eppendorf microtubes containing 3 to 5 ceramic spheres from the Lysing Matrix D tubes. Tissue was ribolysed at speed settings 6.0 for 20 seconds.

Cells grown in wells of 24-well trays were homogenised in 200µl hot 1xSB by pipetting up and down and the solubilised cells collected in 500µl Eppendorf microtubes.

Protein from bronchial biopsies was also isolated from the organic phase left over after RNA extraction using the TRIzol Reagent method, following the manufacture's protocol. Firstly the DNA was precipitated by adding 0.3ml of 100% ethanol per 1ml TRIzol Reagent used for the initial homogenisation. The samples were then mixed by inversion, left at 15 to 30°C for 2-3 minutes and the DNA sedimented by spinning at 2000 rmp for 5 minutes at 2 to 8°C. The Phenol ethanol supernatant was then removed into 2200µl Eppendorf tubes for protein isolation. 1.5ml of isopropyl alcohol per 1ml of TRIzol Reagent was added to precipitate the protein. The samples were left for 10 minutes at 15-30°C. The protein precipitate was sedimented at 12000 g for 10 minutes at 2 to 8°C resulting in a large visible protein pellet. The protein pellet was then washed in 2ml of a solution containing 0.3M guanidine hydrochloride in 95% ethanol for 3 times. During each wash cycle the pellet was left in the wash solution for 20 minutes at room temperature and then centrifuged at 7500 g for 5 minutes at 4°C. After the final wash the protein pellet was gently vortexed using a TopMix (FB15025, Thermo Fisher Scientific, Loughborough, UK) in 2ml of 100% ethanol, left for 20 minutes and centrifuged as above with the wash solution. These samples can be stored in 100% ethanol at minus 20°C for at least 1 year.

The protein pellet was further processed by drying the pellet in a heatblock (DRI-BLOCK® DB-2P, TECHNE, Barloworld Scientific Ltd, Stone, UK) at 50°C for 5 minutes. After this, 200µl of 1x SB was added to the pellet and pipetted up and down to dissolve the pellet. Complete dissolution of the protein pellet required incubating the sample at 50°C for about 20 minutes and sonication in a MSE Soniprep 150 (MSE Limited, London, UK) for about 30 seconds. After this the samples were centrifuged at 3000 rpm for 2 minutes.
All samples homogenised or dissolved in 1xSB were sonicated for 30 to 40 seconds and either used immediately for SDS-PAGE or stored at minus 20°C for future use.
Protein samples extracted from bronchial biopsies were run on a SDS-polyacrylamide gel and stained with Coomassie Brilliant Blue. Comparable bands could be detected for protein which was extracted from biopsies using the TRIzol Reagent method or protein from directly in 1x sample buffer homogenised biopsies (Figure 2.20).

SDS-polyacrylamide gel electrophoresis

Proteins were separated using discontinuous sodium dodecylsulphate polyacrylamide gel electrophoresis (SDS-PAGE) under reducing conditions (Laemmli 1970). The gel solutions of appropriate percentage were prepared and polymerisation initiated by addition of ammonium persulphate (APS) (electrophoresis grade, ≥ 98%,A 3678, Sigma-Aldrich Company Ltd., Gillingham, UK)and TEMED (*N*,*N*,*N*′,*N*′-Tetramethylethylenediamine (electrophoresis grade,~ 99%, T 9281, Sigma-Aldrich, UK).
A Mini-PROTEAN® 3 Cell system (Figure 2.14) (Catalogue# 165-3301, 165-3302, BIO-RAD, Hercules, CA, USA) was used to cast two 1mm thick gels for SDS-PAGE. Two glass spacer plates and two short plates were wiped with a tissue soaked in 10%SDS followed by methanol to ensure that plates were clean and dry. The plates were assembled in the Casting Frame and in the Casting Stand (Figure 2.15). 15ml of separation gel mix was prepared using 15ml of 10%-separation gel stock, 49µl of 10% freshly made APS and 7.5µl of TEMED. A plastic pipette was used to pour the gel down the back plate into the gel cassettes and the gel solution was immediately overlaid with 3mm of water saturated isopropyl alcohol to exclude oxygen, an inhibitor of gel polymerisation. The gels were allowed to polymerise for 45 minutes and were then rinsed with distilled water. Excess water blotted with filter paper. 5ml of stacking gel mix was prepared by combining 5ml of stacking gel stock with 16.7µl of APS and 3.8µl of TEMED. The mix was poured onto the top of the separation gels and a 10 or 15 well comb was inserted without trapping any air bubbles. This was allowed to set for 30 to 40 minutes. Once set, the combs were removed from the gel and the gel cassette sandwich was removed from the Casting Frame and placed into the Electrode Assembly with the short glass plate facing inward. This was placed into the Clamping Frame and the clamps were closed (Figure 2.16). The inner chamber was filled to the top with chilled running buffer to

ensure that all wells were filled with buffer. Protein molecular weight markers (Full Range Rainbow RPN800, Amersham Biosciences, Little Chalfont, UK or Precision Plus Protein™ Kaleidoscope standards, BIO-RAD, Hercules, CA, USA) and samples prepared in 1xSB were heated in a heat block at 95°C for 5 minutes and 5µl marker and 20µl of sample per well was loaded (max 30 µl for 15-well comb) using a pipette with fine gel loading tip. The Electrode Assembly in the Clamping Frame was placed into the Mini Tank and the tank was filled with running buffer. The Lid was placed on the Mini Tank by aligning the colour coded banana plugs and jacks (Figure 2.14) and the electrical leads were connected to the POWER PACK 300 (BIO-RAD, Hercules, CA, USA). The electrophoresis was started with constant 160 volts for about 60 minutes until the bromphenol blue dye front reached the bottom of the separation gel. The power pack was stopped and the gels removed and marked at a corner to allow later identification. The gels were either stained for protein or separated proteins transferred onto a membrane for Western blotting.

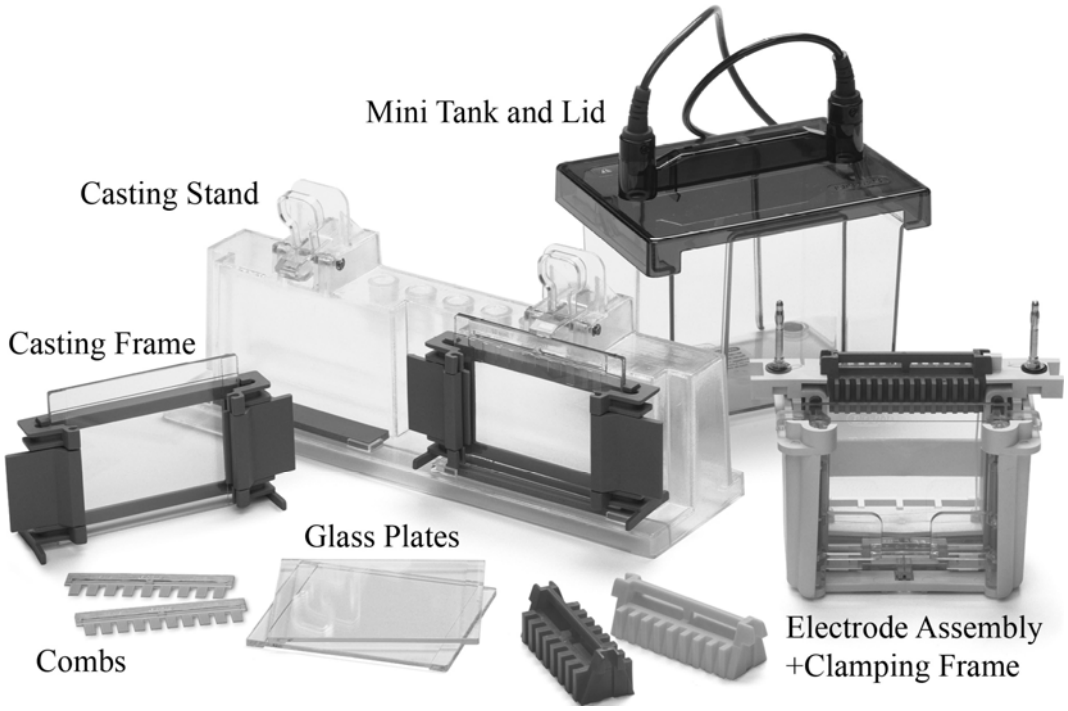

Figure 2.14 Mini-PROTEAN® 3 system.

Mini-PROTEAN® 3 system components (adapted from Mini-PROTEAN® 3 Cell Instruction Manual, BIO-RAD)

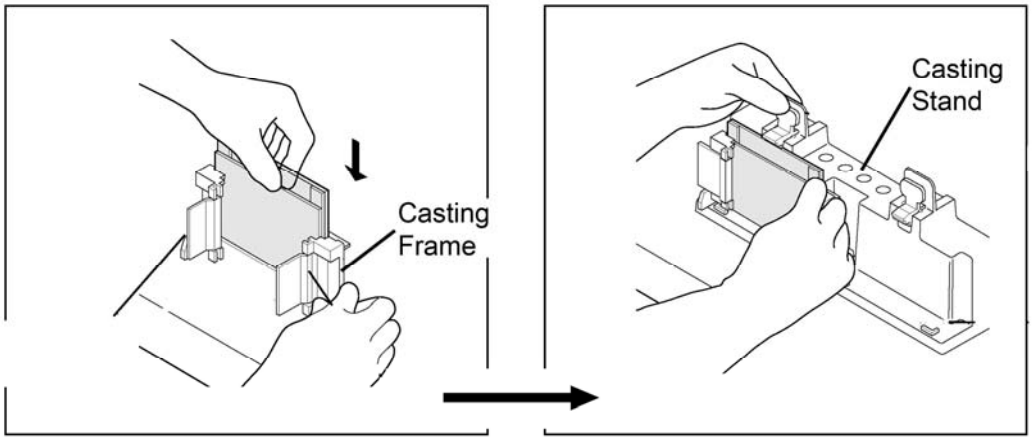

Figure 2.15 Assembling the Mini-PROTEAN 3 Casting Frame and Casting Stand.

(adapted from Mini-PROTEAN® 3 Cell Instruction Manual, BIO-RAD).

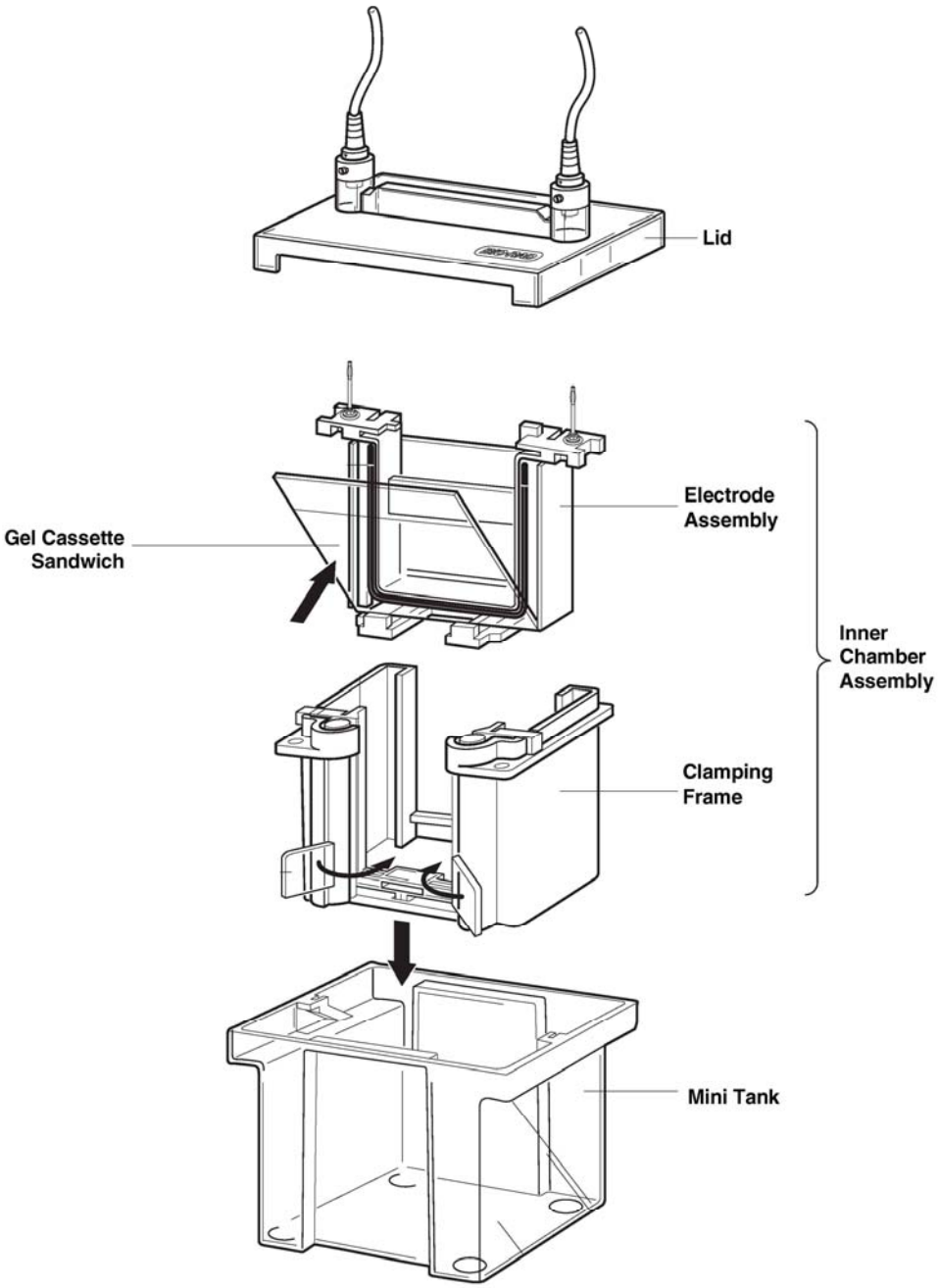

Figure 2.16 Assembling of Mini-PROTEAN 3 cell.

(adapted from Mini-PROTEAN® 3 Cell Instruction Manual, BIO-RAD).

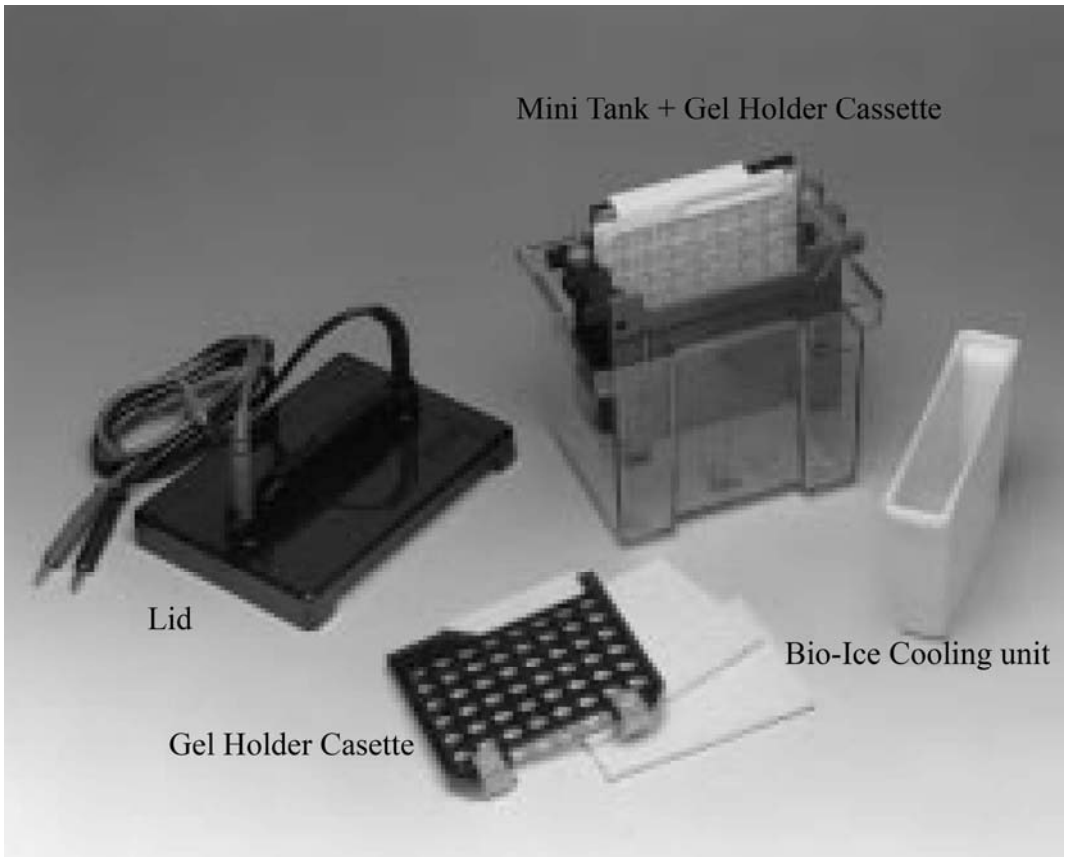

Figure 2.17 Mini Trans-Blot® Electrophoretic Transfer Cell.

Mini Trans-Blot® Electrophoretic Transfer Cell components (adapted from Mini Trans-Blot® Electrophoretic Transfer Cell Instruction Manual, BIO-RAD)

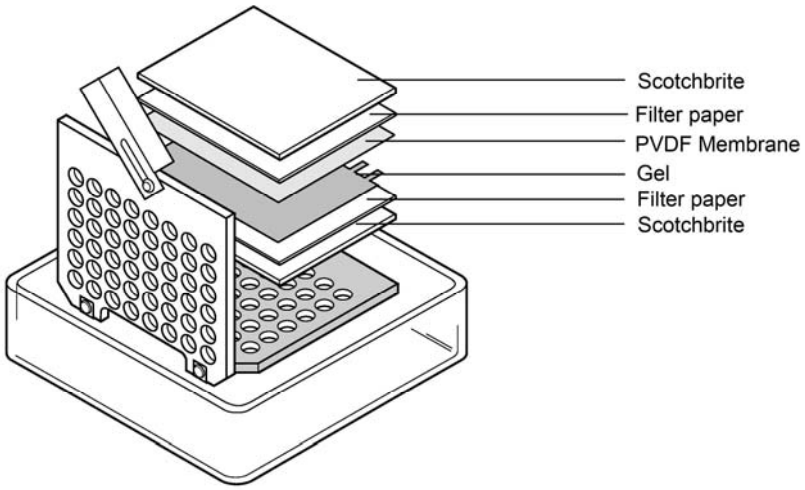

Figure 2.18 Assembly of Gel Sandwich.

(adapted from Mini Trans-Blot® Electrophoretic Transfer Cell Instruction Manual, BIO-RAD)

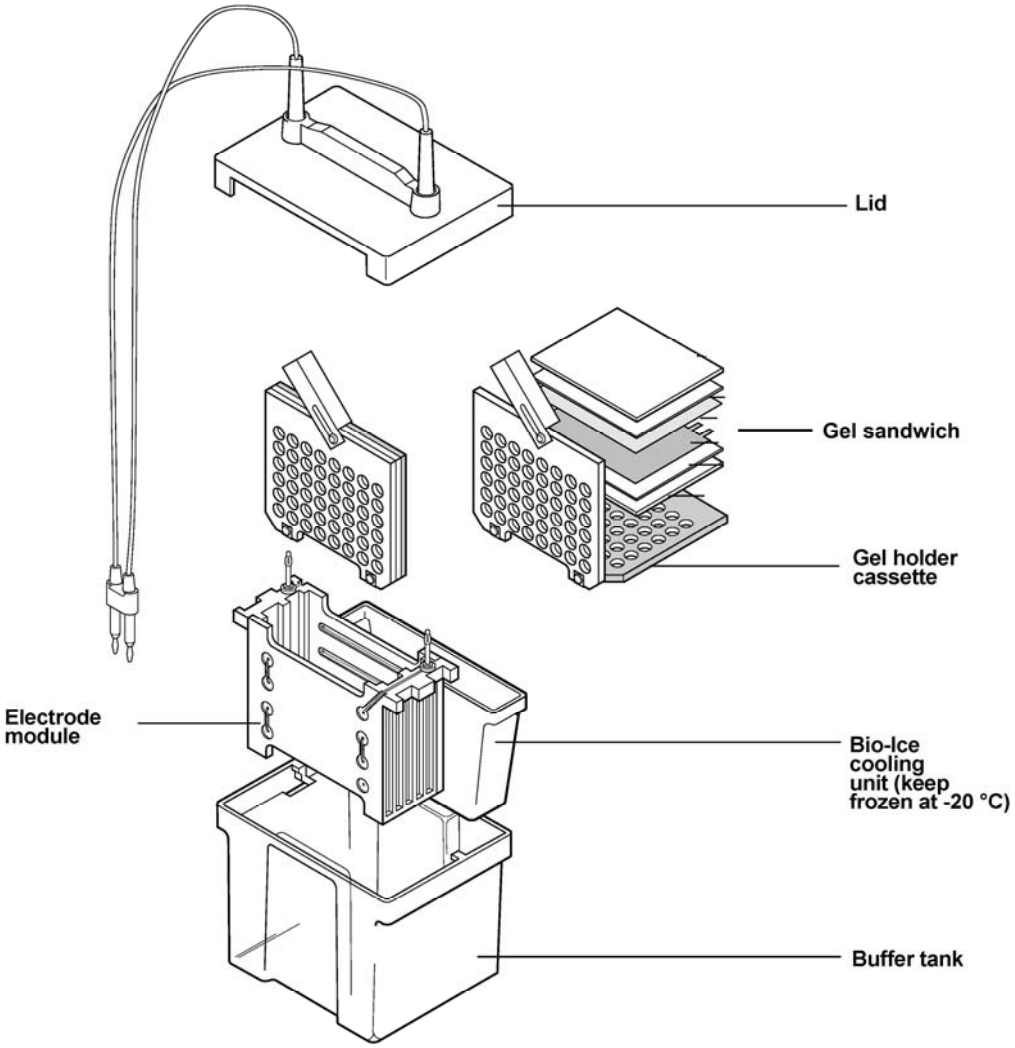

Figure 2.19Assembly of Mini Trans Blot Cell.

(adapted from Mini Trans-Blot® Electrophoretic Transfer Cell Instruction Manual, BIO-RAD)

Coomassie Brilliant Blue protein staining

Proteins contained in gels were stained using Coomassie Brilliant Blue dye. The gels were placed in 20ml of stain and agitated on a shaker for 1 hour at room temperature. They were then transferred into destain solution for 15 to 20 minutes, or until the gels were virtually clear with blue stained bands visible. The destain solution was replaced with fresh solution when it became saturated with dye. The gels were then transferred onto filter paper wetted in distilled water, covered with cling film and dried onto the filter paper using a gel dryer (GEL DRYER, Model 583, BIO-RAD, Hercules, CA, USA) (Figure 2.20).

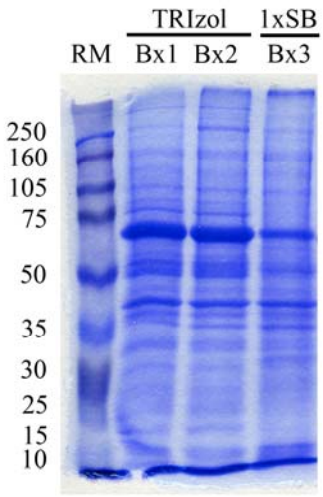

Figure 2.20 Coomassie Brilliant Blue stain of SDS-PAGE gel.

Coomassie Brilliant Blue stain of SDS-PAGE gel, dried on a filter paper. 20µl of protein sample in 1x sample buffer (SB) were loaded from 3 biopsies (Bx1, 2, 3) from the same subject. Bx1 and Bx2 were ribolysed in TRIzol for initial RNA extraction and later isolation of protein and Bx3 was ribolysed straight into 1xSB. 10µl of Rainbow Molecular Weight Marker (RM) was loaded showing bands from 10 to 250kDa.

Western blotting

Proteins were transferred electrophoretically from the SDS-PAGE gel onto a hydrophobic polyvinylidene difluoride membrane (Hybond-P PVDF membrane, Amersham Biosciences, Little Chalfont, UK) and then subjected to immunostaining and detection using Amersham ECL (enhanced chemiluminescence) Plus Western blotting Detection System (RPN 2132, GE Healthcare, UK Limited, Little Chalfont, UK).

The gel obtained from the SDS-PAGE electrophoresis was placed carefully into cold transfer buffer for 15 minutes, to remove salts and to preshrink the gel. Hybond-P PVDF membranes were cut to the size of the gel and pre-wetted in methanol for 3 minutes followed by 3 minutes in water and 15 minutes in transfer buffer. The Mini Trans-Blot® Electrophoretic Transfer Cell system (BIO-RAD, Hercules, CA, USA) consists of a gel holder cassette containing the gel sandwich which is assembled according to Figure 2.18 and then placed into the Electrode Module that is together with an Bio-Ice cooling unit (kept frozen with transfer buffer at minus 20°C) inserted into the into the Mini Tank. The tank was completely filled with transfer buffer and a standard magnetic stir bar (flea) was added to the tank. The tank was placed in a box containing ice and placed on a stirrer to help to maintain even buffer temperature and ion distribution in the tank.

The Lid was placed on the Mini Tank by aligning the colour coded banana plugs and jacks (Figure 2.17) and the electrical leads were connected to the POWER PACK 300 (BIO-RAD, Hercules, CA, USA). The electrophoresis was started with constant 90 volts and amps limit 350mA for about 120 minutes.

Once transferred the blotted membrane was removed and air dried on a piece of dry filter paper and the position of the markers marked with pencil before immuno-detection of the transferred proteins. The Hybond-P PVDF membranes were pre-wet in methanol for 3 minutes followed by 3 minutes in water and then 10 minutes in 1xPBS/0.1%Tween buffer on a shaker (Stuart miniorbital shaker SSM1 Barloworld Scientific - USA or LUCKAM model R100 rotatest shaker Luckham Ltd, Burgess Hill, UK). Nonspecific binding sites were blocked by incubation in 10ml of blocking buffer (5% milk, 1xPBS/0.1%Tween) for 60 minutes. The primary antibody was diluted in 5 to 10ml blocking buffer (Table 2.14), added to the membrane and either incubated at room temperature for 1 hour or in a cold room at 4°C over night. To asses specificity primary antibody that was pre-adsorbed with immunising peptide was incubated in the presence of 30-fold excess immunising peptide for 15 minutes before adding to the membranes (Table 2.14). The membranes were then washed with high salt wash buffer (0.4M NaCl, 1xPBS, 0.1% Tween) for 4 times, once for 15 minutes and 3 times for 5 minutes each time. Secondary antibody was made up in 5 or 10ml of blocking buffer (Table 2.14) added to the membrane which was incubated for 60 minutes. The membranes were washed in wash buffer for 4 times, once for 15 minutes and 3 times for

5 minutes each time. Antibody binding was visualised using enhanced chemiluminescence according to the manufacturer's instruction. Luminescence was detected using Amersham Hyperfilm™ ECL (GE Healthcare, UK Limited, Little Chalfont, UK).
The membranes were placed onto filter paper to remove excess wash buffer and were then placed protein side up onto cling film. The membrane was covered with 2ml/blot of ECL-PLUS solution (2mls solution A and 50µl Solution B) for 5 minutes. The membrane was then blotted onto filter paper and placed protein side down onto another piece of cling film. This was folded over to form an envelope.
The enveloped membrane was exposed to film in a darkroom for 1 to 30 minutes. The film was then developed in 1 in 10 diluted developer solution for 60 seconds and fixed in 1in5 diluted fixative solution for 60 seconds (Fotosped PD5 Print Developer, and FX20 Rapid Fixer, Fotospeed, Corsham, UK).

Once probed with a particular antibody, the membrane can be stripped of all bound antibodies and reprobed with other antibodies of different specificity. After visualisation using ECL, blots were stored in cling film at 4°C. Western blot stripping buffer was prepared and placed into a container with a tight lid. The buffer was pre-warmed to 50°C and the blot was immersed into the solution. After incubation at 50°C for 30 minutes with occasional agitation, the blot was removed and washed for 10 minutes in 1xPBS/0.1%Tween buffer. The blot was then blocked and reprobed with the appropriate primary and secondary antibodies, as described above.

WESTERN BLOTTING			
Primary antibodies	**Company**	**Concentration**	**WB dilution**
Rabbit Antibody to ADAM33; Cytoplasmic domain (RP3-ADAM-33)	Triple Point Biologics, Inc., Forest Grove, OR, USA	1.0mg/ml	1:5,000 as previously described (Powell *et al.* 2004)
Monoclonal Anti-Pan Cytokeratin (mixture mouse IgG1 and IgG2a isotypes) (C2562)	Sigma-Aldrich, Missouri, USA		1:10,000
Immunising peptide	**Company**	**Concentration**	**WB antibody pre-absorbed**
P3-ADAM-33 P.O.# RCMB 06419	Triple Point Biologics, Inc.,	4mg/ml	30 fold molar excess (60µl of stock dilution (3.33µl P3 in 1ml 1xPBS) in 10ml of blocking buffer + 2µl RP3) for 15 minutes
Secondary antibodies	**Company**	**Concentration**	**WB dilution**
Peroxidase AffiniPure Goat Anti-Rabbit IgG (H+L) (Code#111-035-003)	Jackson ImmunoResearch Lab., Inc., West Grove, PA, USA	0.8mg/ml	1:10,000
Polyclonal Rabbit Anti-Mouse Immunoglobulins/HRP Code# P0260	DakoCytomation, Glostrup, Denmark	1g/L	1:2000

Table 2.14 Western blotting antibodies and peptides.

Primary antibodies, immunising peptide and secondary antibodies used in Western blotting.

SDS-PAGE and WESTERN BLOTTING solutions and buffer					
Separation Gel Stock Solutions	**7.5%**	**10%**	**12.5%**	**15%**	**20%**
30% (w/v) acrylamide/0.8% (w/v)bis acrylamide	22.5ml	30.0ml	37.5ml	45.0ml	60.0ml
1.5M Tris-HCl, pH 8.8	22.5ml	22.5ml	22.5ml	22.5ml	22.5ml
dHO	44.6ml	37.1ml	29.6ml	22.1ml	7.1ml
20%(w/v) SDS	0.45ml	0.45ml	0.45ml	0.45ml	0.45ml
Stacking Gel Stock	30% (w/v) acrylamide/0.8% (w/v)bis acrylamide			12.5ml	
dH_2O	0.5M Tris-HCl, pH 6.8			25.0ml	
	dH_2O			62.0ml	
	20%(w/v) SDS			0.50ml	
Separation Gel mix	Separation Gel Stock			15.0ml	
(for two 1mm thick mini gels)	10% (w/v) ammonium persulphate			49.0µl	
	TEMED			7.5µl	
Stacking Gel mix	Stacking Gel Stock			5.0ml	
	10% (w/v) ammonium persulphate			16.7µl	
	TEMED			3.8µl	
10% (w/v) ammonium persulphate	Ammonium persulphate			0.1g	
(freshly prepared)	dH_2O			1.0ml	
5x Sample Buffer	0.3125M Tris-HCl pH 6.8			10.41ml: 1.5M	
	50% glycerol			25.0ml	
	25% 2-mercaptoethanol			12.5ml	
	10% SDS			5.0g	
	0.01% bromophenol blue			5.0mg	
1x Running Buffer; pH 8.3	0.025M Tris			15.15g	
	0.192M glycine			72.0g	

	0.1% (w/v) SDS	25ml; 20%SDS
	pH 8.3 with HCl Made up to 5 litres with dH_2O	
Transfer Buffer; pH 8.0-8.3	25mM Tris	15.15g
	192mM glycine	72.0g
	20% (v/w) methanol	1000ml
	Made up to 5 litres with dH_2O, check pH 8.3 do not adjust	
5x Phosphate Buffered Saline (PBS)	727mM NaCl	425g
	45mM Na_2HPO_4	64g
	5.7mM NaH_2PO_4 H_2O	7.8g
	dH_2O	10L
Wash Buffer	1xPBS	200ml; 5xPBS
	0.1% Tween 20	1.0ml
	Made up to 1 litres with dH_2O	
High Salt Wash Buffer	0.4M NaCl	23.8g in 1 litre of Wash buffer
Blocking Buffer	1xPBS	200ml; 5xPBS
	0.5% (v/v) Tween 20	1.0ml
	5% (w/v) dried low fat skimmed milk powder	50.0g
Coomassie Brilliant Blue R-250 staining solution	0.00125% (w/v) Coomassie Brilliant Blue R-250	

	45% (v/v) methanol	
	45% (v/v) dH_2O	
	10%(v/v) glacial acetic acid	
Gel De-staining solution	25% (v/v) methanol	
	65% (v/v) dH_2O	
	10% (v/v) glacial acetic acid	
Western Blot Stripping Buffer	100mM 2-mercaptoethanol	0.7ml
	2% (w/v) SDS	20.0ml; 10%SDS
	62.5mM Tris pH 6.7	6.25ml; 1M Tris-HCl (pH 6.8)
	Made up to 100 ml in H_2O	

Table 2.15 Solutions and buffers used in SDS-PAGE and Western blotting.

2.4 Section: Immunochemistry

In order to localise the expression of ADAM33 protein in cells and tissue immunochemistry was performed. Primary and secondary antibodies and immunising peptides used for immunochemistry can be found in Table 2.16.

2.4.1 Fluorescent labelling of antibodies

A Zenon® Alexa Fluor® 546 Rabbit IgG Labelling Kit (Excitation 556/Emission 573nm) (Cat# Z-25304, Invitrogen detection technologies, Molecular Probes® Europe BV, Leiden, The Netherlands) was used to label polyclonal rabbit anti-ADAM33 antibodies (Figure 2.21) and negative control rabbit immunoglobulin. The Zenon labelling reagent contains a fluorophore-labelled goat Fab fragment. The affinity purified labelled Fab fragment binds to the Fc portion of the intact rabbit IgG antibody resulting in a Fab-antibody complex which occurs in less than 5 minutes. Excess Fab fragment is bound by adding of a nonspecific rabbit IgG, which prevents cross-labelling of the Fab fragment in experiments where multiple primary antibodies of the same species are used.
1µg of polyclonal Rabbit anti-ADAM33 antibody (Triple Point Biologics, Inc., Forest Grove, OR, USA) and 1µg of Rabbit negative control IgG (Code# X0903, DakoCytomation, Glostrup, Denmark) was prepared in1xPBS (Volume ≤20µl). 5 µl of Zenon rabbit IgG labelling reagent (Component A) was added to the antibody solution (molar ration 3:1) and incubated for 5 minutes at room temperature protected from light. At this stage antibodies could be stored at 4°C for several weeks with the addition of 2mM sodium azide as a preservative. As only one rabbit antibody was labelled the addition of 5µl of Zenon blocking reagent (Component B) was omitted. The complexes were applied to the samples within 30 minutes.

2.4.2 Immunocytochemistry (ICC)

(adapted from Molecular Probes Zenon® Rabbit IgG Labelling Kit Product Information sheet, MP25300, revised: 23-Apri-2003)

Lung epithelial cells from the NIH-H292 (H292) cell line (ATCC® Number: CRL-1848™, LGC Promochem, Middlesex, UK) that do not express ADAM33 were grown in 4 and 8-well chamber slides (Nunc, Lab-Tek II Chamber Slide System, Fisher Scientific UK Ltd, Loughborough, UK) and transiently transfected with a vector containing full length ADAM33 and green fluorescent protein (GFP) (gift from Robert Powell).

Cells were fixed in 4% paraformaldehyde (PFA) for 15 minutes at room temperature. They were washed in 1xPBS for 2 times for 3-5 minutes each. After this the cells were permeabilised in 1xPBS, 0.1%Triton®-X-100 (T8532, Sigma-Aldrich, UK) (PBS-T) for 5 minutes and then blocked in PBS-T containing 1%BSA (A2153, Albumin from bovine serum, Sigma-Aldrich, UK) (PBS-T-BSA) for 30 minutes at room temperature. Cells were then incubated with fluorescently labelled ADAM33 antibody, antibody pre-adsorbed with 20fold excess immunising peptide or a negative control IgG each prepared in PBS-T-BSA for 30-60 minutes at room temperature protected from light. Antibodies were titrated to establish the optimal working dilution. The cells were washed in 1x PBS for 2 times for 3-5 minutes and then subjected to a second fixation in 4%PFA for 15 minutes at room temperature. The cells were washed again in 1xPBS for 3 times for 3-5 minutes and the nuclei were counterstained with TO-PRO®-3 (1:1000) (Catalogue# T3605, TO-PRO®-3 iodide (Excitation 642/Emission 661nm),1 mM solution in DMSO, Invitrogen detection technologies, Molecular Probes® Europe BV, Leiden, The Netherlands) for 5 minutes. After a last wash in 1xPBS 3 times for 3-5 minutes a drop of VectaShield® Hard♦Set™ mounting medium (Cat# H-1400, Vector Laboratories, Inc., Burlingame, CA, USA; VC-H-1400; Alexis, UK) was placed onto the slides and they were covered with a cover slip. Confocal microscopy was done using a LEICA TCS SP2 confocal microscope (Leica, Mannheim, Germany).

2.4.3 Immunohistochemistry (IHC)

GMA embedding

Bronchial biopsies and HEL tissue pieces were placed into ice cold acetone containing 2mM phenyl methyl sulphonyl fluoride (35mg/100ml) and 20mM iodoacetamide (370mg/100ml) and left for fixation overnight at -20°C. The next day the fixative was replaced by acetone at room temperature for 15 minutes and then methyl benzoate at room temperature for another 15 minutes. Then the tissue was infiltrated with processing solution: 5% methyl benzoate in glycol methacrylate (GMA solution A) at 4°C 3 times for 2 hours after which it was embedded in freshly prepared embedding solution in Taab flat bottomed embedding (Taab Laboratories Equipment Ltd., Reading, UK) capsules, placing the specimen in the bottom of the capsule and filling to the brim with resin and closing the lid to exclude air. The capsules were left at 4°C to polymerise overnight and then stored in airtight boxes at -20°C. GMA embedding was performed by Jon Ward, Helen Rigden and Janet Underwood from the Histochemistry Research Unit.

Section and staining of bronchial biopsies

GMA embedded bronchial biopsies were cut into ultrathin 2μm thick section using an ultra-microtome (Reichert Ultracut S, Leica, Germany). Sections of all biopsies were stained with toluidine blue, images taken, submucosal area measured and evaluated for smooth muscle content. Cutting of first sections and staining with toluidine blue for evaluation for submucosal area and smooth muscle content was performed by Dr Tim Shaw. One biopsy per subject containing submucosal smooth muscle was selected on the basis of greatest submucosal area for immunostaining and staining and analysis of immunostaining was done blinded.

Consecutive 2μm sections were cut and immunostained for ADAM33 and αSMA as described previously (Britten *et al.* 1993) according to the local histochemistry research unit immunohistochemistry staining protocol. All primary antibodies and secondary antibodies were titrated in GMA embedded human nasal polyps (control tissue) to find the optimal working dilution. Consecutive sections of samples were cut by Jon Ward, Helen Rigden and Janet Underwood.

ADAM33 was detected using the same RP3 antibody as used for Western blotting (working dilution: 1:500, 1.0μg/ml) and αSMA antibody with a mouse monoclonal antibody (A2547, Sigma-Aldrich, Inc., UK; working dilution: 1:40000). Detection was performed using biotinylated secondary antibodies (swine anti rabbit and rabbit anti mouse at dilutions 1:1200 and 1:300(DakoCytomation, Glostrup, Denmark)) complexed with streptavidin-horseradish-peroxidase and visualised using H_2O_2 with the chromagen diaminobenzidine (DAB) (LIQUID DAB, HK153-5KE, BioGenex, San Ramon, CA, USA). 100μl of 15% sodium azide were added to 5ml of DAB solution to prevent non-specific staining in GMA embedded tissue.

To confirm the specificity of the antibody, control staining was performed using ADAM33 antibody after pre-adsorption with a 5-fold molar excess of the immunising peptide (P3, Triple Point Biologics, Inc., OR, USA). A negative control with Tris buffered saline (TBS) instead of the primary antibody was also performed. Images were taken with a Zeiss Axioskop2 MOT using a digital camera Zeiss AxioCam colour and image analysis was performed blinded using an Open Zeiss KS 400 Image analysis system (Carl Zeiss, Oberkochen, Germany). To control for the variation in smooth muscle content and in biopsy size analysing the αSMA and ADAM33 positive stained area were performed in two ways: (1) by placing a mask around the total area of αSMA positive smooth muscle bundles, measuring the positive stained area of αSMA and ADAM33 in the same mask and calculating each relative to the mask area and (2) by measuring the αSMA and ADAM33 positive stained area relative to the submucosal area. The software template for computer

assisted image analysis was developed with the help of Roger Alston and Aton Page from the Biomedical Imaging Unit.

Section and staining of HEL tissue

GMA embedded HEL tissue was cut into ultrathin 2µm thick section using an ultra-microtome. Sections of all samples were stained with toluidine blue and selected for immunostaining. Consecutive 2µm sections were cut and immunostained for ADAM33 and αSMA as described for the bronchial biopsies. GMA embedding and cutting of sections were performed by Jon Ward, Helen Rigden and Janet Underwood from the Histochemistry Research Unit.

2.4.4 Whole mount immunochemistry

(adapted and modified from protocol used by Tollet J et al.) (Tollet *et al.* 2002)
Bronchial biopsies and HEL tissue were dissected into small pieces under a dissecting microscope and then fixed in freshly prepared 4% paraformaldehyde (PFA) overnight. After washing twice in PBS, the tissue was cleared in dimethyl sulfoxide (3x 10 min), washed and then non-specific binding sites blocked using 1% bovine serum albumin (BSA) in PBS/0.1% Triton®X-100 (PBS-BSA-TX) for 1h. Immunostaining was performed using the ADAM33 antibody (RP3; working dilution 1:100, 10µg/ml) directly labelled with a Zenon™ Alexa Fluor® 546 Rabbit IgG Labelling Kit (Z25304; Molecular Probes, UK) together with FITC-conjugated mouse monoclonal anti αSMA antibody (F3777;Sigma-Aldrich, UK; working dilution 1:200) at 4°C overnight. The tissue was washed in PBS-BSA-TX for (4-5 x 5 min) and then fixed with 4% PFA for 15 min for a second time before washing (4-5 x 5 min) and counterstaining the nuclei with TO-PRO®-3 iodide (T-3605; Molecular Probes, UK; working dilution 1:1000) for 15 min. The tissue was then washed and mounted on a glass slide in two drops of VectaShield® Hard Set™ mounting medium (Cat# H-1400, Vector Laboratories, Inc., Burlingame, CA, USA; VC-H-1400; Alexis, UK) using a Gen Frame® (AB-0577; ABgene, UK) as distance holder covered by a glass cover slide. In some cases, tissue pieces were incubated with unlabelled ADAM33 antibody and then incubated with a secondary Alexa Fluor® 546 $F(ab')_2$ fragment of goat anti-rabbit IgG (H+L) (A11071; Molecular Probes, Ivitrogen, UK; working dilution 1:200) together with FITC conjugated mouse monoclonal anti αSMA antibody (F3777;Sigma-Aldrich, UK; working dilution 1:200) at 4°C overnight. The tissue was then washed without a second fixation step, counterstained and mounted as described above. Control pieces of lung tissue were

immunostained with the Zenon™ Alexa Fluor® labelled anti ADAM33 antibody preadsorbed with a 20-fold molar excess of the immunising peptide (P3) and with Zenon™ Alexa Fluor® labelled control Rabbit IgG (X0903, DakoCytomation, Glostrup, Denmark) at the same concentrations. Confocal microscopy was performed using a LEICA TCS SP2 confocal microscope (Leica, Mannheim, Germany).

Confocal microscopy

Dual stained (one antibody and nuclear stain) ADAM33-GFP transfected cells and Triple-stained (two antibodies and a nuclear stain) whole pieces of human bronchial tissue or HEL tissue were imaged on a Leica SP2 Confocal laser scanning microscope, using simultaneous excitation at 488, 546 and 633 nm. The 3 lasers Argon laser with lines: 458, 488, 514nm, Green HeNe laser: 543nm, and Red HeNe laser 633nm were used to excite the fluorophores FITC (A:495 /E:519nm), Alexa Fluor 546 (A:556 /E:573nm) and TO-PRO-3 (A:642 /E:661nm). Their fluorescence spectrum allowed the use for dual and triple stain (Figure 2.22).

A z-series was obtained through the thickness of the cells/tissues from which representative optical sections or maximum projection images were extracted as appropriate. In cases were overlapping emission spectra caused "bleed through", fluorochromes were excited sequentially rather than simultaneously.

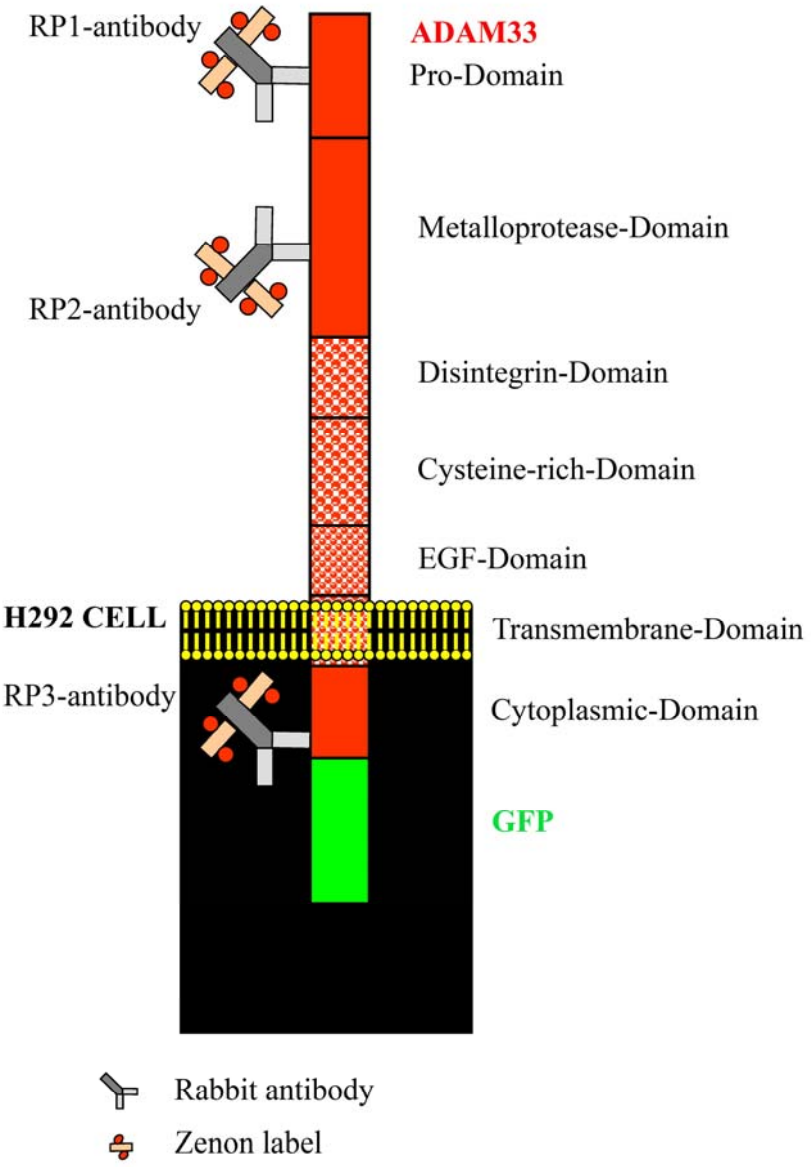

Figure 2.21 Diagram of ADAM33-GFP staining with ADAM33 antibodies.

Diagram of full length ADAM33 plus Green Fluorescence Protein (GFP) transiently transfected into NCI-H292 epithelial cells. RP1, 2 and 3 antibodies are affinity purified polyclonal Rabbit anti human ADAM33 antibodies, raised against peptides from 3 different domains of ADAM33. The antibodies were labelled with a Zenon® Alexa Fluor® 546 Rabbit IgG Labelling Kit (Z25304; Molecular Probes™, Invitrogen™, UK). The Zenon label exists of a fluorochrome labelled Goat-Fab fragment of Fc-specific anti-Rabbit IgG antibody, which binds to the Fc-segment of the RP1 to 3 antibodies.

IMMUNOCHEMISTRY			
Primary antibody	**Company**	**Conc.**	**Working dilution**
Rabbit Antibody to ADAM33; Propeptide domain (RP1-ADAM-33)	Triple Point Biologics, Inc., Forest Grove, OR, USA	1.0mg/ml	1:500 (IHC) 1:100 (ICC) 1:100 (Whole mount)
Rabbit Antibody to ADAM33; Aminoterminal end (RP2-ADAM-33)	Triple Point Biologics, Inc., Forest Grove, OR, USA	1.0mg/ml	1:100 (ICC)
Rabbit Antibody to ADAM33; Cytoplasmic domain (RP3-ADAM-33)	Triple Point Biologics, Inc., Forest Grove, OR, USA	1.0mg/ml	1:100 (ICC)
Monoclonal Anti-α-Smooth Muscle Actin Clone 1A4 Fitc conjugate.(F3777)	Sigma-Aldrich, Missouri, USA	2.0mg/ml	1:200 (Whole mount)
Monoclonal Anti-α-Smooth Muscle Actin Clone 1A4 (A2547)	Sigma-Aldrich, Inc., UK;	2,2mg/ml	1:40,000 (IHC)
Negative Control Rabbit Immunoglobulin Fraction	DakoCytomation, Glostrup, Denmark	20.0g/L diluted to 1.0mg/ml	1:100 (ICC and Whole mount)
Immunising peptide	**Company**	**Conc.**	**Antib. pre-absorbed**
P1-ADAM-33 P.O.# RCMB 06419	Triple Point Biologics, Inc.,	4mg/ml	5-20 fold molar excess for 15 minutes
P2-ADAM-33 P.O.# RCMB 06419 Amino acid sequence: rrtrk ylelyivadh tlfltrhrnl nhtkqrllev	Triple Point Biologics, Inc.,	4mg/ml	5-20fold molar excess for 15 minutes
P3-ADAM-33 P.O.# RCMB 06419	Triple Point Biologics, Inc.,	4mg/ml	5-20 fold molar excess for 15 minutes

Secondary antibody	Company	Conc.	WB dilution
Polyclonal Swine Anti-Rabbit Immunoglob. /Biotin Code# E0431	DakoCytomation, Glostrup, Denmark	1.2g/L	1:1200 (IHC)
Polyclonal Rabbit Anti-Mouse Immunoglob. /Biotin Code# E0413	DakoCytomation, Glostrup, Denmark	0.8g/L	1:300 (IHC)
Alexa Fluor® 546 $F(ab')_2$ fragment of goat anti-rabbit IgG (H+L) (A11071)	Molecular Probes, Ivitrogen, UK	2mg/ml	1:200 (Whole mount)

Table 2.16 Antibodies and peptides used in immunochemistry.

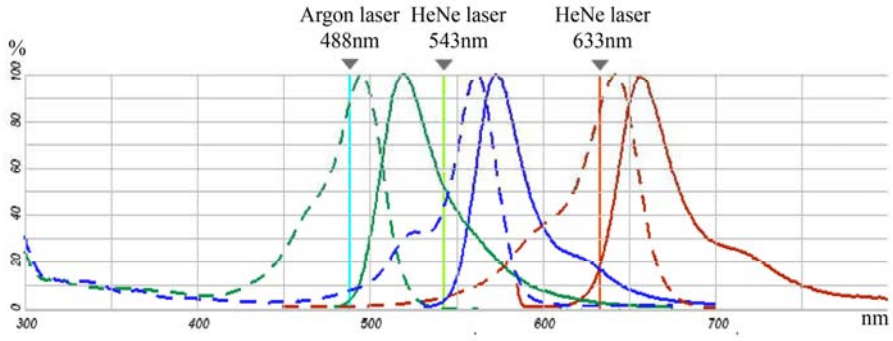

Figure 2.22 Absorption spectra used with confocal microscopy.

Absorption (A) and Emission (E) fluorescence spectra for FITC (green) (A:495 /E:519nm), Alexa Fluor 546 (blue) (A:556 /E:573nm) and TO-PRO-3 (red) (A:642 /E:661nm) adapted from the online Molecular Probes Fluorescence Spectra Viewer. Broken line = absorption spectrum; Full line = emission spectrum. Excitation maxima of 3 lasers used with the LEICA TCS SP2 confocal microscope are indicated by black arrow heads.

2.5 Section: In vivo exposures

The effect of a maternal environment on the offspring from allergic and non-allergic mouse mothers was studied. A/J mice were used who have the asthma susceptibility locus (BHR-1) which is syntenic to human ADAM33.

In vivo exposure studies were designed in Southampton and performed in collaboration with David J.P Bassett of the Ford Motor Company Fund Exposure Facility, Eugene Applebaum College of Pharmacy and Health Sciences at Wayne State University, Detroit, MI, USA. Prior to commencing the study, approval was sought from and granted by the Institutional Animal Investigation Committee (IACUC) at Wayne State University. All procedures met US government guidelines and the facilities, including those for animal exposure, were fully accredited by the Association for Assessment and Accreditation of Laboratory Animal Care International (AAALAC). The mouse exposure experiments, assessments of lung inflammation and lung physiology were performed by Xiufeng Gao and David Bassett at Wayne State University.

Mouse strain

Specific pathogen-free 5 week old male and female inbred A/J mice (weighing 20-25g) were obtained from Harlan-Sprague Dawley, Inc. (Indianapolis, Indiana, USA). Mice were maintained throughout the experiment on low dust corn cob bedding in high efficiency particulate filtered air with free access to filtered water and a standard rodent diet.

An initial pilot study of ADAM33 mRNA expression of newborn mouse lungs (day 24 post conception) showed a significant decrease in ADAM33 in the offspring from Ovalbumin compared to the saline challenged mothers (22.6±1.5 vs 53.6±7.0, mean±standard deviation, $p = 0.002$, $n = 3$ in each group). The minimum sample size for a t-test was determined using SigmaStat for Windows version 3.5. This was calculated on the basis of the difference between the means of the 2 groups (31.0) and minimal expected difference (22.6) that would still give a meaningful result and the maximal expected standard deviation (7.0). This resulted in minimum sample sizes of 2 and 4respectively with a desired power of 0.8 and a desired alpha level of $\alpha=0.05$ which would be appropriate to show significant differences. Similarly, based on previously observed variances and mean differences of greater than 50% in Penh values in ova-allergic Balb/c mice, it was calculated that this study would require a minimum number of 5 mouse mothers per exposure and time point, in order to ensure that there is a greater than 80% chance of detecting similar effect with a confidence level of 95%. Calculation of sample size for Penh measurements was performed by David Bassett Wayne State University. Therefore, it was planned to mate 10 mice with about 50% pregnancy rate for each time point and number of offspring of 4-5 per pregnant mouse.

Mouse sensitisation & mating

Following a week of acclimatisation within the animal facility the female mice were sensitised by intra-peritoneal injection with 0.2ml of 0.9% sterile isotonic saline containing 10µg of ovalbumin and 2mg aluminium hydroxide at day 21 and again at day 7 before the time of mating (Figure 2.23) Two days before mating the female mice were placed into a cage containing the dirty bedding of the male mouse to prime the female mice and to induce oestrus. The male mouse was introduced for a period of two days prior to exposure to either saline or ovalbumin aerosols. Eleven to twelve days later, pregnancy was confirmed by increased maternal weight. Days post conception were indentified as ED15 and ED18-20 of the harvested fetuses and ED22-24 and 4 weeks post-partum of the offspring using standardised charts of maternal weight change and of fetal length and appearance (Foster *et al.* 1983).

Exposure experiments

Following the mating the female mice were either exposed to saline (control) or ovalbumin (1% w/v in sterile isotonic saline) aerosols in a nose-only exposure system (CH Technologies, Inc., Westwood, NJ USA) (Figure 2.24). To confirm inflammation of the lung in ovalbumin exposed female mice non-pregnant animals were used to assess lung inflammation by inflammatory cells recovered in broncheoalveolar lavage fluid from the lungs (Figure 2.26).

Aerosols were generated using collision nebulisers that provide a relatively monodispersed aerosol of 0.25µm mean aerodynamic diameter and diluent air, adjusted to provide an aerosol concentration of 25mg ovalbumin/m^3. The aerosol was monitored using a DUSTTRAK™ Aerosol Monitor (TSI Incorporated**,** Shoreview, MN, USA) Diluent air was chemical and high efficiency particulate filtered with relative humidity controlled to 45-55%. Exposures were conducted for a period of 1 hours per day, 3 days per week for 3 weekly cycles.

Pregnant mice were anaesthetised with sodium pentobarbital (50-50 mg/kg body weight, i.p.) for the removal of the embryos and harvesting of maternal lung tissue. Embryo and newborn tissues were harvested following sacrifice by a Schedule 1 method (cervical dislocation and neural tube dissection) according to experimental schedule (Figure 2.23). The lungs from day 15, day 18-20, day 22-24 post conception and week 4 post partum were removed under a dissecting microscope and collected in RNA*later*® Ambion, Inc. (Catalogue# R0901; Sigma Chemical Co, St Louis, IL, USA) stored at 4°C overnight and then minus 20°C until shipment on dry ice for RNA extraction in Southampton, UK. Tissue preserved in

RNA*later*® was homogenised in Trizol for RNA extraction and RT-qPCR according to the protocol described above (See section 2.3.1).

Assessment of lung inflammation

Ventilated lungs of anaesthetised mice (sodium pentobarbital; 50-60mg/kg body weight) were first perfused with warm isotonic saline (37°C) via the pulmonary artery to remove blood components prior to extensive bronchoalveolar lavage (BAL) with an initial 1ml of phosphate buffered saline (PBS; pH 7.4) and then 5 additional lavages with 0.8ml PBS containing 3mM EDTA to ensure maximal recovery of inflammatory cells (Bassett *et al.* 2001; DeLorme *et al.* 2002). The combined cell population was then counted and subjected to differential analyses by staining with modified Wright's stain for the identification of macrophages, lymphocytes, neutrophils and eosinophils (Figure 2.26).

Assessment of lung physiology

Changes in mouse airway responsiveness to the bronchoconstrictor methacholine in adult mice and offspring were determined using a previously described whole body plethysmograph (Hamelmann *et al.* 1997), equipped with a pneumotachograph, pressure transducer, and a computer data acquisition system (BUXCO Electronics, Inc., Troy, NY, USA) (Figures 2.25). Airway responsiveness to aerosols with increasing methacholine concentrations were indicated by changes in the breathing pattern as determined by analysis of the pressure waveform that generates an empirical measure of the enhanced pause in expiration (Penh). This Penh parameter has previously been defined as the ratio of the peak chamber pressure on expiration (PEP) and the peak negative pressure on inspiration (PIP) times the pause in breathing indicated by $(T_E - T_R)/T_E$ where T_E represents the time for expiration and T_R the time to reach 36% of chamber pressure on expiration (Hamelmann *et al.* 1997). Following 20 minutes of acclimatisation, mice were exposed for 2 minutes to aerosols with increasing concentrations of methacholine up to 50mg/ml for 4 week offspring mice, with 5 minutes recovery between each concentration during which time measurements of chamber pressure were recorded and analysed for Penh based on mean values obtained following 20 completed breathes meeting established criteria using Buxco's BioSystem XA software (BUXCO Electronics, Inc., Troy, NY, USA) (Hamelmann *et al.* 1997; Temelkovski *et al.* 1998; Tsuchiya *et al.* 2003) (Whitehead *et al.* 2003). Although Penh measurements as a non-invasive method for evaluation of lung function have been extensively used and cited in the literature its use has raised some controversial debates about its usefulness in the evaluation of airway function (Bates and IRVIN 2003; Bates *et al.* 2004) (Lundblad *et al.* 2007; Finkelman 2008). Penh is derived from empiric analysis of changes in breathing pattern in unrestrained animals using a barometric plethysmography. Although Hamelmann

et al demonstrated that Penh measurements paralleled increased sensitivity of methacholine obtained by an invasive technique that directly measured airway resistance in an allergic airway inflammation mouse model (Hamelmann *et al.* 1997), Penh is a dimensionless parameter that is not a direct physical measurement. Therefore, already in 1999 it was suggested by Drazen et al that 'Penh measures should be confirmed with a measurement of airway obstruction based on physical principles rather than signal processing' in order to establish the reliability of Penh as a surrogate for bronchoconstriction (Drazen *et al.* 1999). The advantage of unrestrained single chamber barometric plethysmography is that it can be used repeatedly for the same animal without needing to sacrifice the animal and might have a role in particular for screening of large animal numbers. Finkelman recently stated in the Journal of Allergy Clinical Immunology that when both, Penh and airway resistance, were used to study sensitivity to methacholine or acetylcholine in mice with airway inflammation that no report showed a strikingly difference when Penh or airway resistance measurements were used (Finkelman 2008). The author suggested that the above named journal 'should now require all contributors who use unrestrained, single-chamber barometric plethysmography for this purpose to confirm the most important points in their articles with an accepted invasive technique' (Finkelman 2008). Based on this background and with the knowledge of the limitations of unrestrained, single-chamber barometric plethysmography Penh was chosen as an initial measurement for the mouse work in this thesis with the plan to confirm data with invasive methods in follow-on future experiments.

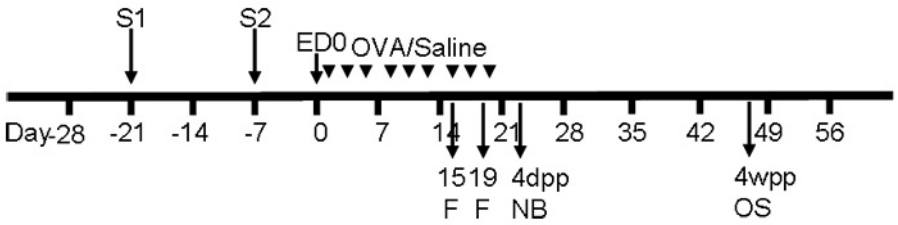

Figure 2.23 Maternal mouse allergic environment experimental outline.

Time points of sensitisation (S1, S2) at day 21 and 14 before mating (ED0) and exposure to ovalbumin or saline (OVA/Saline). Lungs from fetuses and newborn (NB) and offspring (OS) were harvested at day 15, 19 and around day 24 post conception (4 days post partum (pp)) and 4 weeks post partum (4wpp).

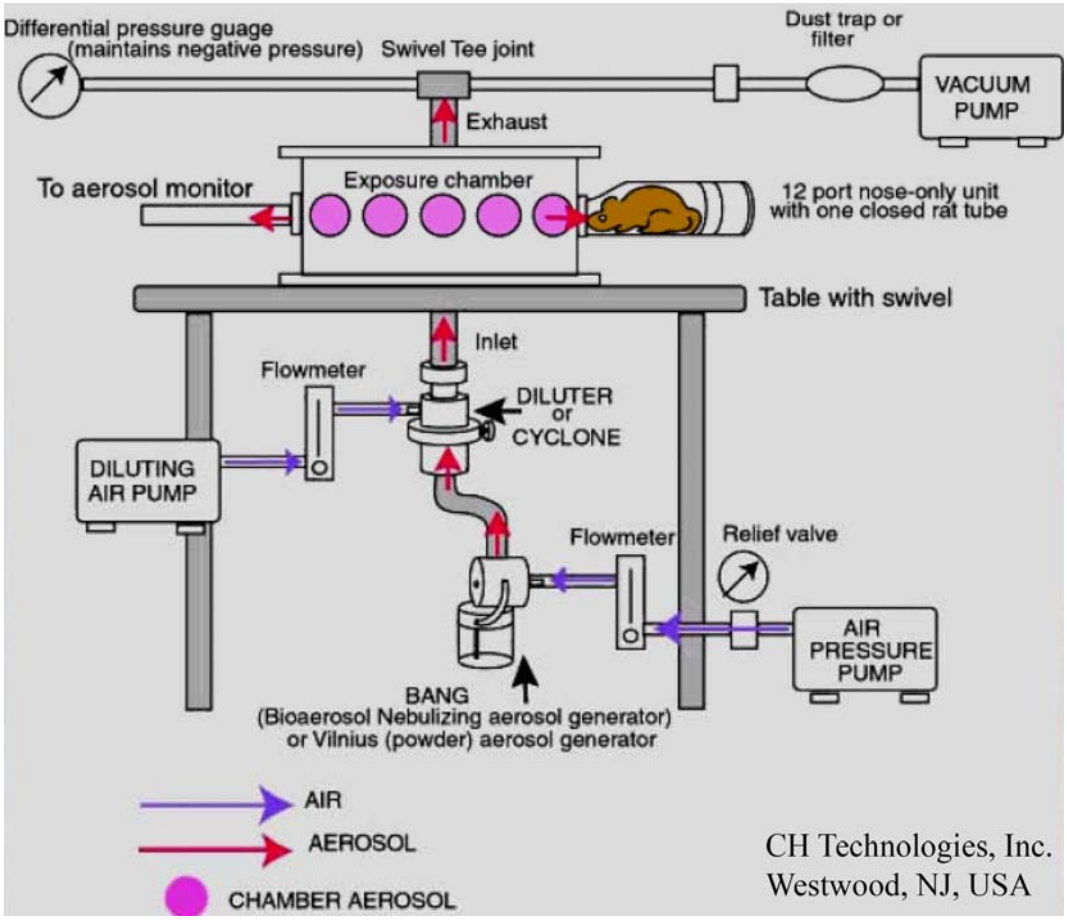

Figure 2.24 Example of nose-only aerosol generation system.

(adapted from CH Technologies, Inc., Westwood, NJ, USA).

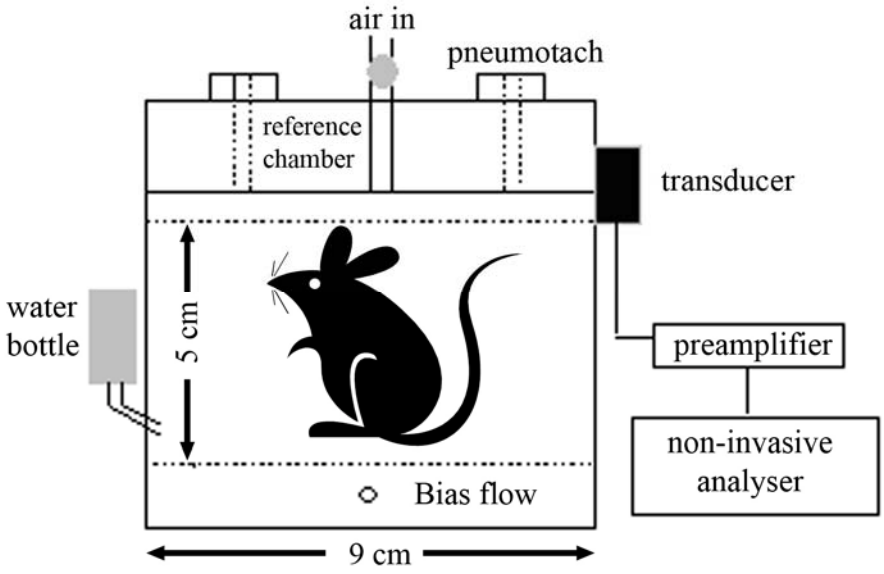

Figure 2.25 Barometric whole body plethysmograph.

The chamber is equipped with a bias air flow (2L/min), pneumotach wire mesh screens by which changes in chamber pressure can be computed using a transducer, amplifier and data logging computer software system (Buxco Instrument Co, Troy, NY). (adapted figure from David Bassett)

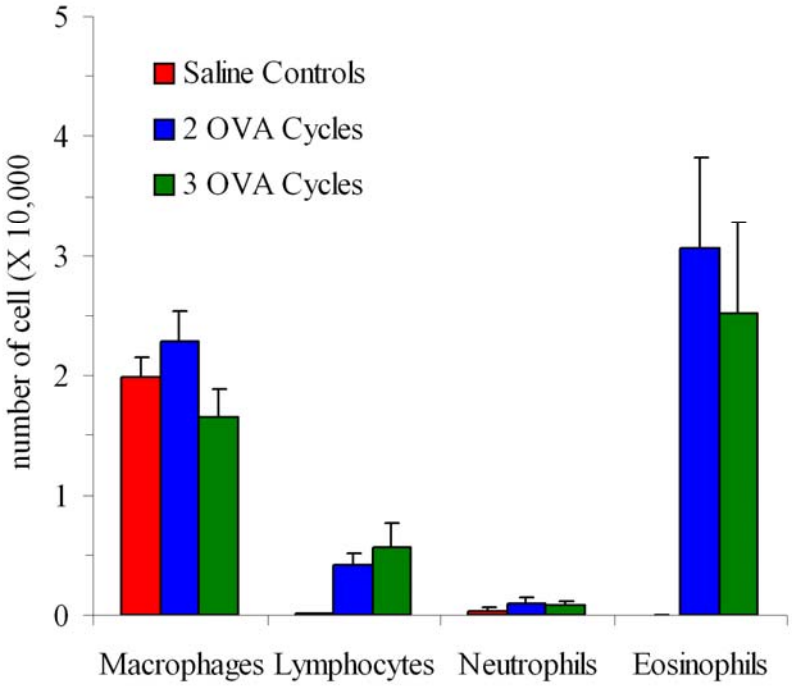

Figure 2.26 Mouse broncheoalveolar lavage inflammatory cells.

Recovery of inflammatory cells from broncheoalveolar lavage of female adult A/J mice after 2 and 3 ovalbumin exposures compared to saline exposure (control). (Figure was contributed by David Bassett)

2.6 Statistics

Data analyses were performed using SigmaStat and SigmaPlot from SPSS (SPSS UK Ltd.,Woking, UK).

All data comparing 2 groups were analysed using parametric Student-t test. Where the test failed normality criteria non-parametric tests (Mann-Whitney Rank Sum Test or Wilcoxon Rank Sum Test) of statistical significance were performed.

Data of more than 2 groups that were normally distributed were compared using One Way Analysis of Variance (ANOVA) and multiple comparisons Bonferrroni t-test. Where the test for normality failed Kruskal-Willis One Way ANOVA on Ranks and multiple comparisons Student-Newman Keuls or Dunnet's method was performed.

Data mouse methacholine challenges were analysed by Two Way ANOVA with comparisons of the means using Student-Keul's multiple range tests. Logarithmic transformation of the data was conducted when variances were found to be heterogeneous by Hartley's test.

Significance was reached when p was less or equal (≤ 0.05).

Chapter 3 Results: ADAM33 in Human adult lung

3.1 Background

Polymorphic variation of *ADAM33* has been associated with asthma and in particular with bronchial hyperresponsiveness (Van Eerdewegh *et al.* 2002) and more recently with COPD (Gosman *et al.* 2007) and Psoriasis (Lesueur 2007). Despite extensive characterisation of ADAM33 at molecular and structural level (Zou *et al.* 2005; Zou *et al.* 2004; Orth *et al.* 2004; Meng *et al.* 2007; Bridges *et al.* 2005) the biological function of ADAM33 protein in health and disease is still unknown. ADAM33 is mainly expressed in mesenchymal cells and several alternatively spliced variants of ADAM33 have been detected in cultured bronchial fibroblasts (Powell *et al.* 2004), but there was no information as to whether these differ quantitatively or qualitatively in tissue from normal and asthmatic subjects.

The first aim of this chapter is to quantify ADAM33 splice variants in bronchial biopsies from normal and asthmatic subjects.
A further aim is to determine the cellular origin of ADAM33 protein by immunolocalisation.

3.2 Results

3.2.1 Analysis of ADAM33 mRNA amplicons in bronchial biopsies & bronchial brushings

Using RT-qPCR primers that recognize alternatively spliced variants of ADAM33 (Figure3.1A), both the α- and β-isoforms of ADAM33 were detected in bronchial biopsy tissue from healthy and mild to moderate asthmatic subjects, although the β-isoform that lacks exon Q (Figure 3.1A) was less abundant compared to that previously found in primary airway fibroblasts (Powell *et al.* 2004). The metalloprotease (MP) domain (exons FGHI) and the putative soluble form of ADAM33 (generated by a 37 bp deletion in exon R) were both rare transcripts relative to the 3'UTR (Figure 3.1B), similar to findings in airway fibroblasts (Powell *et al.* 2004). Analysis of ADAM33 mRNA in biopsies from 13 normal and 14 mild to moderate asthmatic subjects (See chapter 2, section 2.1.1, Table 2.1) did not reveal any significant difference in the level of expression of any splice variant between normal and asthmatic subjects. Furthermore, within a cross-section of the asthmatic group, treatment with corticosteroids did not result in any difference in the pattern of ADAM33 expression. As ADAM33 is expressed in mesenchymal cells (Van Eerdewegh *et al.* 2002), mRNA expression for α-smooth muscle actin (αSMA), a marker of smooth muscle cells and myofibroblasts was also measured. This showed no significant difference in αSMA expression between normal and mild to moderate asthmatic subjects and analysis of ADAM33 splice variants relative to αSMA did not reveal any significant disease-related differences comparing mild to moderate asthmatic with normal control subjects (Figure 3.1C).

These findings are in contrast to a recent report of increased ADAM33-alpha isoform mRNA expression in bronchial biopsies from subjects with severe and moderated asthma compared to mild asthmatic and healthy subjects (Foley *et al.* 2007). Although considered to be a mesenchymal cell-specific gene, this recent report has also suggested epithelial cell expression of ADAM33 in severe asthma (Foley *et al.* 2007). In order to study ADAM33 mRNA expression in biopsies and bronchial brushings, containing bronchial epithelial cells, from normal subjects and patients with severe asthma, three probe based RT-qPCR assays were used that were intron spanning. These assays allowed assessment of the alpha, beta and the metalloprotease containing isoforms of ADAM33 as in the biopsy study of mild to moderate asthmatic subjects. The assays were validated using HEK293 cells that were transfected with a cDNA encoding the full length of ADAM33. It was shown that the ADAM33 EGF alpha and MP domain assays were of comparable efficiency (Figure 3.2A).

The ADAM33 EGF beta assay could not be tested in the cells, as the recombinant cells expressed only the full length alpha isoform of ADAM33. However, the efficiency of this assay was 97.8% when tested using cDNA from primary human bronchial fibroblasts. In contrast with findings in HEK293 cells expressing full length of ADAM33, the MP domain was poorly expressed compared to the alpha isoform in bronchial fibroblasts (Figure 3.2B), as previously reported (Powell *et al.* 2004).

To investigate whether ADAM33 expression is increased in severe asthma, the three probe based RT-qPCR assays for ADAM33 were used to evaluate mRNA in bronchial biopsies from 15 severe asthmatics and 8 healthy controls (See chapter 2, section 2.1.1, Table 2.2). Contrary to the recent report (Foley *et al.* 2007), no significant difference between ADAM33 expression in biopsies from healthy or severe asthmatic subjects could be found (Figure 3.3), which could not have been accounted for by differences in smooth muscle content of the biopsies, as αSMA expression was similar in both groups (Figure 3.3).

When these assays were used to evaluate ADAM33 mRNA in 14 bronchial brushings form 6 healthy and in 16 bronchial brushings from 9 severe asthmatic subjects (See chapter 2, section 2.1.1, Table 2.3), no positive signal was detectable, even though a strong signal was detected using primary fibroblasts as a positive control (Figure 3.4A). Failure to detect a positive signal for ADAM33 mRNA was not due to poor quality or quantity of RNA extracted from the brushings, as strong signals were detected for the housekeeping genes (average Ct values 20 to 21) and the epithelial specific gene, MUC5AC, whereas low signals were detected for the myofibroblast marker, αSMA (Figure 3.4B).

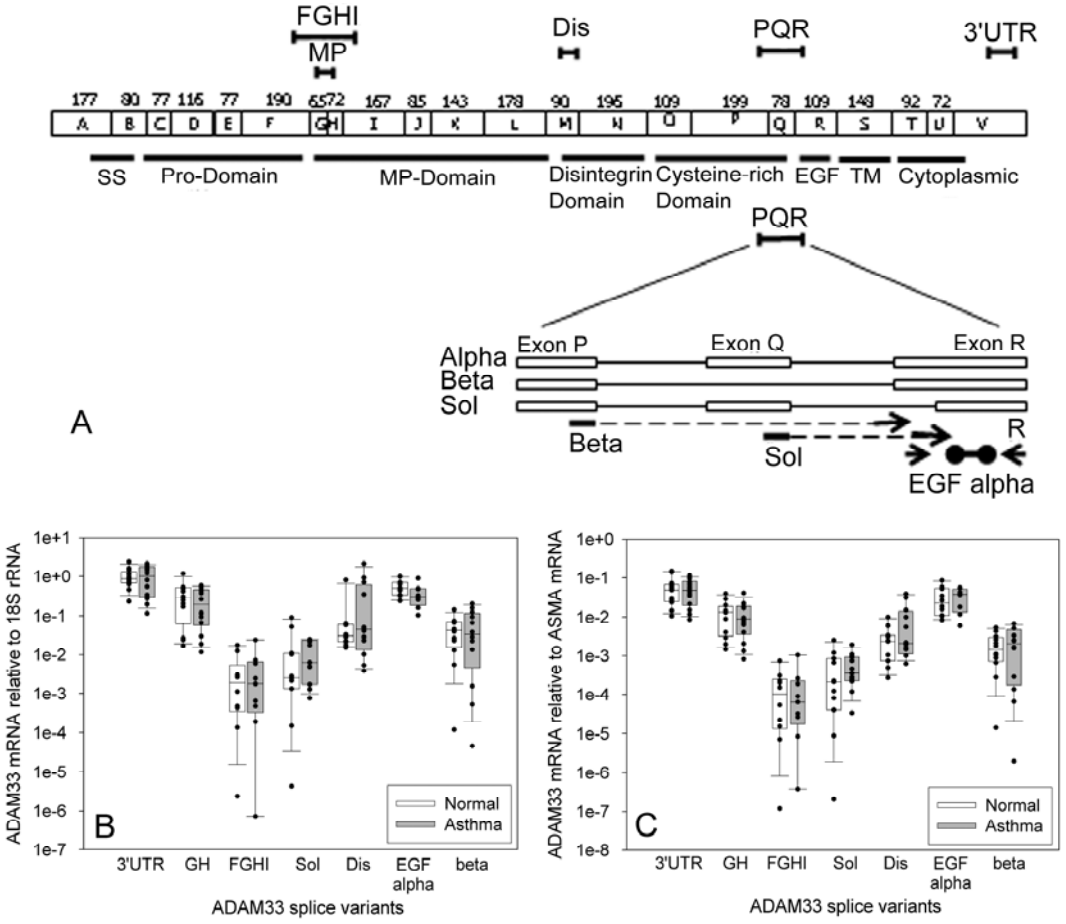

Figure 3.1 ADAM33 splice variant expression in bronchial biopsies.

A) The exon structure and domain organisation of ADAM33 and location of the TaqMan primers: primers for GH, FGHI, Sol and beta were intron spanning and primers for 3'UTR, EGF alpha and Dis were placed in a single exon of ADAM33. B and C) ADAM33 mRNA splice variant expression relative to 18S ribosomal RNA (B) and αSMA (C) respectively in bronchial biopsies from normal (n=11-13) and asthmatic subjects (n=8-14). The average Ct value ± standard deviation for each amplicon was: 3'UTR: 28.81±1.10; GH: 30.41±1.72; FGHI: 38.76±4.13; Sol: 37.04±2.98; Dis: 33.93±1.23; EGF alpha: 29.87±0.82; beta: 33.77±2.582; 18s rRNA: 12.57±1.01, αSMA: 29.87±0.824. The minus reverse transcription controls (RT-) and the negative water controls were not detectable (no amplification curve) for most amplicons other than: Dis: 39.32±6.86; 18S rRNA: 33.50±1.22. Note that expression data are plotted on a log scale. Data were analysed by the Mann Witney U test.

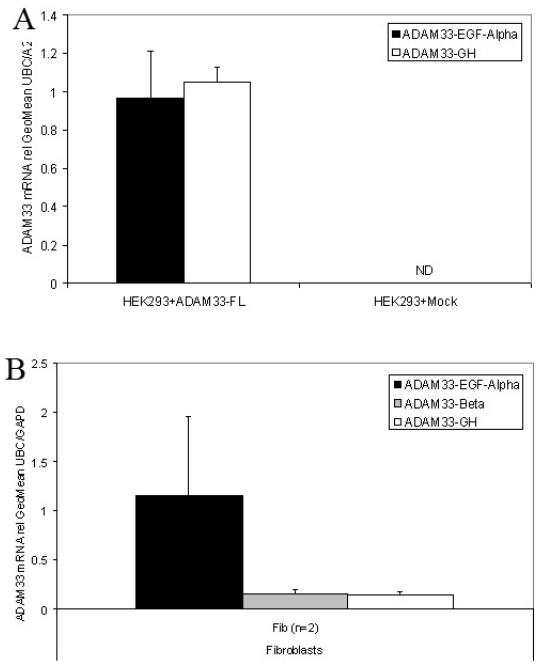

Figure 3.2 Validation of probe-based RT-qPCR assays for ADAM33

All assays are intron spanning. HEK293 cells transfected with full length ADAM33 (HEK293-ADAM33FL) were analysed for expression of ADAM33 mRNA (A) for primer sets located in the EGF domain (ADAM33-EGF-Alpha) and the MP domain (ADAM33-GH) which showed equal expression. No ADAM33 mRNA could be detected in the Mock-transfected cells (HEK293-Mock). When the same primer sets and a primer set for the beta-form of ADAM33 (ADAM33-Beta) were tested in primary fibroblasts (B) ADAM33 mRNA expression showed high expression of the Alpha-isoform containing the EGF domain with low expression of the Beta-isoform and MP-isoform similar to findings by Powel et al (Powell *et al.* 2003).

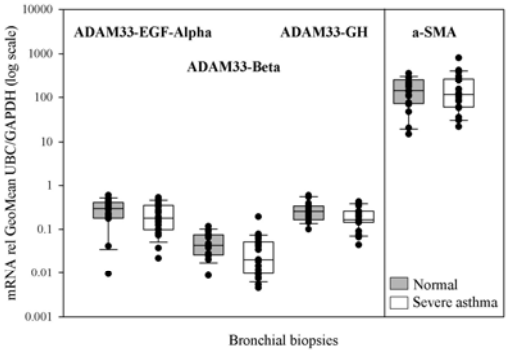

Figure 3.3 ADAM33 and αSMA expression in bronchial biopsies.

RT-qPCR for 3 ADAM33 isoforms and αSMA in bronchial biopsies from healthy (normal) (n=8) and asthmatic (severe asthma) subjects (n=15). No significant difference could be detected between healthy and severe asthmatic subjects.

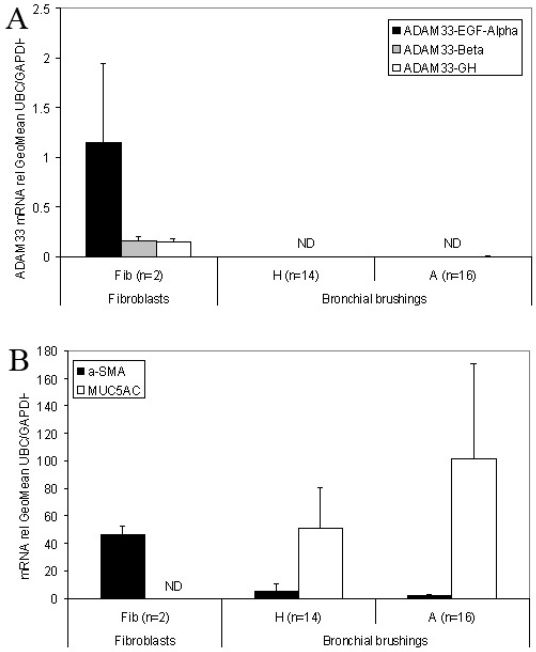

Figure 3.4 ADAM33, αSMA, MUC5AC expression in bronchial brushings.

Epithelial cells from bronchial brushings from healthy (H) and asthmatic (A) subjects were analysed for ADAM33 mRNA using RT-qPCR. Compared to the fibroblasts none of the 3 isoforms of ADAM33 were detected (ND) in the bronchial brushings (A). RT-qPCR for αSMA and MUC5A in fibroblasts showed strong expression of αSMA mRNA, a marker for mesenchymal cells but no expression of MUC5AC, a marker for epithelial cells. In contrast in bronchial brushings MUC5AC was strongly expressed with only weak expression of αSMA (B).

3.2.2 Validation of three Rabbit anti human ADAM33 antibodies using H292 lung epithelial cells transfected with full length ADAM33+GFP using immunocytochemistry and confocal microscopy.

After studying ADAM33 mRNA expression in bronchial biopsies it was important also to study ADAM33 protein expression in bronchial biopsies using immunohistochemistry.
In order to test the quality and specificity of three commercial affinity purified polyclonal Rabbit anti human ADAM33 antibodies, H292 lung epithelial cells, that do not express ADAM33 were transiently transfected with a vector containing full length ADAM33 and green fluorescent protein (GFP) (gift from Robert Powell). The cells, fixed in 4% paraformaldehyde, were stained with anti-ADAM33 antibodies or control IgG that were labelled with a Zenon® Alexa Fluor® 546 Rabbit IgG Labelling Kit (Figure 3.5); control experiments used antibodies that were pre-adsorbed with the immunising peptide. Once stained, cells were analysed by laser confocal microscopy.
The three rabbit antibodies RP1, 2 &3 from Triple Point Biologics, Inc. were tested. All antibodies were raised against synthetic peptides corresponding to sequences in human ADAM33 and were purchased as peptide-affinity purified preparations. The antibodies were concentrated to 1mg/ml with addition of 0.05% sodium azide as preservative and 50% glycerol as cryoprotectant. RP1 is an antibody that recognises the Pro-domain of ADAM33, RP2 the amino-terminal end containing the MP domain and RP3 the cytoplasmic domain (Figure 3.5). RP1 and RP2 antibodies showed only weak staining (red) (Figure 3.6B & 3.7 B) of the ADAM33-GFP expression cells (green) (Figures 3.6 & 3.7, A & D) with only low co-localisation and some none-green cells also showed a positive signal (yellow) (Figure 3.6C & 3.7 C). The positive staining could only be partially blocked in the presence of the immunising peptides, P1 and P2, (Figure 3.6E & 3.7 E), suggesting that these two antibodies have a low affinity for their specific domains (Pro and MP) in full length ADAM33. In contrast, RP3 antibody showed the strongest positive staining (Figure 3.8B) of ADAM33-GFP expressing cells (Figure 3.8A & D) which co-localised very well with the GFP expressing cells (Figure 3.8C) and could be almost fully blocked in the presence of the immunising peptide P3 (Figure 3.8E&F), suggesting that this antibody against the cytoplasmic domain of ADAM33 showed the best quality and highest specificity of all three antibodies. Zenon® labelled Rabbit IgG used at the same concentration as the three antibodies did not show staining (Figure 3.9, A-C); there was also no auto-fluorescence detectable in cells with only the buffer (PBS) and without an antibody (Figure 3.9,D-F).

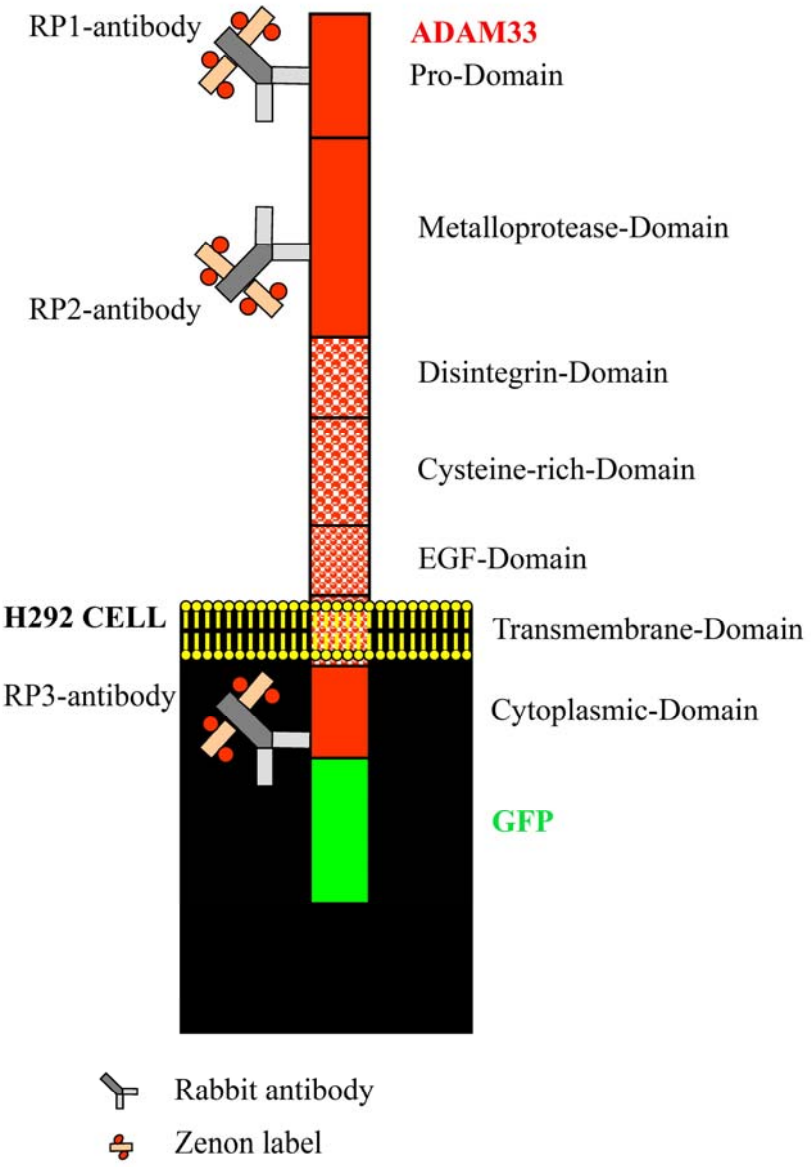

Figure 3.5 Diagram of full-length ADAM33-GFP in H292 epithelial cells.

Full length ADAM33 plus Green Fluorescence Protein (GFP) transiently transfected into NCI-H292 epithelial cells. RP1, 2 and 3 antibodies are affinity purified polyclonal Rabbit anti human ADAM33 antibodies, raised against peptides from 3 different domains of ADAM33. The antibodies were labelled with a Zenon® Alexa Fluor® 546 Rabbit IgG Labelling Kit (Z25304; Molecular Probes™, Invitrogen™, UK). The Zenon label exists of a fluorochrome labelled Goat-Fab fragment of Fc-specific anti-Rabbit IgG antibody, which binds to the Fc-segment of the RP1 to 3 antibodies.

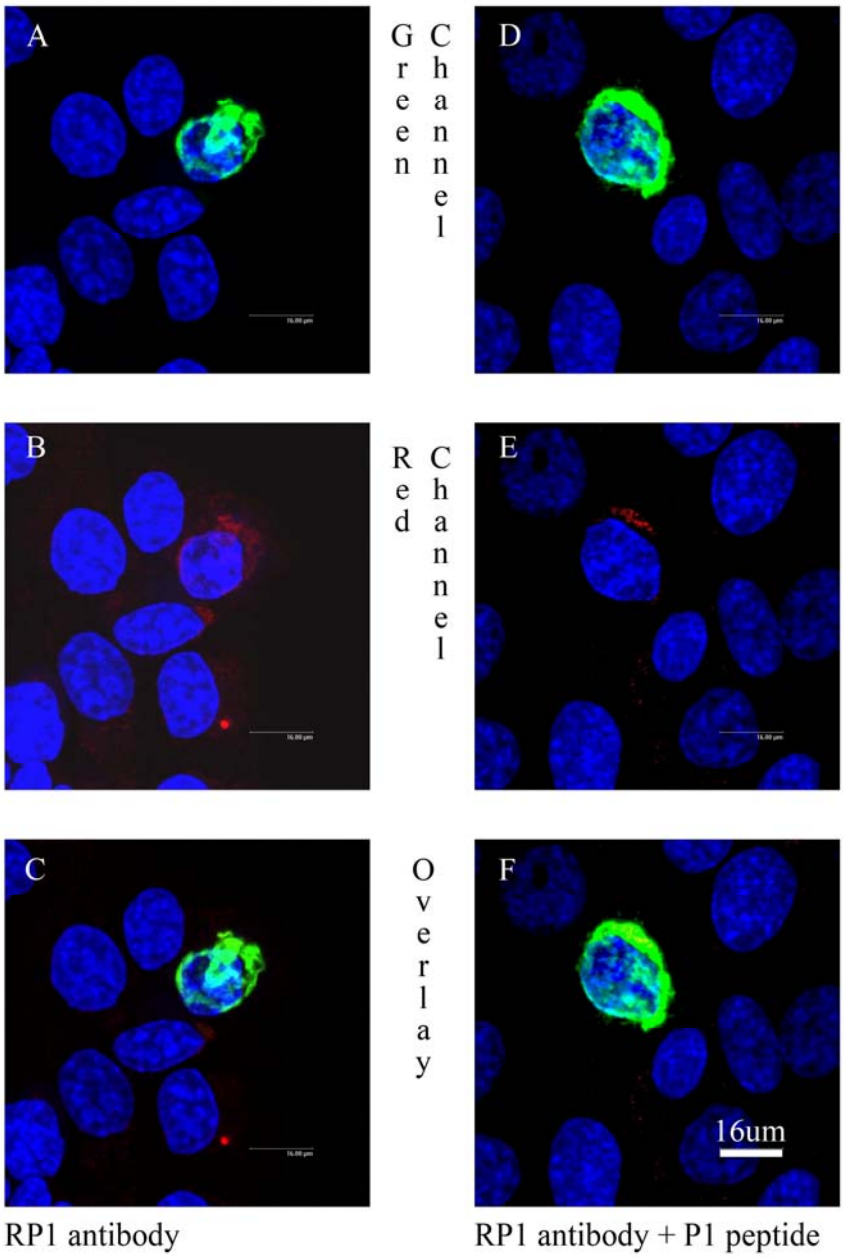

Figure 3.6 Immunocytochemistry with ADAM33 antibody RP1.

Green and red channel and overlay images using confocal microscopy of NCI H292 epithelial cells transiently transfected with full length ADAM33 coupled to Green Fluorescent Protein, fixed in 4% paraformaldehyde and stained with Zenon® labelled RP1 antibody without (red) (A,B,C) and with the blocking peptide P1 (D,E,F). The cell nuclei were counterstained with TO-PRO3 (blue).

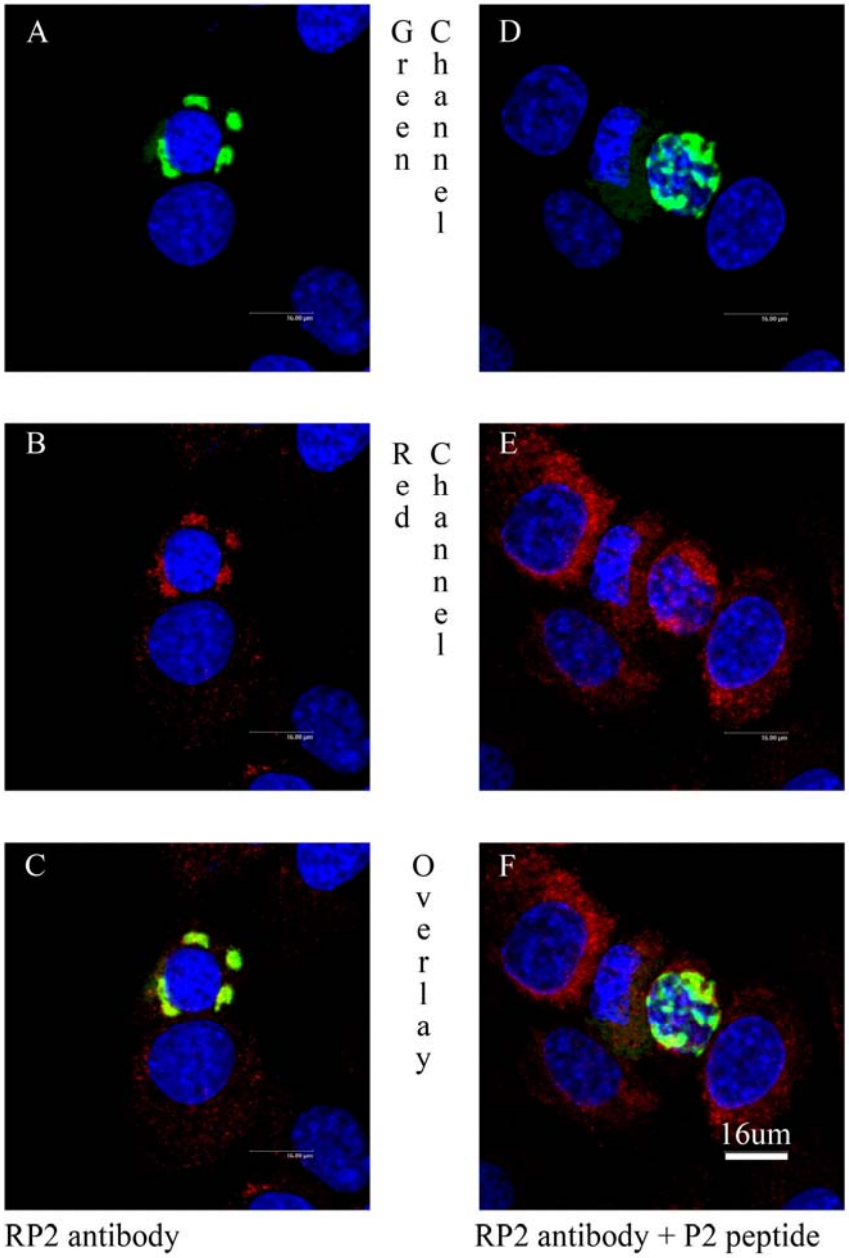

Figure 3.7 Immunocytochemistry with ADAM33 antibody RP2.

Green and red channel and overlay images using confocal microscopy of NCI H292 epithelial cells transiently transfected with full length ADAM33 coupled to Green Fluorescent Protein, fixed in 4% paraformaldehyde and stained with Zenon® labelled RP2 antibody without (red) (A,B,C) and with the blocking peptide P2 (D,E,F). The cell nuclei were counterstained with TO-PRO3 (blue).

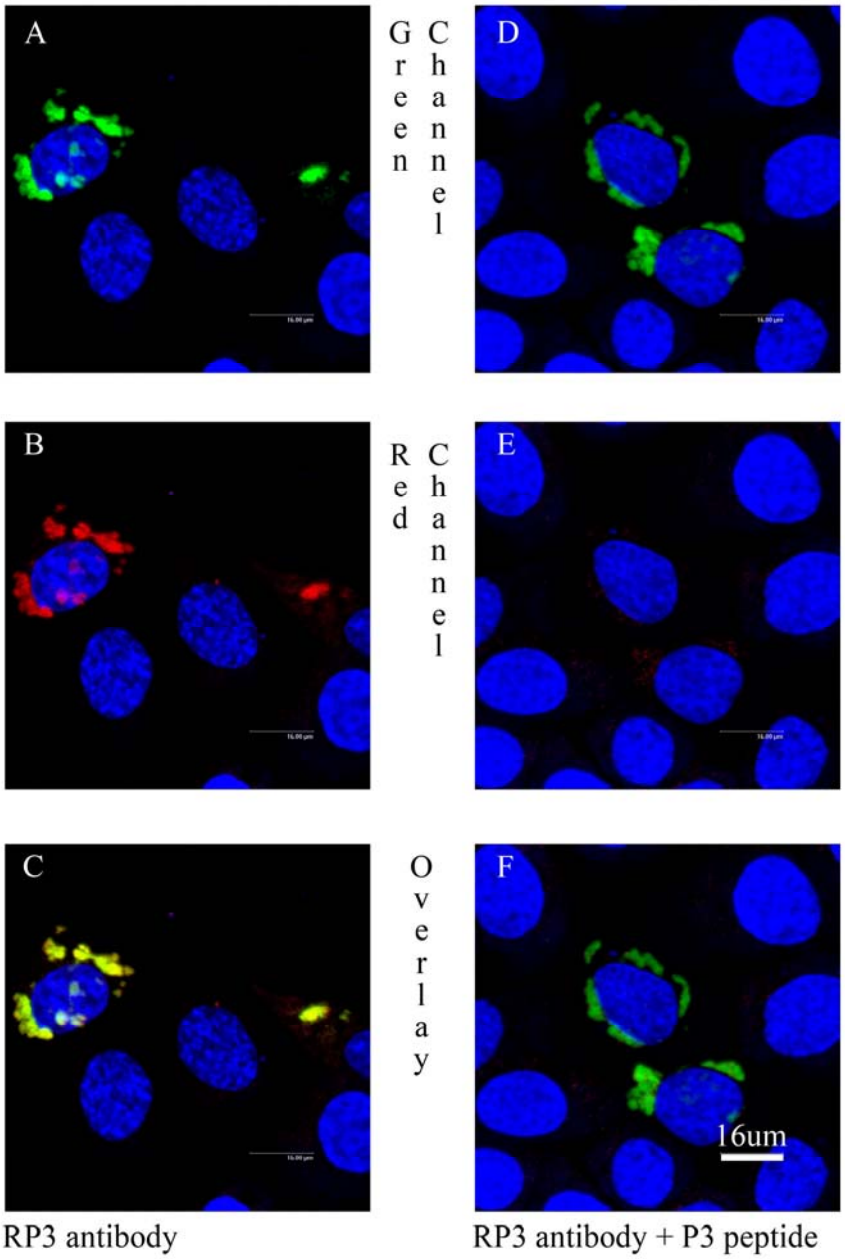

Figure 3.8 Immunocytochemistry with ADAM33 antibody RP3.

Green and red channel and overlay images using confocal microscopy of NCI H292 epithelial cells transiently transfected with full length ADAM33 coupled to Green Fluorescent Protein, fixed in 4% paraformaldehyde and stained with Zenon® labelled RP3 antibody without (red) (A,B,C) and with the blocking peptide P3 (D,E,F). The cell nuclei were counterstained with TO-PRO3 (blue).

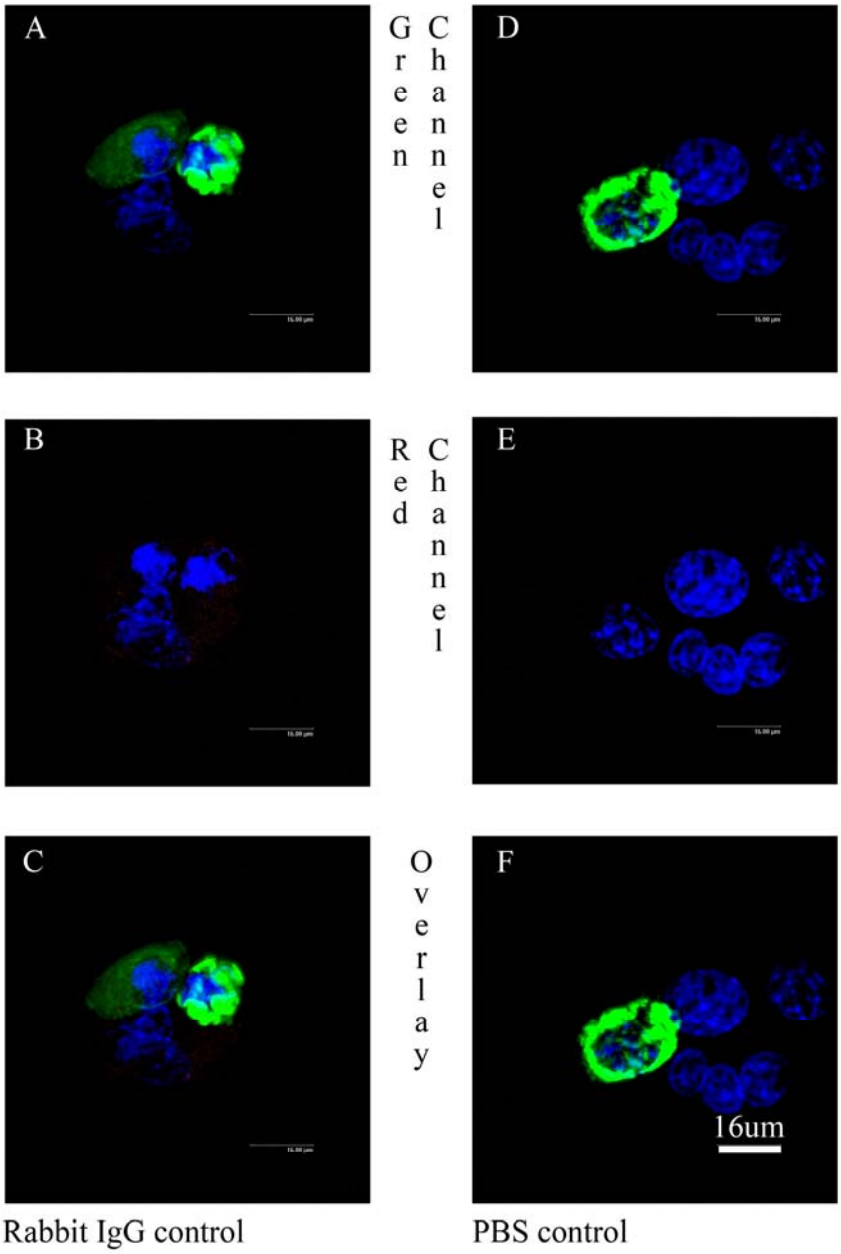

Figure 3.9 Immunocytochemistry with isotype antibody and PBS.

Green and red channel and overlay images using confocal microscopy of NCI H292 epithelial cells transiently transfected with full length ADAM33 coupled to Green Fluorescent Protein, fixed in 4% paraformaldehyde and stained with Zenon® labelled Rabbit IgG (A,B,C) and Phosphate Buffered Saline (PBS) (D,E,F) as controls. The cell nuclei were counterstained with TO-PRO3 (blue).

3.2.3 Immunohistochemical analysis and localisation of ADAM33 in bronchial biopsies

The next step was to localise ADAM33 protein expression in bronchial biopsies by immunohistochemical staining using the RP3 antibody against the cytoplasmic domain of ADAM33 which allowed detection of all potential isoforms of ADAM33 with exception of the putative soluble form.

On average 2.5 biopsies (range: 1-4) were taken from each subject in both groups (asthmatic and controls). Sections of all GMA embedded biopsies were stained with toluidine blue, images taken, submucosal area measured and evaluated for smooth muscle content. 19 out of 30 biopsies (63%) (Average 1.6 per subject) in the asthmatic group (n=12) contained smooth muscle compared to 21 of 38 biopsies (55%) (Average 1.4 per subject) in the control group (n=15). There was no significant difference in number of biopsies per subject containing smooth muscle in the asthmatic and control subjects (p=0.56) (Data were provided by Tim Shaw). One biopsy per subject containing submucosal smooth muscle was selected on the basis of greatest submucosal area for immunostaining. There was no significant difference between control and asthmatic subjects in submucosal area of all biopsies as well as the biopsies chosen for IHC.

Through use of serial thin sections (2μm), it was possible to demonstrate localisation of ADAM33 in αSMA positive cells (Figure 3.10). Immunostaining for ADAM33 (Figure 3.10B) was predominantly within the αSMA smooth muscle bundles (Figure 3.10A), however, single cells in the submucosa and around vessels were also positively stained for ADAM33 (Figure 3.10B). Although immunostaining of the muscle and submucosal cells was blocked in the presence of the immunizing peptide (Figure 3.10C), the weak staining of the bronchial epithelial cells was not fully blocked by the immunizing peptide and probably represents non-specific cross-reactivity with epithelial cytokeratins, as demonstrated below. Analysis of the ADAM33 and αSMA positive stained area relative to the total area of smooth muscle bundles in serial sections showed no significant difference in expression of ADAM33 and αSMA protein in asthmatic compared with control subjects (Figure 3.11). Similarly, no significant difference ($p>0.05$) was observed between normal and asthmatic subjects if ADAM33 or αSMA immunostaining were expressed relative to submucosal area.

To explore further the distribution of ADAM33 and αSMA in bronchial biopsies, tissue pieces were processed for immunofluorescence confocal microscopy. Using a FITC-conjugated antibody, αSMA positive myofibroblasts or migratory smooth muscle cells could be easily visualised by the green immunostaining of the actin filaments (Figure 3.10D & G).

These cells were also ADAM33 positive (Figure 3.10E) and showed yellow co-localisation when the green αSMA and red ADAM33 channels were overlaid (Figure 3.10F). In addition to its presence in the αSMA-positive cells, ADAM33 immunostaining was also occasionally detected in cells with no obvious αSMA staining (Figure 3.10F, arrowhead); these may be fibroblasts or primitive smooth muscle precursors. No immunostaining was detected when the ADAM33 antibody was pre-adsorbed with the immunising peptide (Figure 3.10H, I).

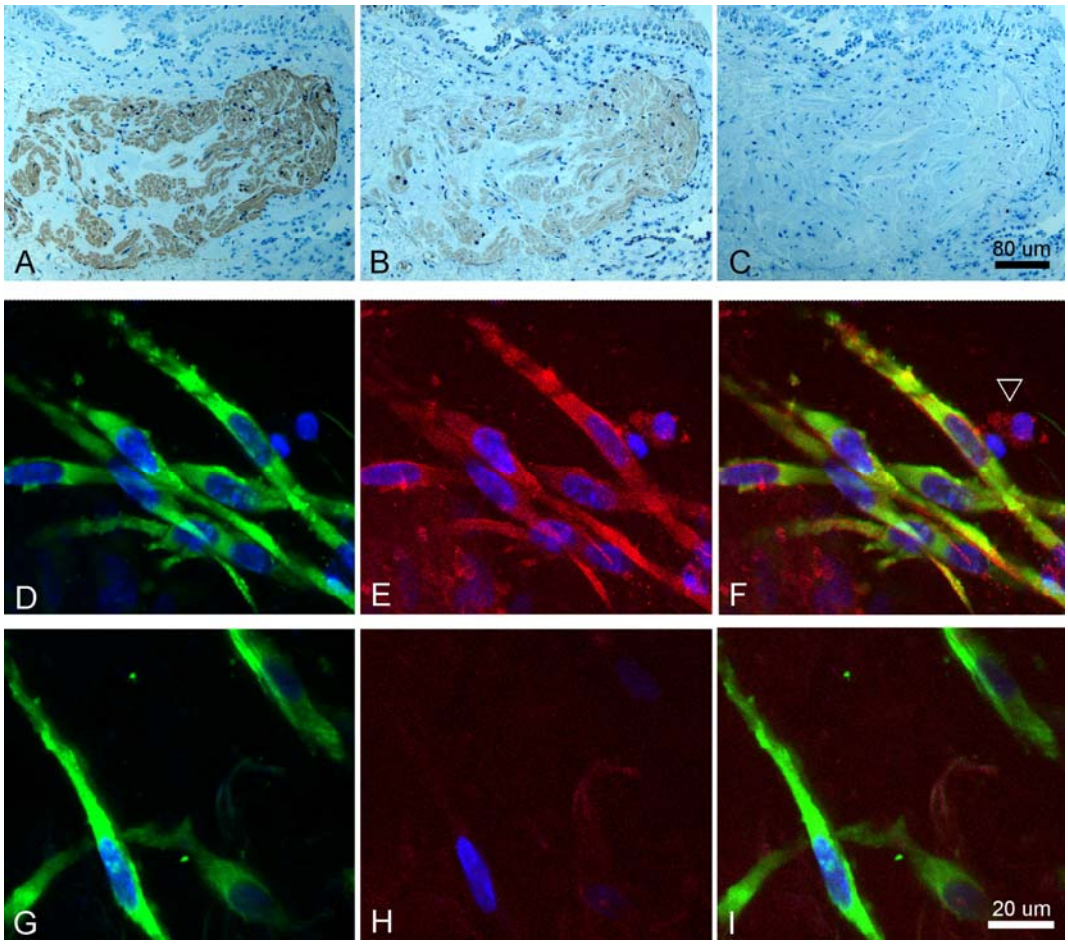

Figure 3.10 Immunohistochemistry and confocal microscopy of bronchial biopsies.

Immunohistochemical analysis (A-C) of serial sections taken from a bronchial biopsy showing the pattern of immunostaining for αSMA (A), ADAM33 (B) or ADAM33 plus immunizing peptide (C). Co-localisation of αSMA and ADAM33 by laser immunofluorescence confocal microscopy (D-I) using whole mounts of bronchial biopsy tissue. Tissue samples were immunostained with FITC conjugated αSMA (green fluorescence; D and G) and Alexa Fluor 546 labelled ADAM33 (red fluorescence, E). Overlay of red and green channels (F) showed that αSMA and ADAM33 were usually co-localised (yellow) within the same cell, however, some cells stained positively for ADAM33 but not for αSMA (white arrow head). ADAM33 immunostaining was markedly reduced when the antibody was preadsorbed with the immunizing peptide (H and I). Nuclei are counterstained with TO-PRO-3® iodide (purple-blue).

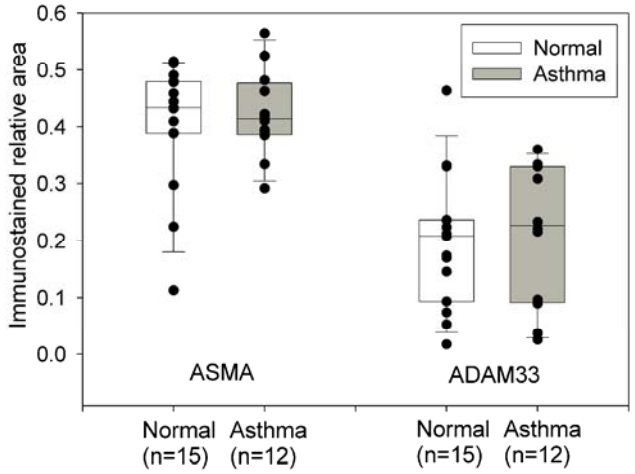

Figure 3.11 Quantitation of ADAM33 and αSMA IHC in bronchial biopsies.

Image analysis of immunostaining in normal and asthmatic bronchial biopsies.

3.2.4 Western Blot analysis of ADAM33 expression in bronchial biopsies, smooth muscle cells and bronchial brushings

In addition to immunofluorescence studies, Western blot analysis was undertaken to characterise ADAM33 protein expression in bronchial biopsies (BBx) and to enable comparison with splice variants in airway smooth muscle cells (SMC). Using the RP3 antibody to the cytoplasmic domain that recognises all predicted variants of ADAM33, with the exception of the putative secreted isoform, several specific bands with molecular weights of 22, 37, 55 and 65 kDa were detected in lysates of SMCs and BBx, but not bronchial epithelial brushings. RP3 antibody also recognises full length ADAM33 in recombinant Cos7 cells. While the immunoreactivity of these bands was blocked in the presence of the immunizing peptide, a strong band at around 50kDa whose reactivity could not be blocked was seen in bronchial biopsies and bronchial brushings (Figure 3.12). Based on a Western blot using a mixture of monoclonal pan cytokeratin antibodies (Figure 3.13) and on its molecular weight and epithelial origin (i.e. presence in bronchial brushings), we suggest that this is a non-specific interaction with epithelial cytokeratins which have molecular weights in this range. Taken together with the mRNA data, these findings suggest that the majority of ADAM33 isoforms in bronchial biopsies and airway smooth muscle cells exist as smaller alternatively spliced variants that lack the metalloprotease domain, as previously reported in bronchial fibroblasts (Powell *et al.* 2004). Based on their recognition by an antibody to the carboxyl tail of ADAM33, the 22 kDa proteins are most likely to contain the carboxyl tail and a short region upstream into EGF and cysteine-rich domain. The lack of mRNA expression and a corresponding lack of any specific immunoreactivity in bronchial brushings are consistent with previous reports that ADAM33 is not expressed in epithelial cells (Van Eerdewegh *et al.* 2002).

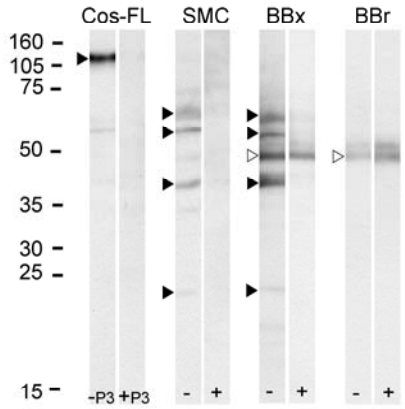

Figure 3.12 Western blots with ADAM33 antibody RP3.

Western blots of lysates from COS7 cells transfected with full length ADAM33 (Cos-FL) (gift from Jim Wicks), airway smooth muscle cells (ASMC), bronchial biopsies (BBx) and bronchial brushings (BBr) were stained with ADAM33 antibody or ADAM33 antibody preadsorbed with the immunizing peptide (P3). Black arrow heads indicate specific ADAM33 bands. The white arrow head shows the non-specific band with a molecular weight of 48 kDa in BBxs, BBrs and HELs that could not be blocked with the immunizing peptide and which was putatively identified as cytokeratin.

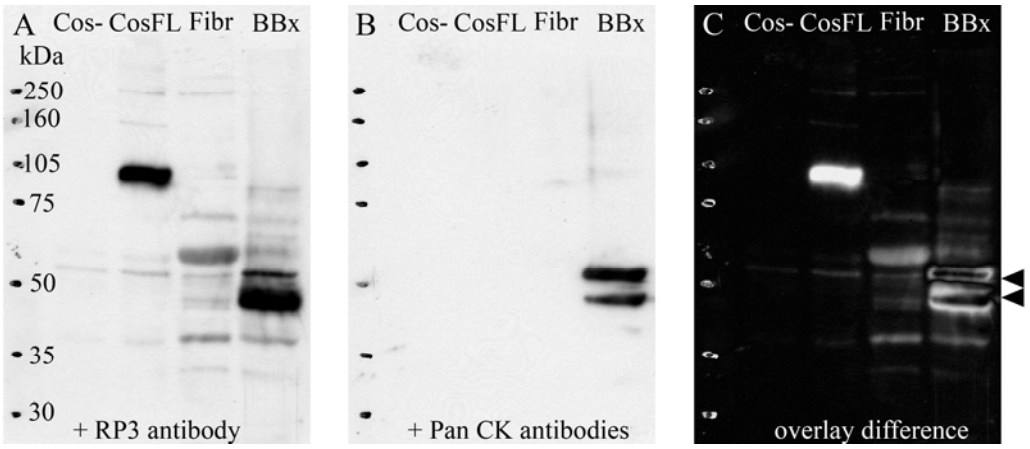

Figure 3.13 Western blots with pan-cytokeratin antibodies.

Western blot of Cos7 without (Cos-) and with ADAM33 full length (CosFL) transfected, Fibroblasts (Fibr) and bronchial biopsy (BBx) from same subject. Membrane was blotted with ADAM33 antibody (RP3) (A), then stripped and re-blotted with Pan cytokeratin antibodies (Pan CK antibodies) (B). The 2 blots were overlaid to show the difference of the 2 blots (C) which showed that 2 cytokeratin bands overlay with 2 non-specific bands in the bronchial biopsy around the molecular weight of 50kDa (black arrows).

3.3 Discussion

The analysis of ADAM33 transcripts in bronchial biopsies from normal and asthmatic subjects revealed a similar profile of ADAM33 splice variant expression as was reported by Powell et al using bronchial fibroblasts (Powell *et al.* 2004). No significant difference could be shown for overall ADAM33 mRNA or individual splice variant expression. This was also confirmed with immunohistochemistry at the protein level using normal and asthmatic bronchial biopsies (Figure 3.11). These data suggest that simple up or down regulation of ADAM33 expression is unlikely to account for its role in the development of asthma, however, some caution should be taken in the interpretation of the data due to the relative small number of subjects which might be insufficient to take into account the influence of ADAM33 genetic variation on protein expression. These data also contrast recent findings (Ito *et al.* 2007; Foley *et al.* 2007). Ito et al reported that ADAM33 protein was more strongly expressed in airway smooth muscle of bronchial biopsies from 4 normal and 4 asthmatic subjects using immunohistochemistry with the RP3 antibody. However, this is a relative small number of subjects and it is not clear how they analysed the staining. It is also in contrast to the findings by Foley et al from the same research group that reported no positive staining for ADAM33 in smooth muscle of bronchial biopsies in normal subjects and positive staining in 100% of severe and moderate and about 30% in mild asthmatic. They also showed a significant increase of epithelial scores for positive staining for ADAM33 as well as ADAM33 mRNA expression in bronchial biopsies from subjects with severe and moderate asthma compared to mild and normal subjects. However, data in this chapter suggest that there is no expression of ADAM33 mRNA in bronchial brushings and hence bronchial epithelial cells and no increase of mRNA expression in bronchial biopsies from severe asthmatic subjects compared to normal subjects. RT qPCR was done with probe based assays that were intron spanning compared to the Sybr green assay done without the report of a specific melt curve in these recent reports. Probe-based assays give only a signal when the probe is incorporated into the amplified sequence resulting in the release of a fluorescent signal which is specific. However, Sybr green assays are based on the incorporation of Sybr green into double stranded DNA during amplification. Therefore, all DNA products including DNA resulting from miss priming or primer dimmer formation of the forward and reverse primer will produce an amplification signal. Only a meltcurve analysis of the RT-qPCR product can tell if the amplification curve has a clean and specific single product signal showing only one peak at the predicted melting temperature (See chapter 2 Section 2.3.3).

Western blot analysis detected several smaller than full length bands in bronchial biopsies and smooth muscle cells (Figure 3.12) consistent with the findings from previous work

(Powell *et al.* 2004), suggesting a lack of the MP domain. This absence suggests that the proteolytical active MP-domain might be tightly controlled and some function of ADAM33 may be linked to the disintegrin, cysteine rich or EGF domains, which may play a role in cell interaction and adhesion.

Using immunohistochemistry and confocal microscopy, the first time finding that ADAM33 occurs predominantly in smooth muscle bundles and in some undifferentiated (αSMA negative) mesenchymal cells are of great importance (Figure 3.10). It suggests that ADAM33 might play an important role in smooth muscle development and function and in development and differentiation of mesenchymal cells, such as fibroblasts/myofibroblasts. These cells play an important role in pre-natal lung development and airway modelling where ADAM33 might lead to abnormal airways early in life that might result in the development of asthma in childhood. The effect of ADAM33 in early life might be 'swamped' by environmental effects in later life and adulthood, hence making it important to study the expression and role of ADAM33 in children.

3.4 Summary of results and novel findings.

- ADAM33 mRNA is expressed in bronchial biopsies.
- ADAM33 splice variant isoform profile is similar to that in fibroblasts (Powell *et al.* 2004).
- ADAM33 mRNA expression does not differ between healthy control and mild to moderate or severe asthmatic subjects.
- RP3 antibody against the cytoplasmic domain of ADAM33 is strong and specific in detecting full length ADAM33 expressed in H292 epithelial cells.
- ADAM33 protein co-localises almost exclusively to smooth muscle cell bundle in adult bronchial biopsies.
- ADAM33 protein expression in adult bronchial biopsies confirmed the mRNA data.
- Western blot analysis showed several isoform bands in bronchial biopsies similar to the one found in smooth muscle cells. The non-specific bands around 50kDa were positive for cytokeratin.

Chapter 4 Results: ADAM33 in Human embryonic lung

4.1 Background

Although the function of ADAM33 is mostly unknown, its selective expression in mesenchymal cells, such as fibroblasts, myofibroblasts and smooth muscle cells, suggests that its function is linked to airway remodelling, an important component of asthma pathophysiology, that might start as early as during the development of the unborn lung. It is also known that maternal atopy/allergy is a strong risk factor for development of BHR and asthma early in life (Young *et al.* 1991) suggesting that a maternal allergic environment has an effect on lung modelling in utero or early in life.

Investigations of function of a novel gene usually begin with over-expression and knock out studies. Although studies in an ADAM33 knock out mouse did not show a major effect on lung development and function in either normal or allergen challenged mice (Chen *et al.* 2006), these studies are difficult to interpret as other ADAM proteins or MMPs may compensate for the absent ADAM33.

In order to study the involvement of ADAM33 in human lung development the first aim of this chapter is to examine the overall expression of ADAM33 as well as particular splice variants in human embryonic lungs in vivo. Therefore, human embryonic lung was studied to assess ADAM33 expression during embryonic lung development to extend work in fibroblasts and in bronchial biopsies and to determined the cellular origin of ADAM33 in HELs.

A second aim is to develop a HEL explant culture model to examine the expression of ADAM33 in HELs in vitro without and in the presence of IL-13, to mimic a maternal allergic environment.

A third aim is to examine the effect of ADAM33 knock down in contrast to knock out on HEL whole tissue pieces and primary fibroblasts using ADAM33 siRNA.

4.2 Results

4.2.1 Analysis of ADAM33 mRNA expression in human embryonic lungs

Initial studies focused on extraction of RNA from fresh HELs obtained 7 to 9 weeks post conception (wpc) (collected by David Wilson & Neil Hanley). This revealed that there was a similar mRNA pattern of splice variant expression analysis of ADAM33, with those found in fibroblasts (Powell *et al.* 2004) and bronchial biopsies with relatively few transcripts encoding the metalloprotease domain exons (FGHI). However, all of the ADAM33 splice variants relative to global ADAM33 (3'UTR) were less expressed than in fibroblasts and bronchial biopsies (Figure 4.1). A possible explanation for this could be that the ADAM33 3'UTR primers (not intron spanning) detect some contamination by genomic DNA, which was not completely digested by DNase treatment.

Comparison of HELs at different time points during the pseudoglandular stage of lung development suggested that ADAM33 mRNA expression increased significantly from 7wpc to 9 wpc (Figure 4.2).

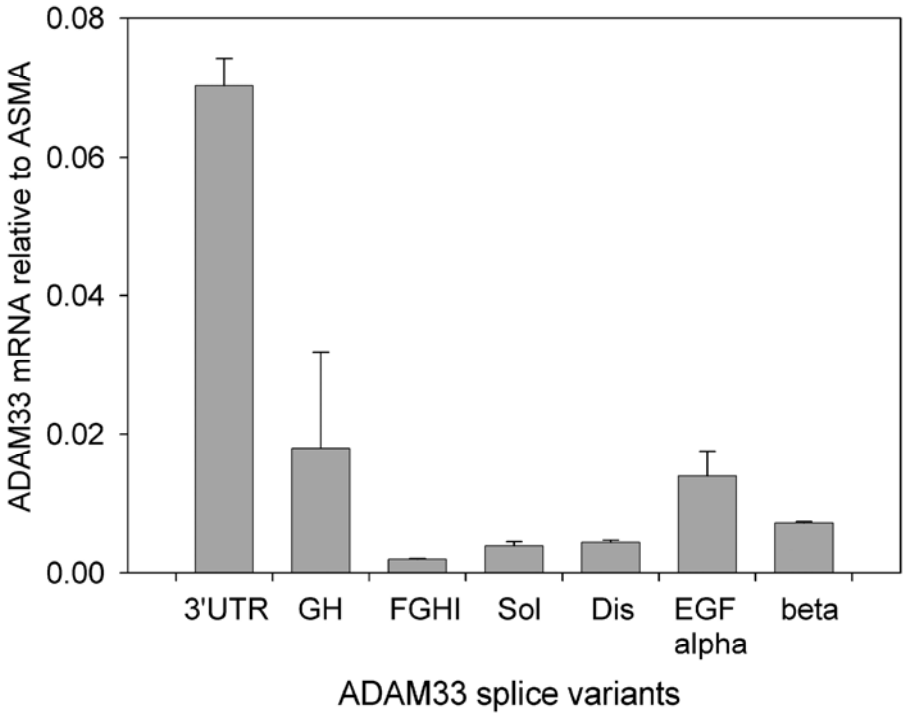

Figure 4.1 ADAM33 splice variant expression in HELs.

ADAM33 splice variant expression relative to αSMA and in human embryonic lung tissue (n=3). The same primers were used as in the adult bronchial biopsies experiments in Figure 3.1.

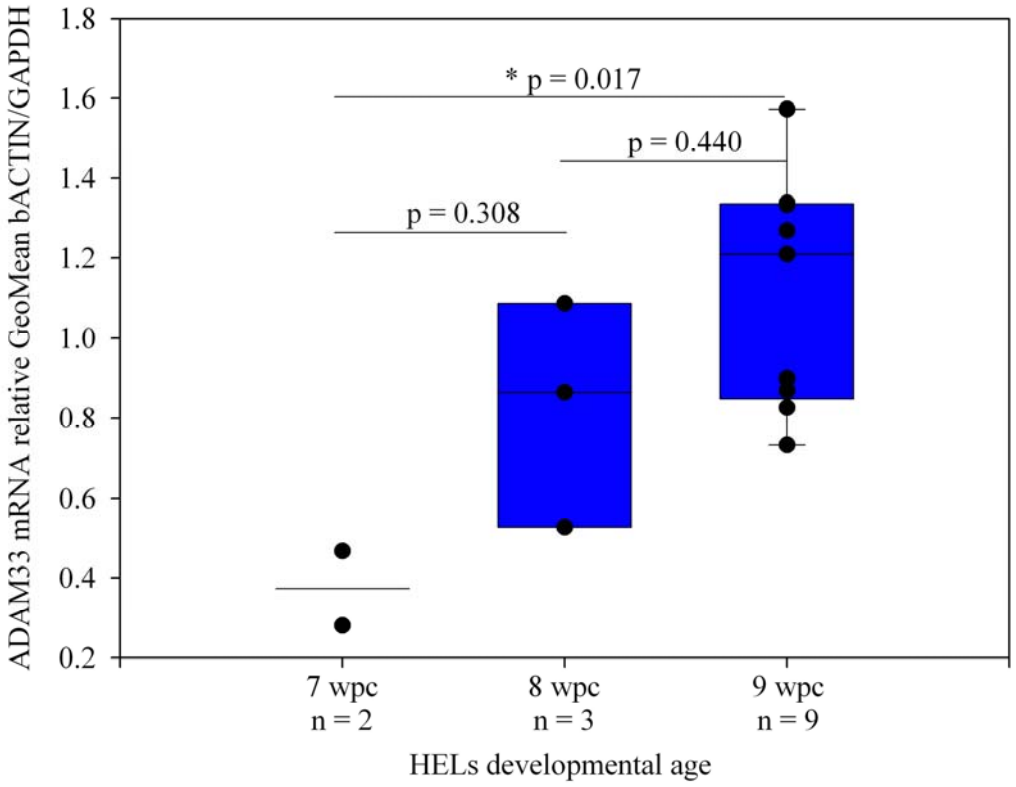

Figure 4.2 ADAM33 expression in HELs.

ADAM33 mRNA expression of HELs at 7, 8 and 9 weeks post conception (wpc). In order to detect global expression of ADAM33 the primers of the 3'UTR (See Figure 3.1) were used to detect ADAM33 in HELs at 3 different gestational time points. Statistical analysis is limited due to restricted availability of embryonic tissue (only 3 time points and low numbers of donors) (One way ANOVA and multiple comparison Bonferroni t-test; * p = significant).

4.2.2 Western Blot analysis of ADAM33 expression in human embryonic lungs

Western blot analysis was undertaken to characterise ADAM33 protein expression in HELs and to enable comparison with splice variants in airway smooth muscle cells (SMC). Using an antibody to the cytoplasmic domain that recognises all predicted variants of ADAM33, with the exception of the putative secreted isoform, several specific bands with molecular weights of 22, 37, 55 and 65 kDa were detected in lysates of SMCs and HEL with an extra strong band at 25 kDa that was evident in embryonic lung samples (Figure 4.3).

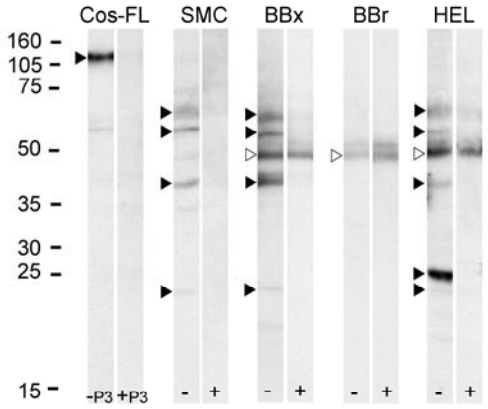

Figure 4.3 Western blotting of HELs.

Western blots of lysates from COS7 cells transfected with full length ADAM33 (Cos-FL) (gift from Jim Wicks), airway smooth muscle cells (ASMC), bronchial biopsies (BBx), bronchial brushings (BBr) and human embryonic lungs (HELs) were stained with ADAM33 antibody or ADAM33 antibody pre-adsorbed with the immunizing peptide (P3). Black arrow heads indicate specific ADAM33 bands. The white arrow head shows the non-specific band with a molecular weight of 48 kDa in BBxs, BBrs and HELs that could not be blocked with the immunizing peptide and which was putatively identified as cytokeratin.

4.2.3 Immunohistochemical analysis and localisation of ADAM33 in human embryonic lungs

Immunohistochemical staining of human embryonic lung tissue in the pseudoglandular stage of lung development around weeks 8-10 of gestation showed specific staining around the embryonic bronchial tree for αSMA (Figure 4.4A) and ADAM33 (Figure 4.4B). However, in contrast with the adult lung (See chapter 3.2, Figure 3.10) where ADAM33 and αSMA immunoreactivity showed a very similar distribution, there were many ADAM33 positive cells in the undifferentiated mesenchyme surrounding the bronchial ducts that were not positive for αSMA (Figure 4.4B). To further explore the relationship between ADAM33 and αSMA distribution, embryonic lung pieces were analysed by immunofluorescent confocal microscopy. Using the FITC-conjugated αSMA antibody, the 3-dimensional structure of the embryonic airways could be visualised easily through the green immunostaining of the actin filaments and there was no detectable αSMA immunostaining outside of these tubular structures (Figures 4.4D & 4.5). By analysing Z-series taken through individual airways, the αSMA immunostaining clearly delineated the boundary between the epithelial cells within the airway and the undifferentiated mesenchyme around the developing airway (Figure 4.4E-L). ADAM33 immunoreactivity, which was detected using a red Alexa Fluor conjugate was absent from the airway epithelial cells, but showed prominent immunostaining in the surrounding mesenchymal cells (Figure 4.4E-L). Analysis of the pattern of red ADAM33 and green αSMA immunostaining confirmed that while ADAM33 did show some yellow co-localisation within the overlay image, the majority was present in undifferentiated mesenchymal cells that showed no detectable αSMA expression (Figure 4.4D-L). ADAM33 staining was not detected when the ADAM33 antibody was pre-adsorbed with the immunising peptide (Figure. 4.6).

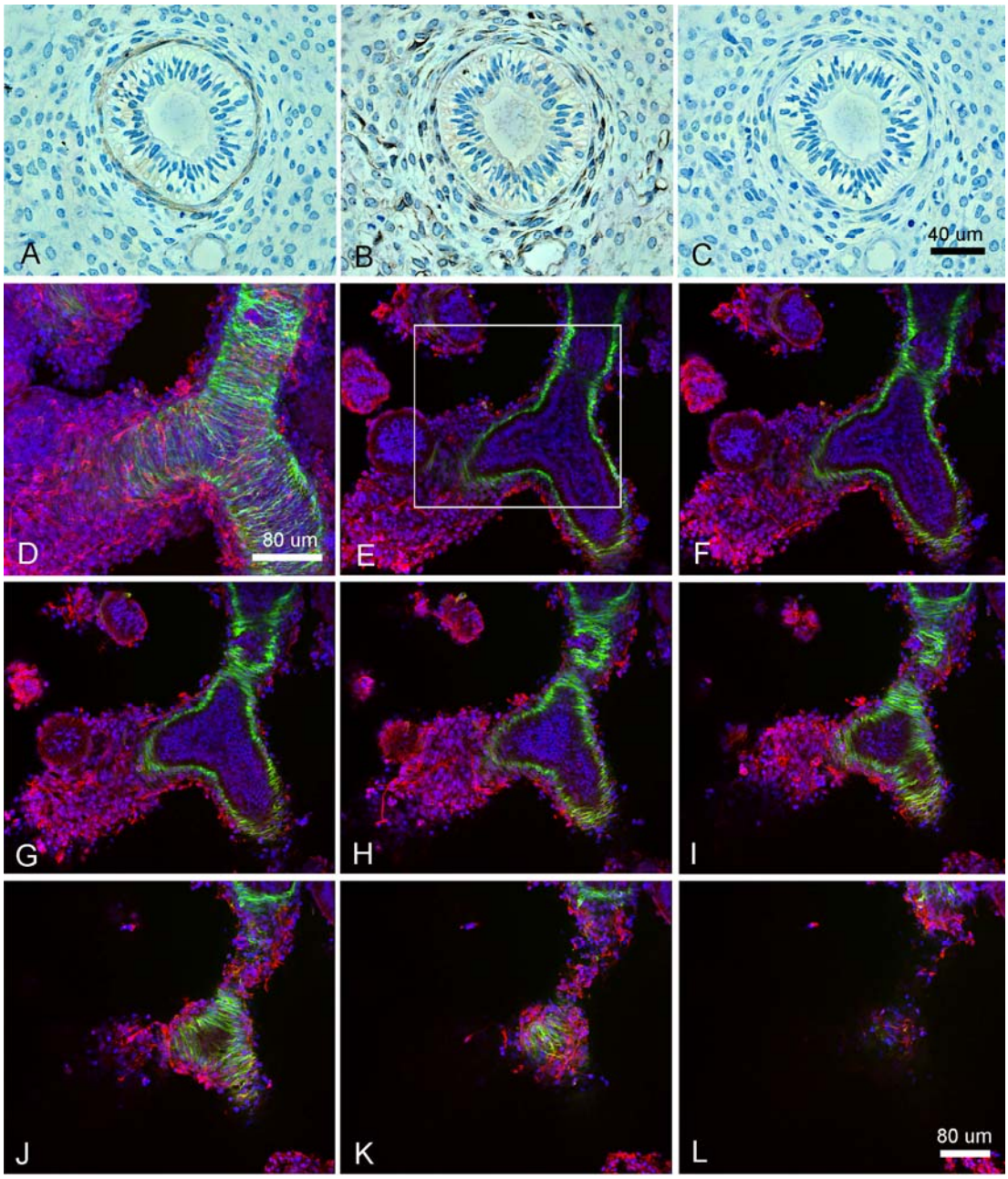

Figure 4.4 Immunohistochemistry and confocal microscopy of HELs.

Immunohistochemical analysis (A-C) of serial sections taken from glycol methacrylate-embedded human embryonic lung showing the pattern of immunostaining for αSMA (A), ADAM33 (B) or ADAM33 plus immunizing peptide (C). Co-localisation of αSMA and ADAM33 by laser immunofluorescence confocal microscopy (D-L) using whole mounts of human embryonic lung tissue. Human embryonic lung pieces were immunostained with FITC conjugated αSMA, Alexa Fluor 546 labelled ADAM33 and the nuclei counterstained with TO-PRO-3® iodide (purple-blue). Plate D shows a 3-dimensional image of an embryonic airway constructed from the z-series (5μm apart) shown in plates E-I (within the white frame). In each plate, red and green channels are overlaid so that yellow pixels indicate areas of co-localisation of αSMA and ADAM33. Data are representative of three independent experiments.

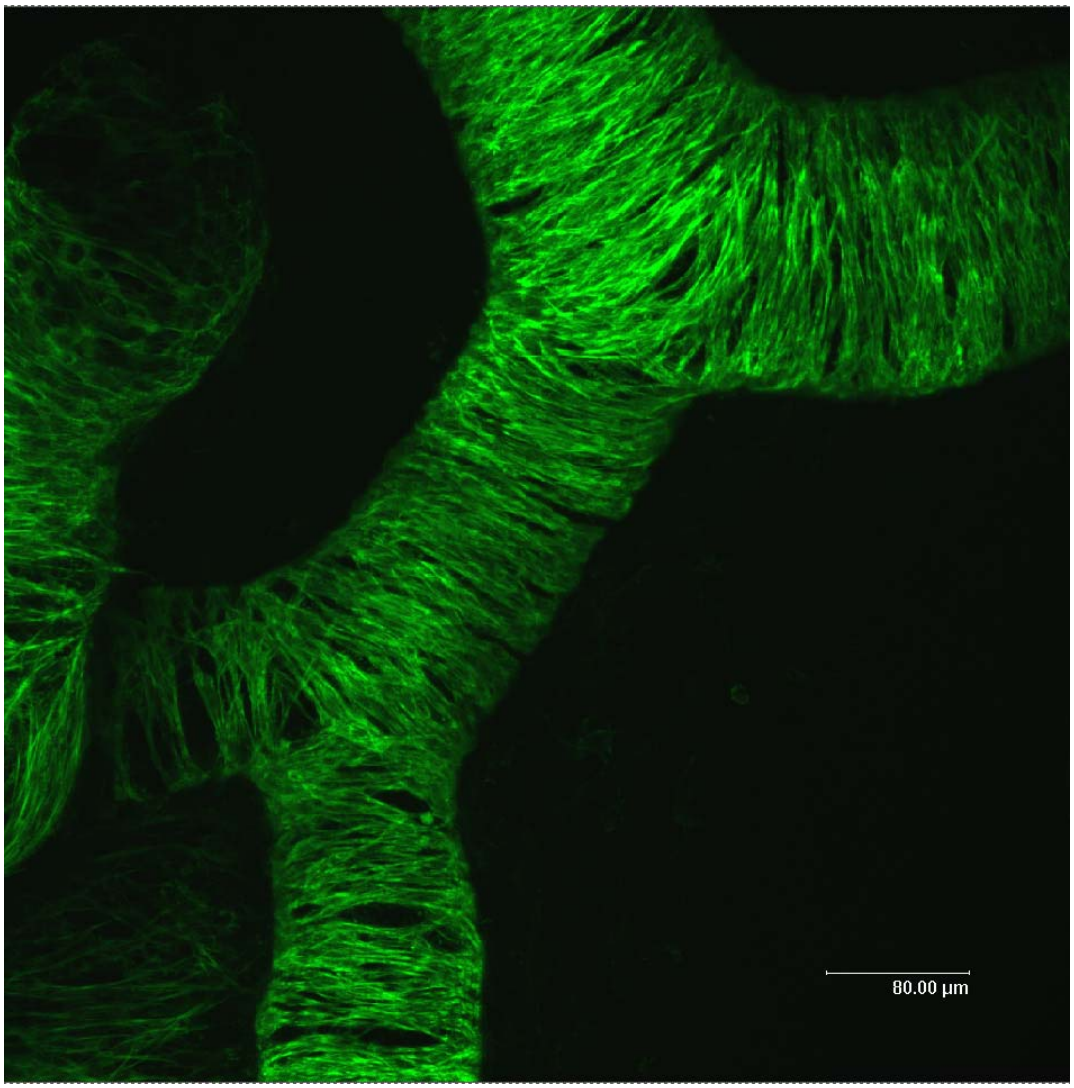

Figure 4.5 Confocal microscopy: αSMA positive cells in HEL.

Confocal microscopy of 8 weeks post conception human embryonic lung showing the structure of primitive smooth muscle tubes stained with FITC labelled anti-αSMA antibodies.

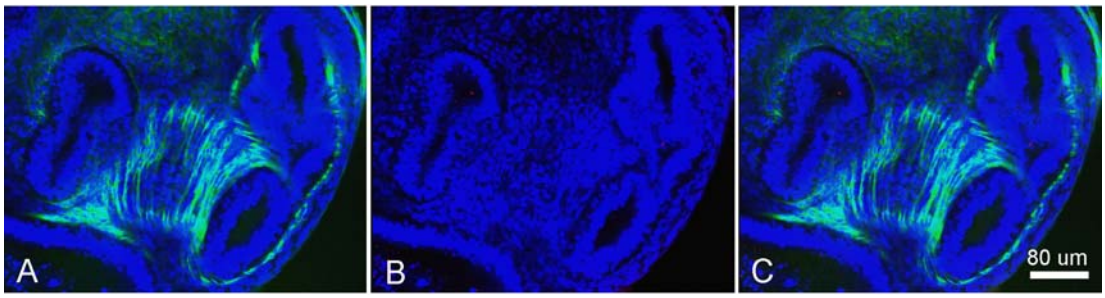

Figure 4.6 Confocal microscopy with pre-adsorbed ADAM33 antibody.

Laser immunofluorescence confocal microscopy using whole mounts of human embryonic lung tissue that were immunostained with FITC conjugated αSMA (green) (A), Alexa Fluor 546 labelled ADAM33 (red) pre-adsorbed with immunising peptide (P3) (B) and the nuclei counterstained with TO-PRO-3® iodide (purple-blue). ADAM33 staining was not detected when the ADAM33 antibody was pre-adsorbed with P3 (B) and therefore, no areas of co-localisation of αSMA and ADAM33 could be detected when red and green channels were overlaid (C).

4.2.4 ADAM33 expression in dissected HELs into tubular structures and surrounding mesenchymal cell mesh

To confirm the immunohistochemical data HELs (n=5) were dissected into the mesenchymal mesh, that has the appearance of cotton wool, and into tubes, that are surrounded by the mesenchymal mesh (Figure 4.7). ADAM33 mRNA expression was studied using RT-qPCR which was significantly higher expressed in the mesenchymal mesh compared to the tubes ($p=0.028$) but no difference could be found compared to the whole HEL ($p=0.25$) (Figure 4.8).

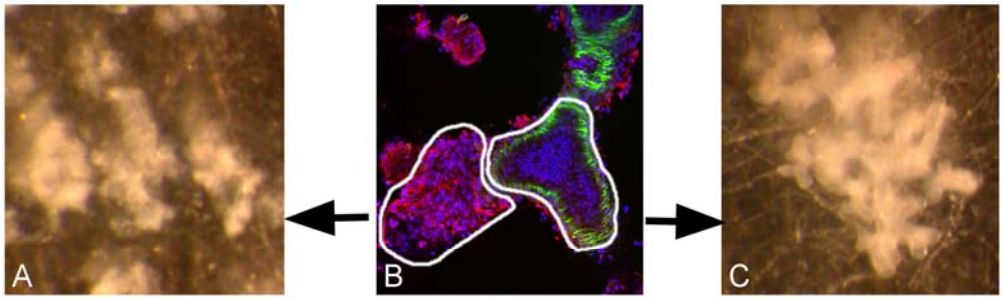

Figure 4.7 HELs dissected into tubes and mesenchyme.

HEL (B) dissected under dissecting microscope into mesenchymal mesh (A) and tubes (C).

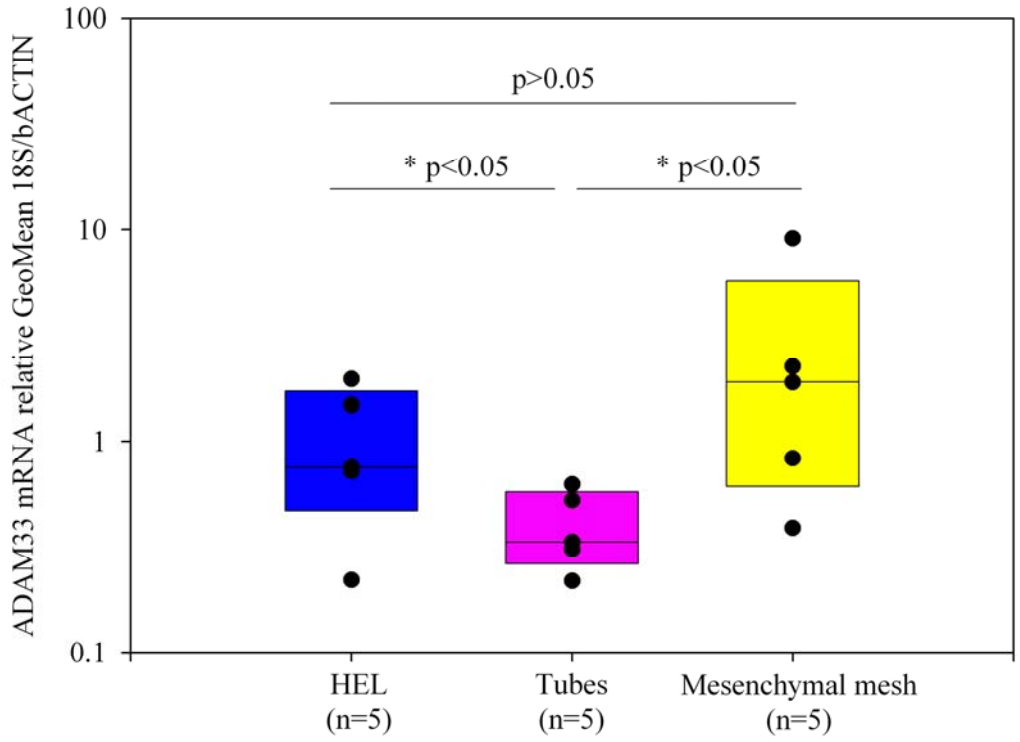

Figure 4.8 ADAM33 expression in tubes and mesenchyme of HELs.

Expression of ADAM33mRNA (primers in 3'UTR) in HELs dissected into tubes and mesenchymal mesh (Kruskal-Wallis One Way ANOVA on ranks and multiple comparison Student-Newman-Keuls method;* $p<0.05$). (* p = significant).

4.2.5 ADAM33 expression in HEL explant cultures

In order to investigate the effect of the maternal environment on ADAM33 expression in HEL development, a new explant culture model was developed. This involved taking small pieces of HELs (1-2mm) and culturing them embedded in extracellular matrix in a transwell culture insert that was placed in a well containing the medium (See chapter 2 section 2.2, Figure 2.1). Incubation of a period of 7 to 18 days showed that they had increased in size and exhibited branching morphogenesis (Figure 4.9 & 4.10).

HEL explants were cultured in serum free medium from 6 to 18 days (Figure 4.10). In these cultures ADAM33 and αSMA mRNA increased significantly after 12 and 18 days in culture compared with D0 (Figure 4.11A+B).

HEL explants were also cultured in the presence of IL-13 at dose of 1 ng/ml based on dose response curves of IL-13 in human primary adult bronchial fibroblasts (L. Andrews - unpublished data). A similar increase of ADAM33 and αSMA mRNA was detected in HEL explants cultured in serum free medium with IL-13 (1ng/ml) (Figure 4.12 A+B). However, HEL explants cultured in the presence of IL-13 to mimic a maternal allergic environment showed a significant depression of ADAM33 mRNA at day 18 in culture compared to the lungs cultured in serum free medium (Figure 4.12A). In contrast, αSMA showed no difference (Figure 4.12B).

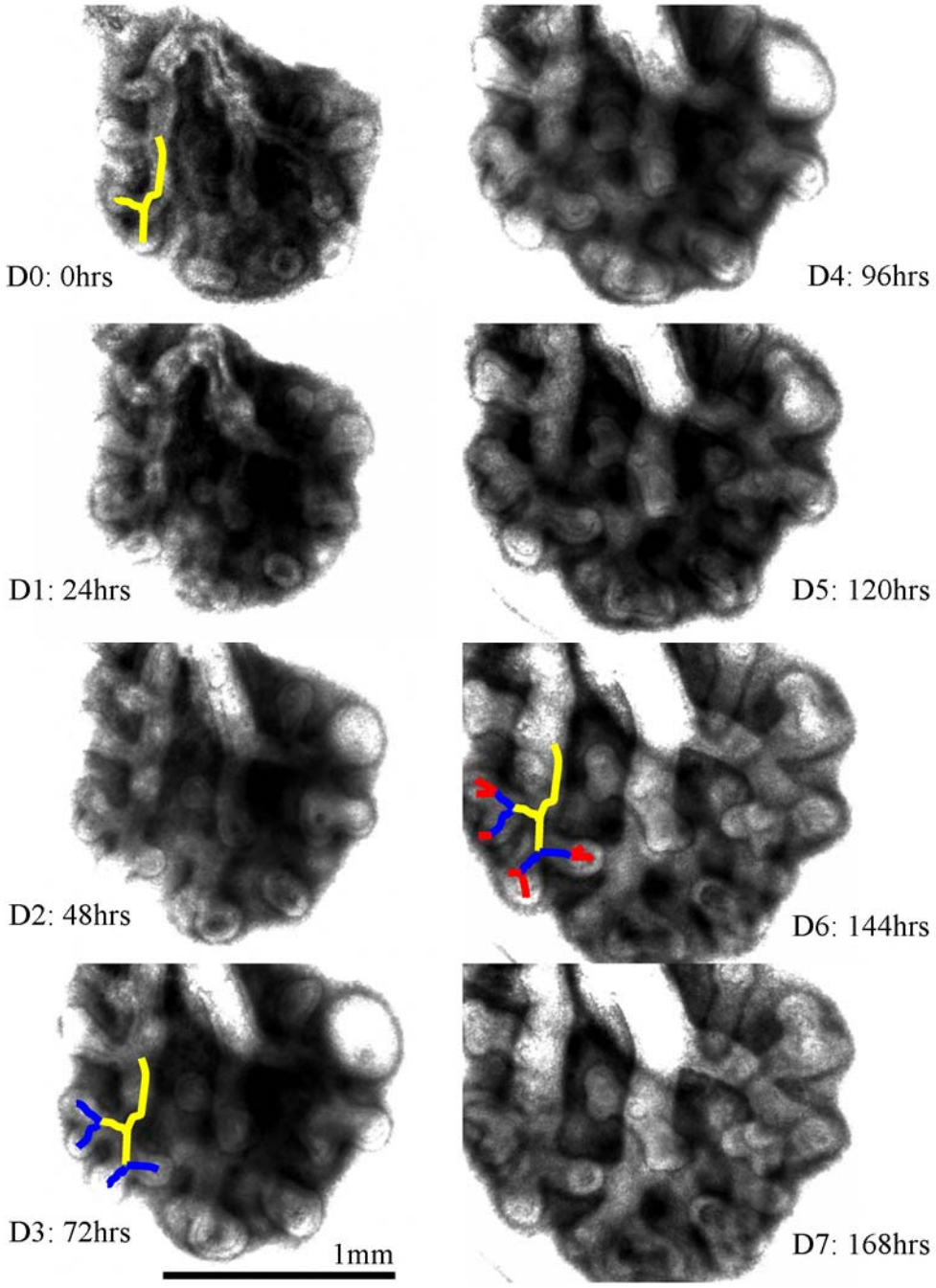

Figure 4.9 Time lapse microscopy of HEL explant culture.

Time lapse of HEL grown for 8 days showing branching morphogenesis (yellow, blue, red) in single images at 24 hours (hrs) intervals for 7 days (D) (See movie 1 in attached CD).

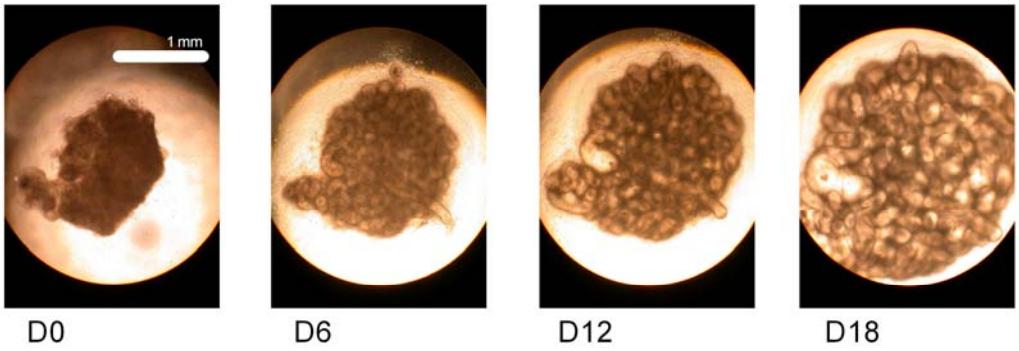

Figure 4.10 Phase contrast microscopy of HEL explant cultures.

Phase contrast images of HEL explants (8 wpc) from day 0 (D0) and cultured for 6 to 18 days (D0-18) in serum free medium.

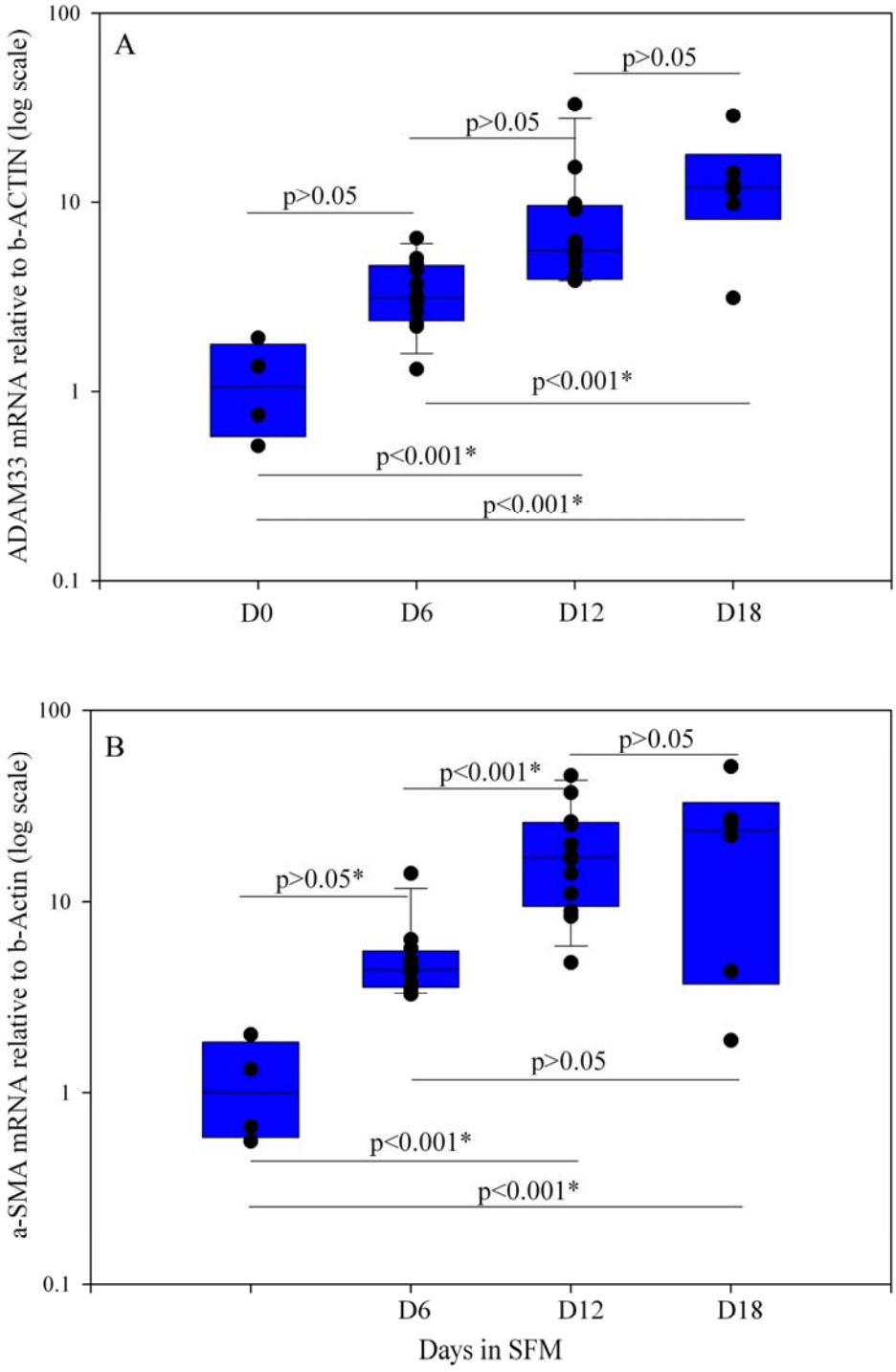

Figure 4.11 ADAM33 and αSMA expression in HEL explant cultures.

A: ADAM33 (primers in the 3'UTR) and B: αSMA mRNA expression of HELs explants from 3 independent donors cultured in serum free medium for 0 to 18 days (D0 to D18) (Kruskal-Wallis One Way ANOVA on ranks and multiple comparison Dunn's method;* $p<0.001$).

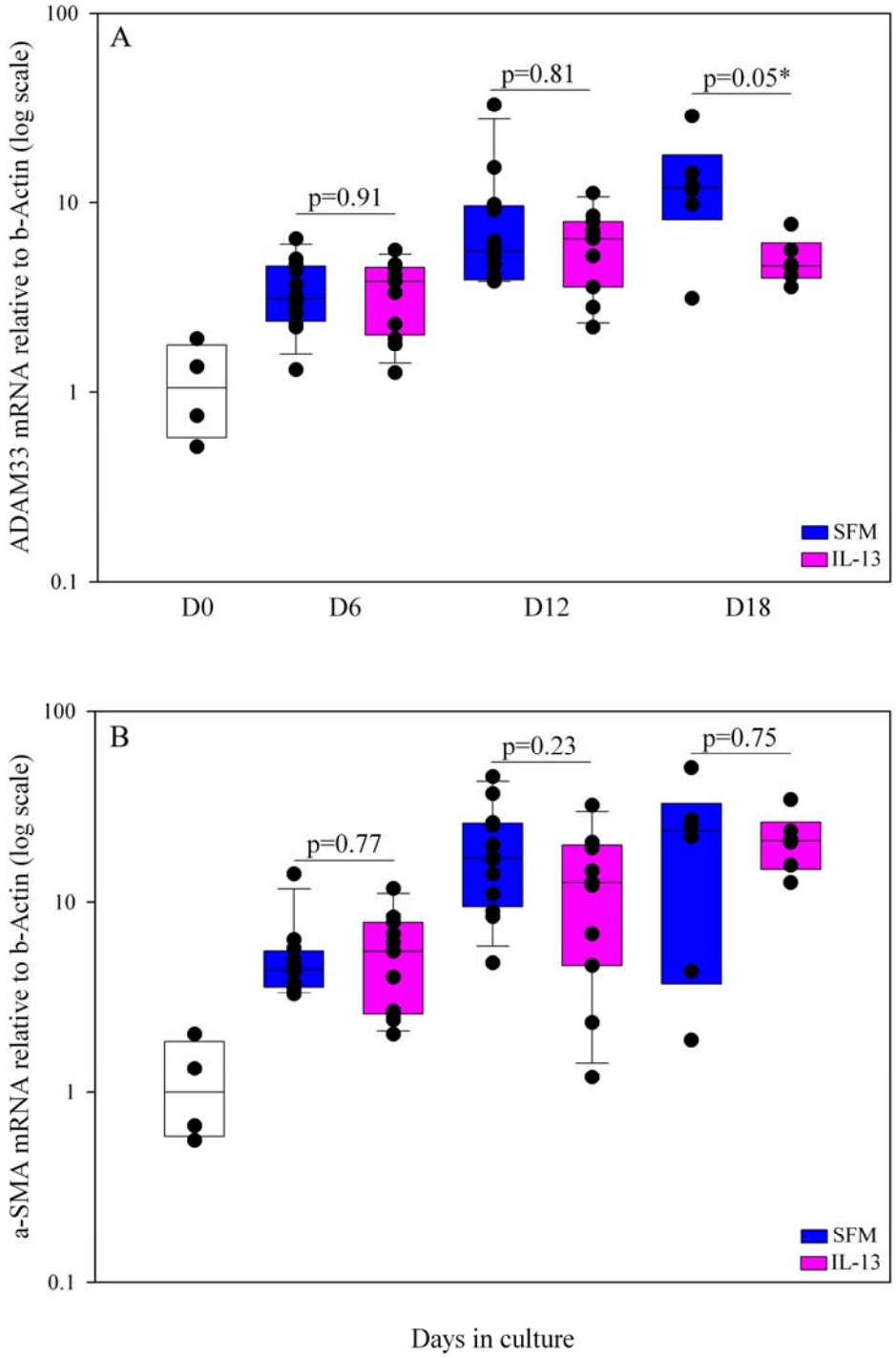

Figure 4.12 A: HEL explants cultures in the presence of IL-13.

ADAM33 (primers in the 3'UTR) and B: αSMA mRNA expression of HELs explants from 3 independent donors cultured in serum free medium (SFM) compared to cultures in SFM + IL-13 (1ng/ml) for 0 to 18 days (D0 to D18) (Mann-Whitney Rank Sum Test;* p = significant).

4.2.6 Transfection optimisation in whole embryonic lung tissue pieces

In order to study the effect of ADAM33 knockdown on human embryonic/fetal developing lung, it was aimed to test different methods of siRNA transfection to be able to achieve the difficult and challenging task to transfect whole pieces of human embryonic/fetal lung.

Transfection of human embryonic/fetal lung with baculoviurs A vector

A modified Baculovirus *Autographa califorinica* multiple nuclear polyhedris virus (ACMNPV) (Baculovirus A) vector has been successfully used to efficiently transfect different mammalian cells and tissue with different DNA constructs (Boyce and Bucher 1996; Condreay *et al.* 1999; Airenne *et al.* 2000; Gao *et al.* 2002; Ho *et al.* 2005). To evaluate if Baculovirus A could be used as a vector for ADAM33 siRNA constructs to transfect whole pieces of human embryonic/fetal lungs (HEL) pilot experiments were undertaken. The aim was to transfect HELs with baculovirus A vector carrying *lacZ* (gift from Christopher McCormick).

Initially a series of different concentrations (0, $5x10^6$, $8x10^6$, $1x10^7$ and $2x10^7$plaque forming units per ml (pfu/ml)) of baculovirus A vector carrying *lacZ* was used to infect 1-2 mm HEL tissue pieces for 24 hours. β-galactosidase activity was assessed by microscopy after fixation and incubation of the tissue pieces with the substrate X-Gal (Figure 4.13A-F). However, only a few cells showed blue positive staining with the highest baculovirus titer (Figure 4.13 F)

To overcome the potential problem of penetration of the vector, HELs were further dissected into the tubular airway structures and the mesenchymal cell mesh that surrounds these primitive airways and again infected with baculovirus A vector carrying *lacZ* at the same titers as in the experiment above. Again only a few cells in the dissected lung tissue showed positive uptake of the vector at the highest titers in form of blue staining (Figure 4.14D & E, 1 & 2).

To check if infection efficiency could be improved by higher titers of the vector (0, $1x10^7$, $2x10^7$, $3x10^7$, $4x10^7$ and $5x10^7$ pfu/ml) were used to infect the 1-2mm HEL tissue pieces. An increase of blue stained cells was observed with these higher titers (Figure 4.15A–F) but low efficiency did not warrant further exploration of the use of baculovirus A vector as transfection method of HEL tissue pieces with a construct containing ADAM33 siRNA.

Transfection of human embryonic/fetal lung with siRNA using chemical transfection reagents.

Chemical transfection of siRNA into human tissue has been successfully performed in adult skin tissue pieces of basal cell carcinoma (Ji *et al.* 2005), however, it is unknown whether siRNA can be transfected into human embryonic tissue.

Initially transfection quality and efficiency was studied by transfecting 1-2 mm HEL tissue pieces with red-fluorescently labelled (Cy3 equivalent) non-functional non-targeting siRNA (siGLO-RISCfree control siRNA = chemically modified siRNA that does not interact with RISC) at 100nM using 4 different Dharmacon transfection reagents (DharmaFECT 1-4 (Dh1-4). Each transfection reagent was used at 3 different concentrations. Phase contrast and fluorescence microscopy revealed no toxicity of Dh1 and Dh4 transfection reagents after 24 and 48 hour in culture and best transfection efficiency at the lowest concentrations. (Figure 4.16A-D).

To check for penetration of siRNA into the tissue, pieces of tissue were fixed in 4% formaldehyde and the nuclei were counterstained and laser confocal microscopy was performed on whole mounted tissue. This showed good penetration of the fluorescently labelled siRNA on the three dimensional image (Figure 4.17 A) and on the single sections taken at about 3um thickness (Figure 4.17B–F).

Human embryonic/fetal lungs were then transfected with a pool of four ADAM33 siRNAs (ADAM33-SMARTpool siRNA (M-004525-00)), a pool of four functional, non-targeting control siRNAs (Control-SMARTpool siRNA), a positive silencing control for GAPDH and the fluorescently labelled control siRNA at 100nM using Dh1 transfection reagent 1 (0.2µl/100µl total transfection medium). RT-qPCR analysis was performed after 24 and 48 hours but no significant gene silencing for ADAM33 or GAPDH could be shown despite good transfection efficiency.

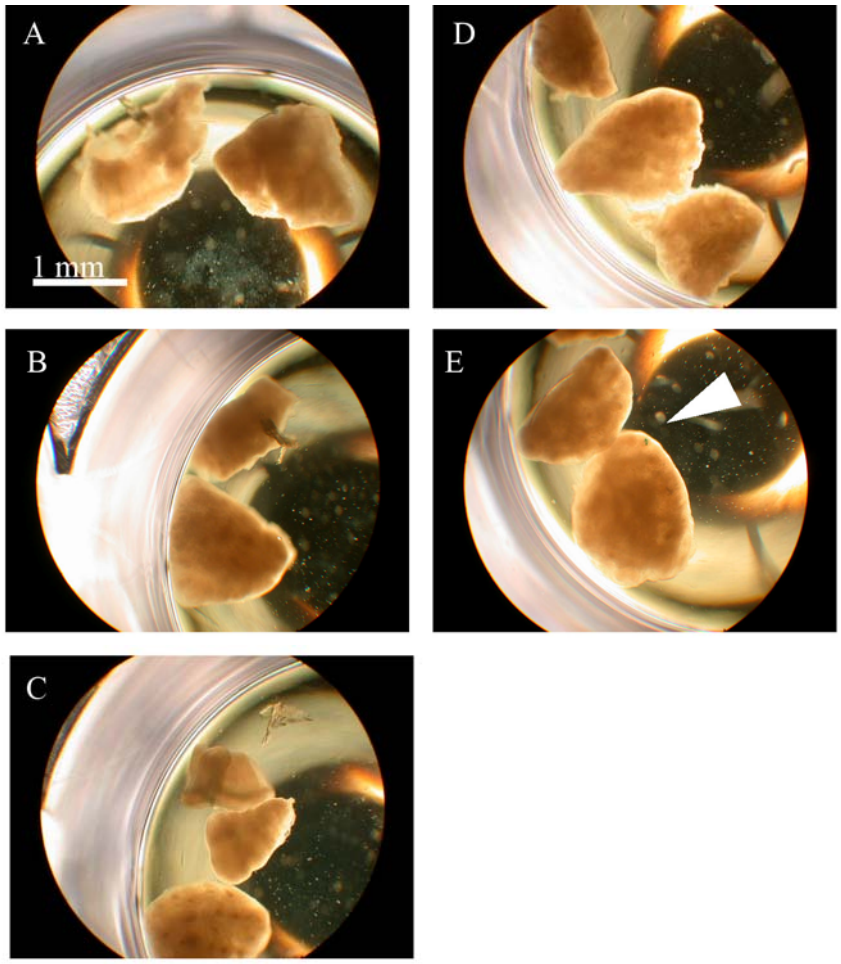

Figure 4.13 Baculovirus A vector transfection of HELs. I.

Human embryonic lungs dissected in 1x2 mm tissue pieces transfected with baculovirus A vector carrying lacZ in 5 titers 0 (A), 5x106 (B), 8x106 (C), 1x107 (D) and 2x107 (E) plaque forming units per ml (pfu/ml) for 24 hours. β-galactosidase activity was assed after fixation in 4% formaldehyde and incubation with the substrate X-Gal (5-bromo-4-chloro-3-indolyl-β-D-galactopyranoside) for at least 4 hours. Only very few cells showed blue staining (white arrow) in the lungs transfected with the highest titer of baculoviurs vector (E).

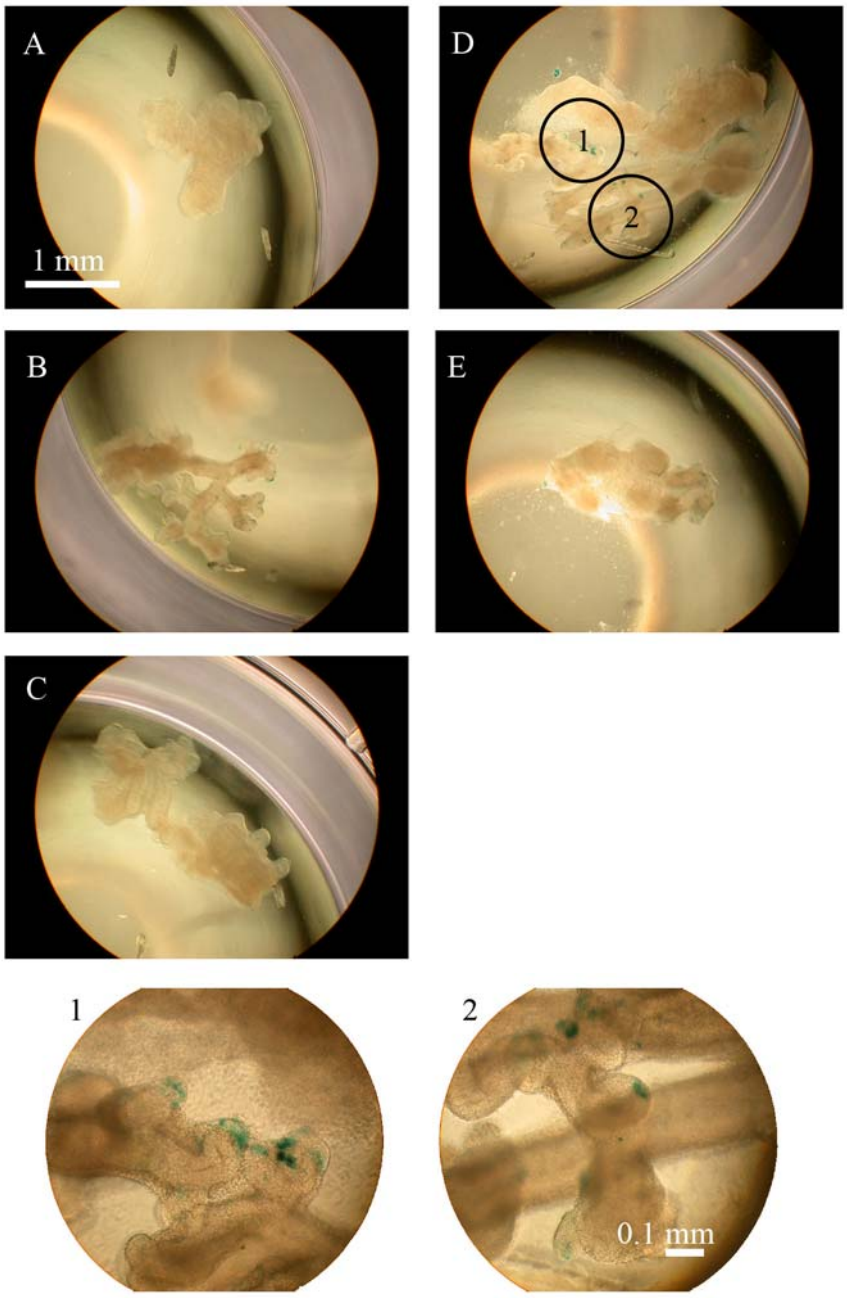

Figure 4.14 Baculovirus A vector transfection of HELs. II.

Human embryonic lungs dissected in primitive bronchial tubular structures transfected with baculovirus A vector carrying lacZ in 5 titers 0 (A), 5x106 (B), 8x106 (C), 1x107 (D) and 2x107 (E) plaque forming units per ml (pfu/ml) for 24 hours. β-galactosidase activity was assessed after fixation in 4% formaldehyde and incubation with the substrate X-Gal (5-bromo-4-chloro-3-indolyl-β-D-galactopyranoside) for at least 4 hours. Cells showing blue staining in the transfected lungs were found with the highest titer of baculoviurs vector (D & E) but were only less than 5% of whole tissue (higher magnifications) (1 & 2).

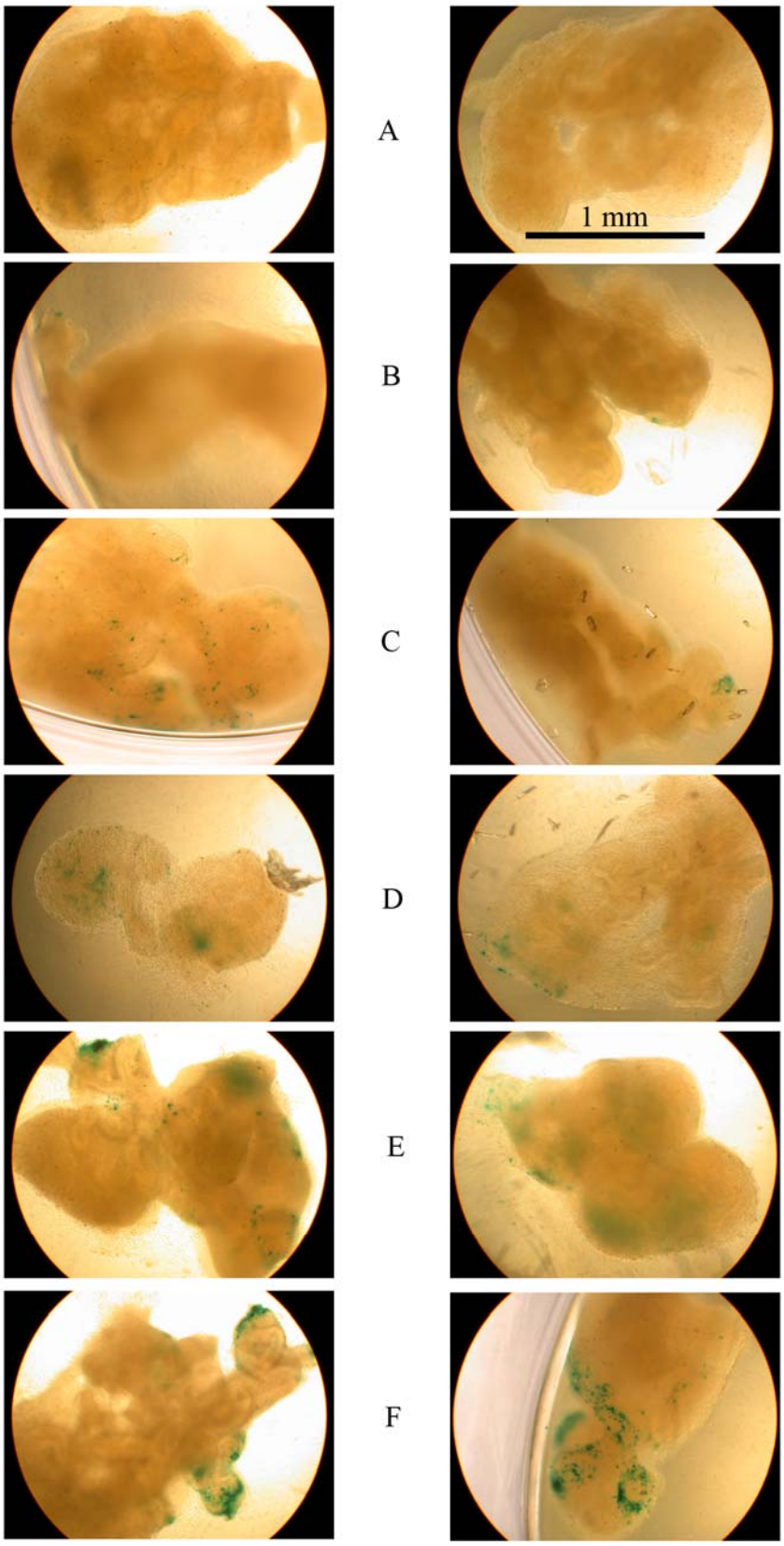

Figure 4.15 Baculovirus A vector transfection of HELs. III.

Human embryonic lungs dissected into 1x2 mm tissue pieces transfected with baculovirus A vector carrying lacZ in 5 titers 0 (A), $1x10^7$ (B), $2x10^7$ (C), $3x10^7$ (D), $4x10^7$ (E) and $5x10^7$ (F) plaque forming units per ml (pfu/ml) for 24 hours. β-galactosidase activity was assessed after fixation in 4% formaldehyde and incubation with the substrate X-Gal (5-bromo-4-chloro-3-indolyl-β-D-galactopyranoside) for at least 4 hours. Higher titers of baculoviurs vector showed more blue stained cells in the transfected lungs but were still less than 5% of whole tissue (D,E,F).

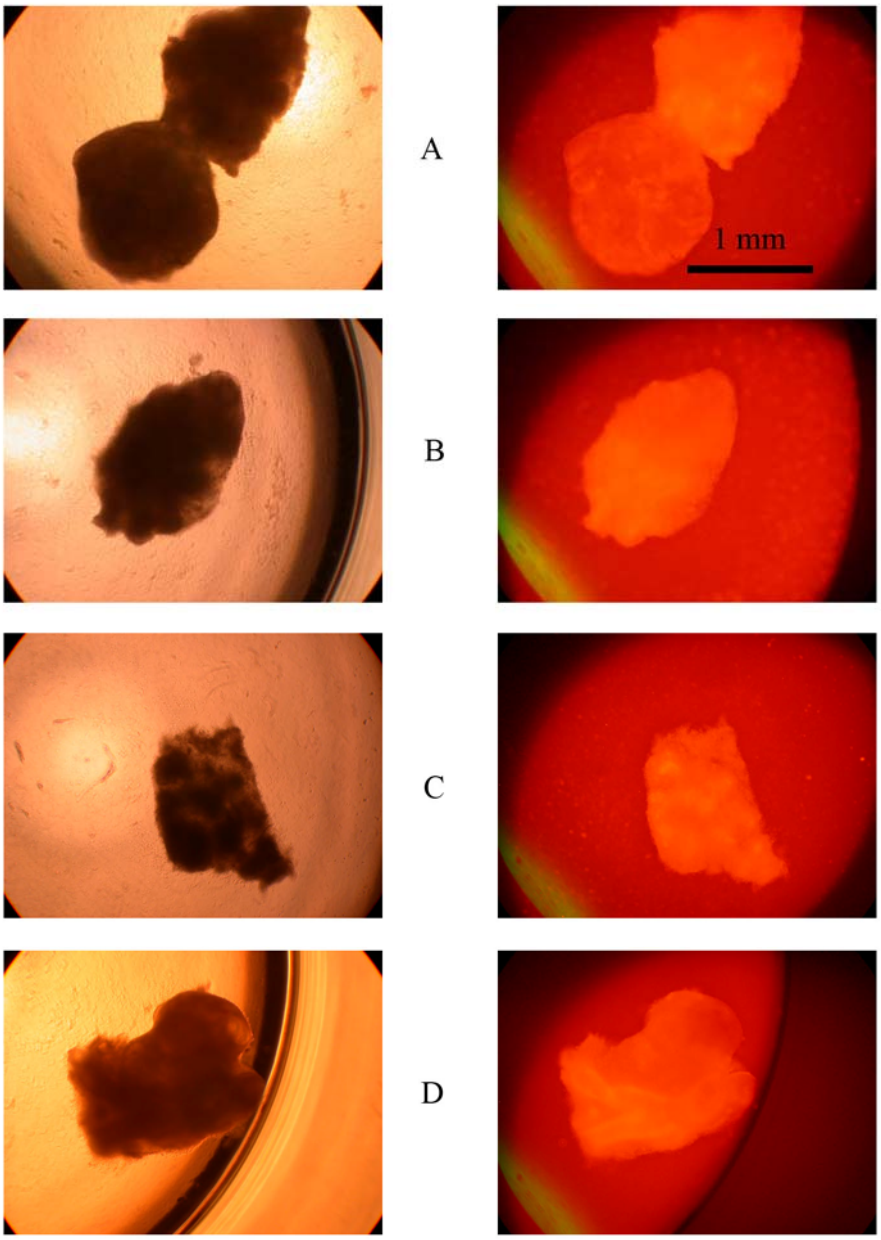

Figure 4.16 Light microscopy of HEL whole tissue siRNA transfection.

Phase contrast (left column) and fluorescence (right column) images of human embryonic lungs dissected into 1x2 mm tissue pieces and transfected with siGLO-RISC-free control siRNA (100nM) using 4 different Dharmacon transfection reagents in 96 well plates for 24 hours. (A) transfection reagent DharmaFECT™ 1 (Dh1, 0.2µl/100µl total transfection medium); (B) DharmaFECT™ 2 (Dh2, 0.2µl/100µl total transfection medium); (C) DharmaFECT™ 3 (Dh3, 0.4µl/100µl total transfection medium); (D) DharmaFECT™ 4 (Dh4, 0.8µl/100µl total transfection medium); All four transfection reagents showed good transfection efficiency with Dh1 and Dh4 showing the least toxicity.

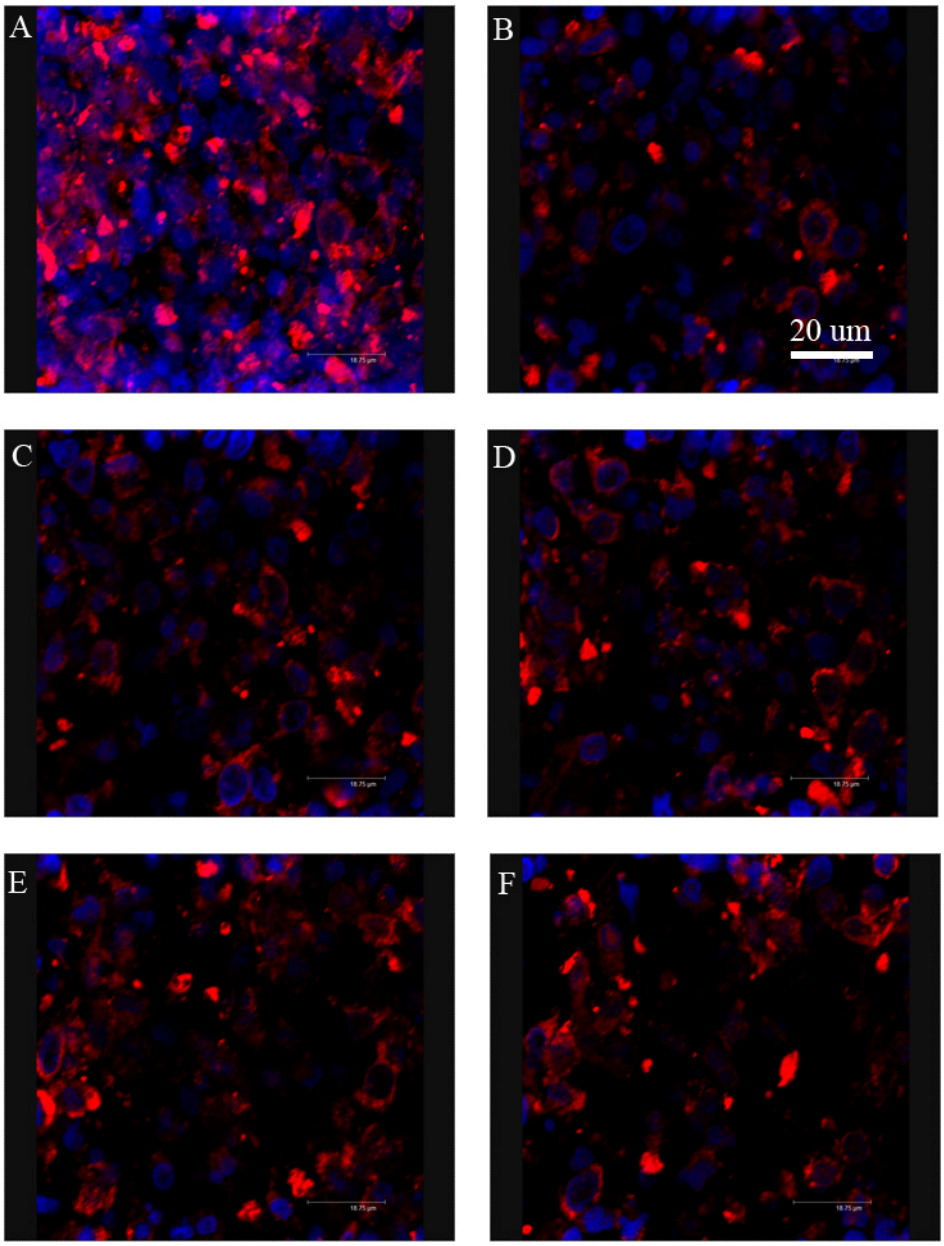

Figure 4.17 Confocal microscopy of HELs whole tissue siRNA transfection.

Laser confocal microscopy images of human embryonic lungs dissected into 1x2 mm tissue pieces and transfected with siGLO-RISC-free control siRNA (100nM) using Dharmacon transfection reagent DharmaFECT™ 1 (Dh1, 0.2µl/100µl total transfection medium) in 96 well plates for 48 hours. Three dimensional image (A) and images of sections 5-9 (B-F) out of 10 (about 3 µm thick) sections, showing good penetration of the fluorescently labelled siRNA.

4.2.7 Transfection optimisation in primary fibroblast cells

It was difficult to achieve reproducible and significant silencing of ADAM33 and other control genes in whole HEL tissue using baculovirus vectors and chemical transfection. Therefore, primary human adult and embryonic/fetal fibroblasts were used to optimise transfection of siRNA to be primarily able to study the effect of ADAM33 siRNA on primary human embryonic/fetal lung fibroblasts.

Optimisation of transfection reagents for siRNA in primary bronchial/lung fibroblasts

Prior to the use of human primary embryonic/fetal lung fibroblasts (HPELF), initially human primary adult bronchial fibroblasts (HPABF) were used to determine the transfection efficiency using different chemical transfection reagents with fluorescently labelled control siRNAs in 96 well plates as well as the feasibility of RNA extraction and RT-qPCR from single 96 wells. These were grown from bronchial biopsies that were obtained from volunteers during bronchoscopy. A further objective was to test the effect of positive silencing control siRNAs on mRNA expression using the transfection reagents that showed highest transfection efficiency and lowest toxicity.

The two transfection reagents from Dharmacon RNA Technologies that showed least toxicity when used in HELs, Dh1 and Dh4, were tested at concentrations recommended by Dharmacon to be used in primary cells. Dh1 (0.2µl/100µl total transfection medium) has been reported to have the highest efficiency and Dh4 (0.4µl/100µl total transfection medium) to have the ability to transfect mouse and rat cells as well. HPABFs were grown to about 70% confluence and transfected with 2 different commercially available fluorescently labelled control siRNAs, siGLO-RISC-free non-functional and non-targeting control siRNA and siGLO-Cyclophilin positive silencing control siRNA at 100 nM. Both control siRNAs showed relative better transfection efficiency with Dh1 after 48 hours (Figure 4.18B & D) compared with Dh4 (Figure 4.18C & E). Only weak uptake was observed in cells grown in the presence of siGLO-RISC-free control siRNA without transfection reagent (Figure4.18A). Initially 96 well plates were used to save precious and expensive reagents for the first optimisation experiments, but it was not known if single wells were sufficient to harvest enough and good quality RNA for RT qPCR. Therefore, RNA extracted from single 96 wells was used for RT-qPCR and 18S rRNA and β-Actin, ADAM33 and αSMA mRNA expression was assessed using probe-based TaqMan primer sets for RT-qPCR. All traces showed low CT-values with 18S rRNA at around 12 cycles, b-Actin at around 20 and ADAM33 and αSMA at 24 and 23 cycles (Figure 4.19A-D) which was similar to results obtained from PHAFs cultured in 6, 12 and 24 well plates suggesting sufficient and good RNA quality from single 96 wells.

mRNA knockdown in primary human adult bronchial fibroblasts.

HPABFs were transfected with RISC-free-control siRNA, GAPDH control siRNA and Cyclophilin control siRNA at 100nM for 48 hours using Dh1 at 0.2µl/100µl total transfection medium and assessed for RNA expression. The GAPDH control siRNA showed >80% of GAPDH (Figure 4.20A) and the Cyclophilin control siRNA showed about 50% knockdown effect (both significant) for their target genes (Figure 4.20B) compared to RISC-free control siRNA.

mRNA knockdown in primary human embryonic/fetal lung fibroblasts.

Then HPELFs were grown to about 70% confluence in 24 well plates instead of initially tested 96 well plates to increase the yield of RNA. Cells were transfected (using same protocols as above) with RISC-free-control siRNA, GAPDH control siRNA at 100nM for 24 and 48 hours and assessed for RNA expression using TaqMan RT-qPCR. GAPDH mRNA showed a 60 to 70% knock down effect which was significant after 24 (Figure 4.21A) and almost significant after 48 hours (Figure 4.21B) using GAPDH control siRNA.

Optimisation of new transfection reagent for siRNA in human primary fetal/embryonic lung fibroblasts.

A new transfection reagent from Roche Applied Science, X-tremeGENE siRNA Transfection Reagent (XG), became available that had advantages over Dharmacon transfection reagent as the medium did not have to be replaced before adding XG and as it was less toxic and therefore did not need changing after 24 hours.

HPELFs were grown to about 70% confluence in 24 well plates and transfected with siGLO-RISCfree non-functional non-targeting control siRNA (Figure 4.22) and siGLO-Cyclophilin positive silencing control siRNA (Figure 4.23) at different concentrations with different amounts of XG transfection reagent (6nM with 1µl XG, 15nM with 2.5µl XG and 30nM with 5µl XG/500µl total transfection medium according to the company's guidelines) for 48 hours. Phase-contrast and fluorescence microscopy images were taken at 24 hours and revealed least toxicity with 1µl and 2.5µl (Figure 4.22B & C; Figure 4.23A & B) XG transfection reagent and highest toxic effect on cells with 5µl of XG (Figure4.22D; Figure 4.23C). RNA was extracted after 48 hours and TaqMan RT-qPCR performed for Cyclophilin mRNA. The greatest and significant knock down was observed at 15nM siRNA with 2.5µl XG transfection reagent/500µl total transfection medium (Figure 4.23).

Further optimisation experiments with lower concentrations of XG transfection reagent (siRNA-buffer on its own (without siRNA) with 1µl XG and siGLO-Cyclophilin control siRNA at 10nM with 0.3µl XG, 15nM with 0.5µl XG, 30nM with 1µl XG and 60nM with

2µl XG transfection reagent/500µl total transfection medium) showed least cell toxicity at 0.3, 0.5 and 1 µl of XG transfection reagent but highest transfection efficiency with 0.5, 1.0 and 2.0 µl of XG transfection reagent (Figure 4.25A-E). TaqMan RT-qPCR for Cyclophilin mRNA showed highest and significant knock down (>50%) at siRNA concentrations of 10 – 30nM (Figure 4.26). Based on these results siRNA was used at 15nM with 1.0 to 2.0µl of XG transfection reagent/500µl medium new knock down experiments.

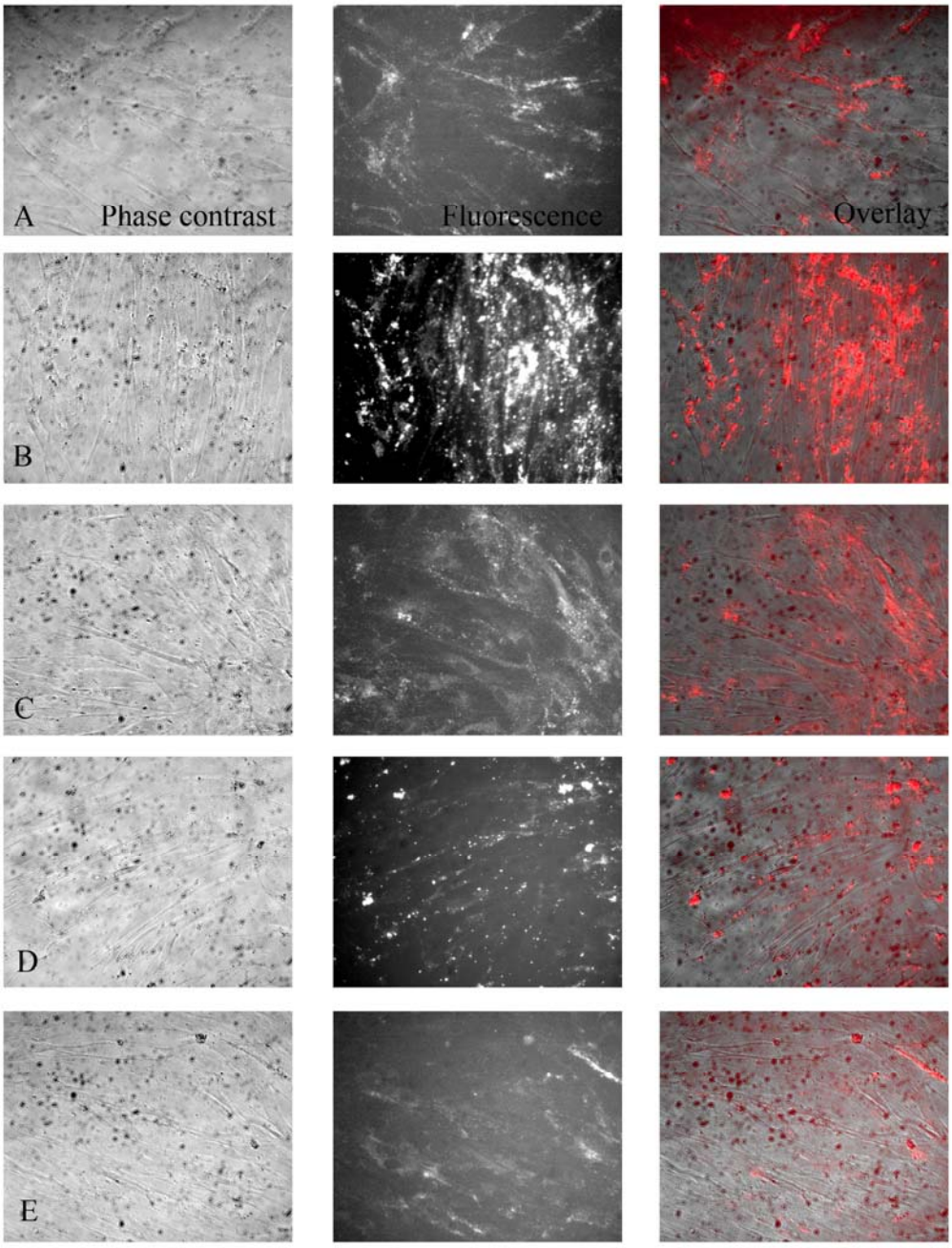

Figure 4.18 Light microscopy of HPABFs transfected with control siRNA.

Phase contrast, fluorescence and overlay images of human primary pulmonary fibroblasts transfected with siRNA in 96 well plates for 48 hours. (A) siGLO-RISC-free control siRNA (100nM) without transfection reagent; (B) siGLO-RISC-free control siRNA (100nM) with DharmaFECT™ 1 (Dh1, 0.2µl/100µl total transfection medium); (C) siGLO-RISC-free control siRNA (100nm) with DharmaFECT™ 4 (Dh4, 0.4µl/100µl total transfection medium); (D) siGLO-Cyclophylin siRNA with Dh1 (0.2µl/100µl of total transfection medium); (E) siGLO-Cyclophylin siRNA with Dh4 (0.4µl/well). The transfection reagent Dh1 showed the highest transfection efficiency and the least toxicity.

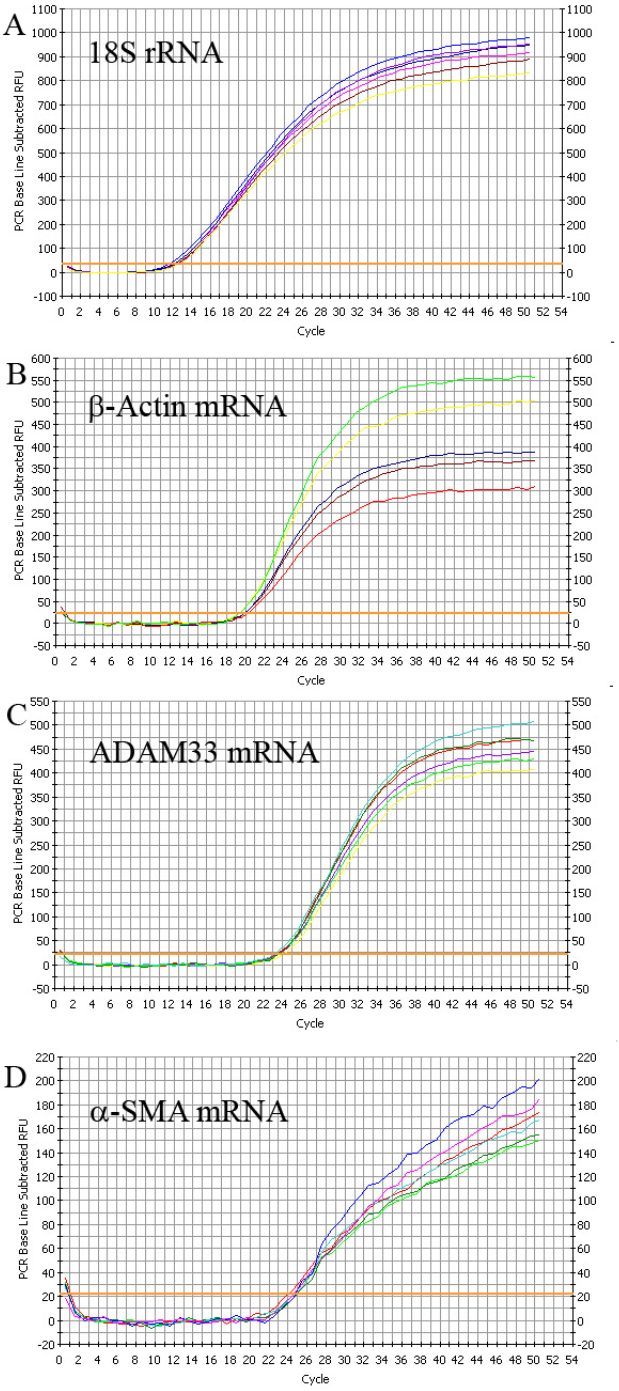

Figure 4.19 RT-qPCR of HPABFs.

PCR Amplification/Cycle Graph of RNA extracted from human primary pulmonary fibroblasts in single wells (n=3) from a 96 well-plate. TaqMan for: 18S rRNA: Ct value 12 (A); β-Actin mRNA: Ct value 20 (B); ADAM33 mRNA (primers in the 3'UTR): Ct value 24 (C); αSMA mRNA: Ct value 23 (D).

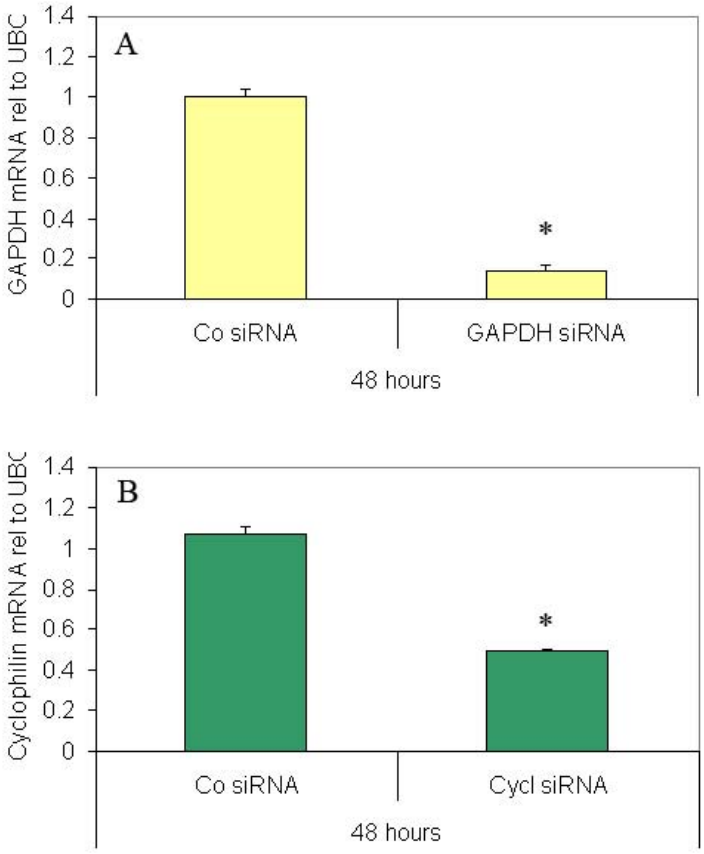

Figure 4.20 RT-qPCR of HPABFs transfected with siRNA.

TaqMan for GAPDH & Cyclophilin mRNA rel to UBC mRNA in human primary pulmonary fibroblasts transfected with siRNA (100nM) for GAPDH, siGLO-Cyclophillin (Cycl) and siGLO-RISC free control (Co) using DharmaFECT™ 1 (0.2µl/100µl total transfection medium) for 48 hours. TaqMan (n=3) showed a gene knock down of about 80% for GADH (A) and 50% for Cyclophilin (B). (* t-test: $p<0.001$)

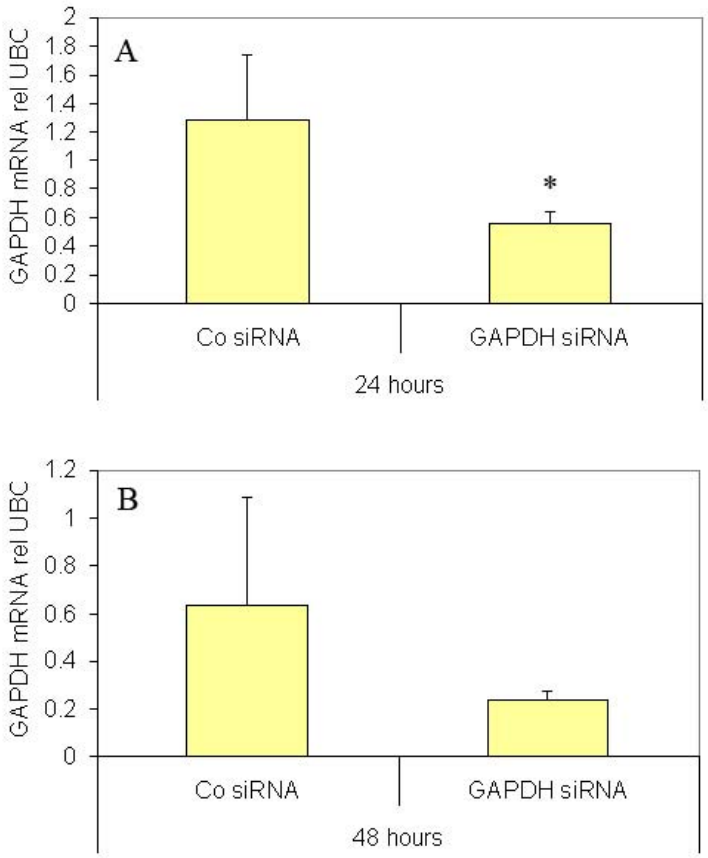

Figure 4.21 RT-qPCR of HPELFs transfected with control siRNA. I.

TaqMan for GAPDH mRNA rel to UBC mRNA in human primary embryonic lung fibroblasts transfected with siGLO-RISCfree control (Co) and GAPDH siRNA (100nM) using DharmaFECT™ 1 (0.2µl/100µl total transfection medium) in a 24 well plate for 24 and 48 hours. TaqMan (n=3) showed a significant gene knock down for GAPDH mRNA at 24 and a tendency at 48 hours (A&B) of about 60 to 70% (* t-test: $p \leq 0.05$)

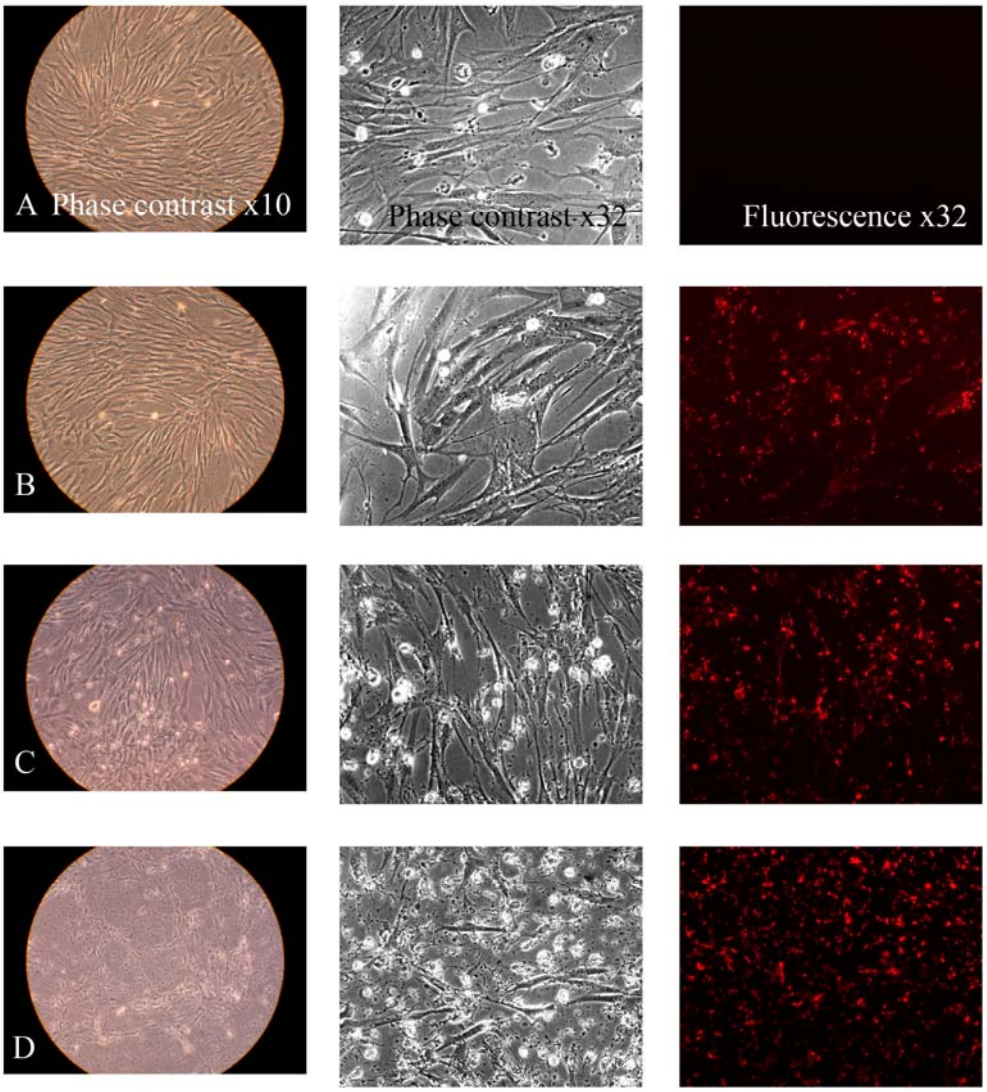

Figure 4.22 Light microscopy of HPELFs transfected with control siRNA. I.

Human primary embryonic lung fibroblasts without transfection reagent (A) and transfected with siGLO-RISCfree non-functional non-targeting control siRNA at 6nM with X-tremeGENE siRNA Transfection Reagent (Roche Applied Science) 1µl (B), at 15nM with 2.5µl (C) and 30nM with 5µl/500µl total transfection medium (D) in a 24 well plate after 24 hours. 1µl of X-tremeGENE showed the least toxicity and good transfection efficiency, 2.5µl had medium toxicity and good transfection efficiency and 5µl was most toxic for the cells.

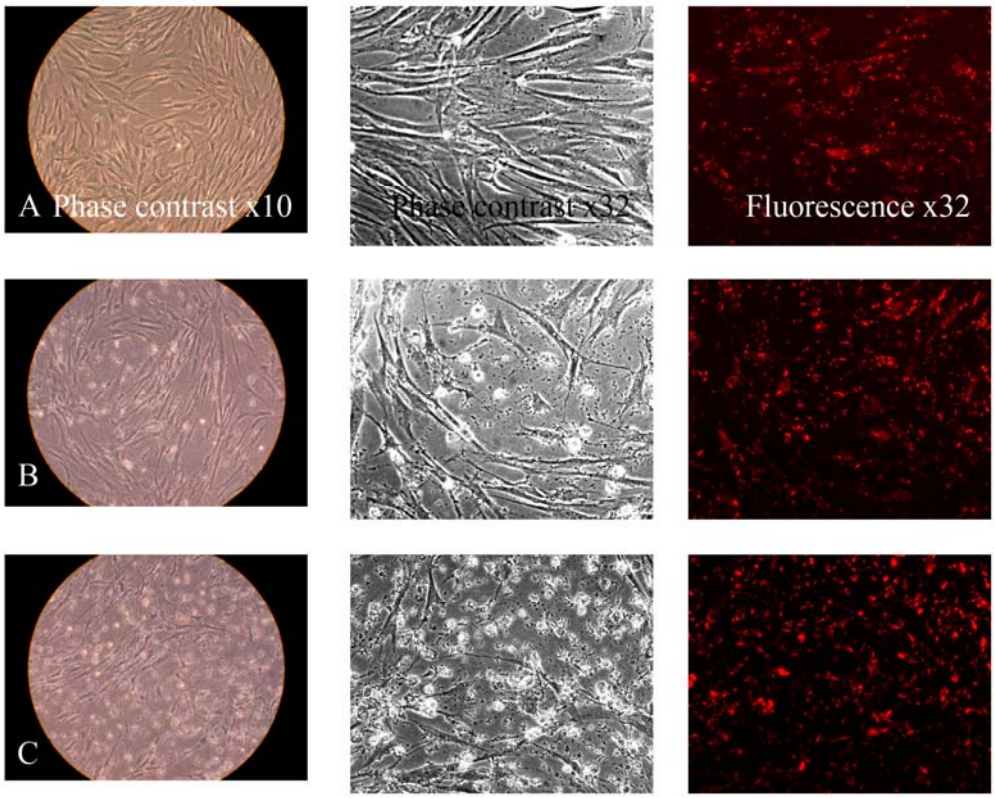

Figure 4.23 Light microscopy of HPELFs transfected with control siRNA. II.

Human primary embryonic lung fibroblasts that were transfected with siGLO-Cyclophilin positive silencing siRNA at 6nM with X-tremeGENE siRNA Transfection Reagent (Roche Applied Science) 1µl (A), at 15nM with 2.5µl (B) and 30nM with 5µl/500µl total transfection medium (C) in a 24 well plate after 24 hours. Similar to the results with siGLO-RISCfree siRNA 1µl of X-tremeGENE showed the least toxicity and good transfection efficiency, 2.5µl had medium toxicity and good transfection efficiency and 5µl was most toxic for the cells.

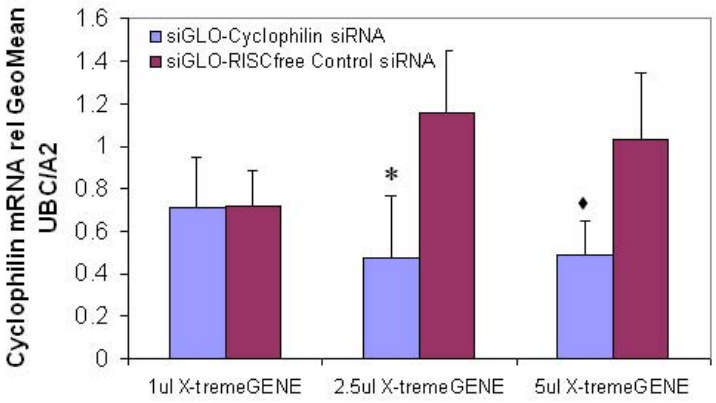

Figure 4.24 RT-qPCR of HPELFs transfected with control siRNA.II.

TaqMan for Cyclophilin mRNA relative to GeoMean of UBC and A2 in human primary embryonic lung fibroblasts transfected with siGLO-Cyclophilin siRNA and siGLO-RISCfree control siRNA at 6nM with 1µl X-tremeGENE siRNA Transfection Reagent (Roche Applied Science), 15nM with 2.5µl and 30nM with 5µl/500µl total transfection medium in a 24 well plate after 48 hours. At 6nM siRNA and 1µl of X-tremeGENE no knockdown was observed whereas the greatest significant knock down was at 15nM and 2.5µl (* t-test: $p<0.05$) and less at 30nM and 5µl of transfection reagent (♦ t-test: $p=0.055$).

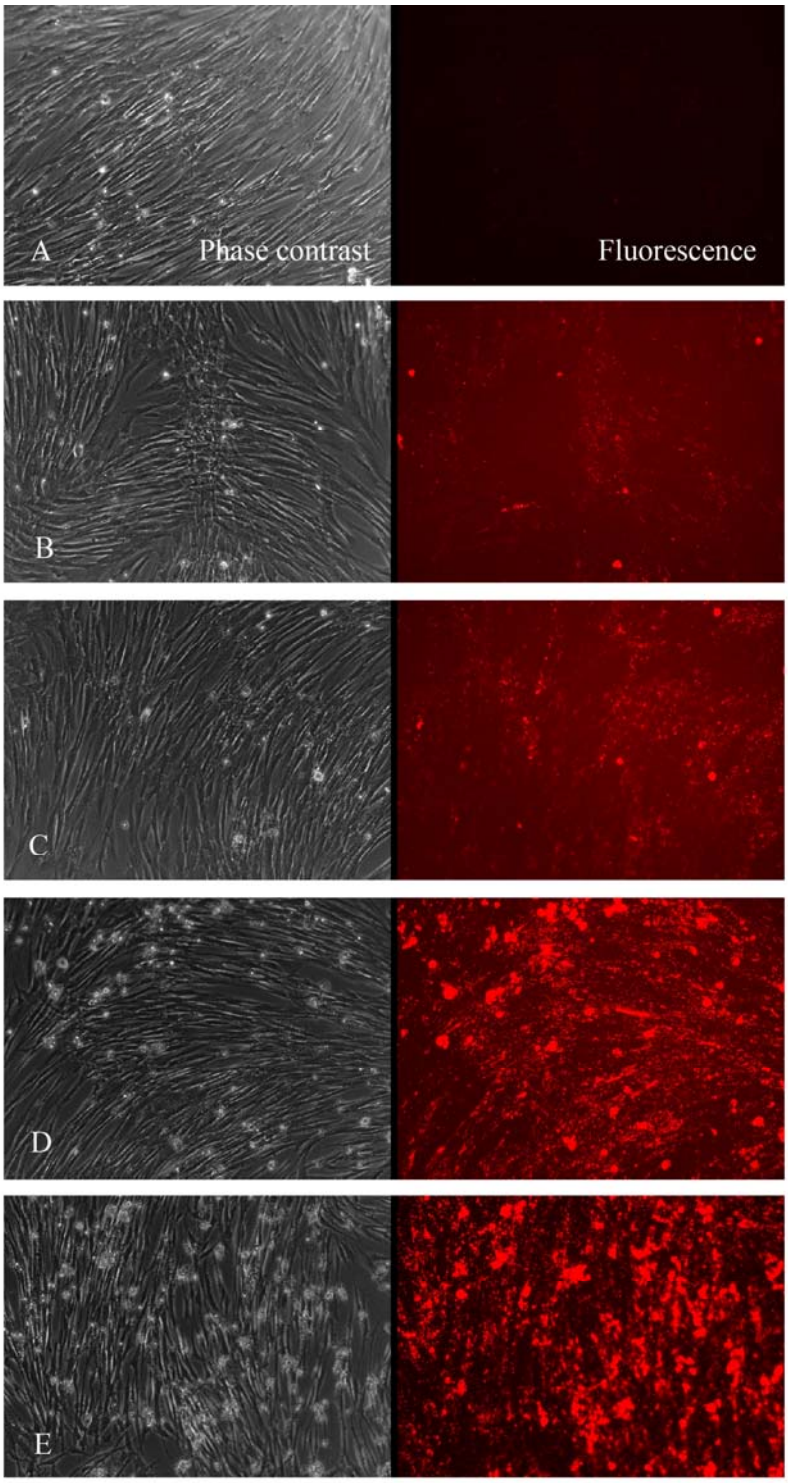

Figure 4.25 Light microscopy of HPELFs transfected with control siRNA. III.

Human primary embryonic lung fibroblasts transfected with siRNA-buffer only without siRNA using X-tremeGENE siRNA Transfection Reagent (Roche Applied Science) 0.5µl (A) and transfected with siGLO-Cyclophilin siRNA at 10nm with 0.33µl (B), at 15nM with 0.5µl (C), 30nM with 1µl (D) and at 60nM with 2µl transfection reagent/500µl total transfection medium (E) in a 24 well plate after 48 hours. 0.5 µl of X-tremeGENE at 15nM siRNA (C) and 1.0µl at 30nM siRNA showed a low toxicity and good transfection efficiency compared with 0.33 and 2µl transfection reagent.

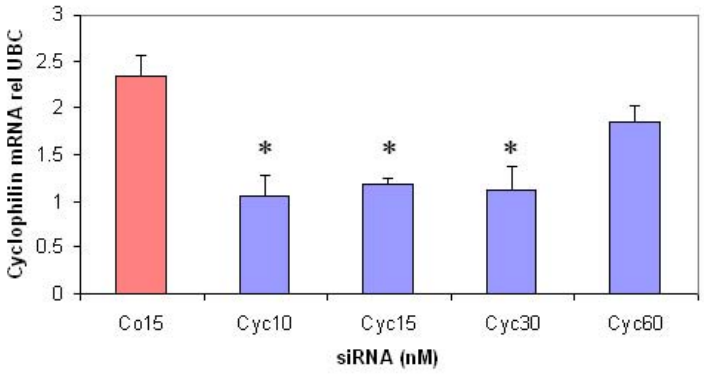

Figure 4.26 RT-qPCR of HPELFs transfected with control siRNA.III.

TaqMan for Cyclophilin mRNA relative to UBC mRNA in human primary embryonic lung fibroblasts transfected with siGLO-Cyclophilin siRNA and siGLO-RISCfree control siRNA (Co15) at 10nM (Cyc10) with 0.33µl X-tremeGENE siRNA Transfection Reagent (Roche Applied Science), 15nM (Cyc15) with 0.5µl, 30nM (Cyc30) with 1µl and 60nM(Cyc60) with 2µl/500µl total transfection medium in a 24 well plate after 48 hours. A significant knock down was demonstrated at 10 to 30 nM siRNA and 0.33 to 1µl of transfection reagent, whereas at 60nM siRNA and 2µl of X-tremeGENE showed increased toxicity and no knockdown was observed. (One Way ANOVA and multiple comparison method Bonferroni t-test; * $p<0.001$),

4.2.8 ADAM33 knock down in primary human bronchial/lung fibroblasts.

ADAM33 siRNA target location

On the basis of frustrated attempts to achieve knock down of ADAM33 in HPAFs and HPEFs with the ADAM33-SMARTpool siRNA (M-004525-00) but successful knockdown of GAPDH using the GAPDH-control-siRNA (Figures 4.27 & 4.28), information about the target location of the four single siRNA duplexes in the pool was sought from the company (Dharmacon). This revealed that all four siRNA duplexes of the M-004524-00 pool were located in the metalloprotease (MP) domain of ADAM33 (Table 4.1), which is known to be lowly expressed in fibroblasts(Powell *et al.* 2004) and hence could possibly explain the lack of effect of this pool. Therefore, Dharmacon provided the position for 2 other ADAM33-SMARTpool sets of which M-004525-01 contained one duplex in the MP domain, one in the Pro-domain and 2 duplexes in the 3'-untranslated region (3'UTR) (Table 4.1). This set was chosen for further knockdown experiments.

HPEFs were grown to about 70% confluence in 24 well plates and transfected with ADAM33-SMARTpool siRNA (M-004525-01), Control-SMARTpool siRNA and GAPDH control siRNA at 15nM using XG transfection reagent at 2µl/500µl total transfection medium for 24 and 48 hours in 3 independent experiments with 3 different HPEFs and all in triplicate. ADAM33 mRNA could be knocked down significantly by >60% after 24hours and >80% after 48hours (Figure 4.29A & F) similar to the effect of GAPDH-control siRNA had on GAPDH mRNA expression (Figure 4.29B &G) (all $p<0.001$). When the same cDNA was analysed for the mesenchymal cell and myo-fibroblast marker, αSMA, a novel, concomitant and significant knock down effect of ADAM33 siRNA on αSMA mRNA expression was observed after 48 hours (Figure 4.29H). mRNA expression of two other genes expressed in mesenchymal cells, TGFβ1 and Collagen1A, were not affected by transfection with siRNA for ADAM33 or GAPDH (Figure 4.29D, I, E & J).
To confirm the effect of ADAM33 SMART-pool siRNA the single duplex siRNAs from M-004525-01 pool (new pool) (Table 4.2) were individually used to transfect HPEFs in comparison with the two ADAM33-SMARTpool, the siGLO-RISCfree-control and GAPDH-control siRNAs at 15nM and with 1µl of XG transfection reagent/500µl total transfection medium for 48 hours. This showed a >50% knockdown of GAPDH mRNA using the GAPDH-control siRNA (Figure 4.30B) and about 40% knockdown of ADAM33 with the new pool compare to about 20% with the old pool of ADAM33 siRNA (Figure

4.30A). The greatest knockdown with the individual siRNA duplexes for ADAM33 was achieved with duplex 6 and 7 (Figure 4.30A), both located in the 3'UTR region (Table 4.2). A concomitant knockdown effect was also seen for αSMA with duplex 7 (Figure 4.30C).

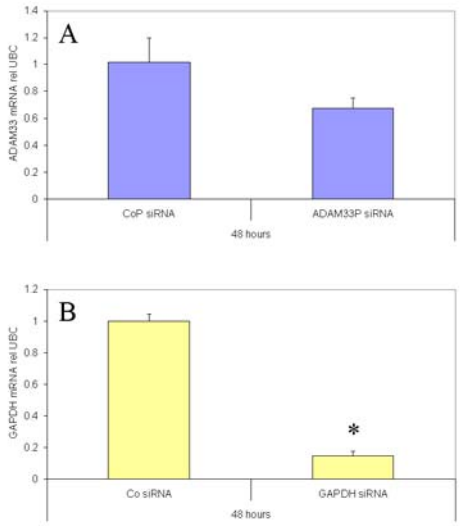

Figure 4.27 RT-qPCR of HPABFs transfected with ADAM33 & controlsiRNA.

TaqMan for ADAM33 (primers in the 3'UTR) and GAPDH mRNA rel to UBC mRNA in human primary adult bronchial fibroblasts (HPABFs) transfected with siRNA (100nM) SMARTpool® of 4 siRNA duplexes (M-004525-00) for ADAM33 (ADAM33P) and Control-pool (CoP), Control and control GAPDH siRNA using DharmaFECT™ 1 (0.2µl/100µl total transfection medium) for 48 hours. TaqMan (n=3) showed no significant knock down using the ADAM33 pool of siRNA (A) but significant gene knock down of about 80% for GADH (B) (* t-test: $p<0.001$).

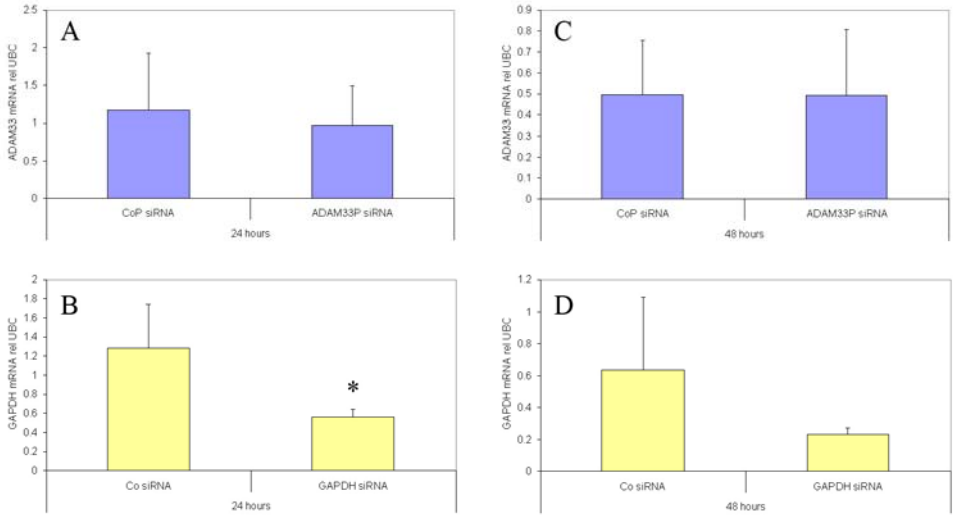

Figure 4.28 RT-qPCR of HPELFs transfected with ADAM33 & control siRNA.I.

TaqMan for ADAM33 (primers in the 3'UTR) and GAPDH mRNA rel to UBC mRNA in human primary embryonic lung fibroblasts (HPELFs) transfected with siRNA (100nM) SMARTpool® of 4 siRNA duplexes (M-004525-00) for ADAM33 (ADAM33P) and Control-pool (CoP), Control and control GAPDH siRNA using DharmaFECT™ 1 (0.2µl/100µl total transfection medium) for 24 and 48 hours. TaqMan (n=3) showed no significant knock down using the ADAM33 pool of siRNA after 24 and 48 hours (A&C) but a significant gene knock down for GAPDH mRNA at 24 (B) and a tendency at 48 hours (D) of about 60 to 70% (* t-test: $p \leq 0.05$)

Human ADAM33, NM_025220 & NM_153202: Standard and ON-Target Plus siGENOME SMARTpool® products from Dharmacon, Inc.				
SMARTpool	Duplex	5' siRNA start position	Exon	Domain
M-004525-00: Standard siGENOME	Duplex 1	713	G	MP
	Duplex 2	786	H	MP
	Duplex 3	742	GH	MP
	Duplex 4	513	F	MP
M-004525-01: Standard siGENOME	Duplex 1	713	G	MP
	Duplex 5	0	A	PRO
	Duplex 6	2525	V	3'UTR
	Duplex 7	2557	V	3'UTR
L-004525-00: ON-Target Plus	Duplex 8	742	GH	MP
	Duplex 9	1292	L	MP
	Duplex 10	1866	P	CYS
	Duplex 11	713	G	3'UTR

Table 4.1 ADAM33 SMARTpool® siRNA.

SMARTpool® siRNA duplexes with 5' starting position in exons and domains of human ADAM33

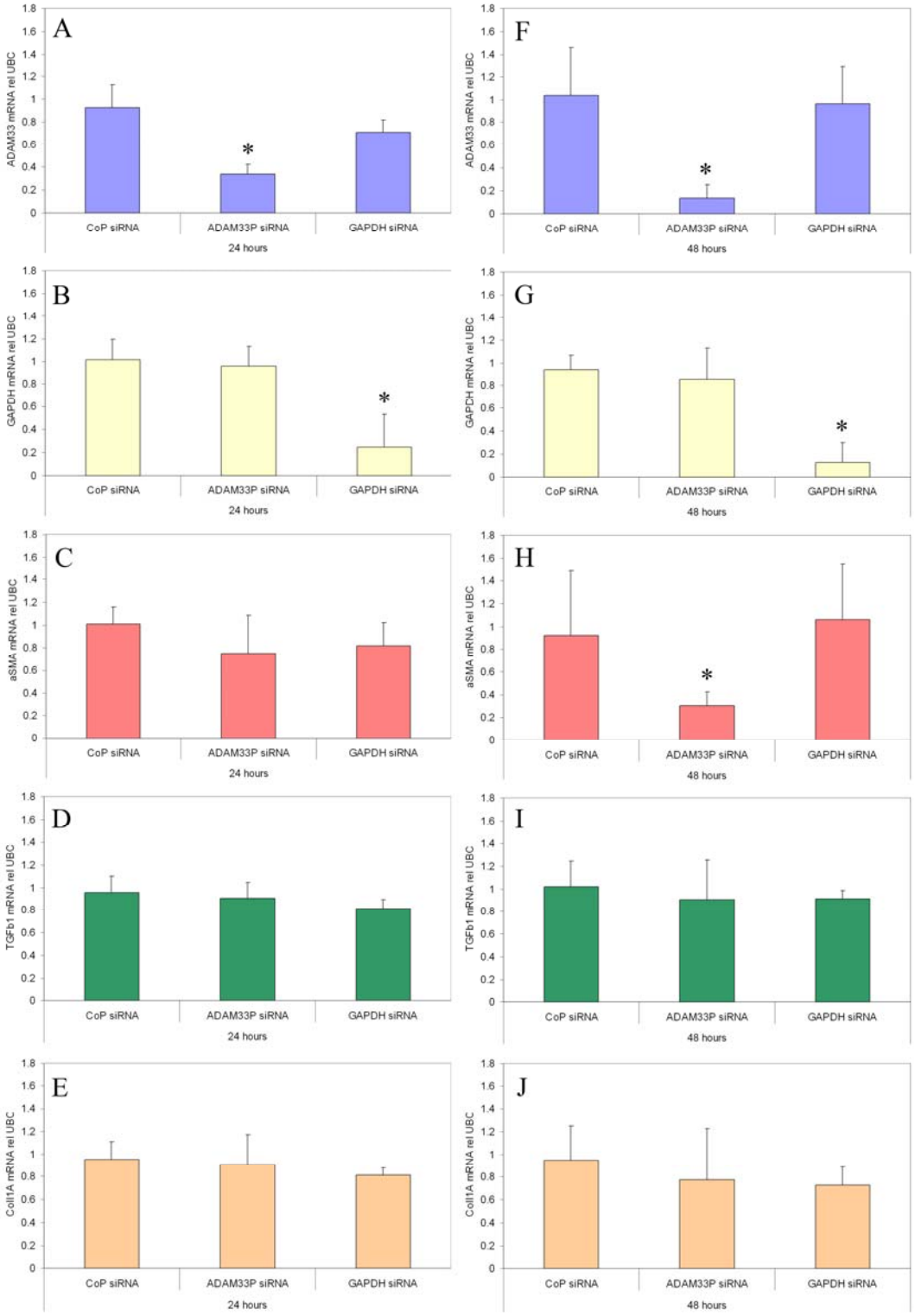

Figure 4.29 RT-qPCR of HPELFs transfected with ADAM33 & control siRNA.II.

TaqMan for ADAM33 (primers in the 3'UTR), GAPDH, αSMA, TGFβ1 and Coll1A mRNA rel to UBC mRNA in human primary embryonic lung fibroblasts (HPELFs) transfected with siRNA (15nM) SMARTpool® of 4 siRNA duplexes (M-004525-01) for ADAM33 (ADAM33P) and Control-pool (CoP), control GAPDH siRNA using X-tremeGENE siRNA Transfection Reagent (Roche Applied Science), (2.5µl/500µl total transfection medium) in a 24 well plate for 24 (A-E) and 48 hours (F-J). TaqMan from 3 independent experiments with 3 different HPELFs and in triplicate showed significant gene knock down for ADAM33 mRNA and GAPDH mRNA at 24 hours (>60% for ADAM33; >70% for GAPDH) (A & B) and 48 hours (>80% for ADAM33; >80% for GAPDH) (F & G). αSMA mRNA was also significantly knocked down after transfection with ADAM33 siRNA at 48 hours (>70% for αSMA) (H) but not at 24 hours (C) . TGFβ1 and Collagen A1 mRNA of two genes also expressed in mesenchymal cells were not affected by transfection with ADAM33 or GAPDH siRNA at 24 (D & E) or 48 hours (I & J) (One Way ANOVA and multiple differences Bonferroni t-test; *$p<0.001$).

Human ADAM33, NM_025220, siGENOME Set of 4 Upgrade, Dharmacon, Inc.			
Set of 4 Upgrade	Duplex	Sense & Anti-sense sequence	Domain
M-004525-01-0002	Duplex 1	S: GGAAGUACCUGGAACUGUAUU AS: 5'-PUACAGUUCCAGGUACUUCCUU	MP
	Duplex 5	S: GAAGAACCAUGGCCUGAUCUU AS: 5'PGAUCAGGCCAUGGUUCUUCUU	PRO
	Duplex 6	S: GGUGAGAGGUAGCUCCUAAUU AS: 5'PUUAGGAGCUACCUCUCACCUU	3'UTR
	Duplex 7	S: AAAGACAGGUGGCCACUGAUU AS: 5'PUCAGUGGCCACCUGUCUUUUU	3'UTR

Table 4.2 ADAM33 siGENOME Set of 4 Upgrade duplexes

siGENOME Set of 4 Upgrade duplexes of Standard siGENOME SMARTpool® M-004525-01 with Sense (S) and Anti-sense (AS) sequence and domains for human ADAM33.

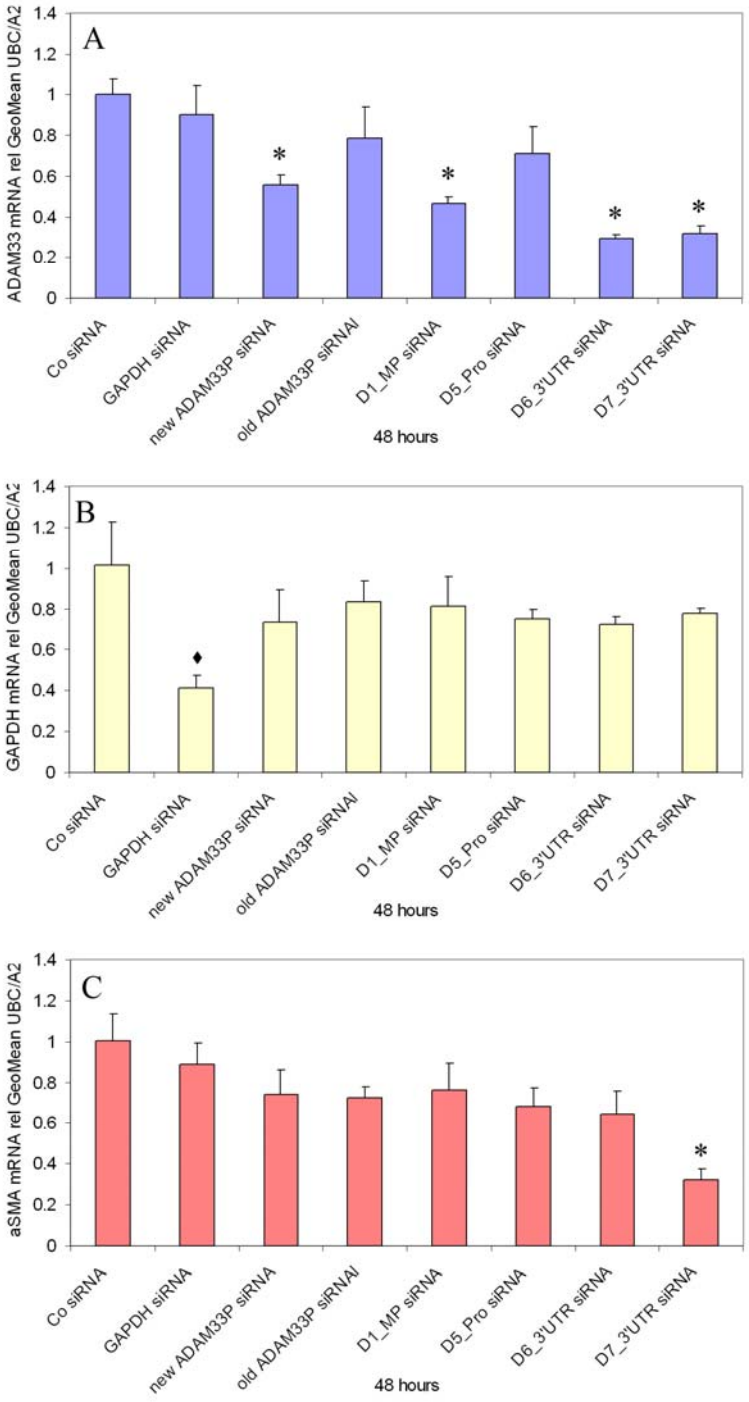

Figure 4.30 RT-qPCR of HPELFs transfected with ADAM33 & contr. siRNA.III.

TaqMan for ADAM33 (primers in the 3'UTR), GAPDH and αSMA mRNA rel to the geometric mean (GeoMean) of UBC and A2 mRNA in human primary embryonic lung fibroblasts (HPELFs) transfected with control (Co) and GAPDH siRNA, two ADAM33 SMARTpool® containing each 4 siRNA duplexes (M-004525-01 and M-004525-01; new A33P and old A33P) and individual four ADAM33 duplex siRNAs (D1_MP, D5_Pro, D6_3'UTR, D7_3'UTR) for ADAM33(15nM) using X-tremeGENE siRNA Transfection Reagent (Roche Applied Science), (1µl/500µl total transfection medium) in a 24 well plate for 48 hours. RT-qPCR showed significant ADAM33 mRNA knocked down by the new ADAM33 pool and duplex 1 (about 40-50%) and most knock down could be shown for duplexes 6 & 7 (about 70%), both located in the 3'UTR of ADAM33 (A). GAPDH mRNA was significantly knocked down by the GAPDH siRNA (about 60%), but was not influenced by the control or any of the ADAM33 siRNAs (B). Significant αSMA mRNA concomitant knock down could be seen in the presence of duplex 7 ADAM33 siRNA (C) (One Way ANOVA and multiple comparison versus control Bonferroni t-test; * ♦ $p<0.001$).

4.3 Discussion

This is the first report demonstrating that ADAM33 mRNA splice variants are expressed in human embryonic lungs showing a similar pattern like in the bronchial fibroblasts and bronchial biopsies and global ADAM33 mRNA expression increases during normal lung development in vivo. However, HEL tissue was only available from a limited number of donors and also a narrow window of lung development (7 to 9 wpc). It would have been desirable to cover a wider gestational range to be able to compare the human findings with the results in the mouse lung development (See chapter 5.2.1), which for ethical reasons is not possible. Western blotting of lysates from the human embryonic lung tissue confirmed the presence of ADAM33 isoforms similar to the bronchial biopsies and smooth muscle cells, however, of particular note was the occurrence of a distinct additional 25kDa isoform of ADAM33. All bands were smaller than the predicted full length molecule consistent with the findings that the majority of mRNA transcripts lack the MP domain. The extra band most likely contains the carboxy tail and a short region upstream of the EGF and cysteine-rich domain. This extra band needs further identification via immunoprecipitation, 2-D gel electrophoresis and mass spectrometry to verify the amino acid sequence of this splice variant of ADAM33. This might be of help to identify which domains of ADAM33 are contained in this extra ADAM33 isoform which might suggest a potential function in HELs. Immunohistochemistry showed that in addition to the presence of ADAM33 in αSMA positive cells, ADAM33 also occurred in undifferentiated mesenchymal cells, which are much more abundant in embryonic lung than bronchial biopsies, suggesting that it may play an important role in smooth muscle development and function as well as in development of other bronchial structures such as the vascular and neuronal network of the airways as well as the differentiation of mesenchymal cells, such as fibroblasts and smooth muscle cells, in these structures. RT-qPCR of HELs dissected into the mesenchymal cell mesh and tubular epithelial structures confirmed the predominant expression of ADAM33 in the mesenchymal cell mesh surrounding the tubular structures. These findings place ADAM33 in HELs during a critical period of lung development suggesting that it may be involved in airway wall 'modelling' and that polymorphic variation may then contribute to the early life origins of asthma.

IL-13 is a Th2 immunoregulatory cytokine with a mass of 17 kDa (Moy *et al.* 2001) which plays an important role in the pathogenesis of allergic asthma and atopy. Maternal IL-13 protein might cross the placental-fetal barrier as there is a significant positive correlation between maternal and fetal cord plasma IL-13 concentrations in paired maternal-fetal cord plasma at 32 weeks gestation (Williams *et al.* 2000). IL-13 has also been localised in

trophoblasts of the placenta in the first trimester of pregnancy using in situ hybridisation and immunohistochemistry (Dealtry *et al.* 1998) and using immunohistochemistry it was detected in the placenta between 16 and 27 weeks of gestation in contrast to its spontaneous release by fetal mononuclear cells which only happens between 27 to 37 weeks of gestation (Williams *et al.* 2000). To determine how environmental factors, such as a maternal Th2 environment, influence the expression of ADAM33 HELs were cultured in the presence of IL-13. A dose response curve was not done due to limited availability of precious HELs, however, the dose was based on previous in house dose response curves from human primary adult bronchial fibroblasts that were cultured in the presence of 0, 0.1, 1 and 10 ng/ml of recombinant IL-13. 1 ng/ml of IL-13 was chosen as there was no significant difference of induction of mRNA or protein in response to 1 or 10 ng/ml and this concentration was closer to physiological levels in serum (< 1ng/ml) (L. Andrews - unpublished data).

Firstly, the newly developed HEL explant culture system showed that human embryonic/fetal lung tissue can be cultured for several weeks and shows branching morphogenesis which makes it a very precious tool for studying mechanisms of lung development in human tissue. Secondly, the HEL explant showed that ADAM33 expression increased significantly over 18 days in culture in vitro consistent with the data showing the increased expression during lung development in vivo. However, when the HELs were cultured in the presence of IL-13 they showed a significant suppression of ADAM33 after 18 days in culture. IL-13 induces TGFβ2 in human bronchial epithelial cells (Richter *et al.* 2001; Wen *et al.* 2002) and over expression of IL-13 in the mouse lung causes airway remodelling (e.g., subepithelial fibrosis, goblet cell metaplasia, and smooth muscle hypertrophy and hyperplasia) (Fulkerson *et al.* 2006). This tissue remodelling seems to be TGFβ1 dependent not only in the lung but also in the colon (Lee *et al.* 2001; Fichtner-Feigl *et al.* 2007) which might be induced through the IL-13a2 receptor(Fichtner-Feigl *et al.* 2006). It was recently shown by Wicks that TGFβ is a potent suppressor of ADAM33 in differentiation of fibroblasts to myofibroblast (Wicks 2006) suggesting that IL-13 might cause a TGFβ dependent ADAM33 mRNA suppression. However, it has also recently been shown that TGFβ induces the release of an active soluble form of ADAM33 protein from HEK293 cells transfected with full length ADAM33, suggesting that TGFβ might induce ADAM33 itself or other proteases to release the active metalloprotease containing isoform from the surface of the cell (Puxeddu *et al.* 2008).

To study the effect of the knock down of ADAM33 on lung development in vitro transfection optimisation studies were first performed in whole HEL tissue pieces and

primary fibroblasts. Initially Baculovirus A vector carrying lacZ, at different concentrations was used as a potential transfection vector for siRNA which showed partial infection of the tissue that was not sufficient to warrant further evaluation of this system. As second transfection method chemical transfection was attempted using four different lipid- based transfection reagents (DharmaFECT 1-4) from Dharmacon. Two transfection reagents (DharmaFECT 1 and 4) showed low toxicity and good transfection efficiency with fluorescently labelled control siRNA which was confirmed by fluorescence microscopy and confocal microscopy, however, no significant down regulation of mRNA could be achieved using control as well as ADAM33 siRNA. Further optimisation of this transfection method of whole tissue pieces is needed. Due to initial unsuccessful knock down attempts and the limited availability of precious HEL tissue primary human adult bronchial fibroblasts and embryonic lung fibroblasts were used to optimise the two chemical transfection reagents used in whole HEL tissue (DharmaFECT 1 and 4) and a novel transfection reagents (X-tremeGENE) from Roche. Primary cell culture is helpful to optimise experimental methods such as the use of siRNA and to dissect functional mechanisms of single proteins in a single cell type which can be challenging in whole tissue. It has its limitation as single cell culture systems can not account for the interaction with different cell types that take place in a 3-dimensional structure. However, whole HEL tissue explant culture experiments have an advantage over primary cell culture as it might shed more light on complex biological processes such as development of the lungs.

All three transfection reagents used in primary lung fibroblasts resulted in successful downregulation of control genes, however due to ease of use the third transfection reagent was chosen to perform the ADAM33 siRNA knock down experiments.

After initial unsuccessful knock down of ADAM33 using a pool of four siRNAs (ADAM33-SMARTpool: M-004525-00) from Dharmacon target location was done which revealed that all four siRNAs were located in the MP-domain of ADAM33, a domain that is known to be lowly expressed in fibroblasts(Powell *et al.* 2004) which might explain the lack of effect. A new pool of four ADAM33 siRNAs (ADAM33-SMARTpool: M-004525-01) was provided by the company two of them targeting the 3'UTR and only one the MP-domain and one the PRO-domain of ADAM33.

When this new pool was used in primary human embryonic lung fibroblasts a significant knock down of ADAM33 after 24 and 48 hours could be achieved comparable to the knock down using GAPDH control siRNA. Other mesenchymal cell specific genes such as TGFβ1 and Collagen1A were not affected, however, of great interest was that αSMA was concomitantly down regulated by the new ADAM33 siRNA pool. This finding raised the question if ADAM33 knock down has a direct effect on αSMA expression or if the siRNAs have an off-target effect. In order to answer this question the individual duplexes of the new

ADAM33 siRNA pool were used in a knock down experiment. This revealed most significant knock down of ADAM33 with the two siRNAs targeted against the 3'UTR, whereas only one duplex also concomitantly down regulated αSMA expression suggesting that this one duplex might have an off-target effect on αSMA.

In human lung, ADAM33 mRNA is expressed in fibroblasts, smooth muscle cells but not epithelial cells (Van Eerdewegh *et al.* 2002). ADAM33 protein is expressed in the smooth muscle cells and (myo)fibroblasts in bronchial biopsies from adult asthmatic and normal subjects (Haitchi *et al.* 2005b; Lee *et al.* 2006; Ito *et al.* 2007; Foley *et al.* 2007) (See Chapter 1) which might play a role in the control of contractility and tonus and/ or differentiation of the smooth muscle. Detection of ADAM33 mRNA and protein in bronchial epithelial cells (Ito *et al.* 2007; Foley *et al.* 2007) is controversial and could not be confirmed as shown in result chapter 1 (Haitchi *et al.* 2007). In human embryonic/fetal lungs ADAM33 protein is strongly expressed in the mesenchymal progenitor cells (Haitchi *et al.* 2005b) suggesting a potential role in lung development. ADAM33 mRNA expression could be significantly knocked down in human primary embryonic/fetal lung fibroblasts (mesenchymal progenitor cells) for the first time and ADAM33 might be closely linked with the differentiation of smooth muscle arising from the mesenchymal progenitor cells that strongly express ADAM33. Therefore, to further study the role of ADAM33 in lung development transfection of whole pieces of human embryonic/fetal lungs with specific ADAM33 duplex siRNA (without off-target effect) will be a crucial step to further evaluate the effect of an ADAM33 knock down on smooth muscle development in the HEL explant culture system. This would allow us to study and measure the effect the knock down of ADAM33 would have on the spontaneous peristaltic contraction (Schittny *et al.* 2000) (in the pseudoglandular stage of lung development) using time lapse microscopy in the explant culture system.

4.4 Summary of results and novel findings

- ADAM33 mRNA splice variants show a similar pattern as in fibroblasts and bronchial biopsies.
- ADAM33 mRNA expression increases significantly during HEL development in vivo.
- ADAM33 protein isoforms can also be detected in HELs with an extra strong band at 25kDa.
- Immunohistochemistry of HEL sections and confocal microscopy of whole mounted HEL tissue pieces revealed strong ADAM33 expression in the mesenchymal progenitor cells that surround the primitive tubular airways.
- ADAM33 mRNA expression in dissected mesenchymal mesh is significantly greater than in the tubular structures confirming the microscopy data.
- Use of new HEL explant model allows studying HEL development in vitro.
- ADAM33 mRNA expression significantly increases in HEL explant cultures in vitro over 18 days.
- ADAM33 mRNA expression in HEL explant cultures is suppressed in the presence of IL-13 after 18 days.
- Human embryonic/fetal lung tissue pieces can be chemically successfully transfected with fluorescently labelled control siRNA but method needs further optimisation
- Primary human adult and embryonic/fetal fibroblasts can be transfected successfully using chemical transfection reagents.
- mRNA can be successfully knocked down in primary human adult and embryonic/fetal fibroblasts using specific siRNA compared to control siRNA.
- ADAM33 mRNA and GAPDH mRNA as control were significantly knocked down by the new ADAM33 siRNA pool and by GAPDH control siRNA in primary human embryonic/fetal lung fibroblasts.
- ADAM33 siRNA pool had a concomitantly mRNA knock down effect on the mesenchymal cell marker αSMA but no effect on other mesenchymal cell markers such as TGFβ1 and Collagen I in primary human embryonic/fetal lung fibroblasts.
- Single duplexes from the ADAM33 siRNA pool are also effectively knocking down ADAM33 mRNA in primary human embryonic/fetal lung fibroblasts and one of them also suppresses αSMA suggesting an off-target effect.

Chapter 5 Results: ADAM33 in Mouse Lung

5.1 Background

The availability of human embryonic/fetal lungs and the newly developed HEL explant culture model allows us to study ADAM33 in human lung development; however, this is restricted to a very narrow developmental window during the pseudoglandular stage. In order to study ADAM33 in vivo over the complete time course of lung development, from the early embryonic stage to the late post partum alveolar stage, a mouse model was chosen. Embryogenesis and in particular lung development is a complex process that starts in utero and is only completed up to 3 years after birth. The epithelial-mesenchymal trophic unit (EMTU) plays a key role in the formation of the primitive bronchial tubular airways parallel to the development of the vascular and neural system (Shannon and Hyatt 2004). This is tightly regulated by different transcription factors and growth factors that are differentially expressed and released by the epithelial and mesenchymal cell units (Perl and Whitsett 1999; Warburton *et al.* 2005; Maeda *et al.* 2007).

ADAM proteins play an important role in biology and disease (Blobel 2005; Manso *et al.* 2006; Yang *et al.* 2006) through shedding of a broad variety of cytokines and growth factors from the cell membrane or extracellular matrix via the metalloprotease or attachment to integrins via the disintegrin domain (Duffy *et al.* 2003). We know that mice deficient of one of the best described ADAM proteins, ADAM17 (TNFα converting enzyme, TACE) show pulmonary hypoplasia and develop respiratory distress at birth (Zhao *et al.* 2001a). Although ADAM33-null mice showed normal growth and development and the deficiency had no effect on allergen-induced airway hyperreactivity, immunoglobulin E production, mucus metaplasia, and airway inflammation in and allergic asthma model (Chen *et al.* 2006) the role of ADAM33 in lung development and pathogenesis of asthma is still not clear. While complete loss of function had no effect on lung development or allergic asthma, this could potentially be explained by full compensation of its function by other ADAM or MMP proteins, Partial loss (knockdown rather than knock out) of function might enable the function of ADAM33 to be explored in normal lung development. Furthermore, gain of function may underlie the contribution of ADAM33 to the pathogenesis of asthma.

In chapter two it has been shown that ADAM33 is mainly expressed in the mesenchymal cell unit that surrounds the primitive airways in human embryonic lungs in contrast to its expression in adult airways where it is strongly associated to the smooth muscle bundles (chapter 1). This suggest that ADAM33 might play a role in smooth muscle development from the primitive embryonic mesenchymal progenitor cells to the mature smooth muscle of the adult airways that are increased in asthma and play an important role in BHR.

The first aim in this chapter is to study the expression of ADAM33 in mouse lung development from the embryonic and fetal period until the full maturation of the lung in the adult animal.

Based on the fact that maternal atopy is a strong risk factor for development of BHR and asthma (Young *et al.* 1991) the second aim of this chapter is to study the effect of an maternal allergic environment on ADAM33 and airway hyperresponsiveness in offspring from ovalbumin sensitised and challenged mouse mothers (during pregnancy).

5.2 Results

5.2.1 ADAM33 mRNA expression in a series of mouse embryonic, fetal, juvenile and adult mouse tissues

To study the expression of ADAM33 during mouse development outbred MF-1 mice were chosen for ease of mating and high number of offspring per litter. Lungs, hearts and brains were dissected from mouse embryos/fetuses embryonic day (ED) 11 to 19 and juvenile mice from postpartum day (PD) 1 (Figure 5.1), 2, 9, 16, 23, 30, 37, 44, 52, 59 and adult mice. RNA was extracted using the TRIzol method. RNA was reverse transcribed for RT quantitative PCR.

Initially ADAM33 mRNA expression in the lungs was analysed using commonly used genes for normalisation, 18S rRNA and GAPDH mRNA. Data analysed relative to 18S rRNA and GAPDH were similar but showed inconsistencies in their expression profile and their fold increase (Figure 5.2A, B) especially around the time of birth and the neonatal period. One possible explanation for this was that the house keeping gene itself was not stable expressed. Embryonic development is a complex process during which significant changes in gene expression occur. These changes include those genes that are often considered to be 'house-keeping genes' (HKGs). Accurate gene quantification within such a complex process can be problematical and for this reason it is particularly important to establish which HKGs are most stably expressed during the process of lung development to enable accurate gene quantification.

geNorm analysis

Therefore, 12 different of the most commonly used HKGs (Table 5.1) were measured and geNorm analysis (Vandesompele *et al.* 2002) was performed (See chapter 2 section 2.3.4) in order to reveal the stability expression of each gene during mouse lung development to be able to study ADAM33 expression with the best normalising genes. The geNorm analysis compares the ratio of the ratio of control genes in different samples to find those that are most stable as previously described (Vandesompele *et al.* 2002). The 12 HKGs were rated for the average expression stability (M) with the most stable producing the lowest M value (Figure 5.3A). The top 2 HKGs cannot be ranked in order because a gene ratio is required to calculate gene stability. The pair-wise variation analysis (V) in normalising signal (NF_n) was also calculated for the data set using geNorm (Figure 5.3B). This measures the degree of variation in normalisation signal that is achieved by using n control genes compared to n+1, with genes added step-wise into the analysis in the order of their gene stability rankings. The

stability of the normalisation signal improves up to the addition of the sixth gene and then deteriorates as the six least stable genes are added to the analysis.
The four mouse HKGs glyceraldehyde-3-phosphate dehydrogenase (GAPDH), ATP synthase subunit (ATP5B), cytochrome c-1 (CYC1) and succinate dehydrogenase complex (SDHA) were most stably expressed (lowest average stability M) in the developing lungs (Figure 5.3A) but also in the hearts and brains.
The combinations of six to seven HKGs were the optimal number of control genes for normalisation reaching a pairwise variation V of less than 0.15, however, the combination of three to four HKGs showed also an acceptable low variability of less than 0.25 (Figure 5.3B).

Gene quantification

When the three most stably expressed HKGs (GAPDH, ATPB, CYC1) were used for normalisation of ADAM33 mRNA expression in the lungs it could be shown that ADAM33 expression increased in four significant (* $p<0.002$) steps during mouse lung development (Figure 5.4A). These corresponded to the stages of normal lung development (See Figure 5.1) and the progression from the embryonic stage (ED11) to pseudoglandular stage (ED12-15), to the canalicular stage (ED16,17), to the saccular alveolar stage (PD1&8) and to the adult stage (AM). However, the greatest increases in ADAM33 expression occurred from ED11 to 12 and then again after birth (** $p<0.001$). (Figure 5.4A) αSMA mRNA expression showed a similar pattern with a significant increase in the early stage of embryonic lung development and post partum (Figure 5.4B). In contrast the transcription factor, forkhead box A1 (FOXA1), another important gene in lung development(Wan *et al.* 2005), showed a much lower expression relative to ADM33 and no incremental changes during lung development (Figure 5.4C).
To compare the expression of ADAM33 and αSMA in lung development with the development of two other mouse organs, the heart and brain, ADAM33 and αSMA were also studied in series of heart and brains. In contrast to the lungs ADAM33 mRNA expression in the heart and lung was much lower than in the lungs and showed a different much flatter expression pattern (Figure 5.5 A-F) suggesting a different role in these two organs.

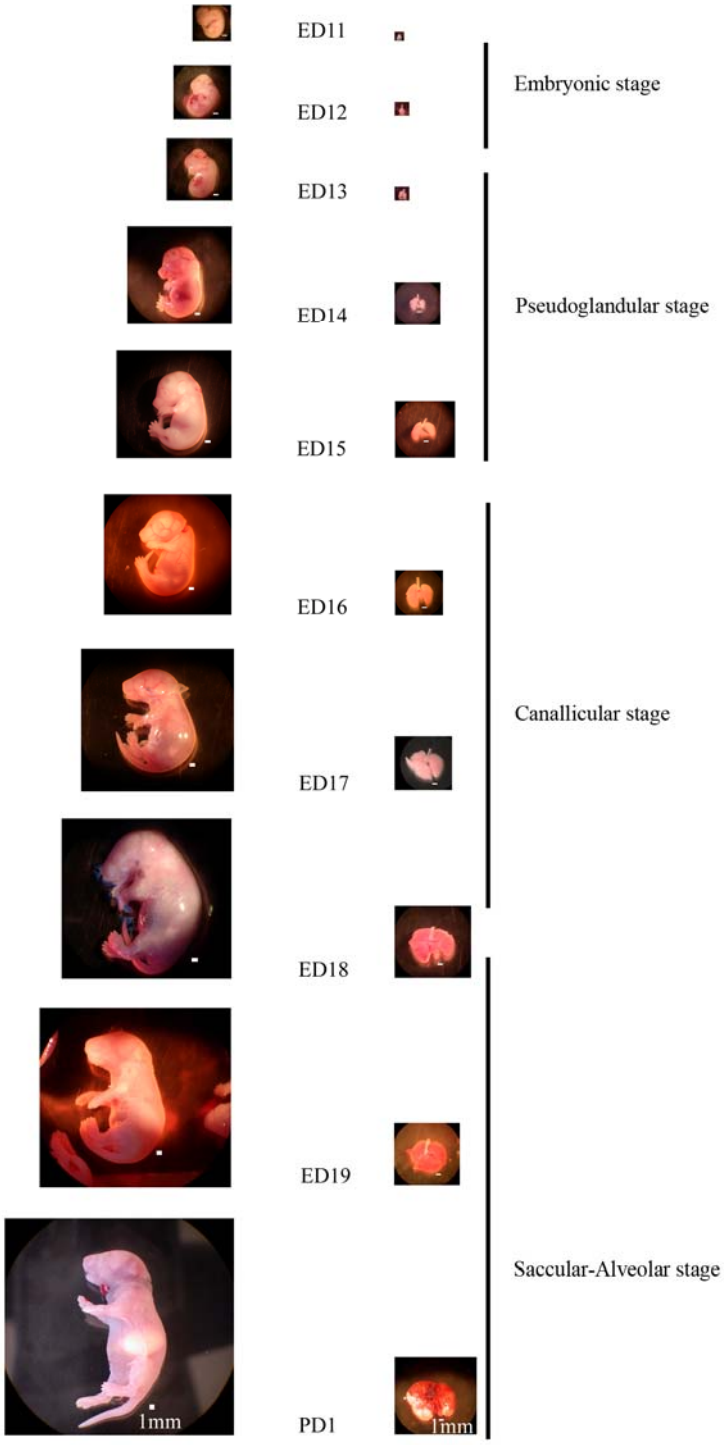

Figure 5.1. Whole embryonic, fetal and postnatal mice and lungs.

Images from MF-1 mouse embryos and embryonic lungs embryonic day (ED) 11-19, juvenile mouse postpartum day (PD) 1 and stages of lung development.

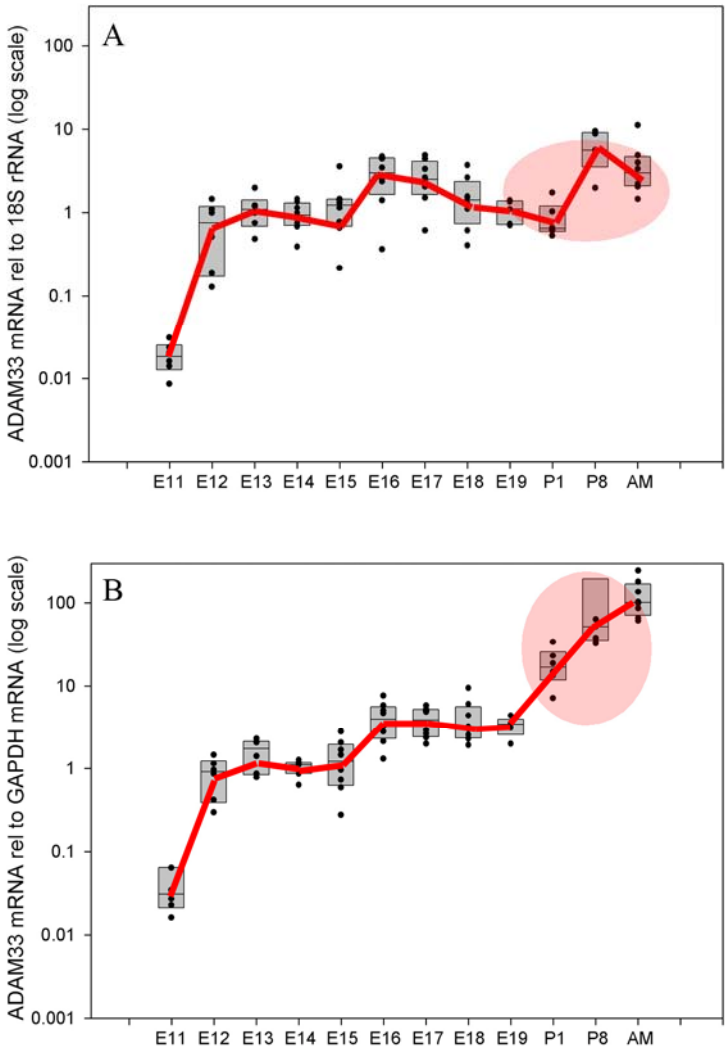

Figure 5.2 RT-qPCR of ADAM33 in a panel of mouse lungs.

ADAM33 mRNA expression in embryonic (E12-E19), postpartum (P1,P8) and adult mouse (AM) lungs (A) relative to 18S rRNA and (B) relative to GAPDH mRNA. The difference in expression pattern (profile and fold increase) is indicated by the coloured ellipses.

Accession Number	Mus musculus Sequence Definition
NM_007393	actin, beta, cytoplasmic (**ACTB**), mRNA.
NM_001001303	glyceraldehyde-3-phosphate dehydrogenase (**GAPDH**), mRNA.
NM_019639	ubiquitin C (**UBC**), mRNA.
NM_009735	beta-2 microglobulin (**B2M**), mRNA.
NM_011740	phospholipase A2 (**YWHAZ**), mRNA.
NM_009438	ribosomal protein L13a (**RPL13A**), mRNA.
NM_007597	calnexin (**CANX**), mRNA.
NM_025567	cytochrome c-1 (**CYC1**), mRNA.
NM_023281	succinate dehydrogenase complex, subunit A (**SDHA**), mRNA.
X00686	**18S** rRNA gene
NM_013506	eukaryotic translation initiation factor 4A2 (**EIF4A2**), mRNA.
NM_016774	ATP synthase subunit (**ATP5B**), mRNA.

Table 5.1 Twelve mouse HKGs detection kit used with geNorm.

Accession numbers and gene names of 12 mouse 'house keeping genes' used for GeNorm analysis in lung development to find the best normalisation genes.

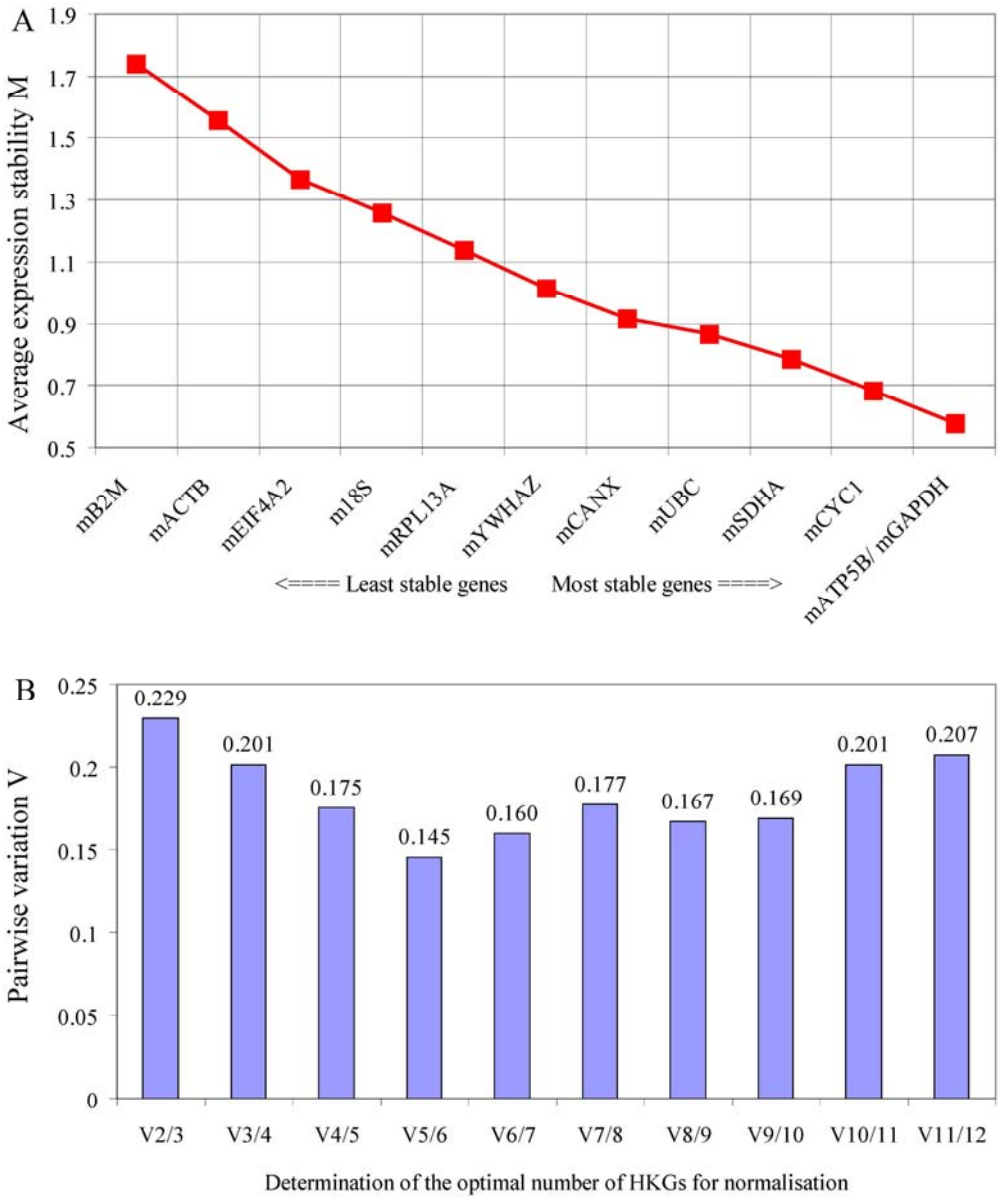

Figure 5.3 geNorm graphs of stability and optimal number for HKGs.

geNorm analysis of 12 house keeping genes: RT-qPCR was performed on cDNA derived from 24 lung samples, 2 each from embryonic day 11 to 19, postpartum day1 and 8 and adult mice. Results were analysed using the geNorm analysis software. (A) Determination of the most stable expressed genes with the lowest M value. The M value is calculated based on changing ratios of genes in the analysis as previously described (Vandesompele *et al.* 2002), such that lower M values indicate more stably expressed genes with and M value < 0.9 indicating relatively stable control genes. (B) Determination of the optimal number of control genes was derived by pairwise variation V analysis between the normalisation factors (NF) of n and n+1 genes. Control genes are added to the calculation in the order of decreasing stability as determined above and a change in NF with n genes compared to NF using n+1 genes. Changes in V values of less than 0.15 are considered optimal number for accurate normalisation.

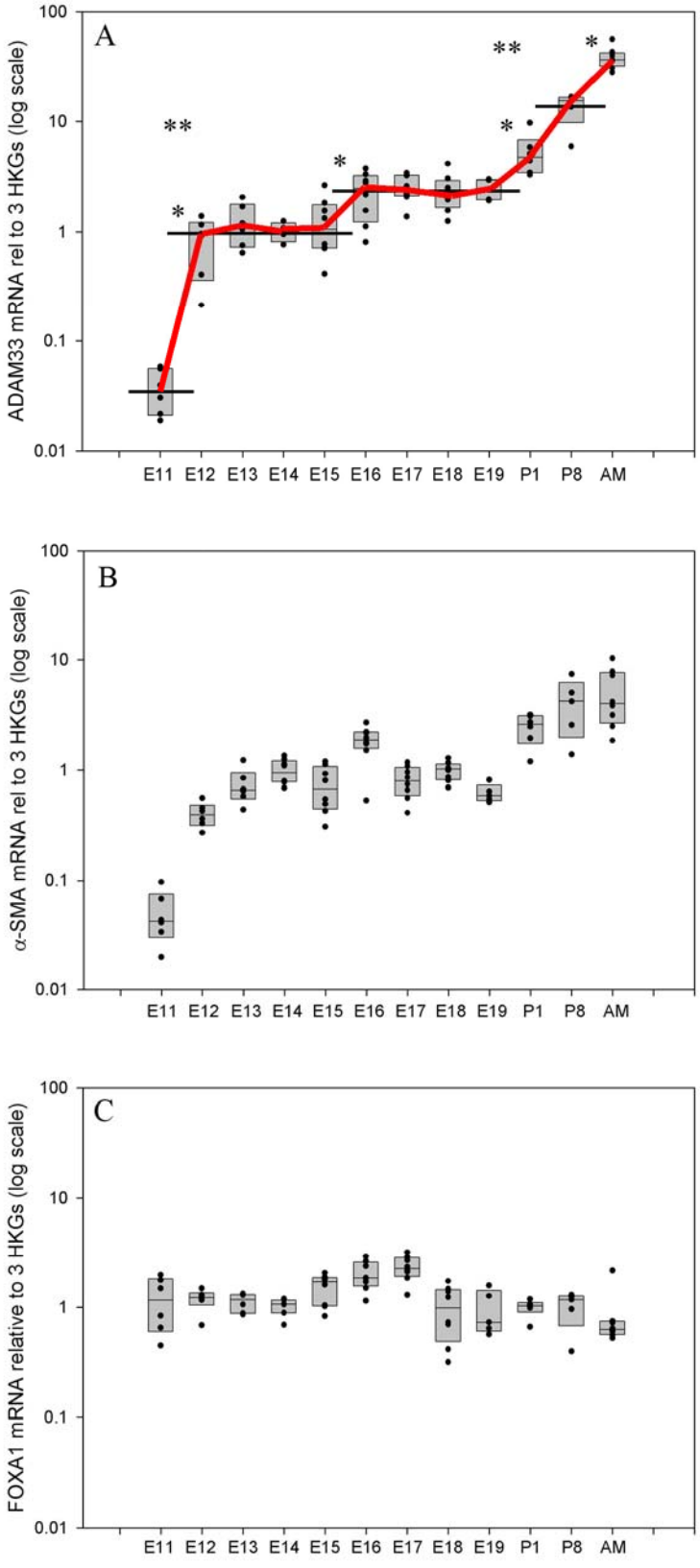

Figure 5.4 RT-qPCR of ADAM33 rel 3HKGs in a panel of mouse lungs.

RNA was extracted from embryonic day 11 to 19 (E11-E19), post partum day 1 and 8 (PD1 & 8) and adult mouse lungs (n=6-8) and RT-qPCR was performed for ADAM33, α-smooth muscle actin (αSMA) and the transcription factor forkhead box A1 (FOXA1). (A) ADAM33 mRNA expression increased significantly in 4 steps (* $p<0.002$)), whereas the biggest increase could be seen early from the embryonic to the pseudoglandular-canalicular stage and later in the postnatal saccular-alveolar stage (Kruskal-Wallis One Way ANOVA on ranks and multiple comparison Dunn's method; ** $p<0.001$). (B) αSMA mRNA expression showed a similar pattern and (C) FOXA1 mRNA expression did not change over all stages of lung development.

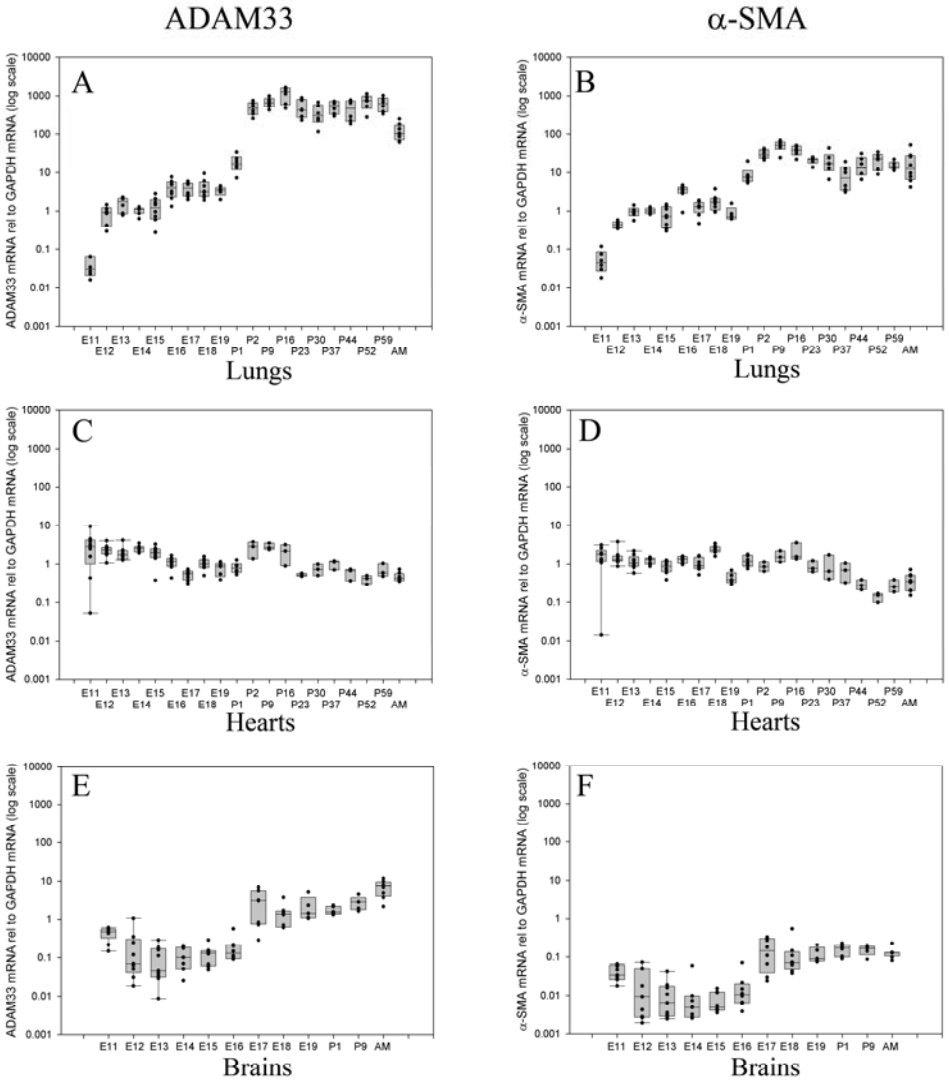

Figure 5.5 RT-qPCR of ADAM33 & αSMA in mouse lungs, hearts and brains.

RT-qPCR for ADAM33 and αSMA was performed in mouse lung, heart and brain series (n=5-9). Data were all analysed rel to GAPDH (delta CT (dCT)) mRNA and relative to the mean of ADAM33 dCTs at embryonic day 14 (ED14) (delta delta CT (ddCT)). ADAM33 and αSMA mRNA expression from embryonic day 11 (E11) to post partum day 59 (P59) and adult mouse (AM) showed a step-wise increase and higher expression level in the lungs (A,B), compared to their expression in the hearts (C,D) and the brains (E,F).

5.2.2 The influence of an allergic maternal environment on ADAM33 and α-smooth muscle actin expression in the lungs of their offspring.

Maternal atopy is a strong risk factor for developing BHR and asthma (Young *et al.* 1991; Sears *et al.* 1996; Arshad *et al.* 2005) early in life. A/J mice (*BHR1* locus positive) (De Sanctis *et al.* 1995) were used to model maternal allergy *in vivo* to study the influence of maternal allergy on ADAM33 and αSMA expression. For allergen exposures, mice were sensitised by intra-peritoneal (i.p.) injection with 0.2 ml of 0.9% sterile isotonic saline containing 10 µg ovalbumin and 2 mg aluminium hydroxide 21 days and 7 days before mating. The pregnant mothers were then exposed to saline (control) or ovalbumin (1% w/v in sterile isotonic saline) aerosols in nose-only exposure systems. Exposures were conducted for a period of 1h per day, 3 days per week for three weeks (Temelkovski *et al.* 1998; Henderson, Jr. *et al.* 2002; Tsuchiya *et al.* 2003). Fetuses and newborn offspring were harvested 15days, 19 days, 24 days post conception and 4 weeks post partum and the lungs were dissected and stored in RNAlater for shipment to and mRNA expression analysis in Southampton. (Work was performed by Xiufeng Gao and David Bassett at Wayne State University, US) (Figure 5.6).

As found in MF-1 mice, ADAM33 mRNA expression increased significantly post partum. However, in lungs of newborn offspring from ovalbumin-allergic mothers ADAM33 mRNA expression was significantly down regulated ($p=0.03$). αSMA mRNA showed also a tendency of down regulation ($p=0.27$) (Figure 5.7A&B). This suggests a direct potential link between environmental influences associated with Th2-type inflammation and ADAM33, acting as a local asthma susceptibility gene.

5.2.3 The influence of an allergic maternal environment on 4 week old offspring and their responsiveness to methacholine

In order to test the influence of a maternal allergic environment on the lung function and in particular the airway reactivity of their offspring ventilatory function tests were performed at the earliest technical feasible time point after birth. Ventilatory function (enhanced pause (Penh)) of four week old offspring from with ovalbumin or normal saline challenged mothers (during pregnancy), was assessed using whole body plethysmography as a measure of airway reactivity to increasing concentrations of inhaled methacholine. (Penh measurements and analysis were performed by Xiufeng Gao and David Bassett at Wayne State University, US). A significant and novel finding is that the reactivity to increasing concentrations of inhaled methacholine was significantly increased in the four week old offspring from mothers challenged with Ovalbumin during pregnancy compared to the offspring from mothers challenged with normal saline during pregnancy. There were no observed differences in the baseline values suggesting that the breathing patterns of the offspring at 4 weeks post-partum were not affected by ovalbumin exposure during pregnancy (Figure 5.8).

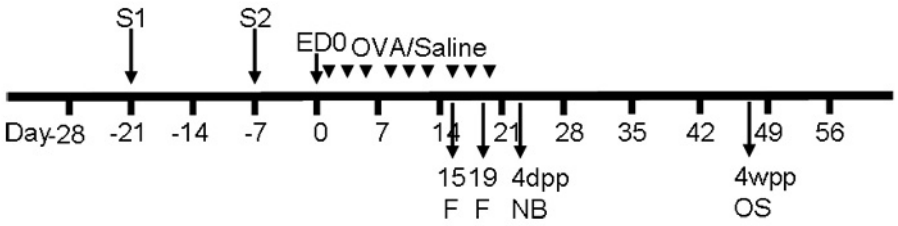

Figure 5.6 Maternal mouse allergic environment experimental outline.

Time points of sensitisation (S1, S2) at day 21 and 14 before mating (ED0) and exposure to ovalbumin or saline (OVA/Saline). Lungs from fetuses and newborn (NB) and offspring (OS) were harvested at day 15, 19 and around day 24 post conception (4 days post partum (pp)) and 4 weeks post partum (4wpp).

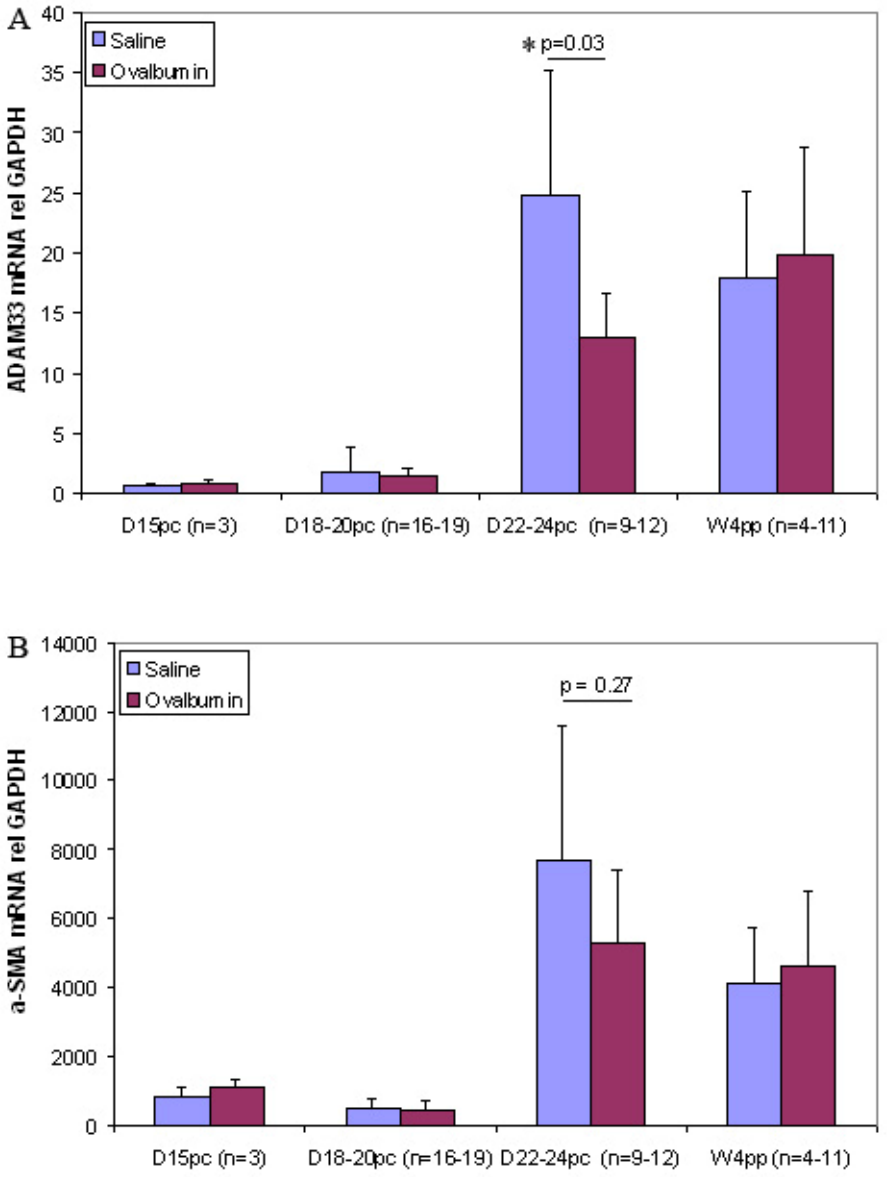

Figure 5.7 RT-qPCR of ADAM33 & αSMA in offspring.

RT-qPCR for ADAM33 and αSMA of lungs harvested from fetuses or offspring of saline or ovalbumin sensitised and exposed A/J mouse mothers at day 15 post conception (D15pc), D18-20pc, D22-24pc and week 4 post partum (W4pp). ADAM33 mRNA (A) was significantly suppressed at day 22-24 post conception in the newborn offspring and αSMA mRNA (B) expression showed a tendency for suppression (t-test, *$p<0.05$).

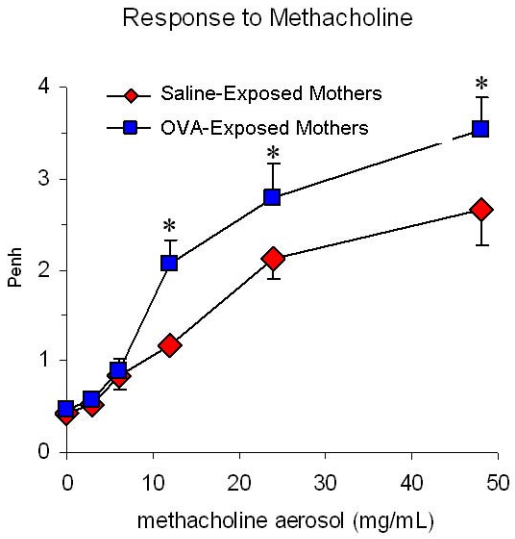

Figure 5.8 Airway responsiveness to methacholine in offspring.

Whole body plethysmography and response to methacholine aerosol of four weeks old offspring from OVA exposed mothers compared with saline exposed mothers (during pregnancy). Data represent the mean Penh values ± SEM obtained from 4weeks post-partum offspring. For analysis 22 offspring form 7 saline exposed mothers and 29 offspring from ovalbumin-exposed mothers were obtained (about 2-4 offspring/mouse mother).(Two Way ANOVA with comparisons of the means using Student-Keul's multiple range tests, * $p<0.05$). (Figure contributed by David Bassett)

5.3 Discussion

ADAM33 expression in different mouse organs during development.

Although no major effect on lung development was seen in a mouse deficient of ADAM33 (Chen *et al.* 2006), other ADAM proteins are involved in normal and abnormal organogenesis, such as ADAM12 in the heart (Asakura *et al.* 2002) and ADAM17 in the lung (Zhao *et al.* 2001b; Zhao *et al.* 2001a).

Loss of function might be compensated by other catalytically active ADAMs, however, over expression or a functional change of the catalytically active ADAM33 might result in a gain in function and potentially influence normal lung development.

The knock-out mouse model might have been of more value if it had used the A/J mouse strain which carries the bronchial hyperresponsiveness locus (*BHR-1*) that is associated with increased BHR (De Sanctis *et al.* 1995) and corresponds to the *ADAM33* locus on mouse chromosome 2 (Yoshinaka *et al.* 2002). This would have allowed assessment of whether loss of ADAM33 directly affected BHR in these mice.

The fact that the human gene for ADAM33 is syntenic to the homologue on mouse chromosome 2 with 70% homology (Yoshinaka *et al.* 2002; Gunn *et al.* 2002) enabled the study of ADAM33 expression in the developing mouse lung and comparison with other developing organs such as the heart and the brain where ADAM proteins play an important role (Duffy *et al.* 2003) (Manso *et al.* 2006; Yang *et al.* 2006).

The initial analysis of the data of ADAM33 expression in the developing lung using commonly used house keeping genes (18s rRNA and GAPDH) showed inconsistency in the expression pattern and the fold increase. Using twelve well known different HKGs and geNorm analysis enabled the discovery of the four most stably expressed HKGs in the developing lung. These were similar or almost the same in the heart and brain tissues and GAPDH was always among the top four most stably expressed genes in all three organs which is not the case in whole mouse embryos at an earlier stage (3.5 – 11.5 dpc)(Willems *et al.* 2006). This finding supports the need for careful assessment of the right HKGs for studies of gene expression in whole organ tissue and complex processes such as lung development and embryogenesis.

ADAM33 is a mesenchymal cell protein and it can be found in the human fetal airways almost exclusively in the mesenchymal progenitor cells that surround the primitive tubular αSMA positive and epithelial cell containing structures whereas in human adult airways it is strongly co-localised to the smooth muscle bundles (See chapter 3). This suggests a differential function of ADAM33 in adult compared to fetal airways that might result in the different function of the airway smooth muscle.

The significant step-wise increments of ADAM33 and αSMA expression over the whole process of mouse lung development and in particular during the early parts and later after birth suggest some important biological or biomechanical stimuli in this process. One possible explanation for the significant increase in the early stages of lung development (embryonic to pseudoglandular stage) might be spontaneous airway contraction (about 1/minute) that are known to occur in the early pseudoglandular stage (Jesudason *et al.* 2005) and can be observed during branching morphogenesis in mouse ED12 lung explant cultures in vitro (Figure 5.9) (See movie 2 in attached CD). This peristaltic movement is thought to promote the growth of the endbuds into the surrounding mesenchyme (Schittny *et al.* 2000). Mechanical stretch from breathing after birth might be an explanation for the most significant increase of ADAM33 expression post partum.

Breathing movements at and after birth (mouse: mean 132//minute two days post partum and 260/minute 8 days post partum(Dauger *et al.* 2004); human: mean of 48 breaths/minute in less than 2 months old infants(Rusconi *et al.* 1994)) are dramatic changes for the newborn lungs resulting in mechanical stretch of the airways. This might enhance ADAM33 as well as αSMA expression in newborn breathing lungs which does not further change over the next 8 weeks post partum (Figure 5.5A)

A further important finding is that ADAM33 is several hundred-fold higher expressed and shows a different expression pattern in the developing lungs compared to the developing hearts and brains. This suggests a different and potentially significant role of ADAM33 in lung development.

The effect of maternal allergy on ADAM33 expression and lung function in their offspring.

Maternal allergy is one of many environmental factors, such as cigarette smoke, alcohol, toxins or drugs and diet, which can have an influence on embryonic and fetal lung development that can result in early life wheezing which might continue in childhood or adult asthma (Young *et al.* 1991; von Mutius 2002; Celedon *et al.* 2002; Lannero *et al.* 2006). Due to the fact that 3 and 5 year old children from a prospective birth cohort study showed an association of impaired lung function in particular with the SNP (F+1) in ADAM33 (Simpson *et al.* 2005a) it was hypothesised that maternal allergy might have an influence on ADAM33 and lung development in utero and post partum.

As discussed above, the gene for ADAM33 in the mouse has also been associated with BHR (*BHR1 locucs*) in A/J mice (De Sanctis *et al.* 1995). Therefore, an animal model of maternal allergy using A/J mice sensitised and exposed to ovalbumin was chosen to study its effect on ADAM33 expression in the fetus, newborn and adolescent offspring as well as the effect of lung function in the adolescent offspring.

The ovalbumin sensitised and challenged adult female mice showed a marked eosinophilic and lymphocytic pulmonary inflammation compared to the normal saline challenged control mice (See chapter 2, section 2.5, Figure 2.26). When the expression of ADAM33 mRNA was studied in their offspring a significant increase of ADAM33 was detected in the lungs from the newborns confirming the findings in the MF-1 mice. However, a significant depression of ADAM33 was observed in the lungs of the newborn mice (2-4 dpp) from ovalbumin challenged compared to saline challenged mothers (Figure 5.7A). Only a tendency of αSMA mRNA depression was seen in the lungs of the same newborn offspring. The finding that ADAM33 is depressed in the lungs of newborns from allergic mothers suggests that maternal allergy may have a direct or indirect influence on the expression of ADAM33 in the mesenchymal progenitor cells. This early post partum effect might reflect a delayed expression of ADAM33 caused by the maternal allergic environment hence being either a marker or possibly related to the cause for delayed lung maturation early in life which might lead to wheezing in children.

The second important finding is that the airway responsiveness to increasing concentrations of inhaled methacholine is significantly increased in 4 week old offspring from allergic mothers compared to non-allergic mothers. It has been previously reported that offspring of asthmatic mouse mothers (BALB/c) showed airway hyperresponsiveness (AHR) and allergic pulmonary inflammation after an intentionally suboptimal OVA sensitisation and exposure protocol that had little effect on offspring from normal mothers, suggesting a maternal transfer of asthma susceptibility. In contrast to these findings our data show already increased AHR in offspring from allergic mothers without OVA sensitisation and exposure

of the offspring. This suggest a different mechanism that maternal allergy in animals with susceptibility to BHR (A/J mice, *BHR-1* positive) might have a direct or indirect effect of modelling of the airways and making them more responsive to methacholine, however the same experiment has to be repeated with animals not susceptible to BHR (BALB/c mice) as a control group.

These data suggest that ovalbumin exposure of sensitised mice during pregnancy results in non-specific airway hyperactivity in the offspring. However, although the non-invasive Penh method has been used extensively to screen for methods to ameliorate allergen-induced lung inflammation and airway hyperreactivity, it does not directly measure changes in airway calibre, required for a detailed assessment of airway reactivity to methacholine challenges that requires the direct measurement of changes in trans-pulmonary pressure (Bates *et al.* 2004). Although investigators have worked towards validating the Penh method by comparing data with other non-invasive and invasive procedures (Glaab *et al.* 2005) (DeLorme and Moss 2002), its use as a measurement of airway hyperreactivity remains controversial. However, Whitehead et al (Whitehead *et al.* 2003) have used the Penh method effectively to compare the baseline methacholine responses of a range of differing mouse strains, consistent with the present investigation.

Morphological studies are also needed to study the potential effect of ADAM33 suppression on the airway structure at the early postpartum time point and the later time point (4 wpp) when ADAM33 expression has caught up but the animals have the increased responsiveness to methacholine. These studies will allow explaining if the increased responsiveness is either due to differences in inflammatory cell content or accounted for by changes in airway structure.

In support of the data from the allergic mice, are the findings in human embryonic/fetal lungs. Exposure of the human embryonic lungs to IL-13 to mimic a maternal allergy in an *in vitro* culture model using human embryonic/fetal lung explants (See Chapter 4) resulted also in suppression of ADAM33 expression by 18 days of culture.

These results suggest that the maternal Th2 environment and maternally derived IL-13 may have an effect on ADAM33 which might affect the structure of the developing airway walls *in utero* predisposing to the development of BHR early in life. Variation in ADAM33 in combination with environmental factors (Saglani and Bush 2007), may lead to abnormal airways leading to the development of BHR in asthma.

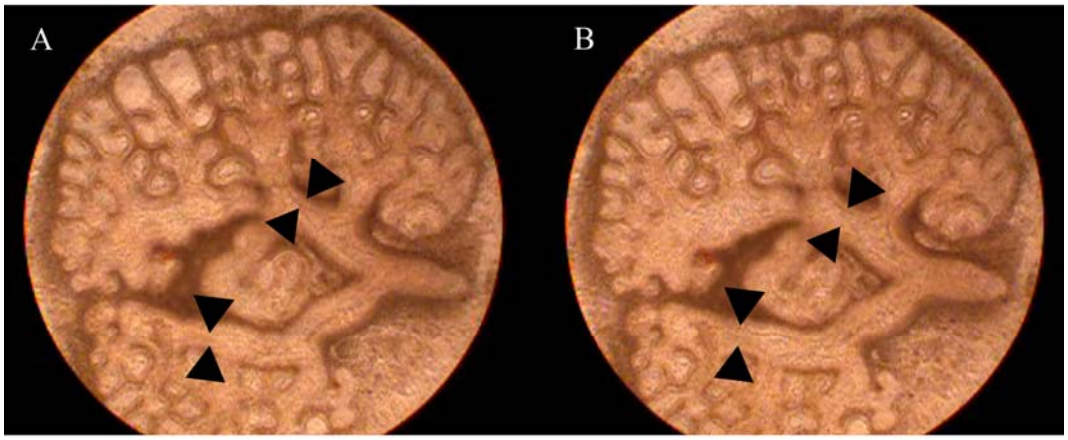

Figure 5.9 Snap shots of spontaneous contraction in ED12 mouse lung.

Snap shots of a real time movie of mouse embryonic day 11/12 lungs cultured for 48 hours showing spontaneous contraction (A) and relaxation (B) of the primitive airways (black arrows). Contractions occurred every 40 seconds with these two images being 40 seconds apart (See movie 2 in attached CD).

5.4 Summary of results and novel findings

- GeNorm analysis enabled determination of the best HKGs to use for mRNA analysis during lung development.
- ADAM33 expression increases in step-wise fashion during lung development in MF-1 mice, most significantly in the early embryonic stage and after births, which might be stretch induced by spontaneous contraction of the pseudoglandular primitive airways and breathing movement after birth.
- ADAM33 expression increases also significantly in A/J mice after birth.
- Maternal allergy suppresses expression of ADAM33 in their newborn offspring.
- Four week old offspring form allergic mothers compared with offspring from normal mothers have a significant increased reactivity to increasing concentrations of methacholine independent of allergen sensitisation and challenge.

Chapter 6 Final discussion

This thesis has concentrated on the expression of ADAM33 in human embryonic and adult tissue and its role in the physiology and pathophysiology in the process of lung development and the origins of asthma that develops later in life.

6.1 Statement of principle findings

Several key findings have been described in this thesis that might have important implications for the role of ADAM33 in lung development and disease (Figure 6.1).

- The first important finding is that ADAM33 is mainly expressed in the mesenchymal progenitor cells that are precursors for the smooth muscle in human embryonic lungs. Although some co-localisation was found with αSMA active positive cells this is different to ADAM33 expression in adult bronchial tissue. Here it was described for the first time that ADAM33 is mainly found in the airway smooth muscle and fibroblasts/myo-fibroblasts of the adult airway suggesting a different role early in life compared to adult life. When different splice variants of ADAM33 were studied in HELs and bronchial biopsies a similar expression pattern was found as previously described in fibroblasts (Powell *et al.* 2004). No differences in relation to disease severity were found; however, there was a distinct extra 25kDa protein band present in the HELs that points to different roles of protein variants at different stage of lung development.
- Another key element of this thesis was the development of a new HEL explant culture model using an 'air-Matrigel-medium interface', which is much closer to the in vivo intra-uterine lung developmental environment and has allowed studying of HELs for several weeks. Using this in vitro model it was shown that ADAM33 increased significantly over a time period of 18 days, which was similar to the findings in vivo from 7 to 9 weeks old HELs suggesting that this model is a valid in vitro tool in studying HEL development. Knock down of ADAM33 in mesenchymal progenitor cells from HELs using siRNA was also achieved, paving the way for knock down experiments in the HEL model. This will allow comparison with the knock-out mouse model where compensational mechanisms may have prevented identification of phenotypic effects of loss of ADAM33 function. This model will allow the study of the effect of ADAM33 knock down under different culture conditions (plus/minus mechanical stress, different extracellular matrix, IL-13 or TGF-β) in co-culture systems.

- Another key finding was that ADAM33 expression over the different stages of MF-1 mouse lung development increased at two distinct time points when spontaneous mechanical stretch of the airways occurs (contractions in pseudoglandular stage and breathing after birth). This suggests that ADAM33 and subsequently associated lung development might be influenced by mechanical stress.
- A further significant finding in this thesis resulted from the study of the effect of an allergic environment on offspring from allergic A/J mouse mothers that carry the BHR susceptibility gene. One effect was the depression of ADAM33 early after birth in the offspring from allergic mothers when compared to the offspring from normal mothers, although both offspring showed a significant increase of ADAM33 expression from intra-uterine to the time after birth, similar to findings in the MF-1 mice. The influence of allergic pathways was confirmed in HELs where ADAM33 suppression was observed after 18 days in culture in the presence of IL-13, mimicking a maternal allergic environment.
- Although no causal relationship with ADAM33 was established, a final important finding was that when lung functions were tested in 4 week old off-spring from the "allergic" A/J mouse mothers and compared with the offspring from normal mothers, they showed significantly increased pulmonary responsiveness to methacholine. This model may offer a novel approach to studying the impact of gene-environment interactions involving ADAM33 and maternal exposures on the subsequent development of asthma.

6.2 Strength and weaknesses of the study

In 2002, ADAM33 was the first described asthma susceptibility gene that was found by positional cloning and its single nucleotide polymorphisms are strongly associated in particular with the asthma phenotype of BHR (Van Eerdewegh *et al.* 2002) suggesting an important role in the airway smooth muscle development or function. However, ADAM33 is still a gene of unknown function with a multidomain structure that could be involved in different functions at different time points of development (Figure 6.1).

To begin studying the physiological role of a new gene it is important to know where and when it is expressed. Previous studies showed that ADAM33 is only expressed in mesenchymal cells and mesenchymal cell containing organs but not in epithelial cells (Van Eerdewegh *et al.* 2002; Umland *et al.* 2003). Data in this study showed for the first time that ADAM33 is mainly expressed in the airway smooth muscle in adult bronchial biopsies (Haitchi *et al.* 2005b) which has subsequently been confirmed by other studies (Lee *et al.* 2006; Ito *et al.* 2007; Foley *et al.* 2007). The localisation to smooth muscle is an important finding however reproducibility of immunohistochemistry findings from bronchial biopsies

could be improved by using more than one section within a single biopsy or between biopsies. Although computer assisted image analysis was done blinded additional analysis by a second or third blinded observer would allow correcting for observer variability.

In contrast to the adult lung, in human fetal lung ADAM33 is predominantly expressed in the progenitor cells in the mesenchymal mesh that surrounds the primitive airway tubular structures (Haitchi *et al.* 2005b) suggesting a different role and function in early lung development.

It is known that the embryonic airway smooth muscle originates from local mesenchymal progenitor cells that are located around the tips of the growing epithelial buds. Mechanical tension, contact with extracellular matrix (laminin) and epithelial paracrine factors seem to regulate bronchial myogenesis (Badri *et al.* 2008). In contrast to the unknown function in the adult airways, embryonic smooth muscle exerts an important physiological function in moving fluid in the primitive airways with spontaneous peristaltic contractions, hence facilitating branching morphogenesis (Schittny *et al.* 2000). Since ADAM33 is present in muscle cells, it is possible that it may play a role in this contractile process and hence, airway development. A shortcoming of these studies is the fact that HELs were only available from 7 to 9 weeks post conception during the first trimester of pregnancy. It would have been of great interest to study the expression of ADAM33 in lung tissue from the second and third trimester of pregnancy.

Although no morphological changes were observed in the lungs of the ADAM33 knock-out mouse model (loss of function), embryonic lungs were not studied in this model (Chen *et al.* 2006). Compensatory mechanisms by other ADAMs or MMPs may obscure the effect of ADAM33. A conditional knock-out mouse model would have allowed studying the effect of loss of ADAM33 at different time points of embryonic lung development which would have been even of more interest if the A/J mouse would have been used as background as this strain has the *BHR1* locus (close to ADAM33) which is associated with increased bronchial hyperresponsiveness (De Sanctis *et al.* 1995). However, it remains important to study the effect of ADAM33 knock-down, rather than knock-out, on embryonic lung mesenchymal progenitor cells and subsequently on airway smooth muscle development. Although initial attempts to knock down ADAM33 in whole HEL tissue were not successful further optimisation of ADAM33 knock-down in whole tissue will be of particular importance using other methods of RNA interference such as electroporation and short hairpin RNA (shRNA) with Lentiviral vector technology. This will allow studying the effect of ADAM33 suppression on changes in pattern and frequency of spontaneous peristaltic contractions in the pseudoglandular stage of lung development (Schittny *et al.* 2000). This might result in abnormal morphological changes in the airway smooth muscle and delayed lung development. The effect of knock down can be studied in vitro by time lapse or video

microscopy of life tissue culture (Pandya *et al.* 2006). Morphological changes can be studied in fixed tissue using whole mount confocal microscopy.

Significant RNAi-mediated downregulation of ADAM33 was finally achieved in primary human embryonic lung fibroblast (mesenchymal progenitor cells) cell culture after unsuccessful attempts in whole tissue. It would have been better to start siRNA transfection experiment first in monolayer fibroblast cell cultures to optimise the siRNA approach in particular with the frustration of having initially used an ineffective set of ADAM33 siRNAs. This system will allow studies of the effect of ADAM33 knock-down on mesenchymal progenitor cells when smooth muscle development is induced in vitro by exposure to mechanical stretch (Yang *et al.* 2000), different extracellular matrices (such as laminin) (Relan *et al.* 1999), growth factors and cytokines such as TGF-β and IL-13. It will also allow study of co-culture with smooth muscle cells, epithelial cells and endothelial cells that all play an important role in the EMTU.

Another important difference between adult and embryonic lung was found in the isoforms of ADAM33 expressed, namely an extra ~25kDa protein in HELs. This extra ADAM33 isoform needs to be confirmed using mass spectroscopy as it might represent a splice variant containing the cytoplasmic tail, the transmembrane domain and part of the EGF domain involved in cell fusion, an important function during early embryogenesis and development. An alternative explanation could be that the 25kDa fragment represents a breakdown product of full length ADAM33. This possibility was first suggested by Wicks et al, who reported an increase of smaller degradation products of ADAM33 in bronchial fibroblasts in the presence of TGF-β (Wicks 2006). Alternatively, it might also be a remnant containing the cytoplasmic tail that is left after ADAM33 has been cleaved from the cell surface resulting in a soluble form of ADAM33 (sADAM33) as reported for the closely related *Xenopus* ADAM13 (Gaultier *et al.* 2002). Such membrane cleavage could be induced by TGF-β which has been shown to cause dose-dependent release of a soluble form of ADAM33 from HEK293 cells that have been transfected with full length ADAM33 (Puxeddu *et al.* 2008). TGF-β plays a pivotal role in controlling fetal branching morphogenesis (Cardoso and Lu 2006) and smooth muscle differentiation in embryonic lungs (Figure 6.1). Contact of mesenchymal progenitor cells with laminin, an important extracellular matrix component of the basement membrane, induces smooth muscle differentiation in embryonic myogenesis (Badri *et al.* 2008). Some extracellular matrix (ECM) components are substrate for other ADAMs, indirectly making the case of ADAM33 effecting ECM modelling. This potential role in embryonic myogenesis needs to be studied by growing mesenchymal progenitor cells plus/minus RNAi on laminin or exposing them to recombinant sADAM33 in the presence of plus/minus TGF-β.

For practical reasons as mentioned above it was not possible to study ADAM33 expression during all stages of human lung development and therefore, a mouse model was studied. The parallel occurrence of a marked increase in ADAM33 mRNA expression with spontaneous mechanical stretch early in embryonic lung development and again postnatally, when the lungs inflate, suggests a physiological effect of stretch on ADAM33. As mechanical stress is important for embryonic airway smooth muscle differentiation originating from the mesenchymal progenitor cells (Badri *et al.* 2008), an association with ADAM33 might be important during this process. Using MRC-5 cells, a human embryonic lung cell line, and a Flexcell™ machine preliminary data have shown that 8% mechanical stretch for 24 and 48 hours significantly induced ADAM33 as well as αSMA mRNA and protein (unpublished data). This strengthens the case for a role of mechanical stress on ADAM33 and subsequently smooth muscle formation and differentiation in the embryonic and postnatal stages of lung development. It would have been important to confirm the mRNA data with protein data in the series of mouse tissue that was fixed in paraformaldehyde and embedded in GMA, however, at the time no working anti-mouse ADAM33 antibody has been available. Future western blotting and immunohistochemistry of lungs from each developmental time point can be done with new antibodies that might become available.

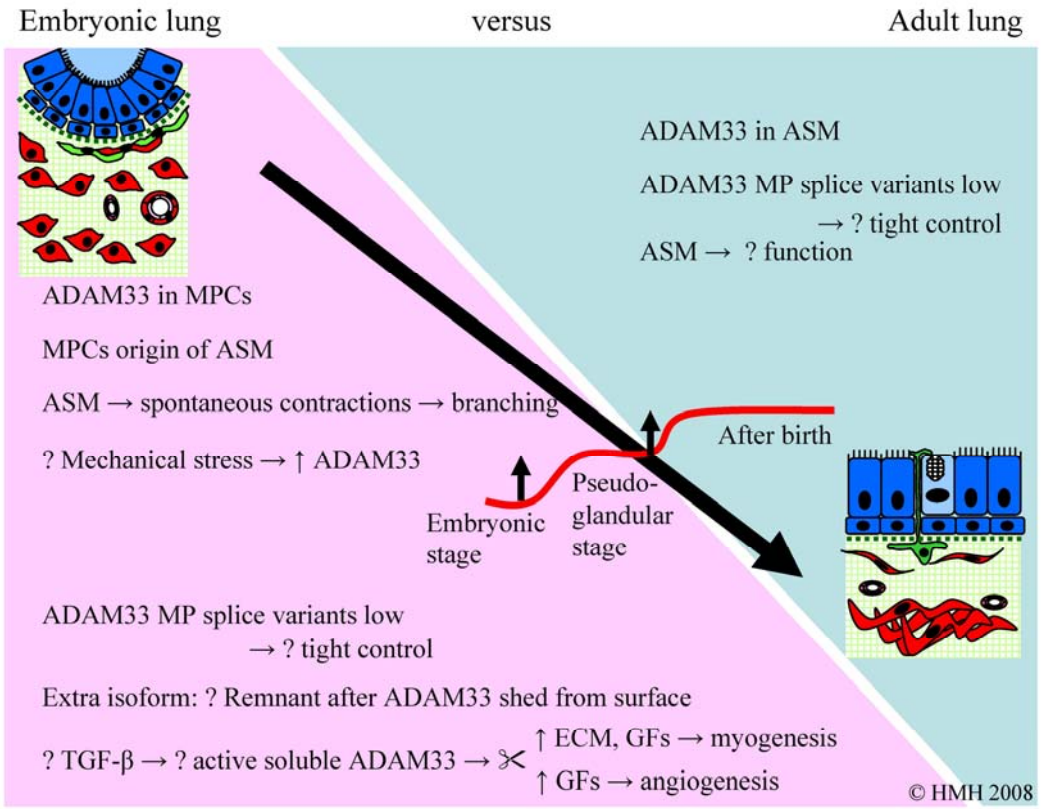

Figure 6.1 Findings and implications in normal embryonic and adult lung.

6.3 Strength and weaknesses in relation to other studies

Often understanding the physiological role of a gene comes from understanding and studying the role of the gene in pathophysiology of disease. Most of our understanding about the role of ADAM33 in pathology comes from genetic studies that have shown association with asthma and BHR, loss of lung function in asthma and COPD. (Van Eerdewegh *et al.* 2002; Jongepier *et al.* 2004; van Diemen *et al.* 2005a; Gosman *et al.* 2007).

Many of the SNPs that showed significant association were located in the intronic regions and 3' end of the gene (Van Eerdewegh *et al.* 2002) which could have an effect on alternative splicing of ADAM33 mRNA. The finding of multiple different ADAM33 splice variants expressed in adult bronchial biopsies from normal and asthmatic subjects (chapter 3) (Haitchi *et al.* 2005b) was very similar to the profile found in adult bronchial fibroblast (Powell *et al.* 2004).

Of great interest was the fact that the variants containing the MP domain, one of the most promising functional domains of ADAM33 as it possesses catalytic activity, were very lowly expressed suggesting tight regulation. However, there was no significant difference of any of the splice variants found between mild-moderate and severe asthmatic and normal subjects. This was also the case when the data were analysed relative to αSMA to normalise for the amount of smooth muscle present in each biopsy. Also no differences in disease specific ADAM33 protein staining in bronchial biopsies in the group with mild-moderate asthma could be detected.

This contrasts with a recent finding of asthma-specific increase of ADAM33 mRNA and protein expression in bronchial biopsies and in particular in epithelial cells from severe asthmatic subjects (Ito *et al.* 2007) (Foley *et al.* 2007). The reported increase of ADAM33 mRNA expression in asthmatic bronchial biopsies could be explained by the fact that the investigators failed to take into account differences in smooth muscle content of their biopsies. Alternatively there might be a difference between the UK and the Canadian population due to an unknown difference in environmental influences. Although no significant difference in ADAM33 mRNA expression in biopsies from severe asthmatic patients in the UK population could be shown, immunohistochemistry needs to be performed on biopsies from severe UK asthmatics to confirm the Canadian findings.

Furthermore, the controversial finding of ADAM33 expression in epithelial cells could be explained by misinterpretation of Sybr green based assays (reports without meltcurve as discussed in chapter 3) and non-specific staining of cytokeratin in epithelial cells using the polyclonal rabbit antibody against the cytoplasmic domain of ADAM33 (see chapter 3). In the present study, no ADAM33 expression was detected in bronchial brushings, comprising 95% bronchial epithelial cells. This is likely to be the result of epigenetic control

mechanisms that suppress ADAM33 expression in epithelial cells, as recently shown by Yang et al (Yang *et al.* 2008).

The conclusion that simple up or down-regulation of ADAM33 cannot explain its role in disease was not surprising as no functional asthma-associated polymorphisms have yet been reported in the promoter region of the gene. However gene polymorphisms might rather be involved in changes of protein function or release of a soluble active form of ADAM33 in disease.

The recent report from a Korean group of a significant increase of a 50kDa soluble form of ADAM33 containing the catalytically active domain in bronchoalveolar lavage fluid (BALF) from asthmatic subjects and its inverse correlation with disease severity and lung function (FEV_1% predicted) was an important finding (Lee *et al.* 2006). However, ADAM33 was detected by dot blotting of BALF with a polyclonal antibody against the catalytic domain of ADAM33 which specificity for ADAM33 needs to be confirmed by mass spectroscopy. Further Western blotting or ELISA studies using antibodies against the catalytic domain of ADAM33 on BALF from asthmatic compared with normal subject are necessary and positive findings need to be confirmed by mass spectroscopy to confirm the findings of the Korean group. It has further been suggested that release or shedding of a soluble form of ADAM33 results in a gain of function in disease, resulting from its detachment from membrane anchorage (Puxeddu *et al.* 2008). This would allow the uncontrolled accumulation of the active protein in the airways and its 'sheddase' activity might activate membrane or matrix bound growth factors and cytokines involved in airway remodelling (Figure 6.2). This would also explain why the ADAM33 knock-out mouse model revealed no functional clues in normal growth and development but also in a disease model (Chen *et al.* 2006), such that loss of function might not be responsible for disease pathogenesis.

Two possible mechanisms for the generation of sADAM33 can be considered. Firstly, the loss of 37 bases in 5'end of exon R might result in a frame shift and give rise to a protein lacking the TM domain, hence a putative secreted isoform (Powell *et al.* 2004). However, as the putative soluble form is expressed at a very low level in bronchial biopsies (see chapter 3), it seems unlikely that this could give rise to the secreted from of the molecule. Alternatively it has recently been demonstrated that sADAM33 is shed from cells expressing full length ADAM33 and its shedding is increased by TGF-β. This may play a pathophysiological role in disease.

Recent public data mining has revealed extended linkage disequilibrium in and around the ADAM33 gene on chromosome 20p13 with a peak recombinatory rate at exon S-V (Wjst 2007), where most of the statistically significant gene variations were initially reported (Van Eerdewegh *et al.* 2002). Some of these SNPs result in amino acid changes in the transmembrane domain and the cytoplasmic tail to effect co-localisation with other

membrane bound proteins or cell signalling. It is suggested that the cytoplasmic tail of ADAM33 protein mediates dimerisation of ADAM33 with itself or another protease such as MT1-MMP (MMP14) (G Murphy, Cambridge, personal communication). Since the expression of TGF-β is markedly increased in asthma (Redington *et al.* 1997) this might induce membrane-based proteases that cleave membrane-associated ADAM33 from the cell surface. Using both in vitro and in vivo models of angiogenesis, the presence of sADAM33 has recently been shown to promote new microvessel formation (Puxeddu *et al.* 2008). This angiogenic property of sADAM33 is consistent with the increased vascularity observed in asthmatic airways and its correlation with disease severity (Orsida *et al.* 1999). (Barbato *et al.* 2006). Angiogenesis is fundamental for supporting both airway inflammation and remodelling (Jackson *et al.* 1997) in particular new vessels can supply nutrients and oxygen to the inflamed tissue, facilitating proliferation of smooth muscle cells, fibroblasts and myofibroblasts. To further study this effect in vivo it will be important to generate a conditional transgenic mouse expressing the human soluble (active and mutant) form of ADAM33. This important model will enable studying the role of sADAM33 in vivo during different stages of lung development and under different environmental influences.

ADAM33 polymorphism F+1 (intronic region in MP domain) has been association with impaired lung function in 3 and 5 years old and S1, ST+5 and V4 (exons and introns in the region of the transmembrane domain and the 3;UTR) in 5 year old children (Simpson *et al.* 2005a). Of particular interest is that one SNP is located close to the MP domain and other SNPs are located in or close to the transmembrane domain and although no direct functional consequences of these are known , the associations suggest a role of ADAM33 in the early life origin of disease.

Mechanical stretch is normal in embryonic and early postnatal lung development and could stimulate a physiological increase of ADAM33 during these early time points. However, in asthma, polymorphisms of ADAM33 might result in abnormal release of ADAM33 to cause abnormal airway smooth muscle, mechanical stress, further ADAM33 induction and increase in smooth muscle (Figure 6.2). This cycle resulting in airway remodelling could already be triggered by intrauterine environmental influences operating during pregnancy (Figure 6.2). It is known that the environment plays an important role in interacting with susceptibility genes such as ADAM33 and maternal asthma is a risk factor for development of BHR and asthma in children. Therefore, it is important to study gene expression in the context of environment (Saglani and Bush 2007). While this is a difficult task to be undertaken in humans, a mouse model (A/J mice) that also exhibits ADAM33 as a susceptibility gene for BHR was chosen to study the effect of a maternal allergic environment on their offspring (De Sanctis *et al.* 1995). When ADAM33 expression was studied in the offspring from

allergic mouse mothers it showed a significant suppression of ADAM33 in the newborn offspring similar to results found in the HEL in the presence of IL-13 suggesting an environment-gene interaction. When lung function was tested in offspring at 4 weeks, a significant increase in BHR to methacholine was shown in response to inhaled ovalbumin challenge of sensitised mothers. Although this is an important and exciting finding it would have been helpful to have a control group without the *BHR1* locus such as Balb/c mice. Other studies of offspring from allergic Balb/c mouse mothers have also shown maternal influences, however, only after the offspring were suboptimal sensitised and challenged with ovalbumin (Hamada *et al.* 2003; Fedulov *et al.* 2007). These studies suggested that transfer of Th2-type mediators (e.g. cytokines, chemokines or autacoids) from the mother to the offspring causes increased susceptibility to the development of the allergic phenotype resulting in lung inflammation and BHR in early life. In contrast to the Balb/c model, the A/J murine model described in this thesis included a known ADAM33 genetic influence linked to BHR. These experiments revealed that an allergic environment in the pregnant mother has a deleterious effect on lung function in the offspring even without suboptimal ovalbumin sensitisation or antigen challenge of the offspring. A possible explanation is that maternal mediators (such as IL-13) are transferred to the offspring and interact with structural cells in the developing lung in the presence of genetic predisposition (Williams *et al.* 2000) (Figure 6.2). As discussed above IL-13 might have an effect on TGF-β and cause suppression of ADAM33 which results in delayed or abnormal embryonic lung development in the absence of inflammation in early life. This could initially trigger wheezing that is followed by asthma in later life in susceptible individuals (Figure 6.2). The delayed expression of ADAM33 in postnatal mice might be a marker of delayed development caused by intrauterine exposure to IL-13 and TGF-β, acting as negative regulators. In support of these findings is the observation that inflammation and remodelling in form of eosinophils and reticular basement membrane thickening seems to be absent in wheezing infants (Saglani *et al.* 2005) but can be found in older children (Cokugras *et al.* 2001; Payne *et al.* 2003; Payne *et al.* 2004; Pohunek *et al.* 2005; de Blic *et al.* 2005; Fedorov *et al.* 2005; Barbato *et al.* 2006) (Saglani *et al.* 2007). Most of these studies used bronchial biopsies and looked at basement membrane thickening as a marker for remodelling. However, functional or structural changes in mesenchymal cells such as smooth muscle and myofibroblasts were not studied although it has recently been shown that biopsies from children with wheeze/asthma are safe (Regamey *et al.* 2008a) and have the highest percentage of muscle (Regamey *et al.* 2007) which is increased in children with asthma (Regamey *et al.* 2008b). Therefore, smooth muscle content should be studied in biopsies from wheezing infants to confirm the absence of remodelling in this early stage of life together with IHC for ADAM33 in infants from allergic or asthmatic mothers. IHC studies of lungs from A/J mouse offspring need also to be done and analysed

for morphological differences in inflammatory cell content and structural changes of the airways in order to explore a potential influence of inflammation or remodelling on BHR in the offspring from ovalbumin challenged mothers.

As smoking during pregnancy is one of the strongest environmental risk factors for developing asthma (Dezateux *et al.* 1999; Dezateux *et al.* 2001; London *et al.* 2001) through its effects on lung morphogenesis and altered mesenchymal function (Sekhon *et al.* 1999; Sekhon *et al.* 2002), it will also be important to study the effect of maternal smoking on ADAM33 and lung function in their offspring by comparing genetic susceptible mice (A/J) with non-susceptible mice (Balb/c). Only recently it has been reported that another important environmental factor, namely air pollution in the form of exposure to diesel derived particles or residual oil fly ash during pregnancy can cause increase susceptibility to allergy in offspring (Fedulov *et al.* 2008; Hamada *et al.* 2007). The effect of ambient air pollution particles on ADAM33 in susceptible mice is not known, making it another very interesting study to be done.

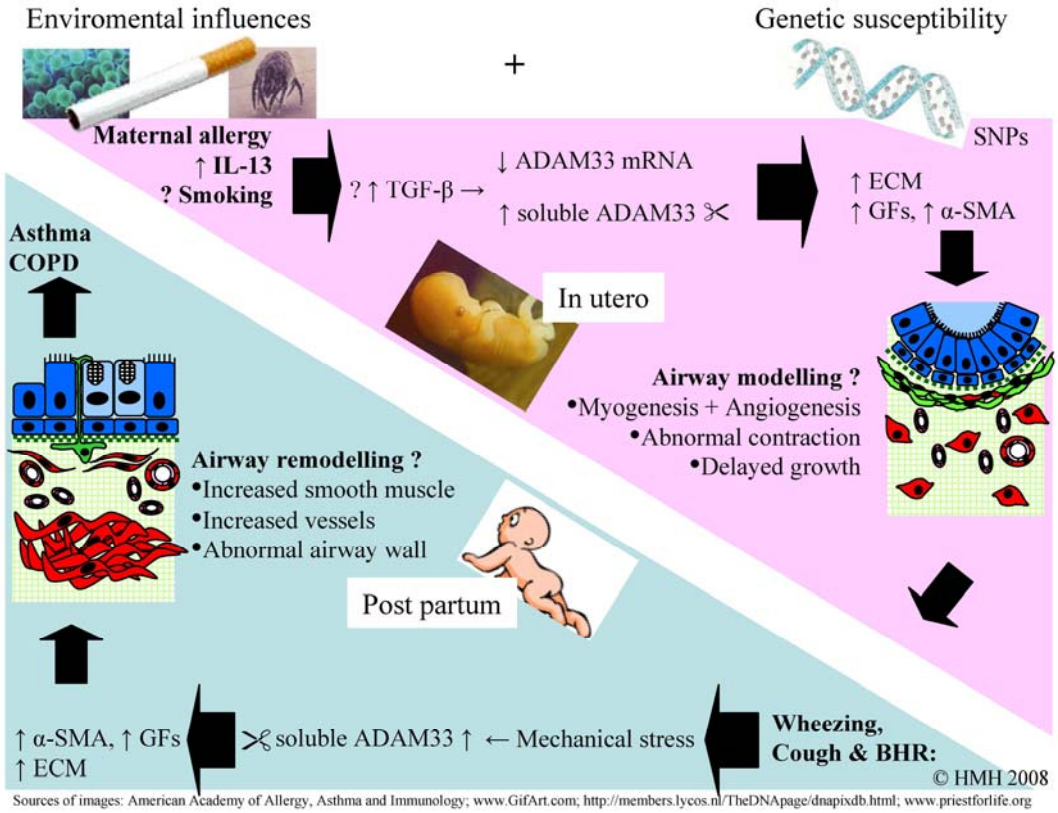

Figure 6.2 Environment-Genetic interaction in early origin of asthma.

6.4 Meaning of the study, unanswered questions and future research

The asthma susceptibility gene *ADAM33* is strongly associated with asthma and in particular BHR. This study showed for the first time that ADAM33 protein is expressed in both differentiated and undifferentiated embryonic mesenchymal cells in human embryonic lungs whereas in human adult bronchial biopsies it is mainly found in smooth muscle cells. The study further showed that although there seems to be some non-specific staining of epithelial cells that no ADAM33 mRNA could be detected in bronchial epithelial cells. It has recently been shown that CpG islands in the promoter region of ADAM33 are methylated in epithelial cells, hence suppressing ADAM33 expression (Yang *et al.* 2008). The prominence of ADAM33 in mesenchymal cells and particular smooth muscle cells suggests a role in the phenotype of BHR. However, it is still not clear what the exact function of ADAM33 is in embryonic lung development and later in adult life.

ADAM33 is strongly expressed in MPCs in the embryonic lung which suggests that it might play a role in differentiation of the MPCs in particular into smooth muscle cells. Further studies in embryonic and fetal lungs from later stages of gestation (MRC tissue bank) might reveal some clues how the expression of ADAM33 protein changes during human lung development and maturation.

This study also led to the development of a HEL explant culture model which allows in vitro studies of human lung development. ADAM33 mRNA increase in culture over18 days. In the presence of IL-13 ADAM33 mRNA was suppressed in the presence of IL-13 at day 18 but it needs to be further studied if IL-13 induces the release of soluble ADAM33 (sADAM33) via induction of TGFβ and if this can be influenced if ADAM33 is knocked down in HEL tissue using siRNA. Furthermore, it was recently reported that increased vessel formation occurred when HEL were cultured in the presence of recombinant ADAM33 containing the catalytic domain (Puxeddu *et al.* 2008). Similar experiments need to be repeated to show if ADAM33 has also a pro-myogenic effect in this explant culture system. This would allow speculating that genetically susceptible subjects (functional important SNPs still unknown) might produce increased soluble form of ADAM33 during embryonic lung development triggered by environmental factors such as maternal allergy, cigarette smoke, pollution or diet. This could lead to abnormal lung modelling before inflammation early in life in subjects susceptible to asthma and BHR.

A soluble form of ADAM33 seems to be increased in asthmatic patients (Lee *et al.* 2006) and sADAM33 has a pro-angiogenic function through its catalytic domain (Puxeddu *et al.* 2008), but the question where sADAM33 is derived from still needs to be answered. The most likely source is the airway myofibroblast and smooth muscle cell. These cells might shed increased sADAM33 from the cell surface in the presence of increased TGF-β.

sADAM33 is then released in the surrounding interstitial tissue where it can cleave extracellular matrix (ECM) and activate growth factors from the cell surface or from the ECM. These factors might have pro-angiogenic and potentially also pro-myogenic function. Further research needs to aim to confirm the presence of sADAM33 in BALF using newly developed and specific monoclonal antibodies to the extracellular domain and in particular to the catalytic domain of ADAM33. These antibodies could be used for immunoprecipitation with subsequent mass spectroscopy to confirm the specificity of the antibodies. Furthermore reliable ELISA kits could be developed to test clinical samples from children and adult asthmatic and control subjects for sADAM33 protein.

When ADAM33 mRNA was studied during all stages of lung developmental in the mouse two significant increases of ADAM33 were observed, one in the pseudoglandular phase and the other after birth. Both time-points are associated with mechanical stretch which can be seen in form of spontaneous contraction of the primitive airways in the pseudoglandular stage and the obvious increased breathing movements after birth. Further studies need to confirm that mechanical stretch is the cause for this induction of ADAM33 using MPCs cultures in a stretch machine. Alternatively or additionally, the biggest increase of ADAM33 after birth might also be influenced by the change form a hypoxic to normoxic environment. Further studies using MPCs cultures under hypoxic conditions that are brought to normoxic conditions are needed.

The maternal allergen exposure study of BHR genetically susceptible mice (A/J mouse, *BHR* locus close to ADAM33) was developed in collaboration with David Bassett from Detroit in the US. This revealed that newborn offspring from allergic mothers had a significant decrease in ADAM33 mRNA expression which confirmed the findings in HEL explant culture experiments in an allergic (IL-13) environment. The mechanism how maternal allergy affects the lungs of their offspring needs to be further studied in particular by using Balb/c mice as control group that are not susceptible to BHR. It would also be important to study in particular sADAM33 in BALF from the offspring from these two different mouse strains using specific antibodies against mouse ADAM33.
Furthermore, tests for airway hyperresponsiveness to methacholine showed a significant increase in responsiveness in 4 week old offspring from allergic mothers compared with non-allergic mothers. This suggests an environmental interaction in form of maternal allergy on offspring that are susceptible to BHR. As these changes were demonstrated initially by Penh measurements these findings need to be confirmed by experiments using invasive lung function studies, which might be a challenge especially in such young animals. Other

environmental factor such as maternal smoking, diet and pollution and their effect on offspring need to be studied in this model.
The construction of an conditional mouse that over-expresses human sADAM33 (catalytically active and mutant form) would be the ultimate research tool to study the influence of gain of function (increased sADAM33) on modelling (vasculogenesis and myogenesis) in fetal/embryonic mouse lungs. This model would also allow studying the effect of maternal allergy or cigarette smoke as in the model described above, which would allow further study of environmental interactions with ADAM33.

The influence of the Th2 cytokine IL-13 and maternal allergy on ADAM33 expression in human and mouse embryonic lungs suggest an important interaction of allergic inflammation and airway wall remodelling early in life predisposing to the development of asthma later in life. To discover disease-specific SNPs it will be important to design large scale longitudinal international studies following lung functions of newborn into adult life and studying association of polymorphisms in ADAM33 in children that become wheezers, persistent wheezers and develop asthma in later life. This needs to be correlated to the parental genetic background and environmental influences during and after pregnancy, such as maternal allergy, smoking, pollution and diet.

It has been a long and difficult road since the first discovery of ADAM33 as an asthma susceptibility gene in 2002, but studies of ADAM33 and its role in asthma and BHR have reached an exciting point of time. The current knowledge and available research tools will enable the further dissection of the function of ADAM33 in health and particular in the early origins of disease. This might provide us with new diagnostic tools and treatment options that might help us to diagnose susceptible individuals early in life and help us to intervene in the early origin (pre- or postnatal) of asthma and prevent it becoming evident.

Appendices

Work presented or published related to thesis

Original papers

HM Haitchi, I Puxxedu, and DE Davies. ADAM33. Current BioData Ltd, UK. Targeted Protein Database (TPDB) 2008 in press.

Y Yang, **HM Haitchi**, J Cakebread, D Sammut, JW Holloway, P Howarth, ST Holgate, DE Davies. Epigenetic mechanisms silence ADAM33 expression in bronchial epithelial cells. J Allergy Clin Immunol. 2008 Jun;121(6):1393-9.

I Puxeddu, YY Pang, A Harvey, **HM Haitchi**, B Nicholas, H Yoshisue, D Ribatti, G Clough, RM Powell, G Murphy, N Hanley, DI Wilson, PH Howarth, ST Holgate & DE Davies. The soluble form of ADAM33 promotes angiogenesis: implications for airway remodelling in asthma. J Allergy Clin Immunol. 2008 Jun;121(6):1400-6.

J Wicks, **HM Haitchi**, DE Davies, ST Holgate, RM Powell. Enhanced upregulation of smooth muscle-related transcripts by TGFbeta in asthmatic (Myo)fibroblasts. Thorax. 2006 Apr;61(4):313-9.

HM Haitchi, RM Powell, TJ Shaw, PH Howarth, S Wilson, DI Wilson, ST Holgate, DE Davies. ADAM33 expression in asthmatic airways and human embryonic lungs. Am J Respir Crit Care Med. 2005 May 1;171(9):958-65.

Reviews

ST Holgate, DE Davies, RM Powell, PH Howarth, **HM Haitchi,** JW Holloway. Locally Acting Genetic and Environmental Factors in Asthma Pathogenesis: A new approach. Eur Respir J. 2007 Apr;29(4):793-803.

ST Holgate, Y Yang, **HM Haitchi,** RM Powell, JW Holloway, H Yoshisue, YY Pang, J Cakebread, DE Davies. The Genetics of Asthma: ADAM33 as an Example of a Susceptibility Gene. Proc Am Thorac Soc. 2006 Jul;3(5):440-3.

ST Holgate, JW Holloway, PH Howarth, S Wilson, **HM Haitchi,** S.Babu, DE Davies, Understanding the pathophysiology of severe asthma to generate new therapeutic opportunities. J Allergy Clin Immunol. 2006 Mar;117(3):496-506.

JW Holloway, TP Keith, DE Davies, RM Powell, **HM Haitchi**, ST Holgate. The discovery and role of ADAM33, a new candidate gene for asthma. Expert Reviews in Molecular Medicine 2004, 6:1-12.

JA Cakebread, **HM Haitchi**, JW Holloway, RM Powell, T Keith, DE Davies, ST Holgate. The role of ADAM33 in the pathogenesis of asthma. Springer Semin Immun (2004)25:361-375.

Abstracts

HM Haitchi, Yang, Y., Sammut, D., Powell RM., Howarth, PH., Holgate, ST., and Davies, DE. ADAM33 expression in bronchial biopsies and epithelial cells in severe asthma. Accepted for oral presentation at ATS May 2008 in Toronto, Canada.

HM Haitchi, Y Yang, J Cakebread, D Sammut, A Harvey, RM Powell, JW Holloway, PH Howarth, ST Holgate, DE Davies. Epigenetic mechanisms silence ADAM33 expression in bronchial epithelial cells. Young investigator price oral presentation at MRS Clinician Scientist in training meeting in Royal College of Physicians, London, 28 February 2008.

HM Haitchi, DJ P Bassett, X Gao, ST Holgate and DE Davies. ADAM33 in lung development and the effect of maternal allergy. Thorax 62[Supplement 3], A37, S90, 2007. Oral presentation at BTS winter meeting December 2007.

HM Haitchi, Yang, Y., Cakebread, J., Sammut, D., Harvey, A., Holloway, J. W., Howarth, P. H., Holgate, S. T., and Davies, D. E. Epigenetic Mechanisms silence ADAM33 Expression in Bronchial Epithelial cells. Thorax 62[Supplement 3], A115, P141, 2007. Poster presentation at BTS winter meeting December 2007.

HM Haitchi, DJ P Bassett, X Gao, ST Holgate and DE Davies. ADAM33 in developing lungs and the effect of maternal allergen sensitization. Am J Respir Crit Care Med 2007, Vol 175:A580, Poster discussion at ATS 2007 in San Francisco, USA.

HM Haitchi, RM Powell, ST Holgate, DE Davies. Stepwise incremental changes in ADAM33 expression during mouse lung development. Thorax 2006 Dec;61(Supplement II):ii44. Oral presentation at the BTS winter meeting, December 2006.

HM Haitchi, RM Powell, ST Holgate, DE Davies. Incremental changes in ADAM33 expression in mouse lung development. ERJ 2006 Sept; 28, Suppl 50:552s. Poster discussion at the European Respiratory Society Congress in Munich, Germany, September 2006.

HM Haitchi, F Bucchieri, A Ribbene, RM Powell, NA Hanley, DI Wilson, ST Holgate, DE Davies. ADAM33, alpha smooth muscle actin and collagen expression in human embryonic lung in vivo and in culture. Proc Am Thorac Soc., 2006, Vol.3, A675. Poster presentation at the International Conference of the ATS in San Diego, US, May 2006.

HM Haitchi, Y Yang, YY Pang, RM Powell, DE Davies, ST Holgate. Functional characterisation of the asthma gene, A Disintegrin and Metalloprotease (ADAM)33. Oral presentation at the Association of Physicians of Great Britain and Ireland 100th Anniversary annual meeting April 2006 in London, Quarterly Journal of Medicine, 2006.

HM Haitchi, F Bucchieri, RM Powell, NA Hanley, DI Wilson, ST Holgate, DE Davies. ADAM33 in Embryonic Airways. Thorax, 2005, Vol 60, Supplement II, S58.

HM Haitchi, RM Powel, TJ Shaw, PH Howarth, SJ Wilson, DI Wilson, ST Holgate, DE Davies. Localisation of ADAM33 to bronchial smooth muscle in asthmatic airways and human embryonic lungs. Thorax, 2005, Vol 60, Supplement II, S130.

HM Haitchi, F Bucchieri, RM Powell, NA Hanley, DI Wilson, ST Holgate, DE Davies. ADAM33 in Embryonic Airways. Eur Respir J, 2005, 22 (Suppl 45): 222s

HM Haitchi, RM Powel, TJ Shaw, PH Howarth, SJ Wilson, DI Wilson, ST Holgate, DE Davies. Localisation of ADAM33 to bronchial smooth muscle in asthmatic airways and human embryonic lungs. Proceedings of the American Thoracic Society, 2005, Vol.2, A506.

HM Haitchi. The Expression of ADAM33, an Asthma Susceptibility Gene, in Asthma and Embryonic Lung Development. Oral presentation at University of Southampton Faculty Postgraduate Conference 2005.

HM Haitchi, RM Powel, TJ Shaw, PH Howarth, SJ Wilson, DI Wilson, ST Holgate, DE Davies. A Disintegrin And Metalloprotease (ADAM)33 is localised to bronchial smooth muscle in asthmatic airways and human embryonic lungs. Abstract presented as poster at Medical Research Society Meeting; Medical Research Society Communications 28th Feb 2005:18P, A36.

HM Haitchi, RM Powell, TJ Shaw, PH Howarth, SJ Wilson, DI Wilson ST Holgate, DE Davies. A Disintegrin And Metalloprotease (ADAM) 33 is localised to bronchial smooth muscle in asthmatic airways and human embryonic lungs. Clinical Scientist in Training Meeting at Royal College of Physicians, London 28.02.2005.

HM Haitchi, RM Powell, TJ Shaw, SK Babu, PH Howarth, ST Holgate, DE Davies. Analysis of Alternatively Spliced Variants of ADAM33 in Bronchial Biopsies from Normal and Asthmatic subjects. Am J Respir Crit Care Med 2004, 169(7):A471.

HM Haitchi, RM Powell, ST Holgate, DE Davies. The Influence of Th2 Cytokines on ADAM33 and Alpha Smooth Muscle Actin (ASMA) Expression in Embryonic Mouse Lung Explant Cultures. Am J Respir Crit Care Med 2004, 169(7):A561.

HM Haitchi, RM Powell, TJ Shaw, SK Babu, PH Howarth, ST Holgate, DE Davies. Expression of ADAM33 splice variants in bronchial biopsies from normal and asthmatic subjects. Eur Respir J, 2003, 22 (Suppl 45): 222s

HM Haitchi, RM Powell, DI Wilson, ST Holgate, DE Davies. ADAM33 Expression in Embryonic Mouse Lung. Am J Respir Crit Care Med, 2003,167(7):A377.

HM Haitchi, RM.Powell, D I.Wilson, ST.Holgate, DE.Davies. ADAM 33 Expression in Embryonic Mouse Lung. Poster presentation at University of Southampton Faculty Postgraduate Conference 2003.

Work presented or published not related to thesis

Original papers

HM Haitchi, H Yoshisue, A Ribbene, SJ Wilson, JW Holloway, NA Hanley, DI Wilson, ST Holgate[1], DE Davies, Chronological expression of Ciliated Bronchial Epithelium 1 during pulmonary differentiation in vivo and in vitro. Manuscript in preparation for submission 2008.

C. Xiao, S. Field, I. Puxeddu, **HM Haitchi**, E. Vernon-Wilson, D. Sammut, N. Bedke, C. Cremin, J. Jones, R. Djukanovic, P. Howarth, S.T. Holgate, P. Monk, S.M. Puddicombe, D.E. Davies, Defective Epithelial Barrier Function in Asthma and its Improvement using and Epithelial-Selective EGF Analogue. Manuscript submitted to Am J Respir Crit Care Med. 2008.

H Yoshisue, SM Puddicombe, SJ Wilson, **HM Haitchi**, RM Powell, DI Wilson, A Pandit, AE Berger, DE Davies, ST Holgate, JW Holloway. Characterization of CBE1, a ciliated cell-specific gene that is induce during mucocillia differentiation of bronchial epithelial cell. Am J Respir Cell Mol Biol. 2004 Nov;31(5):491-500.

H Donninger, R Glashoff, **HM Haitchi**, JA Syce, R Ghildyal, E van Rensburg, and PG Bardin . Rhinovirus induction of the CXC Chemokine ENA-78 in Bronchial Epithelium. J Infect Dis, 2003:187:1809-1817.

Reviews

HM Haitchi, ST Holgate. New strategies in treatment and prevention of allergic diseases. Expert Opin Investigational Drugs (2004)13(2)107-124.

Abstracts

HM Haitchi, H Yoshisue, RM Powell, F. Bucchieri, NA Hanley, DI Wilson, ST Holgate and DE Davies. Chronological expression of Ciliated Bronchial Epithelim (CBE) 1 in mouse and human pulmonary differentiation. Am J Respir Crit Care Med 2007, Vol 175:A582, Poster discussion at ATS 2007 in San Francisco, USA.

HM Haitchi, H Yoshisue, RM Powell, F Bucchieri, NA Hanley, DI Wilson, ST Holgate and DE Davies Chronological expression of Ciliated Bronchial Epithelim (CBE) 1 in mouse and human pulmonary differentiation. Thorax 2006 Dec;61(Supplement II):ii44. Oral presentation at the BTS winter meeting, December 2006.

HM Haitchi, H Yoshisue, RM Powell, F Bucchieri, NA Hanley, DI Wilson, ST Holgate and DE Davies The temporal expression of Ciliated Bronchial Epithelium (CBE) 1 in embryonic lungs. ERJ 2006 Sept; 28, Suppl 50:557s. Oral presentation at the European Respiratory Society Congress 2006 in Munich, Germany.

HM Haitchi. IL-13 has no effect on MUC5AC expression in human embryonic lung explants - a role for IL-13Rα2? Poster presentation at University of Southampton Faculty Postgraduate Conference 2006

HM Haitchi, F Bucchieri, RM Powell, NA Hanley, DI Wilson, ST Holgate, DE Davies. IL-13 has no effect on MUC5AC expression in human embryonic lung explants – a role for IL-13Rα2? Proc Am Thorac Soc., 2006, Vol.3, A34. Poster discussion at the International Conference of the ATS in San Diego, US, May 2006.

Book/book chapter

HM Haitchi, MT Krishna, JH Holloway, G Dent, MG Buckley, ST Holgate. Chapter: "Asthma: Clinical Aspects and Mucosal Immunology." In Mucosal Immunology, Third Edition, edited by Jiri Mestecky, John Bienenstock, Michael E. Lamm, Llyod Mayer, Jerry R. McGhee, and Warren Strober. Elsevier Academic Press; 3rd edition, Volume 2, Chapter 82: 1416-1432, 2005, ISBN 0-12-491543-4.

Bibliography

List of publications referred to in this thesis

Aberg N (1993) Familial occurrence of atopic disease: genetic versus environmental factors. *Clin.Exp.Allergy* **23,** 829-834.

Ahmadi KR, Goldstein DB (2002) Multifactorial Diseases: Asthma Genetics Point the Way. *Current Biology* **12,** R702-R704.

Airenne KJ, Hiltunen MO, Turunen MP, Turunen AM, Laitinen OH, Kulomaa MS, Yla-Herttuala S (2000) Baculovirus-mediated periadventitial gene transfer to rabbit carotid artery. *Gene Ther.* **7,** 1499-1504.

Aliotta JM, Passero M, Meharg J, Klinger J, Dooner MS, Pimentel J, Quesenberry PJ (2005) Stem cells and pulmonary metamorphosis: New concepts in repair and regeneration. *J Cell Physiol* **204,** 725-741.

Allen M, Heinzmann A, Noguchi E, Abecasis G, Broxholme J, Ponting CP, Bhattacharyya S, Tinsley J, Zhang Y, Holt R, Jones EY, Lench N, Carey A, Jones H, Dickens NJ, Dimon C, Nicholls R, Baker C, Xue L, Townsend E, Kabesch M, Weiland SK, Carr D, von Mutius E, Adcock IM, Barnes PJ, Lathrop GM, Edwards M, Moffatt MF, Cookson WOCM (2003) Positional cloning of a novel gene influencing asthma from Chromosome 2q14. *Nat Genet* **35,** 258-263.

Amrani Y, Panettieri RA (2003) Airway smooth muscle: contraction and beyond. *The International Journal of Biochemistry & Cell Biology* **35,** 272-276.

An SS, Bai TR, Bates JH, Black JL, Brown RH, Brusasco V, Chitano P, Deng L, Dowell M, Eidelman DH, Fabry B, Fairbank NJ, Ford LE, Fredberg JJ, Gerthoffer WT, Gilbert SH, Gosens R, Gunst SJ, Halayko AJ, Ingram RH, Irvin CG, James AL, Janssen LJ, King GG, Knight DA, Lauzon AM, Lakser OJ, Ludwig MS, Lutchen KR, Maksym GN, Martin JG, Mauad T, McParland BE, Mijailovich SM, Mitchell HW, Mitchell RW, Mitzner W, Murphy TM, Pare PD, Pellegrino R, Sanderson MJ, Schellenberg RR, Seow CY, Silveira PS, Smith PG, Solway J, Stephens NL, Sterk PJ, Stewart AG, Tang DD, Tepper RS, Tran T, Wang L (2007) Airway smooth muscle dynamics: a common pathway of airway obstruction in asthma. *Eur Respir J* **29,** 834-860.

An SS, Fredberg JJ (2007) Biophysical basis for airway hyperresponsiveness. *Can.J Physiol Pharmacol.* **85,** 700-714.

Aravin AA, Hannon GJ, Brennecke J (2007) The Piwi-piRNA Pathway Provides an Adaptive Defense in the Transposon Arms Race. *Science* **318,** 761-764.

Arshad SH, Kurukulaaratchy RJ, Fenn M, Matthews S (2005) Early life risk factors for current wheeze, asthma, and bronchial hyperresponsiveness at 10 years of age. *Chest* **127,** 502-508.

Asakura M, Kitakaze M, Takashima S, Liao Y, Ishikura F, Yoshinaka T, Ohmoto H, Node K, Yoshino K, Ishiguro H, Asanuma H, Sanada S, Matsumura Y, Takeda H, Beppu S, Tada M, Hori M, Higashiyama S (2002) Cardiac hypertrophy is inhibited by antagonism of ADAM12 processing of HB-EGF: metalloproteinase inhibitors as a new therapy. *Nat.Med.* **8,** 35-40.

Asthma UK (2004a) Living on a Knife Edge. *Report.* 1-24.

Asthma UK (2004b) Where Do We Stand? Asthma in the UK today. *Report.* 1-16.

Atherton HC, Jones G, Danahay H (2003) IL-13-induced changes in the goblet cell density of human bronchial epithelial cell cultures: MAP kinase and phosphatidylinositol 3-kinase regulation. *AJP - Lung Cellular and Molecular Physiology* **285,** L730-L739.

Bacharier LB, Boner A, Carlsen KH, Eigenmann PA, Frischer T, Gotz M, Helms PJ, Hunt J, Liu A, Papadopoulos N, Platts-Mills T, Pohunek P, Simons FE, Valovirta E, Wahn U, Wildhaber J (2008) Diagnosis and treatment of asthma in childhood: a PRACTALL consensus report. *Allergy* **63,** 5-34.

Badri KR, Zhou Y, Schuger L (2008) Embryological Origin of Airway Smooth Muscle. *Proceedings of the American Thoracic Society* **5,** 4-10.

Bai TR, Knight DA (2005) Structural changes in the airways in asthma: observations and consequences. *Clin.Sci.(Lond)* **108,** 463-477.

Barbato A, Turato G, Baraldo S, Bazzan E, Calabrese F, Panizzolo C, Zanin ME, Zuin R, Maestrelli P, Fabbri LM, Saetta M (2006) Epithelial Damage and Angiogenesis in the Airways of Children with Asthma. *American Journal of Respiratory and Critical Care Medicine* **174,** 975-981.

Bassett D, Elbon-Copp C, Otterbein S, Barraclough-Mitchell H, Delorme M, Yang H (2001) Inflammatory cell availability affects ozone-induced lung damage. *J Toxicol.Environ.Health A* **64,** 547-565.

Bates J, Irvin C, Brusasco V, Drazen J, Fredberg J, Loring S, Eidelman D, Ludwig M, Macklem P, Martin J, Milic-Emili J, Hantos Z, Hyatt R, Lai-Fook S, Leff A, Solway J, Lutchen K, Suki B, Mitzner W, Pare P, Pride N, Sly P (2004) The Use and Misuse of Penh in Animal Models of Lung Disease. *American Journal of Respiratory Cell and Molecular Biology* **31,** 373-374.

Bates JHT, IRVIN CG (2003) Measuring lung function in mice: the phenotyping uncertainty principle. *Journal of Applied Physiology* **94,** 1297-1306.

Beasley R, Roche WR, Roberts JA, Holgate ST (1989) Cellular events in the bronchi in mild asthma and after bronchial provocation. *Am Rev.Respir Dis* **139,** 806-817.

Beasley R (1998) Worldwide variation in prevalence of symptoms of asthma, allergic rhinoconjunctivitis, and atopic eczema: ISAAC. *The Lancet* **351,** 1225-1232.

Bentwich I, Avniel A, Karov Y, Aharonov R, Gilad S, Barad O, Barzilai A, Einat P, Einav U, Meiri E, Sharon E, Spector Y, Bentwich Z (2005) Identification of hundreds of conserved and nonconserved human microRNAs. *Nat Genet* **37,** 766-770.

Beqaj S, Jakkaraju S, Mattingly RR, Pan D, Schuger L (2002) High RhoA activity maintains the undifferentiated mesenchymal cell phenotype, whereas RhoA down-regulation by laminin-2 induces smooth muscle myogenesis. *The Journal of Cell Biology* **156,** 893-903.

Bernards R (2006) Exploring the Uses of RNAi -- Gene Knockdown and the Nobel Prize. *The New England Journal of Medicine* **355,** 2391-2393.

Berry MA, Hargadon B, Shelley M, Parker D, Shaw DE, Green RH, Bradding P, Brightling CE, Wardlaw AJ, Pavord ID (2006) Evidence of a Role of Tumor Necrosis Factor {alpha} in Refractory Asthma. *The New England Journal of Medicine* **354,** 697-708.

BIO-RAD. iCycler iQ™ Multi-Color Real-Time PCR Detection System: Operating Instructions. [170-8740]. 2001. BIO-RAD Laboratories, Hercules, CA, USA.

Bisgaard H, Hermansen MN, Loland L, Halkjaer LB, Buchvald F (2006) Intermittent Inhaled Corticosteroids in Infants with Episodic Wheezing. *The New England Journal of Medicine* **354,** 1998-2005.

Black JL, Johnson PR (2002) Factors controlling smooth muscle proliferation andairway remodelling. *Curr Opin Allergy Clin Immunol.* **2,** 47-51.

Black JL, Roth MI, Lee JI, Carlin ST, Johnson PRA (2001) Mechanisms of Airway Remodeling . Airway Smooth Muscle. *American Journal of Respiratory and Critical Care Medicine* **164,** 63S-666.

Black RA, Rauch CT, Kozlosky CJ, Peschon JJ, Slack JL, Wolfson MF, Castner BJ, Stocking KL, Reddy P, Srinivasan S, Nelson N, Boiani N, Schooley KA, Gerhart M, Davis R, Fitzner JN, Johnson RS, Paxton RJ, March CJ, Cerretti DP (1997) A metalloproteinase disintegrin that releases tumour-necrosis factor- alpha from cells. *Nature* **385,** 729-733.

Black RA, White JM (1998) ADAMs: focus on the protease domain. *Current Opinion in Cell Biology* **10,** 654-659.

Blakey J, Halapi E, Bjornsdottir US, Wheatley A, Kristinsson S, Upmanyu R, Stefansson K, Hakonarson H, Hall IP (2005) Contribution of ADAM33 polymorphisms to the population risk of asthma. *Thorax* **60,** 274-276.

Blobel CP (2000) Remarkable roles of proteolysis on and beyond the cell surface. *Curr Opin Cell Biol* **12,** 606-612.

Blobel CP (2005) ADAMs: key components in EGFR signalling and development. *Nat Rev Mol Cell Biol* **6,** 32-43.

Borger P, Tamm M, BLACK JL, Roth M (2006) Asthma: Is It Due to an Abnormal Airway Smooth Muscle Cell? *American Journal of Respiratory and Critical Care Medicine* **174,** 367-372.

Bourdin A, Neveu D, Vachier I, Paganin F, Godard P, Chanez P (2007) Specificity of basement membrane thickening in severe asthma. *Journal of Allergy and Clinical Immunology* **119,** 1367-1374.

Boyce FM, Bucher NL (1996) Baculovirus-mediated gene transfer into mammalian cells. *Proc Natl.Acad.Sci.U.S.A* **93,** 2348-2352.

Bradding P (2007) Mast cell regulation of airway smooth muscle function in asthma. *European Respiratory Journal* **29,** 827-830.

Bridges LC, Sheppard D, Bowditch RD (2005) ADAM disintegrin-like domain recognition by the lymphocyte integrins alpha4beta1 and alpha4beta7. *Biochemical Journal* **387,** 101-108.

Brightling CE, Bradding P, Symon FA, Holgate ST, Wardlaw AJ, Pavord ID (2002) Mast-cell infiltration of airway smooth muscle in asthma. *The New England Journal of Medicine* **346,** 1699-1705.

Brightling CE, Ammit AJ, Kaur D, BLACK JL, Wardlaw AJ, Hughes JM, Bradding P (2005) The CXCL10/CXCR3 Axis Mediates Human Lung Mast Cell Migration to Asthmatic

Airway Smooth Muscle. *American Journal of Respiratory and Critical Care Medicine* **171,** 1103-1108.

British Thoracic Society (BTS), Scottish Intercollegiate Guidelines Network (SIGN) (2007) 'British Guidelines on the Management of Asthma.' A national clinical guideline. Available from: http://www.brit-thoracic.org.uk/evidence_tables.html,

British Thoracic Society Bronchoscopy Guidelines Committee (2001) British Thoracic Society guidelines on diagnostic flexible bronchoscopy. *Thorax* **56 Suppl 1,** i1-21.

Britten KM, Howarth PH, Roche WR (1993) Immunohistochemistry on resin sections: a comparison of resin embedding techniques for small mucosal biopsies. *Biotech.Histochem.* **68,** 271-280.

Burgess JK, JOHNSON PRA, Ge Q, Au WW, Poniris MH, McParland BE, King G, Roth M, BLACK JL (2003) Expression of Connective Tissue Growth Factor in Asthmatic Airway Smooth Muscle Cells. *American Journal of Respiratory and Critical Care Medicine* **167,** 71-77.

Bush A (2008) How early do airway inflammation and remodeling occur? *Allergol.Int.* **57,** 11-19.

Busse W, Rosenwasser L (2003) Mechanisms of asthma. *J Allergy Clin Immunol* **111,** S799-S804.

Busse WW, Lemanske RF (2001) Asthma. *The New England Journal of Medicine* **344,** 350-362.

Buxbaum JD, Liu KN, Luo Y, Slack JL, Stocking KL, Peschon JJ, Johnson RS, Castner BJ, Cerretti DP, Black RA (1998) Evidence that tumor necrosis factor alpha converting enzyme is involved in regulated alpha-secretase cleavage of the Alzheimer amyloid protein precursor. *J Biol Chem.* **273,** 27765-27767.

Cardoso WV (2000) Lung morphogenesis revisited: old facts, current ideas. *Dev Dyn* **219,** 121-130.

Cardoso WV (2001) MOLECULAR REGULATION OF LUNG DEVELOPMENT. *Annual Review of Physiology* **63,** 471-494.

Cardoso WV, Lu J (2006) Regulation of early lung morphogenesis: questions, facts and controversies. *Development* **133,** 1611-1624.

Celedon JC, Litonjua AA, Ryan L, Platts-Mills T, Weiss ST, Gold DR (2002) Exposure to cat allergen, maternal history of asthma, and wheezing in first 5 years of life. *The Lancet* **360,** 781-782.

Celli G, LaRochelle WJ, Mackem S, Sharp R, Merlino G (1998) Soluble dominant-negative receptor uncovers essential roles for fibroblast growth factors in multi-organ induction and patterning. *Embo J* **17,** 1642-1655.

Cerretti DP, DuBose RF, Black RA, Nelson N (1999) Isolation of two novel metalloproteinase-disintegrin (ADAM) cDNAs that show testis-specific gene expression. *Biochem.Biophys.Res.Commun.* **263,** 810-815.

Chen C, Huang X, Sheppard D (2006) ADAM33 Is Not Essential for Growth and Development and Does Not Modulate Allergic Asthma in Mice. *Molecular and Cellular Biology* **26,** 6950-6956.

Cheng L, Enomoto T, Hirota T, Shimizu M, Takahashi N, Akahoshi M, Matsuda A, Dake Y, Doi S, Enomoto K, Yamasaki A, Fukuda S, Mao XQ, Hopkin JM, Tamari M, Shirakawa T (2004) Polymorphisms in ADAM33 are associated with allergic rhinitis due to Japanese cedar pollen. *Clinical Experimental Allergy* **34,** 1192-1201.

Chinoy MR (2003) Lung growth and development. *Front Biosci.* **8,** D392-D415.

Chomczynski and Piotr. Shelf-stable product and process for isolating RNA, DNA and proteins. 826984[5,346,994]. 13-9-1994. United States. 28-1-1992.

Cockcroft DW, Davis BE (2006) Mechanisms of airway hyperresponsiveness. *Journal of Allergy and Clinical Immunology* **118,** 551-559.

Cokugras H, Akcakaya N, Seckin, Camcioglu Y, Sarimurat N, Aksoy F (2001) Ultrastructural examination of bronchial biopsy specimens from children with moderate asthma. *Thorax* **56,** 25-29.

Condreay JP, Witherspoon SM, Clay WC, Kost TA (1999) Transient and stable gene expression in mammalian cells transduced with a recombinant baculovirus vector. *Proc Natl.Acad.Sci.U.S.A* **96,** 127-132.

Contoli M, Message SD, Laza-Stanca V, Edwards MR, Wark PAB, Bartlett NW, Kebadze T, Mallia P, Stanciu LA, Parker HL, Slater L, Lewis-Antes A, Kon OM, Holgate ST, Davies DE, Kotenko SV, Papi A, Johnston SL (2006) Role of deficient type III interferon-[lambda] production in asthma exacerbations. *Nat Med* **12,** 1023-1026.

Copenhaver CC, Gern JE, Li Z, Shult PA, Rosenthal LA, Mikus LD, Kirk CJ, Roberg KA, Anderson EL, Tisler CJ, DaSilva DF, Hiemke HJ, Gentile K, Gangnon RE, Lemanske RF, Jr. (2004) Cytokine response patterns, exposure to viruses, and respiratory infections in the first year of life. *Am J Respir Crit Care Med* **170,** 175-180.

Cossar D, Bell J, Strange R, Jones M, Sandison A, Hume R (1990) The alpha and pi isoenzymes of glutathione S-transferase in human fetal lung: in utero ontogeny compared with differentiation in lung organ culture. *Biochim.Biophys Acta* **1037,** 221-226.

Cox G, Thomson NC, Rubin AS, Niven RM, Corris PA, Siersted HC, Olivenstein R, Pavord ID, McCormack D, Chaudhuri R, Miller JD, Laviolette M, the AIR Trial Study Group (2007) Asthma Control during the Year after Bronchial Thermoplasty. *The New England Journal of Medicine* **356,** 1327-1337.

Dauger S, Durand E, Cohen G, Lagercrantz H, Changeux JP, Gaultier C, Gallego J (2004) Control of breathing in newborn mice lacking the beta-2 nAChR subunit. *Acta Physiol Scand.* **182,** 205-212.

Davies DE (2001) The bronchial epithelium: translating gene and environment interactions in asthma. *Curr Opin Allergy Clin Immunol* **1,** 67-71.

Davies DE, Wicks J, Powell R, Puddicombe S, Holgate S (2003) Airway remodeling in asthma: New insights. *J Allergy Clin Immunol* **111,** 215-225.

de Blic J, Tillie-Leblond I, Emond S, Mahut B, ng Duy TL, Scheinmann P (2005) High-resolution computed tomography scan and airway remodeling in children with severe asthma. *Journal of Allergy and Clinical Immunology* **116,** 750-754.

De Sanctis GT, Merchant M, Beier DR, Dredge RD, Grobholz JK, Martin TR, Lander ES, Drazen JM (1995) Quantitative locus analysis of airway hyperresponsiveness in A/J and C57BL/6J mice. *Nat.Genet.* **11,** 150-154.

De Sanctis G, Daheshia M, Daser A (2001) Genetics of airway hyperresponsiveness. *J Allergy Clin Immunol* **108,** 11-20.

Dealtry GB, Clark DE, Sharkey A, Charnock-Jones DS, Smith SK (1998) Expression and localization of the Th2-type cytokine interleukin-13 and its receptor in the placenta during human pregnancy. *Am J Reprod.Immunol* **40,** 283-290.

Del Mastro RG, Turenne L, Giese H, Keith TP, Van EP, May KJ, Little RD (2007) Mechanistic role of a disease-associated genetic variant within the ADAM33 asthma susceptibility gene. *BMC Med Genet* **8,** 46.

DeLorme MP, Yang H, Elbon-Copp C, Gao X, Barraclough-Mitchell H, Bassett DJ (2002) Hyperresponsive airways correlate with lung tissue inflammatory cell changes in ozone-exposed rats. *J Toxicol.Environ.Health A* **65,** 1453-1470.

DeLorme MP, Moss OR (2002) Pulmonary function assessment by whole-body plethysmography in restrained versus unrestrained mice. *Journal of Pharmacological and Toxicological Methods* **47,** 1-10.

Demayo F, Minoo P, Plopper CG, Schuger L, Shannon J, Torday JS (2002) Mesenchymal-epithelial interactions in lung development and repair: are modeling and remodeling the same process? *AJP - Lung Cellular and Molecular Physiology* **283,** L510-L517.

Desai TJ, Malpel S, Flentke GR, Smith SM, Cardoso WV (2004) Retinoic acid selectively regulates Fgf10 expression and maintains cell identity in the prospective lung field of the developing foregut. *Dev Biol* **273,** 402-415.

Devereux G, Barker RN, Seaton A (2002) Antenatal determinants of neonatal immune responses to allergens. *Clinical Experimental Allergy* **32,** 43-50.

Dezateux C, Stocks J, Dundas I, Fletcher ME (1999) Impaired Airway Function and Wheezing in Infancy . The Influence of Maternal Smoking and a Genetic Predisposition to Asthma. *American Journal of Respiratory and Critical Care Medicine* **159,** 403-410.

Dezateux C, Stocks J, Wade AM, Dundas I, Fletcher ME (2001) Airway function at one year: association with premorbid airway function, wheezing, and maternal smoking. *Thorax* **56,** 680-686.

Drazen JM, Finn PW, De Sanctis GT (1999) MOUSE MODELS OF AIRWAY RESPONSIVENESS: Physiological Basis of Observed Outcomes and Analysis of Selected Examples Using These Outcome Indicators. *Annual Review of Physiology* **61,** 593-625.

Drazen JM, Weiss ST (2002) Genetics: inherit the wheeze. *Nature* **418,** 383-384.

Drey EA, Kang MS, McFarland W, Darney PD (2005) Improving the accuracy of fetal foot length to confirm gestational duration. *Obstet.Gynecol.* **105,** 773-778.

Duan JJW, Chen L, Wasserman ZR, Lu Z, Liu RQ, Covington MB, Qian M, Hardman KD, Magolda RL, Newton RC, Christ DD, Wexler RR, DeCicco CP (2002) Discovery of ã-Lactam Hydroxamic Acids as Selective Inhibitors of Tumor Necrosis Factor á Converting Enzyme: Design, Synthesis, and Structure-Activity Relationships. *Journal of Medicinal Chemistry* **45,** 4954-4957.

Duffy MJ, Lynn DJ, Lloyd AT, O'Shea CM (2003) The ADAMs family of proteins: from basic studies to potential clinical applications. *Thromb.Haemost.* **89,** 622-631.

Dunnill MS (1971) The pathology of asthma. *Ciba Found.Study Group* **38,** 35-46.

Dunnill MS, Massarella GR, Anderson JA (1969) A comparison of the quantitative anatomy of the bronchi in normal subjects, in status asthmaticus, in chronic bronchitis, and in emphysema. *Thorax* **24,** 176-179.

Eder W, Ege MJ, von Mutius E (2006) The Asthma Epidemic. *The New England Journal of Medicine* **355,** 2226-2235.

Elbashir SM, Harborth J, Lendeckel W, Yalcin A, Weber K, Tuschl T (2001) Duplexes of 21-nucleotide RNAs mediate RNA interference in cultured mammalian cells. *Nature* **411,** 494-498.

Elias JA, Lee CG, Zheng T, Ma B, Homer RJ, Zhu Z (2003) New insights into the pathogenesis of asthma. *Journal of Clinical Investigation* **111,** 291-297.

Elliot J, Vullermin P, Robinson D (1998) Maternal Cigarette Smoking Is Associated with Increased Inner Airway Wall Thickness in Children Who Die from Sudden Infant Death Syndrome. *American Journal of Respiratory and Critical Care Medicine* **158,** 802-806.

Evans JP (2001) Fertilin beta and other ADAMs as integrin ligands: insights into cell adhesion and fertilization. *Bioessays* **23,** 628-639.

Evans MJ, Van Winkle LS, Fanucchi MV, Plopper CG (1999) The attenuated fibroblast sheath of the respiratory tract epithelial-mesenchymal trophic unit. *Am J Respir Cell Mol Biol* **21,** 655-657.

Expert Panel Report 3 (2007) Expert Panel Report 3 (EPR-3): Guidelines for the Diagnosis and Management of Asthma-Summary Report 2007. *Journal of Allergy and Clinical Immunology* **120,** S94-S138.

Fedorov IA, Wilson SJ, Davies DE, Holgate ST (2005) Epithelial stress and structural remodelling in childhood asthma. *Thorax* **60,** 389-394.

Fedulov AV, Leme AS, Kobzik L (2007) Duration of allergic susceptibility in maternal transmission of asthma risk. *Am J Reprod.Immunol* **58,** 120-128.

Fedulov AV, Leme A, Yang Z, Dahl M, Lim R, Mariani TJ, Kobzik L (2008) Pulmonary Exposure to Particles during Pregnancy Causes Increased Neonatal Asthma Susceptibility. *American Journal of Respiratory Cell and Molecular Biology* **38,** 57-67.

Fichtner-Feigl S, Fuss IJ, Young CA, Watanabe T, Geissler EK, Schlitt HJ, Kitani A, Strober W (2007) Induction of IL-13 triggers TGF-beta1-dependent tissue fibrosis in chronic 2,4,6-trinitrobenzene sulfonic acid colitis. *J Immunol.* **178,** 5859-5870.

Fichtner-Feigl S, Strober W, Kawakami K, Puri RK, Kitani A (2006) IL-13 signaling through the IL-13[alpha]2 receptor is involved in induction of TGF-[beta]1 production and fibrosis. *Nat Med* **12,** 99-106.

Finkelman FD (2008) Use of unrestrained, single-chamber barometric plethysmography to evaluate sensitivity to cholinergic stimulation in mouse models of allergic airway disease. *Journal of Allergy and Clinical Immunology* **121,** 334-335.

Fire A, Xu S, Montgomery MK, Kostas SA, Driver SE, Mello CC (1998) Potent and specific genetic interference by double-stranded RNA in Caenorhabditis elegans. *Nature* **391,** 806-811.

Fixman ED, Stewart A, Martin JG (2007) Basic mechanisms of development of airway structural changes in asthma. *European Respiratory Journal* **29,** 379-389.

Foley SC, Mogas AK, Olivenstein R, Fiset PO, Chakir J, Bourbeau J, Ernst P, Lemiere C, MARTIN JG, Hamid Q (2007) Increased expression of ADAM33 and ADAM8 with disease progression in asthma. *Journal of Allergy and Clinical Immunology* **119,** 863-871.

Foresi A, Bertorelli G, Pesci A, Chetta A, Olivieri D (1990) Inflammatory markers in bronchoalveolar lavage and in bronchial biopsy in asthma during remission. *Chest* **98,** 528-535.

Foster HL, Small JD, Fox JG (1983) 'The Mouse in Biomedical Research: Normative Biology, Immunology, and Husbandry.' (Academic Press, Inc.: Orlando, San Diego, New York, Austin, Boston, London, Sidney, Tokyo, Toronto)

Fredberg JJ (1998) Airway smooth muscle in asthma: flirting with disaster. *Eur.Respir.J.* **12,** 1252-1256.

Frey U, Kuehni C, Roiha H, Cernelc M, Reinmann B, Wildhaber JH, Hall GL (2004) Maternal Atopic Disease Modifies Effects of Prenatal Risk Factors on Exhaled Nitric Oxide in Infants. *American Journal of Respiratory and Critical Care Medicine* **170,** 260-265.

Fulkerson PC, Fischetti CA, Rothenberg ME (2006) Eosinophils and CCR3 regulate interleukin-13 transgene-induced pulmonary remodeling. *Am J Pathol.* **169,** 2117-2126.

Gao R, McCormick CJ, Arthur MJP, Ruddell R, Oakley F, Smart DE, Murphy FR, Harris MPG, Mann DA (2002) High efficiency gene transfer into cultured primary rat and human hepatic stellate cells using baculovirus vectors. *Liver International* **22,** 15-22.

Garlisi CG, Zou J, Devito KE, Tian F, Zhu FX, Liu J, Shah H, Wan Y, Motasim Billah M, Egan RW, Umland SP (2003) Human ADAM33: protein maturation and localization. *Biochemical and Biophysical Research Communications* **301,** 35-43.

Garton KJ, Gough PJ, Blobel CP, Murphy G, Greaves DR, Dempsey PJ, Raines EW (2001) Tumor necrosis factor-alpha-converting enzyme (ADAM17) mediates the cleavage and shedding of fractalkine (CX3CL1). *J Biol Chem.* **276,** 37993-38001.

Gaultier A, Cousin H, Darribere T, Alfandari D (2002) ADAM13 Disintegrin and Cysteine-rich Domains Bind to the Second Heparin-binding Domain of Fibronectin. *Journal of Biological Chemistry* **277,** 23336-23344.

Gaultier C, Bourbon J, Post M (2000) 'Lung development.' (Oxford University Press:

Gil FR, Lauzon AM (2007) Smooth muscle molecular mechanics in airway hyperresponsiveness and asthma. *Can.J Physiol Pharmacol.* **85,** 133-140.

Gilmore IR, Fox SP, Hollins AJ, Sohail M, Akhtar S (2004) The Design and Exogenous Delivery of siRNA for Post-transcriptional Gene Silencing. *Journal of Drug Targeting* **12,** 315-340.

Gilpin BJ, Loechel F, Mattei MG, Engvall E, Albrechtsen R, Wewer UM (1998) A Novel, Secreted Form of Human ADAM 12á(Meltrin alpha) Provokes Myogenesis in Vivo. *Journal of Biological Chemistry* **273,** 157-166.

Glaab T, Ziegert M, Baelder R, Korolewitz R, Braun A, Hohlfeld JM, Mitzner W, Krug N, Hoymann HG (2005) Invasive versus noninvasive measurement of allergic and cholinergic airway responsiveness in mice. *Respir Res* **6,** 139.

Global Initiative for Asthma (2004) 'GINA Workshop Report (Updated 2004)Global Strategy for Asthma Management and Prevention.'No. NIH Publication No 02-3659,

Global Initiative for Asthma (2006) 'GINA Workshop Report (Revised 2006) Global Strategy for Asthma Management and Prevention.'No. NIH Publication No 02-3659,

Global Initiative for Asthma (2007) 'GINA Workshop Report (Updated 2007) Global Strategy for Asthma Management and Prevention.' Available from: http://www.ginasthma.com,No. NIH Publication No 02-3659,

Gold DR, Fuhlbrigge AL (2006) Inhaled Corticosteroids for Young Children with Wheezing. *The New England Journal of Medicine* **354,** 2058-2060.

Gonzales LW, Ballard PL, Ertsey R, Williams MC (1986) Glucocorticoids and thyroid hormones stimulate biochemical and morphological differentiation of human fetal lung in organ culture. *J Clin Endocrinol.Metab* **62,** 678-691.

Gosman MME, Marike Boezen H, van Diemen CC, Snoeck-Stroband JB, Lapperre TS, Hiemstra PS, ten Hacken NHT, Stolk J, Postma DS, the GLUCOLD Study Group (2007) A disintegrin and metalloprotease 33 and chronic obstructive pulmonary disease pathophysiology. *Thorax* **62,** 242-247.

Grimm D, Kay MA (2007) Therapeutic application of RNAi: is mRNA targeting finally ready for prime time? *J Clin Invest* **117,** 3633-3641.

Guilbert TW, Morgan WJ, Zeiger RS, Mauger DT, Boehmer SJ, Szefler SJ, Bacharier LB, Lemanske RF, Jr., Strunk RC, Allen DB, Bloomberg GR, Heldt G, Krawiec M, Larsen G, Liu AH, Chinchilli VM, Sorkness CA, Taussig LM, Martinez FD (2006) Long-Term Inhaled Corticosteroids in Preschool Children at High Risk for Asthma. *The New England Journal of Medicine* **354,** 1985-1997.

Gunn TM, Azarani A, Kim PH, Hyman RW, Davis RW, Barsh GS (2002) Identification and preliminary characterization of mouse Adam33. *BMC.Genet.* **3,** 2.

Haitchi HM, Holgate ST (2004) New strategies in the treatment and prevention of allergic diseases. *Expert Opin.Investig.Drugs* **13,** 107-124.

Haitchi HM, Krishna MT, Holloway JH, Dent G, Buckley MG, Holgate ST (2005a) Asthma: Clinical Aspects and Mucosal Immunology. In 'Mucosal Immunology'. (Eds J Mestecky, ME Lamm, W Strober, J Bienenstock, JR McGhee, and L Mayer) pp. 1415-1432. (Elsevier Academic Press: Burlington, San Diego, London)

Haitchi HM, Puxeddu I, Davies DE (2008) ADAM33. *Targeted Protein Database*.

Haitchi, H. M., Yang, Y., Cakebread, J., Sammut, D., Harvey, A., Holloway, J. W., Howarth, P. H., Holgate, S. T., and Davies, D. E. Epigenetic Mechanisms silence ADAM33 Expression in Bronchial Epithelial cells. Thorax 62[Supplement 3], A115. 2007.

Haitchi HM, Powell RM, Shaw TJ, Howarth PH, Wilson SJ, Wilson DI, Holgate ST, Davies DE (2005b) ADAM33 Expression in Asthmatic Airways and Human Embryonic Lungs. *American Journal of Respiratory and Critical Care Medicine* **171,** 958-965.

Hakonarson H, Kim C, Whelan R, Campbell D, Grunstein MM (2001) Bi-Directional Activation Between Human Airway Smooth Muscle Cells and T Lymphocytes: Role in Induction of Altered Airway Responsiveness. *The Journal of Immunology* **166,** 293-303.

Hamada K, Suzaki Y, Leme A, Ito T, Miyamoto K, Kobzik L, Kimura H (2007) Exposure of pregnant mice to an air pollutant aerosol increases asthma susceptibility in offspring. *J Toxicol.Environ.Health A* **70,** 688-695.

Hamada K, Suzaki Y, Goldman A, Ning YY, Goldsmith C, Palecanda A, Coull B, Hubeau C, Kobzik L (2003) Allergen-Independent Maternal Transmission of Asthma Susceptibility. *The Journal of Immunology* **170,** 1683-1689.

Hamelmann E, Schwarze J, Takeda K, Oshiba A, Larsen GL, Irvin CG, Gelfand EW (1997) Noninvasive measurement of airway responsiveness in allergic mice using barometric plethysmography. *Am J Respir Crit Care Med* **156,** 766-775.

Hanley NA, Hagan DM, Clement-Jones M, Ball SG, Strachan T, Salas-Cortes L, McElreavey K, Lindsay S, Robson S, Bullen P, Ostrer H, Wilson DI (2000) SRY, SOX9, and DAX1 expression patterns during human sex determination and gonadal development. *Mech Dev* **91,** 403-407.

Have-Opbroek AA (1991) Lung development in the mouse embryo. *Exp.Lung Res.* **17,** 111-130.

Henderson WR, Jr., Tang LO, Chu SJ, Tsao SM, Chiang GK, Jones F, Jonas M, Pae C, Wang H, Chi EY (2002) A role for cysteinyl leukotrienes in airway remodeling in a mouse asthma model. *Am J Respir Crit Care Med* **165,** 108-116.

Hern WM (1984) Correlation of fetal age and measurements between 10 and 26 weeks of gestation. *Obstet.Gynecol.* **63,** 26-32.

Hersh CP, Raby BA, Soto-Quiros ME, Murphy AJ, Avila L, Lasky-Su J, Sylvia JS, Klanderman BJ, Lange C, Weiss ST, Celedon JC (2007) Comprehensive Testing of Positionally Cloned Asthma Genes in Two Populations. *American Journal of Respiratory and Critical Care Medicine* **176,** 849-857.

Hinz B, Phan SH, Thannickal VJ, Galli A, Bochaton-Piallat ML, Gabbiani G (2007) The Myofibroblast: One Function, Multiple Origins. *American Journal of Pathology* **170,** 1807-1816.

Hirota T, Hasegawa K, Obara K, Matsuda A, Akahoshi M, Nakashima K, Shirakawa T, Doi S, Fujita K, Suzuki Y, Nakamura Y, Tamari M (2006) Association between ADAM33 polymorphisms and adult asthma in the Japanese population. *Clinical & Experimental Allergy* **36,** 884-891.

Hirst SJ, Walker TR, Chilvers ER (2000) Phenotypic diversity and molecular mechanisms of airway smooth muscle proliferation in asthma. *Eur Respir J* **16,** 159-177.

Ho YC, Chung YC, Hwang SM, Wang KC, Hu YC (2005) Transgene expression and differentiation of baculovirus-transduced human mesenchymal stem cells. *J Gene Med.* **7,** 860-868.

Hohlberg CJ, Morgan WJ, Wright AL, Martinez FD (1998) Differences in Familial Segregation of FEV1 between Asthmatic and Nonasthmatic Families . Role of a Maternal Component. *American Journal of Respiratory and Critical Care Medicine* **158,** 162-169.

Holgate ST (2000) Epithelial damage and response. *Clinical Experimental Allergy* **30 Suppl 1,** 37-41.

Holgate ST (2002) Asthma: more than an inflammatory disease. *Curr Opin Allergy Clin Immunol.* **2,** 27-29.

Holgate ST, Davies DE, Lackie PM, Wilson SJ, Puddicombe SM, Lordan JL (2000) Epithelial-mesenchymal interactions in the pathogenesis of asthma. *J.Allergy Clin.Immunol.* **105,** 193-204.

Holgate ST, Davies DE, Powell RM, Howarth PH, Haitchi HM, Holloway JW (2007) Local genetic and environmental factors in asthma disease pathogenesis: chronicity and persistence mechanisms. *European Respiratory Journal* **29,** 793-803.

Holgate ST, Holloway JW (2005) Is big beautiful? The continuing story of ADAM33 and asthma. *Thorax* **60,** 263-264.

Holgate S (1999) Genetic and environmental interaction in allergy and asthma. *J Allergy Clin Immunol* **104,** 1139-1146.

Holgate ST (2007) Epithelium dysfunction in asthma. *Journal of Allergy and Clinical Immunology* **120,** 1233-1244.

Holgate ST, Polosa R (2006) The mechanisms, diagnosis, and management of severe asthma in adults. *The Lancet* **368,** 780-793.

Holloway, J. W., Jongepier, H., Beghe, B., Koppelman, G. H., Holgate, S. T., and Postma, D. S. The genetics of asthma. Eur Resp Mon 23, 26-56. 2003.

Holt PG (1996) Primary allergic sensitization to environmental antigens: perinatal T cell priming as a determinant of responder phenotype in adulthood. *The Journal of Experimental Medicine* **183,** 1297-1301.

Hotoda N, Koike H, Sasagawa N, Ishiura S (2002) A secreted form of human ADAM9 has an alpha-secretase activity for APP. *Biochem.Biophys.Res.Commun.* **293,** 800-805.

Howard T, Postma D, Jongepier H, Moore W, Koppelman G, Zheng S, Xu J, Bleecker E, Meyers D (2003) Association of a disintegrin and metalloprotease 33 (ADAM33) gene with asthma in ethnically diverse populations. *J Allergy Clin Immunol* **112,** 717-722.

Howarth PH, Babu KS, Arshad HS, Lau L, Buckley M, McConnell W, Beckett P, Al Ali M, Chauhan A, Wilson SJ, Reynolds A, Davies DE, Holgate ST (2005) Tumour necrosis factor (TNF{alpha}) as a novel therapeutic target in symptomatic corticosteroid dependent asthma. *Thorax* **60,** 1012-1018.

Howarth PH, Wilson J, Djukanovic R, Wilson S, Britten K, Walls A, Roche WR, Holgate ST (1991) Airway inflammation and atopic asthma: a comparative bronchoscopic investigation. *Int.Arch Allergy Appl Immunol* **94,** 266-269.

Huang J, Bridges LC, White JM (2005) Selective Modulation of Integrin-mediated Cell Migration by Distinct ADAM Family Members. *Molecular Biology of the Cell* **16,** 4982-4991.

Illi S, von Mutius E, Lau S, Niggemann B, Grnber C, Wahn U (2006) Perennial allergen sensitisation early in life and chronic asthma in children: a birth cohort study. *The Lancet* **368,** 763-770.

Inanlou MR, Baguma-Nibasheka M, Keating MM, Kablar B (2006) Neurotrophins, airway smooth muscle and the fetal breathing-like movements. *Histol.Histopathol.* **21,** 931-940.

Ioannidis JP, Ntzani EE, Trikalinos TA, Contopoulos-Ioannidis DG (2001) Replication validity of genetic association studies. *Nat Genet* **29,** 306-309.

Ioannidis JP, Trikalinos TA, Ntzani EE, Contopoulos-Ioannidis DG (2003) Genetic associations in large versus small studies: an empirical assessment. *Lancet* **361,** 567-571.

ISSAC Steering Committee (1998) Worldwide variations in the prevalence of asthma symptoms: the International Study of Asthma and Allergies in Childhood (ISAAC). *European Respiratory Journal* **12,** 315-335.

Ito I, Laporte JD, Fiset PO, Asai K, Yamauchi Y, MARTIN JG, Hamid Q (2007) Downregulation of a disintegrin and metalloproteinase 33 by IFN-[gamma] in human airway smooth muscle cells. *Journal of Allergy and Clinical Immunology* **119,** 89-97.

Jackson JR, Seed MP, Kircher CH, Willoughby DA, Winkler JD (1997) The codependence of angiogenesis and chronic inflammation. *The FASEB Journal* **11,** 457-465.

Jakkaraju S, Zhe X, Pan D, Choudhury R, Schuger L (2005) TIPs Are Tension-Responsive Proteins Involved in Myogenic versus Adipogenic Differentiation. *Developmental Cell* **9,** 39-49.

James AL, Pare PD, Hogg JC (1989) The mechanics of airway narrowing in asthma. *Am.Rev.Respir.Dis.* **139,** 242-246.

Jeffery PK (2004) Remodeling and inflammation of bronchi in asthma and chronic obstructive pulmonary disease. *Proc Am Thorac.Soc* **1,** 176-183.

Jeffery PK, Wardlaw AJ, Nelson FC, Collins JV, Kay AB (1989) Bronchial biopsies in asthma. An ultrastructural, quantitative study and correlation with hyperreactivity. *Am Rev Respir Dis* **140,** 1745-1753.

Jesudason EC, Smith NP, Connell MG, Spiller DG, White MR, Fernig DG, Losty PD (2005) Developing rat lung has a sided pacemaker region for morphogenesis-related airway peristalsis. *American Journal of Respiratory Cell and Molecular Biology* **32,** 118-127.

Ji J, Wernli M, Mielgo A, Buechner SA, Erb P (2005) Fas-ligand gene silencing in basal cell carcinoma tissue with small interfering RNA. *Gene Ther.* **12,** 678-684.

Johnson PR, Roth M, Tamm M, Hughes M, Ge Q, King G, Burgess JK, Black JL (2001) Airway smooth muscle cell proliferation is increased in asthma. *Am.J.Respir.Crit Care Med.* **164,** 474-477.

Jongepier H, Boezen HM, Dijkstra A, Howard TD, Vonk JM, Koppelman GH, Zheng SL, Meyers DA, Bleecker ER, Postma DS (2004) Polymorphisms of the ADAM33 gene are associated with accelerated lung function decline in asthma. *Clinical Experimental Allergy* **34,** 757-760.

Kabesch M, Carr D, Weiland SK, von Mutius E (2004) Association between polymorphisms in serine protease inhibitor, kazal type 5 and asthma phenotypes in a large German population sample. *Clinical Experimental Allergy* **34,** 340-345.

Kaur B, Anderson HR, Austin J, Burr M, Harkins LS, Strachan DP, Warner JO (1998) Prevalence of asthma symptoms, diagnosis, and treatment in 12-14 year old children across Great Britain (international study of asthma and allergies in childhood, ISAAC UK). *BMJ* **316,** 118-124.

Kedda MA, Duffy DL, Bradley B, O'HEHIR RE, Thompson PJ (2006) ADAM33 haplotypes are associated with asthma in a large Australian population. *Eur J Hum Genet* **14,** 1027-1036.

Keith, T., Little, R. D., Van Eerdewegh, P., and et al. Human genes relating to respiratory disease and obesity. Ed. Genome Therapeutics Corporation. [US patent 09/627,465]. 2004.

Kheradmand F, Werb Z (2002) Shedding light on sheddases: role in growth and development. *Bioessays* **24,** 8-12.

Koh MS, Irving LB (2007) The natural history of asthma from childhood to adulthood. *International Journal of Clinical Practice* **61,** 1371-1374.

Kurisaki T, Wakatsuki S, Sehara-Fujisawa A (2002) Meltrin beta mini, a new ADAM19 isoform lacking metalloprotease and disintegrin domains, induces morphological changes in neuronal cells. *FEBS Lett.* **532,** 419-422.

Laemmli UK (1970) Cleavage of Structural Proteins during the Assembly of the Head of Bacteriophage T4. *Nature* **227,** 680-685.

Laitinen T, Polvi A, Rydman P, Vendelin J, Pulkkinen V, Salmikangas P, Makela S, Rehn M, Pirskanen A, Rautanen A, Zucchelli M, Gullsten H, Leino M, Alenius H, Petays T, Haahtela T, Laitinen A, Laprise C, Hudson TJ, Laitinen LA, Kere J (2004) Characterization of a common susceptibility locus for asthma-related traits. *Science* **304,** 300-304.

Lambert RK, Wiggs BR, Kuwano K, Hogg JC, Pare PD (1993) Functional significance of increased airway smooth muscle in asthma and COPD. *J.Appl.Physiol* **74,** 2771-2781.

Lannero E, Wickman M, Pershagen G, Nordvall L (2006) Maternal smoking during pregnancy increases the risk of recurrent wheezing during the first years of life (BAMSE). *Respiratory Research* **7,** 3.

Larche M (2007) Regulatory T Cells in Allergy and Asthma. *Chest* **132,** 1007-1014.

Larche M, Akdis CA, Valenta R (2006) Immunological mechanisms of allergen-specific immunotherapy. *Nat Rev Immunol* **6,** 761-771.

Laursen LC, Taudorf E, Borgeskov S, Kobayasi T, Jensen H, Weeke B (1988) Fiberoptic bronchoscopy and bronchial mucosal biopsies in asthmatics undergoing long-term high-dose budesonide aerosol treatment. *Allergy* **43,** 284-288.

Lazaar AL, Panettieri RA, Jr. (2005) Airway smooth muscle: a modulator of airway remodeling in asthma. *J Allergy Clin.Immunol* **116,** 488-495.

Lee CG, Homer RJ, Zhu Z, Lanone S, Wang X, Koteliansky V, Shipley JM, Gotwals P, Noble P, Chen Q, Senior RM, Elias JA (2001) Interleukin-13 Induces Tissue Fibrosis by Selectively Stimulating and Activating Transforming Growth Factor {beta}1. *The Journal of Experimental Medicine* **194,** 809-822.

Lee JH, Park HS, Park SW, Jang AS, Uh ST, Rhim T, Park CS, Hong SJ, Holgate ST, Holloway JW, Shin HD (2004) *ADAM33* polymorphism: association with bronchial hyper-responsiveness in Korean asthmatics. *Clinical Experimental Allergy* **34,** 860-865.

Lee JY, Park SW, Chang HK, Kim HY, Rhim T, Lee JH, Jang AS, Koh ES, Park CS (2006) A Disintegrin and Metalloproteinase 33 Protein in Patients with Asthma: Relevance to Airflow Limitation. *American Journal of Respiratory and Critical Care Medicine* **173,** 729-735.

Lemanske R, Busse W (2003) 6. Asthma. *J Allergy Clin Immunol* **111,** 502-519.

Lenfant C, Khaltaev N (1995) 'Global initiative for asthma global strategy for asthma management and prevention NHLBI/WHO workshop report.' National Institutes of Health National Heart, Lung and Blood Institute,No. Publication Number 95-3659,

Lesueur F (2007) ADAM33, a New Candidate for Psoriasis Susceptibility. *PLoS ONE* **2,** e906.

Li, Y-L., Zhou, J., Burns, D., Yao, W., and Jalluri, R. K. Substituted cyclic hydorxamates as inhibitors of matrix metalloproteinases. Ed. Incyte Corporation. [PCT/US2004/033945]. 28-4-2005. US.

Lind DL, Choudhry S, Ung N, Ziv E, Avila PC, Salari K, Ha C, Lovins EG, Coyle NE, Nazario S, Casal J, Torres A, Rodriguez-Santana JR, Matallana H, Lilly CM, Salas J, Selman M, Boushey HA, Weiss ST, Chapela R, Ford JG, Rodriguez-Cintron W, Silverman EK, Sheppard D, Kwok PY, Gonzalez BE (2003) ADAM33 is not associated with asthma in Puerto Rican or Mexican populations. *Am J Respir Crit Care Med* **168,** 1312-1316.

Litonjua AA, Carey VJ, Burge HA, Weiss ST, Gold DR (1998) Parental History and the Risk for Childhood Asthma . Does Mother Confer More Risk than Father? *American Journal of Respiratory and Critical Care Medicine* **158,** 176-181.

London SJ, James GW, Avol E, Rappaport EB, Peters JM (2001) Family history and the risk of early-onset persistent, early-onset transient, and late-onset asthma. *Epidemiology* **12,** 577-583.

Lordan JL, Bucchieri F, Richter A, Konstantinidis A, Holloway JW, Thornber M, Puddicombe SM, Buchanan D, Wilson SJ, Djukanovic R, Holgate ST, Davies DE (2002) Cooperative Effects of Th2 Cytokines and Allergen on Normal and Asthmatic Bronchial Epithelial Cells. *The Journal of Immunology* **169,** 407-414.

Lum L, Wong BR, Josien R, Becherer JD, Erdjument-Bromage H, Schlondorff J, Tempst P, Choi Y, Blobel CP (1999) Evidence for a role of a tumor necrosis factor-alpha (TNF-alpha)-converting enzyme-like protease in shedding of TRANCE, a TNF family member involved in osteoclastogenesis and dendritic cell survival. *J Biol Chem.* **274,** 13613-13618.

Lundblad LKA, Irvin CG, Hantos Z, Sly P, Mitzner W, Bates JHT (2007) Penh is not a measure of airway resistance! *European Respiratory Journal* **30,** 805.

Macaubas C, de Klerk NH, Holt BJ, Wee C, Kendall G, Firth M, Sly PD, Holt PG (2003) Association between antenatal cytokine production and the development of atopy and asthma at age 6 years. *The Lancet* **362,** 1192-1197.

Maeda Y, Dave V, Whitsett JA (2007) Transcriptional Control of Lung Morphogenesis. *Physiological Reviews* **87,** 219-244.

Manso AM, Elsherif L, Kang SM, Ross RS (2006) Integrins, membrane-type matrix metalloproteinases and ADAMs: potential implications for cardiac remodeling. *Cardiovasc.Res.* **69,** 574-584.

Masoli M, Fabian D, Holt S, Beasley R (2004a) 'Global Burden of Asthma.' Developed for the Global Initiative for Asthma. Available from: http://www.ginasthma.com,

Masoli M, Fabian D, Holt S, Beasley R (2004b) The global burden of asthma: executive summary of the GINA Dissemination Committee report. *Allergy* **59,** 469-478.

McCaffrey AP, Meuse L, Pham TT, Conklin DS, Hannon GJ, Kay MA (2002) Gene expression: RNA interference in adult mice. *Nature* **418,** 38-39.

McKay S, Sharma HS (2002) Autocrine regulation of asthmatic airway inflammation: role of airway smooth muscle. *Respir.Res.* **3,** 11.

Mendelsohn C, Lohnes D, Decimo D, Lufkin T, LeMeur M, Chambon P, Mark M (1994) Function of the retinoic acid receptors (RARs) during development (II). Multiple abnormalities at various stages of organogenesis in RAR double mutants. *Development* **120,** 2749-2771.

Meng JF, McFall C, Rosenwasser LJ (2007) Polymorphism R62W results in resistance of CD23 to enzymatic cleavage in cultured cells. *Genes Immun* **8,** 215-223.

Minoo P, King RJ (1994) Epithelial-Mesenchymal Interactions in Lung Development. *Annual Review of Physiology* **56,** 13-45.

Morgan WJ, Stern DA, Sherrill DL, Guerra S, Holberg CJ, Guilbert TW, Taussig LM, Wright AL, Martinez FD (2005) Outcome of Asthma and Wheezing in the First 6 Years of Life: Follow-up through Adolescence. *American Journal of Respiratory and Critical Care Medicine* **172,** 1253-1258.

Moss ML, Jin SL, Milla ME, Bickett DM, Burkhart W, Carter HL, Chen WJ, Clay WC, Didsbury JR, Hassler D, Hoffman CR, Kost TA, Lambert MH, Leesnitzer MA, McCauley P, McGeehan G, Mitchell J, Moyer M, Pahel G, Rocque W, Overton LK, Schoenen F, Seaton T, Su JL, Becherer JD, . (1997) Cloning of a disintegrin metalloproteinase that processes precursor tumour-necrosis factor-alpha. *Nature* **385,** 733-736.

Moy FJ, Diblasio E, Wilhelm J, Powers R (2001) Solution structure of human IL-13 and implication for receptor binding. *Journal of Molecular Biology* **310,** 219-230.

Nakajima H, Takatsu K (2007) Role of cytokines in allergic airway inflammation. *Int.Arch Allergy Immunol* **142,** 265-273.

Nath D, Slocombe PM, Stephens PE, Warn A, Hutchinson GR, Yamada KM, Docherty AJ, Murphy G (1999) Interaction of metargidin (ADAM-15) with alphavbeta3 and alpha5beta1 integrins on different haemopoietic cells. *Journal of Cell Science* **112 (Pt 4),** 579-587.

Nath D, Slocombe PM, Webster A, Stephens PE, Docherty AJ, Murphy G (2000) Meltrin gamma(ADAM-9) mediates cellular adhesion through alpha(6)beta(1)integrin, leading to a marked induction of fibroblast cell motility. *Journal of Cell Science* **113 (Pt 12),** 2319-2328.

National Asthma Campaign (2001) Out in the open; A true picture of asthma in the UK today, Asthma Audit 2001. *The Asthma Journal* **6**.

National Institute of Health (1985) National Institutes of Health workshop summary. Summary and recommendations of a workshop on the investigative use of fiberoptic bronchoscopy and bronchoalveolar lavage in individuals with asthma. *J Allergy Clin.Immunol* **76,** 145-147.

Noakes PS, Hale J, Thomas R, Lane C, Devadason SG, Prescott SL (2006) Maternal smoking is associated with impaired neonatal toll-like-receptor-mediated immune responses. *Eur Respir J* **28,** 721-729.

Noakes PS, Holt PG, Prescott SL (2003) Maternal smoking in pregnancy alters neonatal cytokine responses. *Allergy* **58,** 1053-1058.

Noguchi E, Ohtsuki Y, Tokunaga K, Yamaoka-Sageshima M, Ichikawa K, Aoki T, Shibasaki M, Arinami T (2006) ADAM33 polymorphisms are associated with asthma susceptibility in a Japanese population. *Clin.Exp.Allergy* **36,** 602-608.

Oguma T, Palmer LJ, Birben E, Sonna LA, Asano K, Lilly CM (2004) Role of Prostanoid DP Receptor Variants in Susceptibility to Asthma. *The New England Journal of Medicine* **351,** 1752-1763.

Orsida BE, Li X, Hickey B, Thien F, Wilson JW, Walters EH (1999) Vascularity in asthmatic airways: relation to inhaled steroid dose. *Thorax* **54,** 289-295.

Orth P, Reichert P, Wang W, Prosise WW, Yarosh-Tomaine T, Hammond G, Ingram RN, Xiao L, Mirza UA, Zou J (2004) Crystal Structure of the Catalytic Domain of Human ADAM33. *Journal of Molecular Biology* **335,** 129-137.

Osler W (1892) 'The Principles and Practice of Medicine.' (D.Appleton and Company: New York)

Page S, Ammit AJ, Black JL, Armour CL (2001) Human mast cell and airway smooth muscle cell interactions: implications for asthma. *Am J Physiol Lung Cell Mol.Physiol* **281,** L1313-L1323.

Pandya HC, Innes J, Hodge R, Bustani P, Silverman M, Kotecha S (2006) Spontaneous contraction of pseudoglandular-stage human airspaces is associated with the presence of smooth muscle-alpha-actin and smooth muscle-specific myosin heavy chain in recently differentiated fetal human airway smooth muscle. *Biol Neonate* **89,** 211-219.

Pang YY (2007) Investigating the proteolytic function of A Disintegrin And Metalloproteinase 33 (ADAM33) and its role in asthma pathogenesis. 'Doctor of Philosophy University of Southampton.

Pang, Y. Y., Nicholas, B., Powell, R. M., Yoshisue, H., Diaz-Mochon, J. J., Murphy, G., Holgate, S. T., and Davies, D. E. Inhibition of ADAM33 by synthetic inhibitors of matrix metalloproteases (MMPs). Proc Am Thorac.Soc 3[Abstracts], A30. 2006.

Pavord ID, Cox G, Thomson NC, Rubin AS, Corris PA, Niven RM, Chung KF, Laviolette M, the RISA Trial Study Group (2007) Safety and Efficacy of Bronchial Thermoplasty in

Symptomatic, Severe Asthma. *American Journal of Respiratory and Critical Care Medicine* **176,** 1185-1191.

Payne DN, Qiu Y, Zhu J, Peachey L, Scallan M, Bush A, Jeffery PK (2004) Airway inflammation in children with difficult asthma: relationships with airflow limitation and persistent symptoms. *Thorax* **59,** 862-869.

Payne DNR, Rogers AV, Adelroth E, Bandi V, Guntupalli KK, Bush A, Jeffrey PK (2003) Early Thickening of the Reticular Basement Membrane in Children with Difficult Asthma. *American Journal of Respiratory and Critical Care Medicine* **167,** 78-82.

Pearce N, Sunyer J, Cheng S, Chinn S, Bjorksten B, Burr M, Keil U, Anderson HR, Burney P (2000) Comparison of asthma prevalence in the ISAAC and the ECRHS. ISAAC Steering Committee and the European Community Respiratory Health Survey. International Study of Asthma and Allergies in Childhood. *Eur.Respir.J.* **16,** 420-426.

Pease JE, Williams TJ (2006) Chemokines and their receptors in allergic disease. *Journal of Allergy and Clinical Immunology* **118,** 305-318.

Perl AK, Wert SE, Nagy A, Lobe CG, Whitsett JA (2002) Early restriction of peripheral and proximal cell lineages during formation of the lung. *Proc Natl.Acad.Sci U.S.A* **99,** 10482-10487.

Perl AK, Whitsett JA (1999) Molecular mechanisms controlling lung morphogenesis. *Clin Genet.* **56,** 14-27.

Peschon JJ, Slack JL, Reddy P, Stocking KL, Sunnarborg SW, Lee DC, Russell WE, Castner BJ, Johnson RS, Fitzner JN, Boyce RW, Nelson N, Kozlosky CJ, Wolfson MF, Rauch CT, Cerretti DP, Paxton RJ, March CJ, Black RA (1998) An Essential Role for Ectodomain Shedding in Mammalian Development. *Science* **282,** 1281-1284.

Piippo-Savolainen E, Korppi M (2008) Wheezy babies-wheezy adults? Review on long-term outcome until adulthood after early childhood wheezing. *Acta Paediatrica* **97,** 5-11.

Pohunek P, Roche WR, Tarzikova J, Kurdmann J, Warner JO (2000) Eosinophilic inflammation in the bronchial mucosa in children with bronchial asthma. *Eur Respir J* **11(suppl 25),** 160s.

Pohunek P, Warner JO, Turzikova J, Kudrmann J, Roche WR (2005) Markers of eosinophilic inflammation and tissue re-modelling in children before clinically diagnosed bronchial asthma. *Pediatric Allergy and Immunology* **16,** 43-51.

Postma DS, Koppelman GH, Meyers DA (2000) The Genetics of Atopy and Airway Hyperresponsiveness. *American Journal of Respiratory and Critical Care Medicine* **162,** 118S-123.

Powell RM, Wicks J, Holloway JW, Davies DE, Holgate ST (2003) Identification and quantification of novel splice variants of ADAM33 reveal distinct tissue expression profiles. *American Journal of Respiratory and Critical Care Medicine* **167,** A440.

Powell RM, Wicks J, Holloway JW, Holgate ST, Davies DE (2004) The splicing and fate of ADAM33 transcripts in primary human airways fibroblasts. *Am J Respir Cell Mol Biol* **31,** 13-21.

Prosise WW, Yarosh-Tomaine T, Lozewski Z, Ingram RN, Zou J, Liu JJ, Zhu F, Taremi SS, Le HV, Wang W (2004) Protease domain of human ADAM33 produced by Drosophila S2 cells. *Protein Expression and Purification* **38,** 292-301.

Puxeddu I, Pang YY, Harvey A, Haitchi HM, Nicholas B, Yoshisue H, Ribatti D, Clough G, Powell RM, Murphy G, Hanley NA, Wilson DI, Howarth PH, Holgate ST, Davies DE (2008) The soluble form of a disintegrin and metalloprotease 33 promotes angiogenesis: Implications for airway remodeling in asthma. *Journal of Allergy and Clinical Immunology* **121,** 1400-1406.

Qiu YM, Luo YL, Lai WY, Qiu SJ (2007a) Association between ADAM33 gene polymorphism and bronchial asthma in South China Han population. *Nan.Fang Yi.Ke.Da.Xue.Xue.Bao.* **27,** 485-487.

Qiu YM, Luo YL, Lai WY, Qiu SJ, Wu YX (2007b) Association of polymorphism of Met764Thr locus allele in ADAM33 gene with bronchial asthma and lung function of asthmatic subjects. *Zhonghua Jie.He.He.Hu Xi.Za Zhi.* **30,** 518-521.

Raby BA, Silverman EK, Kwiatkowski DJ, Lange C, Lazarus R, Weiss ST (2004) ADAM33 polymorphisms and phenotype associations in childhood asthma. *J Allergy Clin Immunol* **113,** 1071-1078.

Raby BA, Weiss ST (2004) ADAM33: where are we now? *Am J Respir Cell Mol Biol* **31,** 1-2.

Rankin JA, Snyder PE, Schachter EN, Matthay RA (1984) Bronchoalveolar lavage. Its safety in subjects with mild asthma. *Chest* **85,** 723-728.

Rawlins EL, Ostrowski LE, Randell SH, Hogan BL (2007) Lung development and repair: contribution of the ciliated lineage. *Proc Natl Acad Sci U.S.A* **104,** 410-417.

Redington A, Madden J, Frew AJ, Djukanovic R, Roche WR, Holgate ST, Howarth PH (1997) Transforming Growth Factor-beta 1 in Asthma . Measurement in Bronchoalveolar Lavage Fluid. *American Journal of Respiratory and Critical Care Medicine* **156,** 642-647.

Regamey N, Hilliard TN, Saglani S, Zhu J, Scallan M, Balfour-Lynn IM, Rosenthal M, JEFFERY PK, Alton EWFW, Bush A, Davies JC (2007) Quality, Size, and Composition of Pediatric Endobronchial Biopsies in Cystic Fibrosis. *Chest* **131,** 1710-1717.

Regamey N, Hilliard TN, Saglani S, Zhu J, Balfour-Lynn IM, Rosenthal M, JEFFERY PK, Alton EWFW, Bush A, Davies JC, Colin AA, Ali-Dinar T (2008a) Endobronchial Biopsy in Childhood. *Chest* **133,** 312-313.

Regamey N, Ochs M, Hilliard TN, Muhlfeld C, Cornish N, Fleming L, Saglani S, Alton EWFW, Bush A, JEFFERY PK, Davies JC (2008b) Increased Airway Smooth Muscle Mass in Children with Asthma, Cystic Fibrosis, and Non-Cystic Fibrosis Bronchiectasis. *American Journal of Respiratory and Critical Care Medicine* **177,** 837-843.

Relan NK, Yang Y, Beqaj S, Miner JH, Schuger L (1999) Cell Elongation Induces Laminin {alpha}2 Chain Expression in Mouse Embryonic Mesenchymal Cells: Role in Visceral Myogenesis. *The Journal of Cell Biology* **147,** 1341-1350.

Richter A, Puddicombe SM, Lordan JL, Bucchieri F, Wilson SJ, Djukanovic R, Dent G, Holgate ST, Davies DE (2001) The contribution of interleukin (IL)-4 and IL-13 to the epithelial- mesenchymal trophic unit in asthma. *American Journal of Respiratory Cell and Molecular Biology* **25,** 385-391.

Roberts CM, Tani PH, Bridges LC, Laszik Z, Bowditch RD (1999) MDC-L, a novel metalloprotease disintegrin cysteine-rich protein family member expressed by human lymphocytes. *J Biol.Chem.* **274,** 29251-29259.

Roche WR, Beasley R, Williams JH, Holgate ST (1989) Subepithelial fibrosis in the bronchi of asthmatics. *Lancet* **1,** 520-524.

Rose MC, Voynow JA (2006) Respiratory Tract Mucin Genes and Mucin Glycoproteins in Health and Disease. *Physiological Reviews* **86,** 245-278.

Rosenthal M, Bush A (2002) The growing lung: normal development, and the long-term effects of pre- and postnatal insults. *Eur Resp Mon* **19,** 1-24.

Roth M, JOHNSON PRA, Borger P, Bihl MP, Rudiger JJ, King GG, Ge Q, Hostettler K, Burgess JK, BLACK JL, Tamm M (2004) Dysfunctional Interaction of C/EBP{alpha} and the Glucocorticoid Receptor in Asthmatic Bronchial Smooth-Muscle Cells. *The New England Journal of Medicine* **351,** 560-574.

Rouse BT (2007) Regulatory T cells in health and disease. *Journal of Internal Medicine* **262,** 78-95.

Rusconi F, Castagneto M, Porta N, Gagliardi L, Leo G, Pellegatta A, Razon S, Braga M (1994) Reference Values for Respiratory Rate in the First 3 Years of Life. *Pediatrics* **94,** 350-355.

Sadeghnejad A, Karmaus W, Arshad SH, Kurukulaaratchy R, Huebner M, Ewart S (2008) IL13 gene polymorphisms modify the effect of exposure to tobacco smoke on persistent wheeze and asthma of childhood, a longitudinal study. *Respir Res* **9,** 2.

Sagane K, Yamazaki K, Mizui Y, Tanaka I (1999) Cloning and chromosomal mapping of mouse ADAM11, ADAM22 and ADAM23. *Gene* **236,** 79-86.

Saglani S, Bush A (2007) The early-life origins of asthma. *Curr Opin.Allergy Clin Immunol* **7,** 83-90.

Saglani S, Malmstrom K, Pelkonen AS, Malmberg LP, Lindahl H, Kajosaari M, Turpeinen M, Rogers AV, Payne DN, Bush A, Haahtela T, MAKELA MJ, JEFFERY PK (2005) Airway Remodeling and Inflammation in Symptomatic Infants with Reversible Airflow Obstruction. *American Journal of Respiratory and Critical Care Medicine* **171,** 722-727.

Saglani S, Payne DN, Zhu J, Wang Z, Nicholson AG, Bush A, JEFFERY PK (2007) Early Detection of Airway Wall Remodeling and Eosinophilic Inflammation in Preschool Wheezers. *American Journal of Respiratory and Critical Care Medicine* **176,** 858-864.

Sakagami T, Jinnai N, Nakajima T, Sekigawa T, Hasegawa T, Suzuki E, Inoue I, Gejyo F (2007) ADAM33 polymorphisms are associated with aspirin-intolerant asthma in the Japanese population. *Journal of Human Genetics* **52,** 66-72.

Sakgami T, Hasegawa T, Yoshizawa H, Suzuki E, Koshino T, Gejyo F (2003) ADAM33 Polymorphisms are Associated with Aspirin Intolerant Asthma in Japanese population. *Am J Respir Crit Care Med* **167,** A750.

Salam MT, Gauderman WJ, McConnell R, Lin PC, GILLILAND FD (2007) Transforming Growth Factor- 1 C-509T Polymorphism, Oxidant Stress, and Early-Onset Childhood Asthma. *American Journal of Respiratory and Critical Care Medicine* **176,** 1192-1199.

Salter HH. On asthma: its pathology and treatment. Ed. Science Press Limited. *In The Evolution of Understanding.*[1], 106-142. 1859. *London*. Classic Papers in Asthma. Edited by Brewis RAL.

Sampson AP (2000) The role of eosinophils and neutrophils in inflammation. *Clin.Exp.Allergy* **30 Suppl 1,** 22-27.

Schedel M, Depner M, Schoen C, Weiland S, Vogelberg C, Niggemann B, Lau S, Illig T, Klopp N, Wahn U, von Mutius E, Nickel R, Kabesch M (2006) The role of polymorphisms in ADAM33, a disintegrin and metalloprotease 33, in childhood asthma and lung function in two German populations. *Respiratory Research* **7,** 91.

Schittny JC, Miserocchi G, Sparrow MP (2000) Spontaneous Peristaltic Airway Contractions Propel Lung Liquid through the Bronchial Tree of Intact and Fetal Lung Explants. *American Journal of Respiratory Cell and Molecular Biology* **23,** 11-18.

Schmidt M, Sun G, Stacey MA, Mori L, Mattoli S (2003) Identification of Circulating Fibrocytes as Precursors of Bronchial Myofibroblasts in Asthma. *The Journal of Immunology* **171,** 380-389.

Seals DF, Courtneidge SA (2003) The ADAMs family of metalloproteases: multidomain proteins with multiple functions. *Genes and Development* **17,** 7-30.

Sears MR, Holdaway MD, Flannery EM, Herbison GP, Silva PA (1996) Parental and neonatal risk factors for atopy, airway hyper-responsiveness, and asthma. *Archives of Disease in Childhood* **75,** 392-398.

Sekhon HS, Jia Y, Raab R, Kuryatov A, Pankow JF, Whitsett JA, Lindstrom J, Spindel ER (1999) Prenatal nicotine increases pulmonary alpha7 nicotinic receptor expression and alters fetal lung development in monkeys. *J Clin Invest* **103,** 637-647.

Sekhon HS, Keller JA, Proskocil BJ, Martin EL, Spindel ER (2002) Maternal Nicotine Exposure Upregulates Collagen Gene Expression in Fetal Monkey Lung . Association with alpha 7 Nicotinic Acetylcholine Receptors. *American Journal of Respiratory Cell and Molecular Biology* **26,** 31-41.

Sekine K, Ohuchi H, Fujiwara M, Yamasaki M, Yoshizawa T, Sato T, Yagishita N, Matsui D, Koga Y, Itoh N, Kato S (1999) Fgf10 is essential for limb and lung formation. *Nat Genet* **21,** 138-141.

Sengler C, Lau S, Wahn U, Nickel R (2002) Interactions between genes and environmental factors in asthma and atopy: new developments. *Respir.Res.* **3,** 7.

Seow CY, Schellenberg RR, Pare PD (1998) Structural and functional changes in the airway smooth muscle of asthmatic subjects. *Am J Respir Crit Care Med* **158,** S179-S186.

Seshasayee D, Lee WP, Zhou M, Shu J, Suto E, Zhang J, Diehl L, Austin CD, Meng YG, Tan M, Bullens SL, Seeber S, Fuentes ME, Labrijn AF, Graus YM, Miller LA, Schelegle ES, Hyde DM, Wu LC, Hymowitz SG, Martin F (2007) In vivo blockade of OX40 ligand inhibits thymic stromal lymphopoietin driven atopic inflammation. *J Clin.Invest* **117,** 3868-3878.

Shannon JM (1994) Induction of alveolar type II cell differentiation in fetal tracheal epithelium by grafted distal lung mesenchyme. *Dev Biol* **166,** 600-614.

Shannon JM, Hyatt BA (2004) Epithelial-mesenchymal interactions in the developing lung. *Annu.Rev Physiol* **66,** 625-645.

Shannon JM, Nielsen LD, Gebb SA, Randell SH (1998) Mesenchyme specifies epithelial differentiation in reciprocal recombinants of embryonic lung and trachea. *Dev Dyn* **212,** 482-494.

Shapiro SD, Owen CA (2002) ADAM-33 Surfaces as an Asthma Gene. *The New England Journal of Medicine* **347,** 936-938.

Shore SA (2004) Airway smooth muscle in asthma--not just more of the same. *N.Engl.J Med* **351,** 531-532.

Silverman ES, Baron RM, Palmer LJ, Le L, Hallock A, Subramaniam V, Riese RJ, McKenna MD, Gu X, Libermann TA, Tugores A, Haley KJ, Shore S, Drazen JM, Weiss ST (2002) Constitutive and Cytokine-Induced Expression of the ETS Transcription Factor ESE-3 in the Lung. *American Journal of Respiratory Cell and Molecular Biology* **27,** 697-704.

Simpson A, Maniatis N, Jury F, Cakebread JA, Lowe LA, Holgate ST, Woodcock A, Ollier WER, Collins A, Custovic A, Holloway JW, John SL (2005a) Polymorphisms in A Disintegrin and Metalloprotease 33 (ADAM33) Predict Impaired Early-Life Lung Function. *American Journal of Respiratory and Critical Care Medicine* **172,** 55-60.

Simpson A, Maniatis N, Jury F, Cakebread JA, Lowe LA, Holgate ST, Woodcock A, Ollier WE, Collins A, Custovic A, Holloway JW, John SL (2005b) Polymorphisms in A Disintegrin and Metalloprotease 33 Predict Impaired Early-Life Lung Function. *American Journal of Respiratory and Critical Care Medicine* 200412-1708OC.

Snyder JM, Johnston JM, Mendelson CR (1981) Differentiation of type II cells of human fetal lung in vitro. *Cell Tissue Res* **220,** 17-25.

Steinman RM, Banchereau J (2007) Taking dendritic cells into medicine. *Nature* **449,** 419-426.

Stick SM, Burton PR, Gurrin L, Sly PD, LeSouef PN (1996) Effects of maternal smoking during pregnancy and a family history of asthma on respiratory function in newborn infants. *The Lancet* **348,** 1060-1064.

Strachan T, Lindsay S, Wilson DI (1997) 'Molecular Genetics of Early Human Development.' (BIOS Scientific Publishers Limited:

Sunyer J, Anto JM, Tobias A, Burney P (1999) Generational increase of self-reported first attack of asthma in fifteen industrialized countries. European Community Respiratory Health Study (ECRHS). *European Respiratory Journal* **14,** 885-891.

Szepfalusi Z, Pichler J, Elsasser S, van Duren K, Ebner C, Bernaschek G, Urbanek R (2000) Transplacental priming of the human immune system with environmental allergens can occur early in gestation. *J Allergy Clin Immunol* **106,** 530-536.

Tang ML, Wilson JW, Stewart AG, Royce SG (2006) Airway remodelling in asthma: current understanding and implications for future therapies. *Pharmacol.Ther.* **112,** 474-488.

Tattersfield AE, Knox AJ, Britton JR, Hall IP (2002) Asthma. *Lancet* **360,** 1313-1322.

Temelkovski J, Hogan SP, Shepherd DP, Foster PS, Kumar RK (1998) An improved murine model of asthma: selective airway inflammation, epithelial lesions and increased

methacholine responsiveness following chronic exposure to aerosolised allergen. *Thorax* **53,** 849-856.

The Childhood Asthma Management Program Research Group (2000) Long-Term Effects of Budesonide or Nedocromil in Children with Asthma. *The New England Journal of Medicine* **343,** 1054-1063.

The ENFUMOSA Study Group (2003) The ENFUMOSA cross-sectional European multicentre study of the clinical phenotype of chronic severe asthma. *European Respiratory Journal* **22,** 470-477.

Tliba O, Amrani Y, Panettieri RA, Jr. (2008) Is Airway Smooth Muscle the "Missing Link" Modulating Airway Inflammation in Asthma? *Chest* **133,** 236-242.

Tollet J, Everett AW, Sparrow MP (2002) Development of neural tissue and airway smooth muscle in fetal mouse lung explants: a role for glial-derived neurotrophic factor in lung innervation. *Am J Respir Cell Mol Biol* **26,** 420-429.

Tsou CL, Haskell CA, Charo IF (2001) Tumor necrosis factor-alpha-converting enzyme mediates the inducible cleavage of fractalkine. *J Biol Chem.* **276,** 44622-44626.

Tsuchiya T, Nishimura Y, Nishiuma T, Kotani Y, Funada Y, Yoshimura S, Yokoyama M (2003) Airway remodeling of murine chronic antigen exposure model. *J Asthma* **40,** 935-944.

Tugores A, Le J, Sorokina I, Snijders AJ, Duyao M, Reddy PS, Carlee L, Ronshaugen M, Mushegian A, Watanaskul T, Chu S, Buckler A, Emtage S, McCormick MK (2001) The Epithelium-specific ETS Protein EHF/ESE-3 Is a Context-dependent Transcriptional Repressor Downstream of MAPK Signaling Cascades. *Journal of Biological Chemistry* **276,** 20397-20406.

Umetsu DT, DeKruyff RH (2006) The regulation of allergy and asthma. *Immunological Reviews* **212,** 238-255.

Umland SP, Garlisi CG, Shah H, Wan Y, Zou J, Devito KE, Huang WM, Gustafson EL, Ralston R (2003) Human ADAM33 messenger RNA expression profile and post-transcriptional regulation. *Am J Respir Cell Mol Biol* **29,** 571-582.

Umland SP, Wan Y, Shah H, Garlisi CG, Devito KE, Braunschweiger K, Gheyas F, Del Mastro R (2004) Mouse ADAM33: Two Splice Variants Differ in Protein Maturation and Localization. *American Journal of Respiratory Cell and Molecular Biology* **30,** 530-539.

van Diemen CC, Postma DS, Vonk JM, Bruinenberg M, Schouten JP, Boezen HM (2005a) A disintegrin and metalloprotease 33 polymorphisms and lung function decline in the general population. *Am J Respir Crit Care Med* **172,** 329-333.

van Diemen CC, Postma DS, Vonk JM, Bruinenberg M, Schouten JP, Boezen HM (2005b) A Disintegrin and Metalloprotease 33 Polymorphisms and Lung Function Decline in the General Population. *American Journal of Respiratory and Critical Care Medicine* **172,** 329-333.

Van Eerdewegh P, Little RD, Dupuis J, Del Mastro RG, Falls K, Simon J, Torrey D, Pandit S, McKenny J, Braunschweiger K, Walsh A, Liu Z, Hayward B, Folz C, Manning SP, Bawa A, Saracino L, Thackston M, Benchekroun Y, Capparell N, Wang M, Adair R, Feng Y, Dubois J, FitzGerald MG, Huang H, Gibson R, Allen KM, Pedan A, Danzig MR, Umland SP, Egan RW, Cuss FM, Rorke S, Clough JB, Holloway JW, Holgate ST, Keith TP (2002)

Association of the ADAM33 gene with asthma and bronchial hyperresponsiveness. *Nature* **418,** 426-430.

Van Rijt LS, Lambrecht BN (2005) Dendritic cells in asthma: a function beyond sensitization. *Clinical & Experimental Allergy* **35,** 1125-1134.

Vandesompele J, De PK, Pattyn F, Poppe B, Van RN, De PA, Speleman F (2002) Accurate normalization of real-time quantitative RT-PCR data by geometric averaging of multiple internal control genes. *Genome Biol* **3,** RESEARCH0034.

Vendelin J, Pulkkinen V, Rehn M, Pirskanen A, Raisanen-Sokolowski A, Laitinen A, Laitinen LA, Kere J, Laitinen T (2005) Characterization of GPRA, a Novel G Protein-Coupled Receptor Related to Asthma. *American Journal of Respiratory Cell and Molecular Biology* **33,** 262-270.

Vermeer PD, Harson R, Einwalter LA, Moninger T, Zabner J (2003) Interleukin-9 Induces Goblet Cell Hyperplasia during Repair of Human Airway Epithelia. *American Journal of Respiratory Cell and Molecular Biology* **28,** 286-295.

Vincent B, Paitel E, Saftig P, Frobert Y, Hartmann D, De Strooper B, Grassi J, Lopez-Perez E, Checler F (2001) The disintegrins ADAM10 and TACE contribute to the constitutive and phorbol ester-regulated normal cleavage of the cellular prion protein. *J Biol Chem.* **276,** 37743-37746.

von Mutius E (2002) Environmental factors influencing the development and progression of pediatric asthma. *J Allergy Clin Immunol* **109,** 525S-532S.

Walley AJ, Chavanas S, Moffatt MF, Esnouf RM, Ubhi B, Lawrence R, Wong K, Abecasis GR, Jones EY, Harper JI, Hovnanian A, Cookson WO (2001) Gene polymorphism in Netherton and common atopic disease. *Nat.Genet.* **29,** 175-178.

Wan H, Dingle S, Xu Y, Besnard V, Kaestner KH, Ang SL, Wert S, Stahlman MT, Whitsett JA (2005) Compensatory Roles of Foxa1 and Foxa2 during Lung Morphogenesis. *Journal of Biological Chemistry* **280,** 13809-13816.

Wang P, Liu QJ, Li JS, Li HC, Wei CH, Guo CH, Gong YQ (2006) Lack of association between ADAM33 gene and asthma in a Chinese population. *International Journal of Immunogenetics* **33,** 303-306.

Wang YH, Liu YJ (2007) OX40-OX40L interactions: a promising therapeutic target for allergic diseases? *J Clin.Invest* **117,** 3655-3657.

Warburton D, Bellusci S, De Langhe S, Del Moral PM, Fleury V, Mailleux A, Tefft D, Unbekandt M, Wang K, Shi W (2005) Molecular Mechanisms of Early Lung Specification and Branching Morphogenesis. *Pediatric Research* **57,** 26R-37.

Warburton D, Tefft D, Mailleux A, Bellusci S, Thiery JP, Zhao J, Buckley S, Shi W, Driscoll B (2001) Do lung remodeling, repair, and regeneration recapitulate respiratory ontogeny? *Am.J.Respir.Crit Care Med.* **164,** S59-S62.

Warburton D, Bellusci S, Del Moral PM, Kaartinen V, Lee M, Tefft D, Shi W (2003) Growth factor signaling in lung morphogenetic centers: automaticity, stereotypy and symmetry. *Respiratory Research* **4,** 5.

Warburton D, Schwarz M, Tefft D, Flores-Delgado G, Anderson KD, Cardoso WV (2000) The molecular basis of lung morphogenesis. *Mechanisms of Development* **92,** 55-81.

Wark PAB, Johnston SL, Bucchieri F, Powell R, Puddicombe S, Laza-Stanca V, Holgate ST, Davies DE (2005) Asthmatic bronchial epithelial cells have a deficient innate immune response to infection with rhinovirus. *The Journal of Experimental Medicine* **201,** 937-947.

Wen FQ, Kohyama T, Liu X, Zhu YK, Wang H, Kim HJ, Kobayashi T, Abe S, Spurzem JR, Rennard SI (2002) Interleukin-4- and interleukin-13-enhanced transforming growth factor-beta2 production in cultured human bronchial epithelial cells is attenuated by interferon-gamma. *Am J Respir.Cell Mol Biol.* **26,** 484-490.

Wenzel SE, Balzar S (2006) Myofibroblast or Smooth Muscle: Do In Vitro Systems Adequately Replicate Tissue Smooth Muscle? *American Journal of Respiratory and Critical Care Medicine* **174,** 364-365.

Werner M, Herbon N, Gohlke H, Altmuller J, Knapp M, Heinrich J, Wjst M (2004) Asthma is associated with single-nucleotide polymorphisms in ADAM33. *Clinical Experimental Allergy* **34,** 26-31.

White, J. M. and Wolfsberg, T. G. **Table of the ADAMs** . Webpage . 2004.
Ref Type: Electronic Citation

Whitehead GS, Walker JK, Berman KG, Foster WM, Schwartz DA (2003) Allergen-induced airway disease is mouse strain dependent. *AJP - Lung Cellular and Molecular Physiology* **285,** L32-L42.

Whitsett J (1998) A lungful of transcription factors. *Nat.Genet.* **20,** 7-8.

Whittaker PA (2003) Genes for asthma: much ado about nothing? *Current Opinion in Pharmacology* **3,** 212-219.

Wicks J (2006) The expression and regulation of ADAM33, a novel asthma susceptibility gene, during myofibroblast differentiation. 'PhD University of Southampton.

Wiester LM, Giachelli CM (2003) Expression and function of the integrin alpha9beta1 in bovine aortic valve interstitial cells. *J Heart Valve Dis.* **12,** 605-616.

Wiggs BR, Moreno R, Hogg JC, Hilliam C, Pare PD (1990) A model of the mechanics of airway narrowing. *J.Appl.Physiol* **69,** 849-860.

Willems E, Mateizel I, Kemp C, Cauffman G, Sermon K, Leyns L (2006) Selection of reference genes in mouse embryos and in differentiating human and mouse ES cells. *Int.J Dev.Biol.* **50,** 627-635.

Williams TJ, Jones CA, Miles EA, Warner JO, Warner JA (2000) Fetal and neonatal IL-13 production during pregnancy and at birth and subsequent development of atopic symptoms. *Journal of Allergy and Clinical Immunology* **105,** 951-959.

Wjst M (2007) Public data mining shows extended linkage disequilibrium around ADAM33. *Allergy* **62,** 444-446.

Yang P, Baker KA, Hagg T (2006) The ADAMs family: coordinators of nervous system development, plasticity and repair. *Prog.Neurobiol.* **79,** 73-94.

Yang Y, Beqaj S, Kemp P, Ariel I, Schuger L (2000) Stretch-induced alternative splicing of serum response factor promotes bronchial myogenesis and is defective in lung hypoplasia. *J Clin Invest* **106,** 1321-1330.

Yang Y, Haitchi HM, Cakebread J, Sammut D, Harvey A, Powell RM, Holloway JW, Howarth P, Holgate ST, Davies DE (2008) Epigenetic mechanisms silence a disintegrin and metalloprotease 33 expression in bronchial epithelial cells. *Journal of Allergy and Clinical Immunology* **121,** 1393-1399.

Yavari R, Adida C, Bray-Ward P, Brines M, Xu T (1998) Human metalloprotease-disintegrin Kuzbanian regulates sympathoadrenal cell fate in development and neoplasia. *Hum.Mol.Genet.* **7,** 1161-1167.

Yin H, Lin H (2007) An epigenetic activation role of Piwi and a Piwi-associated piRNA in Drosophila melanogaster. *Nature* **450,** 304-308.

Yoshinaka T, Nishii K, Yamada K, Sawada H, Nishiwaki E, Smith K, Yoshino K, Ishiguro H, Higashiyama S (2002) Identification and characterization of novel mouse and human ADAM33s with potential metalloprotease activity. *Gene* **282,** 227-236.

Young S, Le Souef PN, Geelhoed GC, Stick SM, Turner KJ, Landau LI (1991) The influence of a family history of asthma and parental smoking on airway responsiveness in early infancy. *The New England Journal of Medicine* **324,** 1168-1173.

Zamel N, McClean PA, Sandell PR, Siminovitch KA, Slutsky AS (1996) Asthma on Tristan da Cunha: looking for the genetic link. The University of Toronto Genetics of Asthma Research Group. *American Journal of Respiratory and Critical Care Medicine* **153,** 1902-1906.

Zhang J, Pare PD, Sandford AJ (2008) Recent advances in asthma genetics. *Respir Res* **9,** 4.

Zhao J, Chen H, Peschon JJ, Shi W, Zhang Y, Frank SJ, Warburton D (2001a) Pulmonary hypoplasia in mice lacking tumor necrosis factor-alpha converting enzyme indicates an indispensable role for cell surface protein shedding during embryonic lung branching morphogenesis. *Dev.Biol* **232,** 204-218.

Zhao J, Chen H, Wang YL, Warburton D (2001b) Abrogation of tumor necrosis factor-alpha converting enzyme inhibits embryonic lung morphogenesis in culture. *Int J Dev.Biol* **45,** 623-631.

Zhu Z, Homer RJ, Wang Z, Chen Q, Geba GP, Wang J, Zhang Y, Elias JA (1999) Pulmonary expression of interleukin-13 causes inflammation, mucus hypersecretion, subepithelial fibrosis, physiologic abnormalities, and eotaxin production. *Journal of Clinical Investigation* **103,** 779-788.

Zou J, Zhang R, Zhu F, Liu J, Madison V, Umland SP (2005) ADAM33 Enzyme Properties and Substrate Specificity. *Biochemistry* **44,** 4247-4256.

Zou J, Zhu F, Liu J, Wang W, Zhang R, Garlisi CG, Liu YH, Wang S, Shah H, Wan Y, Umland SP (2004) Catalytic Activity of Human ADAM33. *Journal of Biological Chemistry* **279,** 9818-9830.

Movie 1

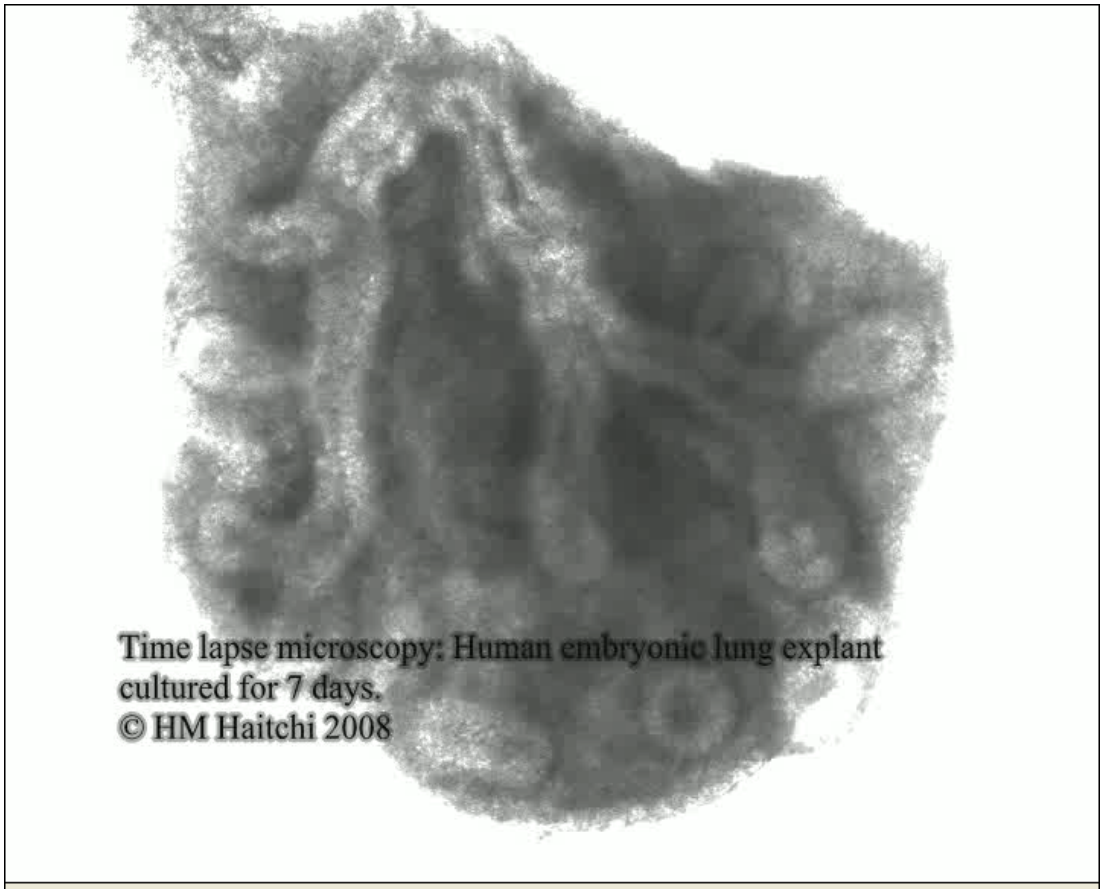

Movie 1_HEL time lapse microscopy_PhD-thesis_HM_Haitchi 2008

Movie 2

Movie 2_MEL video live microscopy_PhD-thesis_HM_Haitchi_2008